Natural Resources Canada | Ressources naturelles Canada

GEOLOGICAL SURVEY OF CANADA
OPEN FILE 9210

Till geochemistry and indicator-mineral methods for exploration in glaciated terrains

Edited by R.C. Paulen and M.B. McClenaghan

2024

Canada

GEOLOGICAL SURVEY OF CANADA
OPEN FILE 9210

Till geochemistry and indicator-mineral methods for exploration in glaciated terrains

Edited by R.C. Paulen and M.B. McClenaghan

2024

© His Majesty the King in Right of Canada, as represented by the Minister of Natural Resources, 2024

Information contained in this publication or product may be reproduced, in part or in whole, and by any means, for personal or public non-commercial purposes, without charge or further permission, unless otherwise specified.
You are asked to:
- exercise due diligence in ensuring the accuracy of the materials reproduced;
- indicate the complete title of the materials reproduced, and the name of the author organization; and
- indicate that the reproduction is a copy of an official work that is published by Natural Resources Canada (NRCan) and that the reproduction has not been produced in affiliation with, or with the endorsement of, NRCan.

Commercial reproduction and distribution is prohibited except with written permission from NRCan. For more information, contact NRCan at copyright-droitdauteur@nrcan-rncan.gc.ca.

This publication is available for free download through the NRCan Open Science and Technology Repository (https://ostrnrcan-dostrncan.canada.ca/).

Recommended citation
Paulen, R.C. and McClenaghan, M.B. (ed.), 2024. Till geochemistry and indicator-mineral methods for exploration in glaciated terrains; Geological Survey of Canada, Open File 9210, 157 p. https://doi.org/10.4095/pbmy2d03m0

Publications in this series have not been edited; they are released as submitted by the author.

ISSN 2816-7155
ISBN 978-0-660-73355-5
Catalogue No. M183-2/9210E-PDF
https://doi.org/10.4095/pbmy2d03m0

Table of Contents

Introduction
Roger C. Paulen and M. Beth McClenaghan 1

Glacial dynamics and glacial sediment dispersal explained
Martin Ross 4

Determination of glacial transport directions
Roger C. Paulen, Riley P.M. Mulligan, and Jessey M. Rice 10

Dirt Detectives: Unravelling buried mineral potential with advanced till sampling techniques
Jessey Rice and M. Beth McClenaghan 24

Strategic applications of shallow overburden drilling for drift prospecting
Dave Sacco 35

Till geochemistry and indicator mineral laboratory methods
Chris Beckett-Brown and M. Beth McClenaghan 41

Tower Resources' rapid discovery from scratch, via glacially dispersed gold grains, of the Lightening and Thunder Au zones within the intensely explored Kamloops district: A recipe for effectively exploring the till-covered Interior Plateau of British Columbia
Stu Averill 58

Volcanogenic massive sulphide exploration in glaciated terrain: till geochemistry, indicator mineral, and boulder tracing methods
M. Beth McClenaghan and Jan M. Peter 66

Exploring for magmatic Ni-Cu-PGE deposits in glaciated terrain: strategies and examples
Dan Layton-Matthews and M. Beth McClenaghan 86

Lithium signatures in till at the Brazil Lake lithium-cesium-tantalum pegmatites, Nova Scotia
Denise Brushett, Chris Beckett-Brown, M. Beth McClenaghan, Roger C. Paulen, and Jessey M. Rice 99

Application of machine learning to till geochemical data
Mohammad Parsa and M. Beth McClenaghan 110

Abitibi Greenstone Belt: Exploration strategies in thick drift terrain
M. Beth McClenaghan, Roger C. Paulen, Jean J. Veillette, and Pierre-Marc Godbout 115

LiDAR in glacial geology and drift exploration: The prospectors'ice-stream landsystem
Syed Bukhari, Nick Eyles, and Roger C. Paulen 133

Glacial dispersal trains and ice streams on the Canadian Shield
Roger C. Paulen, Nick Eyles, Martin Ross 140

Using indicator minerals to explore for porphyry Cu deposits and their related critical minerals
Chris Beckett-Brown and M. Beth McClenaghan 148

Introduction

Roger C. Paulen and M. Beth McClenaghan

Geological Survey of Canada, 601 Booth Street, Ottawa, Ontario K1A 0E8

This publication is a compilation of short papers that present established and new drift prospecting methods and concepts for mineral exploration for a broad range of commodities in glaciated terrain. These extended abstracts were originally prepared to accompany the "Till geochemistry and indicator mineral methods for exploration in glaciated terrains" short course that was held March 1–2, 2024 for the Prospectors and Developers Association Convention (PDAC 2024) in Toronto. This workshop was organized by the Geological Survey of Canada (GSC) and funded by the GSC's Geo-mapping for Energy and Minerals Program (GEM-GeoNorth), Targeted Geoscience Initiative (TGI-6), and Critical Minerals Geoscience and Data (CMGD) initiative.

As the world shifts away from a hydrocarbon-based economy, there is an increasing need for secure supplies of domestically sourced minerals that are critically needed for the green and digital economy. Canada has a list of 31 minerals (Fig. 1) considered to be "critical". These critical minerals are i) essential for Canada's economic security and its supply, ii) required for the country's national transition to a low-carbon economy, or iii) necessary for a sustainable source for our partners and allies (Government of Canada, 2021).

Canada is a glaciated landscape, extensively modified by continental-scale glaciations that have deposited glacial sediments and created landforms that may potentially be covering these critical resources. These short papers provide the fundamental knowledge and tools needed to explore for critical minerals by making use of this glaciated landscape and the sediments. The concepts and examples presented in this volume are applicable to glaciated terrain globally.

Glacial erosion, sediment mixing, transport, and deposition have dispersed metal-rich debris down-ice from mineralized bedrock. These dispersal patterns



Figure 1. A list of Canada's 31 critical minerals depicted in the shape of a maple leaf.

Recommended citation:

Paulen, R.C. and McClenaghan, M.B. 2024. Till geochemistry and indicator mineral methods for exploration in glaciated terrains: Introduction to the course; *in* Till Geochemistry and Indicator Mineral Methods for Exploration in Glaciated Terrains, (ed.) R.C. Paulen and M.B. McClenaghan; Geological Survey of Canada, Open File 9210, p. 1–3. https://doi.org/10.4095/pbmy2d03m0

COMMON INDICATOR MINERALS

- Kimberlite indicator minerals (KIM)
- Gold grains
- Native copper
- Platinum Group minerals
- Sulphide minerals
- Metamorphosed massive sulphide minerals, e.g., gahnite
- Magmatic Ni-Cu-PGE minerals
- Cu-Mo-Au porphyry minerals
- Scheelite, wolframite
- Cassiterite, tourmaline
- Cinnabar
- Fluorite, topaz
- Uraninite, thorianite
- REE minerals
- LCT pegmatites (spodumene, columbite-tantalite, tourmaline)

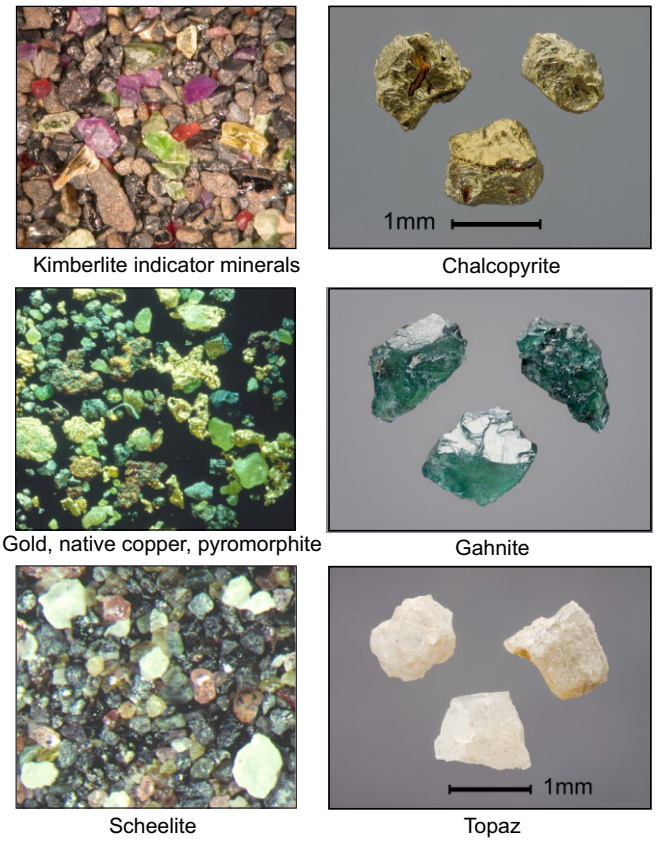


Figure 2. List of indicator minerals that can be routinely recovered from till samples in support of critical mineral exploration.

may be the result of one or more phases of ice flow. Spatially, the dispersal trains are much larger exploration targets than their bedrock sources and can vary in length from a few tens of metres to >100 km. A combination of boulder tracing, till geochemistry, and indicator mineral methods can be used to detect dispersal trains and trace mineralization up-ice to its source.

Boulder tracing and till geochemistry have been widely used in mineral exploration for detecting glacial dispersal in Fennoscandia and Canada since the 1970s. Indicator mineral methods have expanded since the 1980s when they were used for diamond and gold exploration. Today, indicator mineral suites are used to explore for a broad range of critical mineral deposit types, including base metals, rare-earth metals, lithium, and uranium (Fig. 2; McClenaghan and Paulen, 2018, and references therein).

This volume begins with a review of the principles of glacial erosion, transportation, and deposition, the formation of a glacial dispersal train, and how to determine glacial transport directions. These fundamentals are accompanied by presentations describing how to collect a till sample and how to analyze it. The use of LiDAR imagery is explained as a modern tool to help guide till sampling. The dynamics of fast-flowing ice (ice streams) from the former continental glaciers and the implications for mineral exploration in areas affected by them are presented. The application of machine learning to the interpretation of till geochemical data, now an essential part of the till methods toolkit, is explained. This volume also presents examples of till geochemical and indicator mineral signatures for five different critical mineral and other deposit types: Li pegmatites, orogenic Au, magmatic Ni-Cu-PGE, VMS-hosted Cu-Pb-Zn, and porphyry Cu. Special considerations for exploration in the Abitibi Greenstone Belt are reviewed because of this belt's exceptionally thick cover of glacial sediments and long history of till sampling combined with its unusually rich endowment of gold and critical metal deposits.

ACKNOWLEDGEMENTS

The editors would like to thank Volker Moeller, Sarah Nazar, and Michelle Connolly from PDAC for their support and logistical assistance that made the short course possible and successful. Isabelle McMartin coordinated the GSC review process for this open file, with support from fellow scientists Etienne Brouard, Janet Campbell, and Alexandre Voinot. Support from the GSC's GEM-GeoNorth, TGI-6, and CMGD management for this short course and the scientists from the GSC who presented, is greatly appreciated.

REFERENCES

Government of Canada, 2021. The Canadian Mineral Strategy. https://www.canada.ca/en/campaign/critical-minerals-in-

canada/canadian-critical-minerals-strategy.html <accessed Feb. 6, 2024>

McClenaghan, M.B. and Paulen, R.C., 2018. Mineral exploration in glaciated terrain; Chapter 20 *in* Past Glacial Environments (Sediments, Forms and Techniques) A new & revised edition, (ed.) J. Menzies and J.J-M. van der Meer; Elsevier, p. 689–751. https://doi.org/10.1016/B978-0-08-100524-8.00022-1

Glacial dynamics and glacial sediment dispersal explained

Martin Ross

Department Earth and Environmental Sciences, University of Waterloo,
200 University Avenue West, Waterloo, Ontario, N2L 3G1

MINERAL EXPLORATION UNDER GLACIAL SEDIMENT COVER

Glacial and post-glacial sediments can be a hindrance to mineral exploration as they can cover the bedrock of interest and introduce additional complexity to the analysis and interpretation of geophysical data. However, glacial sediment derived from the direct erosion of bedrock by an actively flowing glacier, i.e., subglacial traction till (Benn and Evans, 2010), can contain minerals from a source of potential economic interest (McClenaghan et al., 2023). The glacial transport of these minerals often creates a mappable dispersal pattern down-ice from their bedrock source that may be several times larger than the ore deposit, and even larger than the entire ore deposit footprint in bedrock (including the alteration halo). Several glacial dispersal patterns (a.k.a. dispersal trains) have been documented in the literature providing numerous examples in different geological and glacial history settings (e.g. McClenaghan et al., 2023 and references therein). Mineral exploration can thus be enhanced in glaciated regions by using information about ice flow direction(s) and the composition of till for a provenance analysis. Using glacial geology knowledge, minerals recovered from till that are indicative of certain ore-forming processes, or related geochemical pathfinders, can be traced like breadcrumbs back to their bedrock source (McClenaghan et al., 2023). This strategy may seem straightforward, and it sometimes is. However, several complicating factors often need to be considered. For instance, dispersal trains may have widely variable lengths and shapes, may be defined and outlined using different variables (e.g. indicator minerals, geochemical pathfinders) and threshold values, and may also be overlapping from multiple sources making it challenging to identify their boundaries and locate potential bedrock source areas. Sometimes, the surficial dispersal pattern is detached from its source, whereas other known sources lack a dispersal train. To reduce the risk of costly misinterpretations, the whole strategy must not only rely on a good knowledge of the glacial history of the region being explored, but also on an understanding of the basic principles of glacial dynamics, glacial sediment transport, and deposition mechanisms. Here, a summary is presented of the basics of glacial dynamics and related sedimentary processes that are involved in the formation of glacial dispersal patterns.

GLACIAL DYNAMICS – THE BASICS

Ice sheets, like those in Antarctica and Greenland today, or the North American Ice Sheet Complex that covered most of Canada during the last glaciation are large ice masses that deform and flow due to gravity. Specifically, the 'driving force' of an ice sheet is controlled by the slope of the ice surface, the thickness of the ice sheet, the density of the ice, and gravitational acceleration (Benn and Evans, 2010). An ice-sheet surface is more elevated, and ice is thicker, in the interior regions than the outer regions of the ice sheet, and ice will thus flow from the higher interior regions to the lower outer regions (Fig. 1). An ice sheet can gain mass via snow precipitation, with the transformation of snow into ice, and it can lose mass via ice melting, sublimation and evaporation, and calving of icebergs (if in contact with a water body) (Fig. 1). If all of this is balanced, the glacier is in equilibrium. However, if either the mass gain or the mass loss is greater than the other, the glacier will either grow in extent and thickness (i.e. positive mass balance) or shrink and thin (i.e. negative mass balance), respectively. In all cases, the slow transfer of mass from the interior regions to the margins will continue with ice flowing towards the outer ice-sheet margins, even when those margins are receding due to a negative mass balance. Some parts of an ice sheet may become stagnant, but generally, ice tends to keep flowing. The ice surface topography can shift due to changes in atmospheric circulation and precipitation, and its internal dynamics. One consequence of this is a shift in the position of ice divides and the orientation of regional ice-flow lines (McMartin and Henderson, 2004; Rice et al., 2019). Ice flow can also shift during ice thinning because the ice-surface slope will increasingly adjust to the subglacial topography. These factors can result in one prospective area having experienced different ice-flow directions due to one or more glaciations. Tracing minerals back to their source in this context can be challenging because the minerals may have

Recommended citation:

Ross, M., 2024. Glacial dynamics and glacial sediment dispersal explained; *in* Till Geochemistry and Indicator Mineral Methods for Exploration in Glaciated Terrains, (ed.) R.C. Paulen and M.B. McClenaghan; Geological Survey of Canada, Open File 9210, p. 4–9. https://doi.org/10.4095/pbmy2d03m0

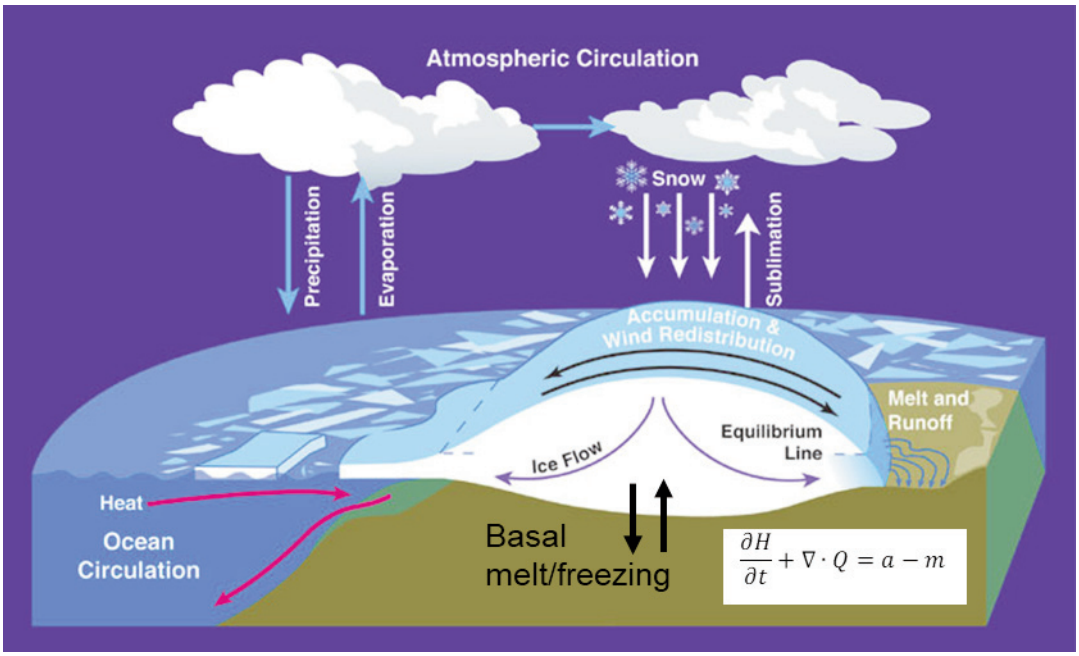


Figure 1. Conceptual model of an ice sheet and its mass balance. The mass balance equation shown is from Hindmarsh (2018), where H (x,y,z) is the ice thickness (H>0), t is time, the flux Q is a vertically integrated horizontal (2HD) ice-flow vector, a is the accumulation/ablation, and m is basal melting/freezing. The image is modified from commons.wikimedia.org.

been transported in two or more ice-flow directions (Parent et al., 1996; Paulen et al., 2013; McClenaghan and Paulen, 2018). It is critical to develop a good knowledge of the regional as well as the local glacial history.

Glacial geologists are particularly interested in what is happening at the base of an ice sheet or, more specifically, at the ice-bed interface where subglacial erosion, sediment transport, and deposition take place. If the interface is below the pressure-melting point (PMP), the conditions are said to be 'cold-based', in which case basal ice-flow velocity will be approaching zero (Fig. 2a). However, the ice above may still flow due to the driving stress. In contrast, if the ice-bed interface is at the PMP, a condition referred to as 'warm-based', then two things can happen: 1) ice at the base will slip on a thin water film (Fig. 2b) or 2) sediments below the interface will undergo deformation (Fig. 2c). Both processes contribute to the forward motion of the ice above. Ice slip, or basal sliding, typically occurs on a hard bed, such as the bedrock surface, but it can also

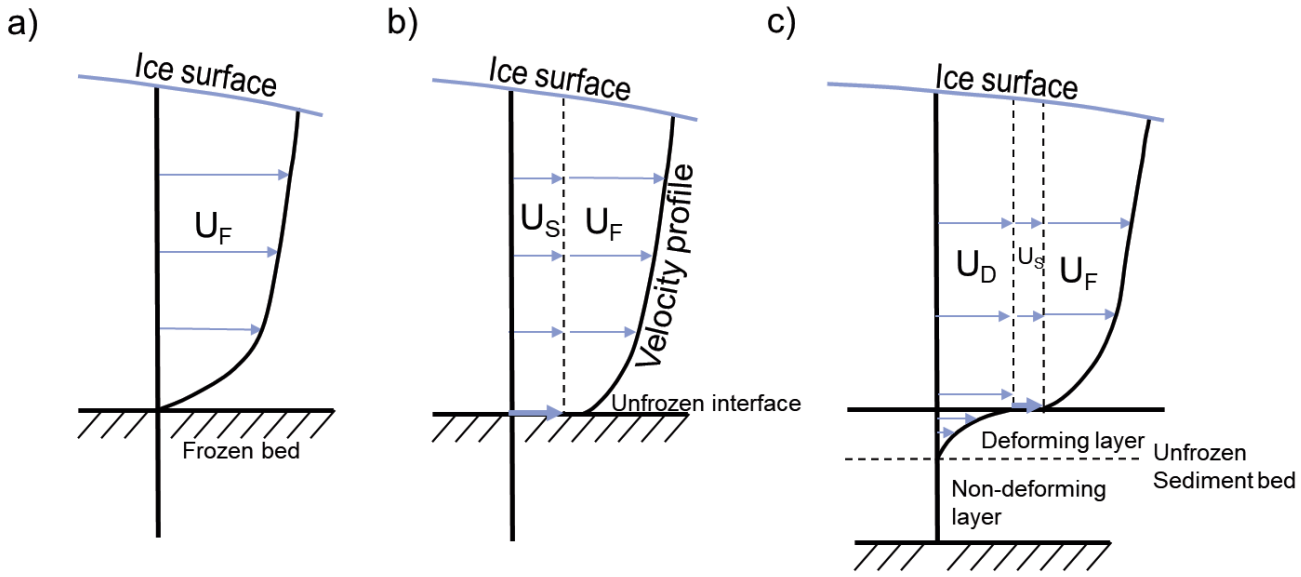


Figure 2. Conceptual ice-flow profiles for **a)** internal ice flow (U_F) only due to a frozen interface (cold-based ice), **b)** internal ice flow and basal sliding (U_S), and **c)** U_F, U_S, and subglacial deformation (U_D). Modified *from* Boulton (1996).

happen locally over a soft bed due to ice-bed decoupling under very low effective stress (i.e. subglacial water pressures are sufficiently high to locally support the weight of the glacier). Subglacial sediment deformation will happen when the shear stress from the moving ice above exceeds the yield strength of the underlying sediment (Benn and Evans, 2010). This is more likely to happen with low-permeability sediment, such as mud-rich till or similar soft fine-grained sediment and relatively low effective pressure (but not low enough for ice-bed decoupling to occur). The latter is a very important process that explains why fast-flowing corridors of ice (referred to as ice streams) exist in the West Antarctic Ice Sheet despite having low driving stresses (Alley et al., 1987). There is compelling evidence across the Canadian glacial landscape indicating that ice streams exerted considerable influence on the Laurentide Ice Sheet's (LIS) dynamics and subglacial sediment transport, on both hard and soft beds (Margold et al., 2015 and references therein).

The processes briefly described above allow for either (a) the preservation under sustained cold-based ice of relict landscapes and sediments in certain glaciated regions or (b) subglacial erosion, transport, and deposition of glacial sediments under warm-based conditions. Subglacial conditions can also vary spatially and temporally. For example, one area may have been cold-based for some time, followed by warm-based conditions, or vice versa. In Canada, this created overprinting or a patchy landscape of disjointed glacial bed pieces that were formed and preserved at different times under different glacial regimes (Ross et al., 2009; Trommelen et al., 2012). As a result, some dispersal trains may be truncated or have complex shapes.

GLACIAL EROSION, TRANSPORT, AND DEPOSITION

In mineral exploration when indicator minerals are found in till, one of the key questions is, how far up-ice is the source? Case studies using known sources and ice-flow history provide useful information (e.g. McClenaghan et al., 2022), but it remains challenging when working in a new area where the source has yet to be found. A good place to start is by developing an understanding of glacial erosion, subglacial sediment transport, and deposition.

The two main processes of bedrock erosion by sliding ice are (1) abrasion and (2) quarrying. Subglacial abrasion results from the sliding of debris-rich basal ice onto a hard bed, typically the bedrock surface. Abrasion rates are controlled by the relative hardness of the clasts protruding from the ice sole compared to that of bedrock, the force pressing the clasts against the hard bed (friction models), the velocity of the sliding clasts, and the debris concentration at the ice-bed interface (Iverson et al., 2003; Rea, 2013). Abrasion tends to produce relatively fine-grained material (e.g. sand and silt). Striations and grooves on polished bedrock surfaces are the product of abrasion (Rea, 2013).

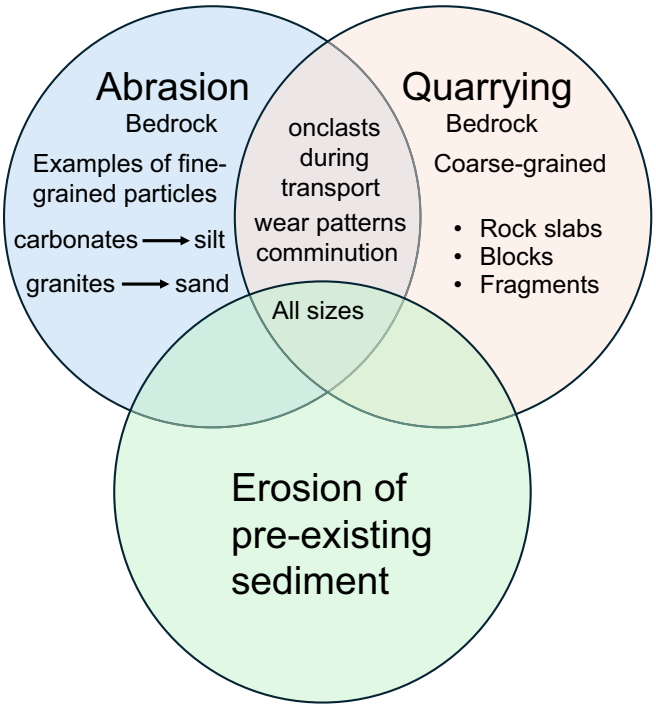


Figure 3. Venn diagram showing the origin (by process) of sediment particles in subglacial traction till from bedrock or pre-existing sediment.

Quarrying initiates with the failure of jointed or fractured bedrock due to large stress gradients and fluctuating water pressures in the down-ice, or the lee-side bedrock steps, under actively flowing ice (Iverson, 1991, 2012; Iverson et al., 2003; Hallet, 1996). Subglacial cavities play a key role as they tend to form down-ice of these steps and will be part of a subglacial linked-cavity drainage system that controls the water pressure. Rock fragments of various sizes may be produced in this way and entrained by ice and incorporated into till. Most large particles from pebbles to glacial erratics (boulders and cobbles) are the product of quarrying. These particles can be further crushed and shaped by frictional processes during transport, which means that a certain proportion of the till matrix originated from larger particles produced by quarrying. Finally, a portion of the till may be derived from the erosion and entrainment of pre-existing unconsolidated sediment of potentially various origins. The origin and production of till particles by these processes is summarized in Figure 3. Now that we know how till particles are produced, the next step is to describe the main ways by which these particles are entrained, transported, and deposited.

Particles of various sizes can be incorporated into basal ice via basal freeze-on and a process called 'rege-

lation intrusion'. For the latter, ice pressing down onto sediments may temporarily melt and penetrate the sediment array and refreeze or 'regelate' in lower pressure spots (Iverson and Semmens, 1995). The sediment then becomes entrapped into basal ice and will move with it. There is a certain limit to how thick the debris-rich basal ice layer can become through this process, but debris can also move further up into the ice via vertical mixing processes (e.g. ice folding) or may be released at the ice-bed interface due to basal melting (Hildes, 2001). All of these processes, along with ice-flow velocity, control the horizontal englacial sediment flux (Hildes, 2001; Melanson et al., 2013). The debris in the moving basal ice will cause friction and thus exert shear traction (Iverson et al., 2003) and may be plastered and deposited onto a hard bed by pressure-melting and other mechanical, frictional processes (Benn and Evans, 2010). This process is referred to as 'lodgement'. As mentioned in the previous section above, subglacial sediments at or near the ice-bed interface may also undergo localized deformation under certain conditions (e.g. Zoet and Iverson, 2020). Subglacial sediment near the ice-bed interface can thus be transported in this way via rotations and other movements. Till is deposited when deformation ceases, which occurs when the sediment strength exceeds shear stress. Due to the complexity of these processes and the multiple cycles and overprinting, subglacial till is best described as 'subglacial traction till' (Benn and Evans, 2010) rather than by assigning a more specific genetic origin (e.g. lodgement, deformation, meltout).

GLACIAL DISPERSAL MAPPING AND MODELLING

Dispersal patterns are the result of the full evolution of clastic sediment transport, which may involve multiple cycles of entrainment, transport, and deposition via the processes described above. It is important to note that dispersal patterns are outlined by mapping the abundance of boulders of selected lithologies, the abundance of selected indicator minerals, or the concentrations of geochemical pathfinders in the till matrix. The abudance or concentration of selected compositions decreases both laterally, away from the dispersal centre line, and in the down-ice direction(s), although some patterns exhibit more complex trends. Most examples in the literature (e.g. McClenaghan et al., 2023) are based on a unique variable (one clast lithology, one indicator mineral, or one geochemical pathfinder). However, recent studies have shown the usefulness of using multivariate analysis and classification algorithms to investigate dispersal patterns (e.g. Rice et al., 2024). Because dispersal trains can be defined and outlined using different methods and compositional variables, their extent and shape may differ, sometimes substantially, from one another over the same area. First, the composition of till is not the same in different size fractions (Shilts, 1993). This is due to various mineralogical, physical, and analytical considerations, but particles of different size fractions may also come from different sources and reflect a different transport mechanism and history. For instance, the boulders perhaps were transported in an englacial position in a single cycle, whereas the smaller particles experienced various transport mechanisms and multiple cycles.

Dispersal patterns are also greatly affected by bedrock topography, in regions of thin and discontinuous till, and by till stratigraphy and surficial landforms in areas of thicker and more continuous till. Dispersal may be blocked, deflected, or fragmented by bedrock obstacles, and bedrock sources nested in a depression, for example, may not always generate a dispersal train (Kelley et al., 2019; Stirling, 2022). Thick, multi-till stratigraphy may also generate complex 3-D dispersal patterns, which are at best only partially captured by surficial till sampling surveys (Kelley et al., 2019).

In the early days of dispersal train mapping and analysis, a common practice was to find the mathematical functions (e.g. exponential, linear) that would give the best fit to the dispersal data and then provide an interpretation of what it meant from a process point of view (Parent et al., 1996; Klassen, 1999). This approach is still useful today, however, Hildes (2001), and more recently Melanson et al. (2013), showed the potential of using ice-sheet and sediment transport models that incorporate the physics at play in the formation of dispersal patterns. These numerical models provide several insights into glacial dynamics, subglacial erosion, and sediment transport and deposition, but they remain challenging to use at a scale useful for mineral exploration and, as a result, have not yet been widely applied for this purpose. Other modelling approaches have been used in fluvial settings (Lipp et al., 2020, 2021), but these forward and inverse sediment transport modelling strategies have yet to be applied to the context of glacial dispersion from mineralized sources. The current strategy of mapping dispersal trains in 2-D and 3-D using survey data and GIS and combining these data with glacial knowledge seems to be the most practical and useful approach to meet mineral exploration needs.

CONCLUSION

Tracing indicator minerals and geochemical pathfinders from till samples back to their bedrock source is a type of "inverse problem" (*see* Lipp et al., 2021, for details) whereby the exploration geologist is trying to determine the location and prospectivity of the source rocks given the composition of glacial sediments and the overall glacial history of the area. For glacial sedi-

ment provenance, this involves mapping dispersal patterns and using their shape and ice-flow information to vector towards a source area of potential interest. In some cases, it is successfully achieved using relatively limited information about the glacial geology. However, the approach is often challenging due to a variety of problems. Dispersal trains may have complex shapes, some are detached from their source, and others are elusive due to being partly buried, truncated, or overprinted by other overlapping dispersal trains. Some sources also lack a dispersal train even though the area was glaciated. All of these situations require a more advanced understanding of glacial dynamics and glacial sediment transport, of the effect of bedrock topography, and of glacial landform formation to reduce exploration risk and increase the likelihood of success. Mineral exploration is increasingly multidisciplinary, and teams trained in advanced glacial geology and glaciology, mineralogy, geochemistry, geophysics, GIS, statistics, and machine learning, as well as numerical modelling can help achieve success in more challenging settings. This is the new, exciting, and promising reality of mineral exploration in glaciated terrain.

REFERENCES

Alley, R.B., Blankenship, D.D., Bentley, C.R., and Rooney, S.T., 1987. Till beneath ice stream B. 3. Till deformation: evidence and implications; Journal of Geophysical Research, v. 92, p. 8921–8929.

Benn, D.I. and Evans, D.J.A., 2010. Glaciers and Glaciation, Second Edition; Routledge, New York, 802 p.

Boulton, G.S., 1996. Theory of glacial erosion, transport and deposition as a consequence of subglacial sediment deformation; Journal of Glaciology, v. 42, p. 43–62.

Hallet, B., 1996. Glacial quarrying: A simple theoretical model; Annals of Glaciology, v. 22, p. 1–8.

Hildes, D.H.D., 2001. Modelling subglacial erosion and englacial sediment transport of the North American ice sheets; Ph.D. thesis, The University of British Columbia, Vancouver, British Columbia, 168 p.

Hindmarsh, R.C.A., 2018. Ice Sheet and Glacier Modelling; Chapter 18 *in* Past Glacial Environments (Second Edition), (ed.) J. Menzies and J.M. van der Meer; Elsevier, p. 607–663.

Iverson, N.R. 1991. Potential effects of subglacial water-pressure fluctuations on quarrying; Journal of Glaciology, v. 37, p. 27–36.

Iverson, N.R., 2012. A theory of glacial quarrying for landscape evolution models; Geology, v. 40, p. 679–682.

Iverson, N.R. and Semmens, D.J., 1995. Intrusion of ice into porous media by regelation: a mechanism of sediment entrainment by glaciers; Journal of Geophysical Research, v. 100, p. 10,219–10,230.

Iverson, N.R., Cohen, D., Hooyer, T.S., Fischer, U.H., Jackson, M., Moore, P.L., Lappegard, G., and Kohler, J., 2003. Effects of basal debris on glacier flow; Science, v. 301, p. 81–84.

Kelley, S.E., Ross, M., Elliott, B., and Normandeau, P.X., 2019. Effect of shifting ice flow and basal topography in shaping three-dimensional dispersal patterns, Lac de Gras region, Northwest Territories, Canada; Journal of Geochemical Exploration, v. 199, p. 105–127.

Klassen, R.A., 1999. The application of glacial dispersal models to the interpretation of till geochemistry in Labrador, Canada; Journal of Geochemical Exploration, v. 67, p. 245–269.

Lipp, A.G., Roberts, G.G., Whittaker, A.C., Gowing, C.J.B., and Fernandes, V.M., 2020. River sediment geochemistry as a conservative mixture of source regions: Observations and predictions from the Cairngorms, UK; Journal of Geophysical Research: Earth Surface, v. 125. https://doi.org/10.1029/2020JF005700

Lipp, A.G., Roberts, G.G., Whittaker, A.C., Gowing, C.J.B., and Fernandes, V.M., 2021. Source region geochemistry from unmixing downstream sedimentary elemental compositions; Geochemistry, Geophysics, Geosystems. v. 22. https://doi.org/10.1029/2021GC009838

Margold, M., Stokes, C.R., and Clark, C.D., 2015. Ice streams in the Laurentide Ice Sheet: Identification, characteristics and comparison to modern ice sheets; Earth-Science Reviews, v. 143, p. 117–146.

McClenaghan, M.B. and Paulen, R.C., 2018. Application of Till Mineralogy and Geochemistry to Mineral Exploration; Chapter 20 *in* Past Glacial Environments (Second Edition), (ed.) J. Menzies and J.M. van der Meer; Elsevier, p. 689–751.

McClenaghan, M.B., Spirito, W.A., Day, S.J.A., McCurdy, M.W., McNeil, R.J., and Adcock, S.W., 2022. Overview of surficial geochemistry and indicator mineral surveys and case studies from the Geological Survey of Canada's GEM Program; Geochemistry: Exploration, Environment, Analysis, v. 22, p. 1–21.

McClenaghan, M.B., Paulen, R.C., Smith, I.R., Rice, J.M., Plouffe, A., McMartin, I., Campbell, J.E., Lehtonen, M., Parsasadr, M., and Beckett-Brown, C.E., 2023. Review of till geochemistry and indicator mineral methods for mineral exploration in glaciated terrain; Geochemistry: Exploration, Environment, Analysis, v. 23, p. 1–43.

McMartin, I. and Henderson, P., 2004. Evidence from Keewatin (Central Nunavut) for paleo-ice divide migration; Géographie Physique et Quaternaire, v. 58, p. 163–186.

Melanson, A., Bell, T., and Tarasov, L., 2013. Numerical modelling of subglacial erosion and sediment transport and its application to the North American ice sheets over the Last Glacial cycle; Quaternary Science Reviews, v. 68, p. 154–174.

Parent, M., Paradis, S.J., and Doiron, A., 1996. Palimpsest glacial dispersal trains and their significance for drift prospecting; Journal of Geochemical Exploration, v. 56, p. 123–140.

Paulen, R.C., McClenaghan, M.B., and Hicken, A.K., 2013. Regional and local ice-flow history in the vicinity of the Izok Lake Zn-Cu-Pb-Ag deposit, Nunavut; Canadian Journal of Earth Sciences, v. 50, p. 1209–1222.

Rice, J.M., Ross, M., Paulen, R.C., Kelley, S.E., Briner, J.P., Neudorf, C.M., and Lian, O.B., 2019. Refining the ice flow chronology and subglacial dynamics across the migrating Labrador Divide of the Laurentide Ice Sheet with age constraints on deglaciation; Journal of Quaternary Science v. 34, p. 519–535.

Rice, J.M., Ross, M., Campbell, H.E., Paulen, R.C., and McClenaghan, B., 2024. Net evolution of subglacial sediment transport in the Quebec-Labrador sector of the Laurentide Ice Sheet; Canadian Journal of Earth Sciences, v. 61, p. 524–542.

Rea, B.R., 2013. Micro- to macroscale forms; *in* Encyclopedia of Quaternary Science (Second Edition), (ed.) C. Mock and S. Elias; Elsevier, p. 865–876.

Ross, M., Campbell, J.E., Parent, M., and Adams, R.S., 2009. Palaeo-ice streams and the subglacial landscape mosaic of the North American mid-continental prairies; Boreas, v. 38, p. 421–439.

Shilts, W.W., 1993. Geological Survey of Canada's contributions to understanding the composition of glacial sediments; Canadian Journal of Earth Sciences, v. 30, p. 333–353.

Stirling, R.A., 2022. Ice flow shift, drumlin, and bedrock topography effects on glacial dispersal from kimberlites in the Lac de Gras region, Northwest Territories, Canada; M.Sc. thesis, University of Waterloo, London, Ontario, 305 p.

Trommelen, M.S., Ross, M., and Campbell, J.E., 2012. Glacial terrain zone analysis of a fragmented paleoglaciologic record, southeast Keewatin sector of the Laurentide Ice Sheet; Quaternary Science Reviews, v. 40, p. 1–20.

Zoet, L.K. and Iverson, N.R., 2020. A slip law for glaciers on deformable beds. Science, v. 368, p. 76–78.

Determination of glacial transport directions

Roger C. Paulen[1], Riley P.M. Mulligan[2], and Jessey M. Rice[1]

[1]Geological Survey of Canada, 601 Booth Street, Ottawa, Ontario K1A 0E8
[2]Ontario Geological Survey, Ministry of Mines, 933 Ramsey Lake Road, Sudbury, Ontario P3E 6B5

ABSTRACT

Effective and efficient mineral exploration in glaciated terrain requires the identification of the erosional and depositional history of ice sheets that impacted the area. Drift prospecting involves the discovery of dispersal trains by geochemical or heavy mineral surveys and subsequent tracing up-ice to the source of the mineralized bedrock source(s). To ensure success in tracing a desired mineral to its bedrock source, it is necessary to know precisely the direction(s) of ice flow that may have influenced its course during transport. Drift prospecting relies heavily on knowledge of former flow dynamics and trajectories of Quaternary glaciers.

Determination of former ice-flow directions is undertaken through analysis of a variety of erosional and depositional landforms and features, including streamlined and other directional landforms in drift and bedrock, striations and other small-scale erosional forms on bedrock or boulders, and in situ measurements of pebbles, boulders, and structural features in till. Exploration success also relies on incorporating local ice-flow observations into regional ice-flow interpretations. Even when clear directional features are identified, the application of ice-flow information to drift prospecting is not always straightforward. Flow directions may change from regional ice flow that is apparently unimpeded by the terrain to topographically controlled (local) flows that exhibit strong changes in ice-flow directions around local topographic features. Regional dispersal trains can be weakly modified, redirected, displaced, or seemingly unaffected by deviations in local topographically controlled ice flow.

Older glacial sediments, landforms, and erosional flow indicators may also be preserved at surface, as a relict terrain, with almost no modification by subsequent ice flows, resulting in major discontinuities in regional ice-flow trends. The dynamic nature of glacial dispersal centres and the widespread occurrence of ice streams, the presence of large continental glaciolacustrine basins, the occurrence of relict landscapes under ice divides, and cold-based ice all interplay with the complexity of the ice sheets that once covered large portions of the Northern Hemisphere.

INTRODUCTION

Drift prospecting involves the identification of dispersal trains in glacial sediments and subsequent tracing to the source by following the glacial flow-path directions to the mineralized bedrock (*see also* DiLabio and Coker, 1989; DiLabio, 1990; Puranen, 1990; Bobrowsky et al., 1995; McClenaghan et al., 2001; Paulen and McMartin, 2009; Ferbey et al., 2017; McClenaghan and Paulen, 2018). Dispersal trains are lithological, mineralogical, or geochemical indicators of economic mineralization that can be traced in glacial deposits to locate their bedrock source (e.g. Klassen, 2001). To ensure success in tracing an indicator back to its bedrock source, it is necessary to know the trajectories of ice flow that eroded the source and influenced the mineralized glacial debris during its transportation and deposition (Hirvas and Nenonen, 1990). Dispersal trains can develop over topographic barriers, cross one or more drainage basins, may be shifted and reworked due to the time-transgressive process of migrating ice-dispersal centres (ice divides), and may be elongated due to ice streaming, with many examples cited in the literature noted above.

Once an ore indicator is discovered in the glacial sediments, it is necessary to know precisely the direction(s) of ice flow that may have influenced its course during transport. This assessment of ice-flow directions should be carried out and confirmed based on the widest possible range of evidence, from large landform indicators down to small outcrop-scale indicators. Often, the dispersal train itself or other indicator trains documented in the area will serve to show the net direction of glacial erosion, entrainment, and deposition, as well as any unexpected patterns, such as displaced dispersal trains. Since local ice-flow directions can deviate quite markedly from regional flow patterns, observations of ice flow on a local scale are essential at or near the site of the ore indicator discovery.

The objective of this short course paper is to illustrate and provide criteria for the recognition of land-

Recommended citation:

Paulen, R.C., Mulligan, R.P.M., and Rice, J.M., 2024. Determination of glacial transport directions; *in* Till Geochemistry and Indicator Mineral Methods for Exploration in Glaciated Terrains, (ed.) R.C. Paulen and M.B. McClenaghan; Geological Survey of Canada, Open File 9210, p. 10–23. https://doi.org/10.4095/pbmy2d03m0

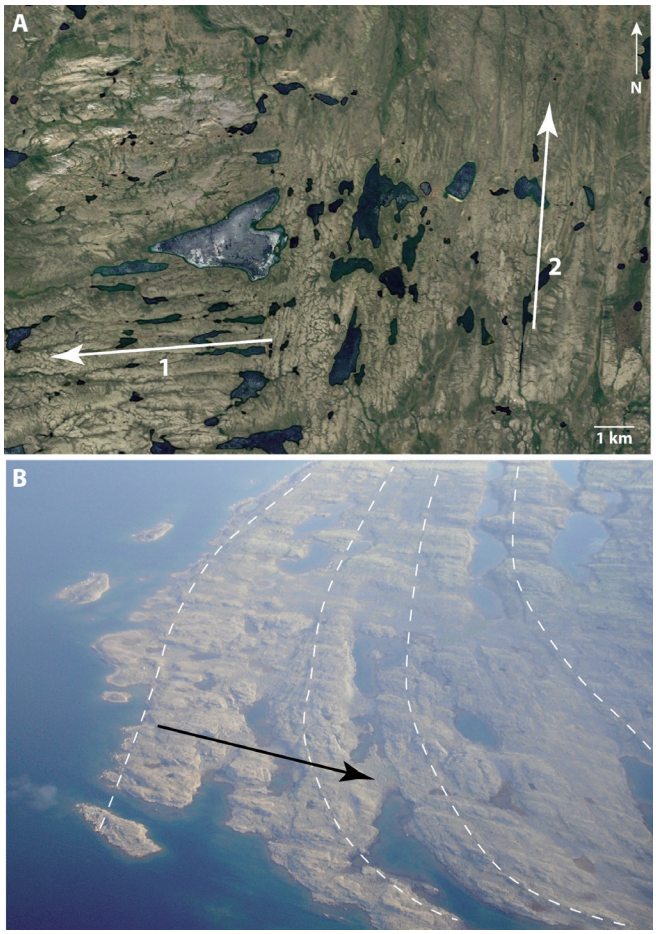


Figure 1. A) Two sets of streamlined subglacial bedforms oriented parallel to former phases of ice flow from the Laurentide Ice Sheet towards the west (1), then north (2), on the northeast margin of Great Bear Lake, Northwest Territories (image source: Landsat 7 with 15 m resolution panchromatic band). **B)** Oblique aerial photograph of thin till over Canadian Shield bedrock, southwest region of Baffin Island. The terrain is dominated by the regional structure of the bedrock geology (white dashed lines) with a light overprinting from the northern Laurentide Ice Sheet (black arrow) with streamlined bedrock and small till ridges.

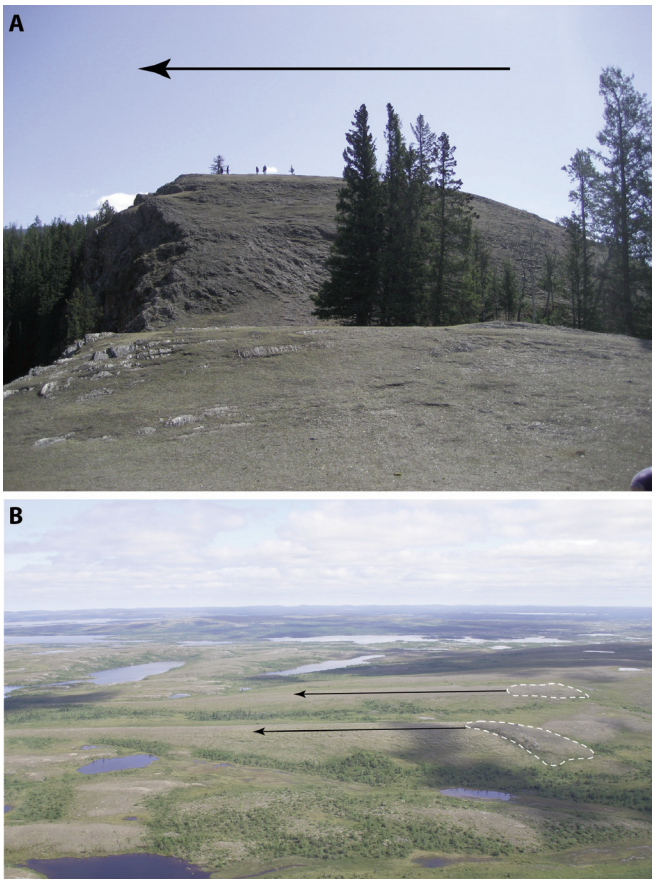


Figure 2. Examples of bedrock-controlled glacial landforms. **A)** A very large glacially sculpted bedrock hill in Jasper National Park (Old Fort Point), called a 'flyggberg'. Ice flow is from right to left (arrow); note the streamlined, up-ice, or stoss side, on the right and the plucked down-ice, or lee, side on the left. There are people on top of the hill for scale. **B)** Outcrop knobs in northeastern Quebec (outlined by white dashed lines) that have long 'tails' of till that have formed in the lee side, or down-ice to form crag-and-tail landforms. Crag-and-tail morphologies are excellent indicators of former trajectories (black arrows) of glacial erosion and depositional processes.

forms and other site-specific glacial features that indicate the former ice-flow directions. This paper, and accompanying presentation, can only provide a broad overview of this topic and the examples presented here represent a minor portion of glacial geomorphology that is summarized in McMartin and Paulen (2009). It is strongly recommended that persons attempting to develop skills in ice-flow reconstruction at any scale using satellite imagery, digital elevation models (DEMs), airphoto interpretation, and/or landform analysis should read additional material such as Mollard's (1996) airphoto atlas, Sauer and Elder's (1982) accompanying guide, and Ryder (1995). In addition, reviews of ice-flow indicators and field methods for ice-flow indicator mapping are provided by Prest (1983), Kujansuu and Saarnisto (1990), Lundqvist (1990), Ryder (1995), and Benn and Evans (1998).

Streamlined landforms are also eroded into local bedrock and are used in the reconstruction of ice-flow directions. Very large bedrock forms, such as flyggbergs (Fig. 2A), usually are rare (Glasser and Warren, 1990), but under the right erosive conditions, large glacially streamlined landforms can develop in hard bedded terrain (i.e. shield cratons), particularly by fast-flowing ice, or ice streams (Krabbendam et al., 2016). Glacially eroded streamlined bedrock hills are commonly termed rock drumlins, and are often enhanced by mantles and streamlined 'tails' of glacial sediments (Lundqvist, 1990; McMartin and Paulen, 2009). These forms typically are asymmetrical with a thinner down-ice tail and thus indicate the direction of ice flow.



Figure 3. Medium- to small-sized glacially-sculpted bedrock landforms with ice-flow directions indicated by arrows. **A)** A stoss-and-lee outcrop above the treeline in northern Labrador. **B)** A stoss-and-lee sculpted outcrop on the Melville Peninsula, Nunavut (rock hammer for scale). **C)** A large stoss-and-lee outcrop that has been cleaned off for landscaping on Sandhamn in the Stockholm archipelago, Sweden (photograph by Jürg Alean, Switzerland). **D)** A house perched on a large glacially sculpted and grooved whaleback bedrock form in Hopedale, Labrador. **E)** A grooved and polished whaleback outcrop on the eastern shore of Georgian Bay, Ontario, which has been cleaned off for landscaping (photograph by Nick Eyles). **F)** A grooved and polished stoss-and-lee landform on the Labrador coastline, near Makkovic (field notebook for scale).

Erosional crag-and-tail landforms produced by the streaming of ice around resistant bedrock obstacles, and subsequent protection of the tail from erosion, are distinct from depositional forms such as large flutings and cavity fills deposited in the lee of basal obstructions, but can still be used to determine regional ice-flow trends (Fig. 2B).

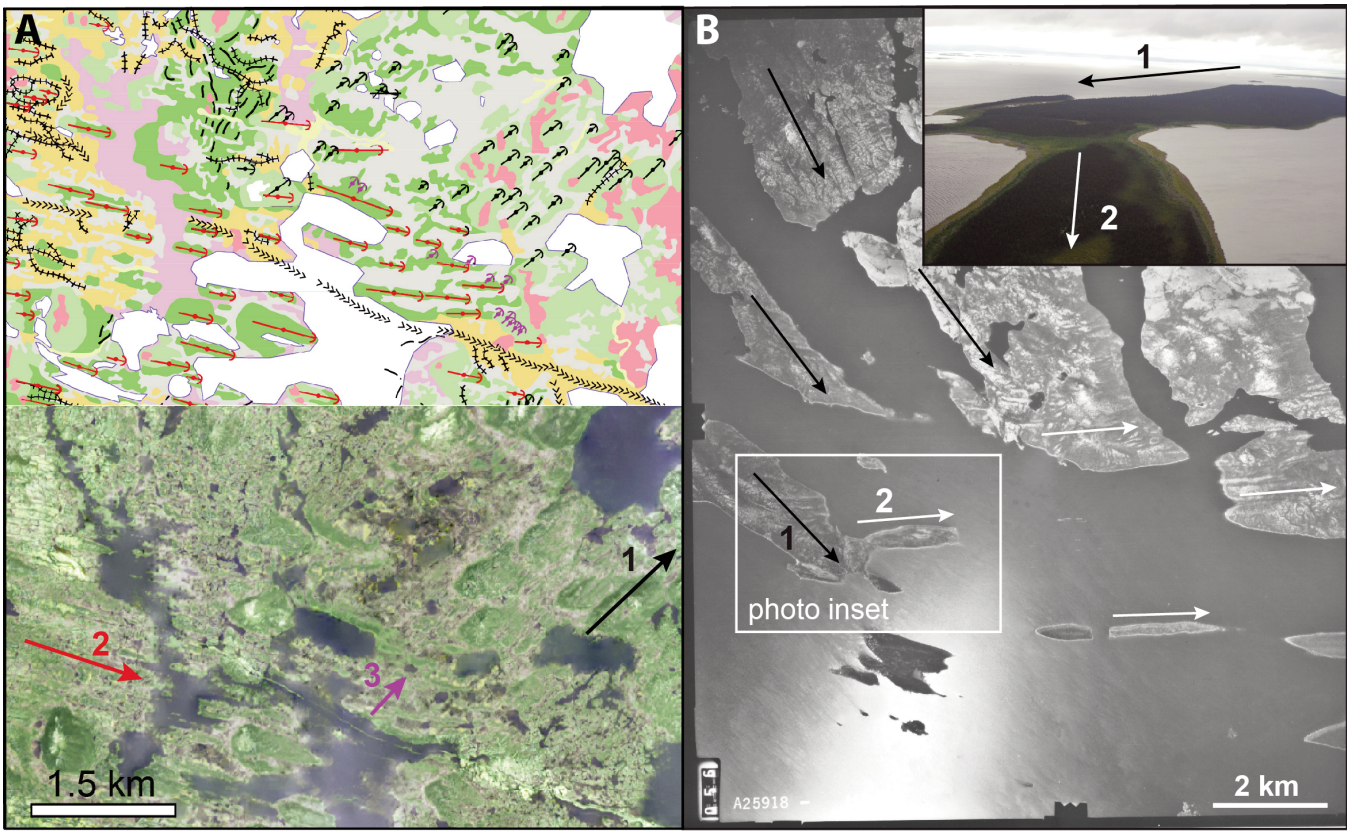
More commonly, relatively medium- to small-sized glacially sculpted bedrock landforms can be observed that can be mapped and measured from airphotos, DEMs, and on the ground. These include roches moutonnées, whalebacks, and bedrock sculpting such as stoss-and-lee forms (Fig. 3). Although these bedrock forms are mostly rounded and shaped by glacial erosion, their mor-



Figure 4. Glacially eroded outcrop morphologies influenced by the bedrock geology with the ice-flow directions indicated by arrows. **A)** Migmatite whereby the biotite-rich melanosome layers have been differentially eroded relative to the quartz-rich leucosome layers (southern shore of the Smallwood Reservoir in Labrador, photo by Beth McClenaghan). **B)** Metasedimentary bedrock with differential erosion between the darker schistose layers and lighter quartzite beds (Belcher Islands, photo by Jean Veillette). **C)** Curvilinear glacial-erosion marks by ice preferentially eroding softer Proterozoic marble relative to the resistant volcanic and granitic bedrock (Cantley, Quebec). **D)** An iron-altered quartzite clast conglomerate, where larger grooves can be seen in the rock matrix, and finer striations on the quartzite clasts (east of Schefferville, Labrador; Canadian two-dollar coin for scale). **E)** Glacial erosion has stripped off the soft regolithic material on this granitic gneiss but preserved the hard corestone, a relic of preglacial chemical weathering. Ice flow at this site is shown by the black solid arrow; note how the glacial ice was deflected around the corestone (dashed black arrow), deviating by almost 90 degrees (coastal Labrador).

phologies can be strongly influenced by the alignments of planes of weakness such as joints, bedding, and foliation or from preglacial weathering (Fig. 4).

In some areas, particularly underneath former ice divides, cross-cutting and superimposed streamlined landforms can be found (e.g. Stea and Brown, 1989; Clark, 1994; McMartin and Henderson, 2004; Rice et al., 2024). These palimpsest streamlined landforms are interpreted to be the result of drastic changes in ice-flow directions, concomitant with adjustments in the overall shape of the ice sheet. Furthermore, the final flow phase indicated by glacial landforms may differ from dominant sediment transport paths (Fig. 5), therefore the evidence from landforms should be filled out



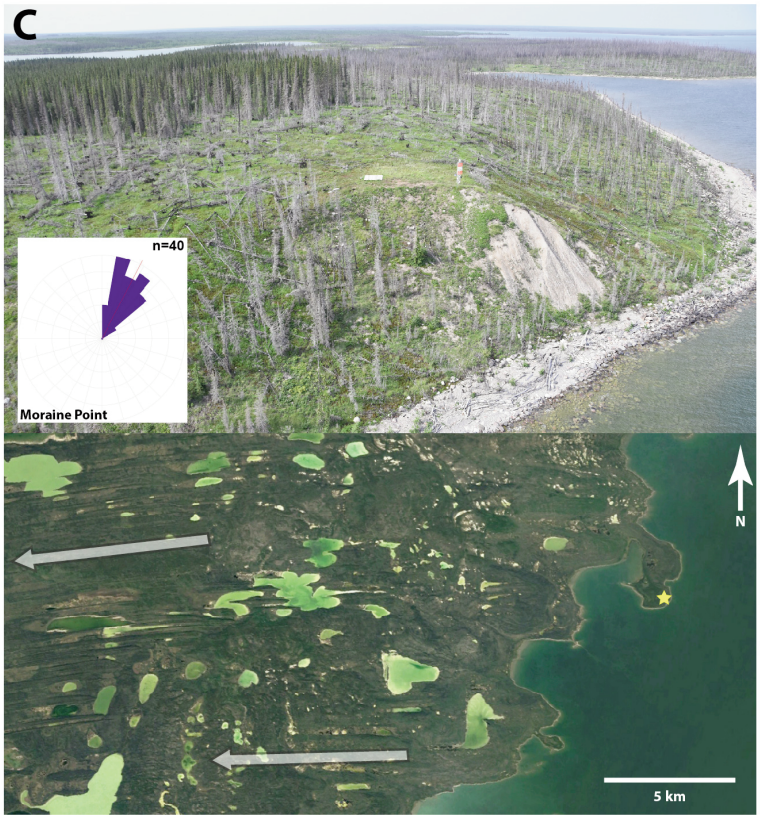


Figure 5. Examples of palimpsest landforms and where there is a discordant trend between the general direction of glacial erosion and transport and the surface landforms, which are often megascale glacial lineations formed by erosion beneath ice streams during deglaciation. **A)** A localized detailed surficial map from southwest of Lac aux Goélands in northeastern Quebec (Paulen et al., 2022; Rice et al., 2024). This region shows the complex evolution of landforms from a strong northeast ice flow (phase 1, black landforms), then a strong east ice flow (phase 2, red landforms), and a weaker deglacial northeast ice flow (phase 3, purple landforms). The few early phase 1 landforms are best preserved in areas of thin to no glacial cover, with major overprinting by phase 2 ice in regions of thicker till deposits that were subsequently modified during a late deglacial ice-flow during phase 3. The change in landscapes is also evident on satellite imagery (Landsat 8 with 15 m resolution panchromatic band). **B)** Examples of cross-cutting landforms on a 1:50 000 scale airphoto from the northwest Smallwood Reservoir, Labrador, where larger and older southeast-trending landforms (1, black arrows) have been reworked by later eastward flow (2, white arrows); note that the inset oblique aerial photo was captured facing west. **C)** An exposure of till at Moraine Point, on the west side of Great Slave Lake, Northwest Territories (yellow star in Landsat image). A clast fabric collected from about 4 m from surface illustrates that the till was accreted from ice flowing to the southwest, subsequently the streamlined landforms at surface to the west strongly reworked the landscape by an westward-flowing ice stream (image source: Landsat 7 with 15 m resolution panchromatic band).

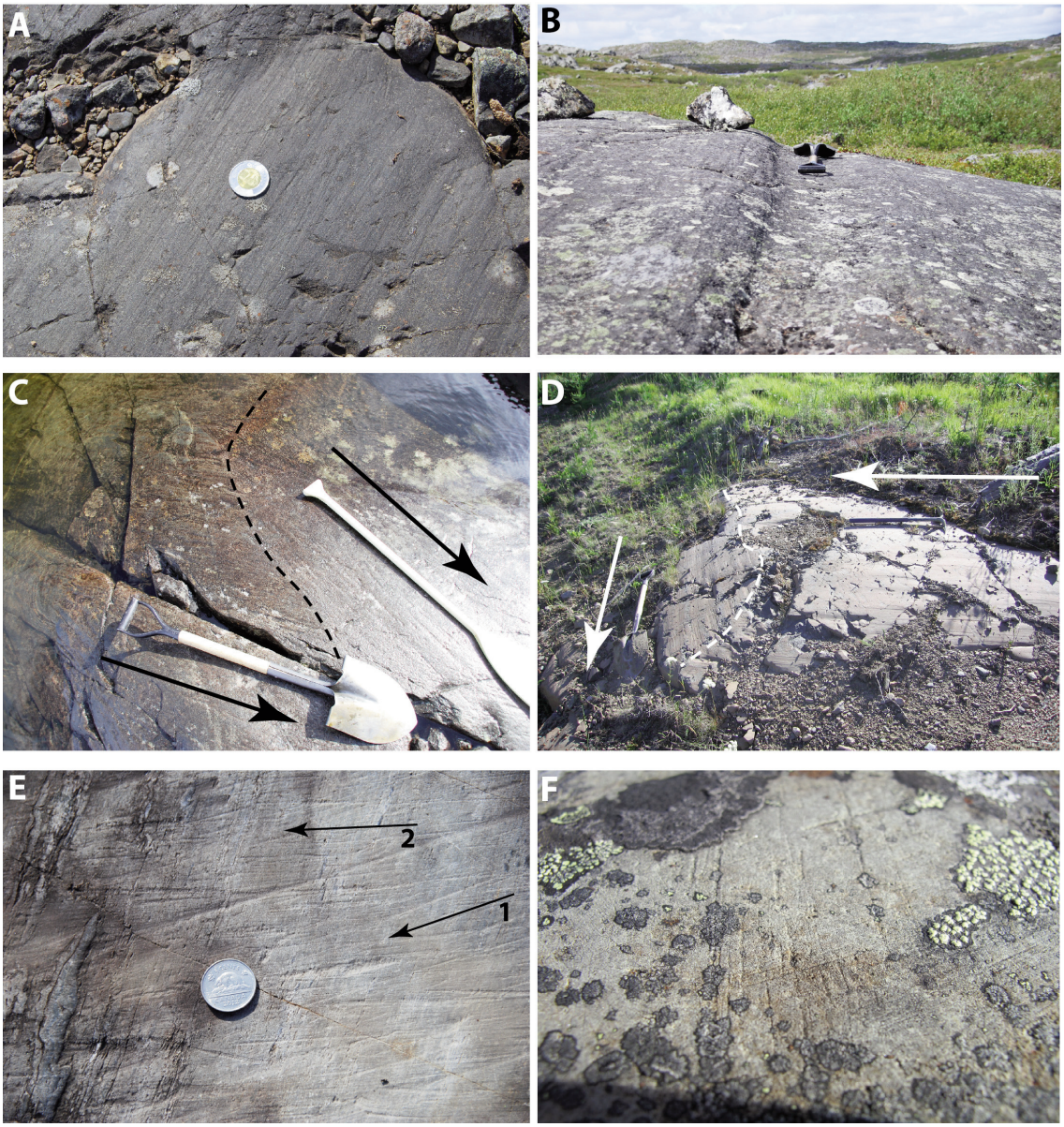


Figure 6. Examples of striated and grooved bedrock. **A)** Striations preserved on a mafic metavolcanic outcrop in eastern Quebec (Canadian two-dollar coin for scale). **B)** A large glacial groove eroded into a granitic gneiss, with shovel inside the groove for scale (eastern Northwest Territories). **C)** An outcrop with faceted surfaces showing an older ice flow (paddle) preserved in the lee side of the younger ice flow (shovel) in eastern Northwest Territories; the dashed line demarks the edge or intersection of the faceted surfaces. **D)** An outcrop with two ice-flow directions at right angles to each other, each preserved on a faceted surface in the central interior of British Columbia (photo by Crystal Huscroft, modified from Plouffe et al., 2009). The older flow (shovel) is preserved in the lee side facet of the younger flow (geo-pick). **E)** On flat surfaces, larger grooves and finer striations help determine the relative ages of the ice-flow phases. The older larger grooves (flow 1) have been overprinted by a younger finer polish (flow 2; Canadian five cent coin for scale). **F)** On flat surfaces with sets of fine cross-cutting striations, it is almost impossible to determine former directions of ice flow and relative ages; this is where other indicators (e.g. outcrop shape and sculpting, behaviour with the nature of the bedrock, e.g., differential erosion around quartz veins or clasts, and associated landforms) are necessary.

with other investigations, such as studies of till provenance, fabric, stratigraphy, and facies, as well as detailed striation mapping (Lundqvist, 1990; McMartin and Paulen, 2009).

EROSIONAL OUTCROP FEATURES

In areas with a thin or moderate till cover, smaller erosional features, indistinguishable on regional imagery, are a reliable means of determining directions and history of ice flow (Rea, 2013). Grooves and striae (striations) are scratches made by rocks embedded in moving ice as they were dragged across bedrock (Fig. 6). Striae are found on smooth glacially polished surfaces; they are quite shallow and may be difficult to see on some lithologies. Striae are best preserved on fine-grained rocks that have not experienced intense post-



Figure 7. A few examples of how to find or reveal striations on bedrock surfaces when they are not freshly exposed in roadcuts, along lakeshores, or rivers. **A)** At a site in western Nunavut, till is carefully scraped away from a glacially eroded bedrock surface. **B)** At the same site as (A) after the outcrop is cleaned, brushed, and moistened, the glacially polished surface is revealed. **C)** Another example of striations preserved along the edge of a sculpted outcrop (Brunton compass for scale). **D)** The use of water on the outcrop surface can help immensely in observing striations and small grooves on this metasedimentary rock (Sharpie marker for scale). **E)** Application of water to this outcrop of glacially smoothed migmatite highlights the striations, making them easier to measure and photograph. **F)** Sometimes, positioning yourself to see the sunlight reflecting off the glacial polish can greatly aid seeing and measuring ice-flow direction (Brunton compass for scale).

glacial weathering. Ultramafic, mafic to intermediate volcanic rocks, limestone, quartzite, and greywacke commonly are the best lithologies to preserve striae. Striae are less common on coarse-textured intrusive rocks, medium- to high-grade metamorphic rocks, and clastic sedimentary rocks, but you can sometimes see fine polishes on quartz veins, which are relatively resistant to post-glacial erosion. Finding striations depends upon a variety of local circumstances, and in places where the bedrock has undergone intense structural jointing and fracturing, the exposed bedrock will not be ideal for the preservation of glacial polish. Additionally, lichen, mosses, and other plant life often obliterate the formerly polished surface of an outcrop. However, striae are easily found where bedrock has been recently exhumed, such as roadcuts and ditches. In more remote regions, some effort is often required to dig around the sculpted edges of an outcrop (Fig. 7).

As with large-scale landforms, the trend of ice flow is easily identified by striae, but determining the direc-

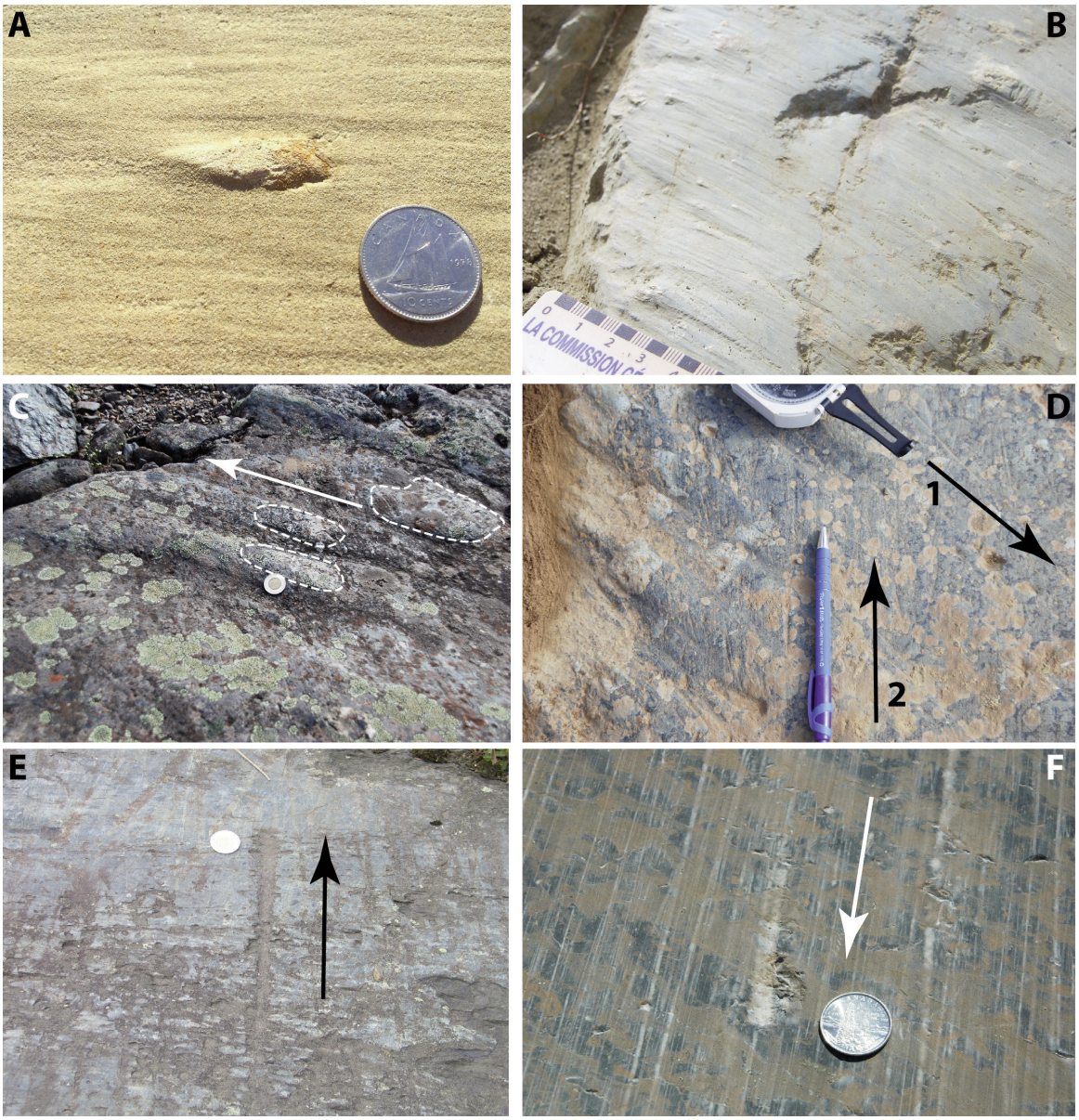


Figure 8. Examples of directional erosional ice-flow indicators with ice-flow direction shown by arrows. **A)** A small rat-tail that has formed in the lee-side of a pebble within a sandstone (ice flow is from right to left; Canadian ten-cent coin for scale). **B)** Very small rat-tails formed from quartz eyes in a metamorphosed rhyolite (ice flow is from left to right). **C)** Large rat-tails formed in migmatite with quartz boudins (outlined by white dashed lines) that were more resistant to glacial abrasion (Canadian two-dollar coin for scale). **D)** Larger rat-tails formed in a metamorphosed volcaniclastic sediment from ice flowing parallel to the Brunton compass (flow phase 1). A later ice-flow phase (2, blue pen) has overprinted finer striations on top of the rat-tails but has not obliterated the forms, which also provides an age relationship. **E)** Large nail-head striations gouged into metasedimentary rock; note how the striation increases in width and depth before it terminates (Canadian two-dollar coin for scale). **F)** Small nail-head striation formed on limestone, which helps determine direction of glacial abrasion on a very flat surface (Canadian twenty-five cent coin for scale).

tion of flow is usually difficult. In some cases, the outcrop surface is sculpted and faceted into a stoss-and-lee form (Fig. 3), which provides a sense of the former ice-flow direction. An excellent directional indicator can be readily determined from striae where differential erosion or abrasion of bedrock that contains hard mineral grains or which is of inhomogeneous nature (e.g. conglomerate, volcaniclastic breccia, quartz veins, etc.) has formed "rat-tails" (i.e. miniature crag-and tail-forms) on an outcrop face. Small knobs of harder rock protrude with tails of softer rock extending down-flow (Fig. 8A–D). Other less reliable features include 'nail-head' striations, which are characterized by individual striations that broaden as the contact point between the rock being transported by the ice and the bedrock surface increases, and end abruptly as the force of friction exceeds the forces of the ice holding the rock at the base of the glacier (Fig. 8E,F).

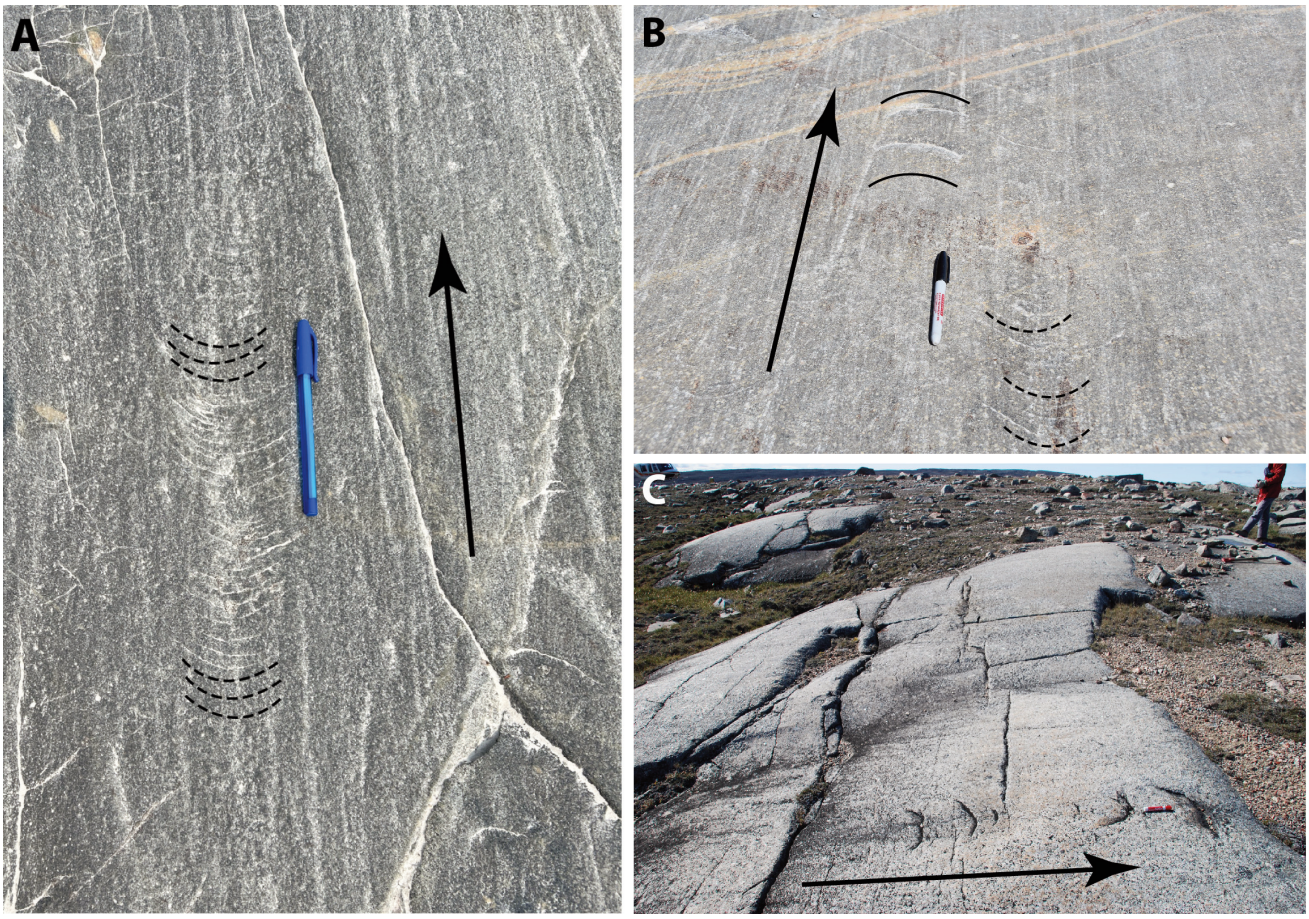


Figure 9. Examples of directional ice-flow indicators, with the ice-flow direction shown by arrows. **A)** Crescentic fractures (some are outlined by dashed black curves) formed into the surface of a silicified mafic xenolith; the apex of the fracture always points up-ice (pen for scale). **B)** A glacially striated and polished gneissic leucogranite with both crescentic fractures (dashed curves) and crescentic gouges (solid curves) (Sharpie marker for scale). **C)** Large crescentic gouges formed on a glacially sculpted tonalite granite. These are formed by glacial quarrying of the rock surface; the apex of the gouge always points down-ice (red whiteboard marker for scale).

Other features related to glacial ice eroding the bedrock include crescentic fractures, which are formed from a hard clast being forced against a bedrock surface that is prone to conchoidal fracturing (e.g. quartzite). The forces being applied to the bedrock surface are from loading (i.e. the weight of the ice sheet) and directional shearing forces from the internal plastic deformation of subglacial sliding of the overriding ice sheet (*see* Ross, 2024), with the fractures propagating into the bedrock surface. These fractures tend to be unidirectional, with the apex of the curved fracture pointing up-ice (Fig. 9A,B). Crescentic gouges are another erosional feature, which tends to occur in coarser grained plutonic and gneissic rocks, and is a form of glacial quarrying (Ross, 2024). The quarrying features tend to have a scalloped nature as material was forced out of the bedrock surface, with the apex of the quarried curve pointing down-ice (Fig. 9B,C). Crescentic gouges may also be influenced by bedrock properties such as fractures, joint sets, and metamorphic fabric and thus are mainly used to support other ice-flow observations.

If directional indicators are so poorly defined that a direction of ice flow cannot be determined with confidence, it may be possible to use known regional ice-flow patterns to infer movement directions at a local area. It is advisable to check the regional interpretations against any local measurements, but be aware that ice flow in areas of rugged topography or former ice-divide regions can deviate more than 90 degrees from the regional flow and, in some cases, flow in opposite directions (Stumpf et al., 2000; Rice et al., 2019). This is because the relative influence of topography on ice-flow is dependent on ice thickness.

DEPOSITIONAL INDICATORS IN TILL

In areas with little or no bedrock exposure, or bedrock with poor preservation potential (e.g. younger Mesozoic of western Canada), deciphering former glacial flow paths is limited to ice-flow indicators such as drift landforms (drumlin ridges and fluted plains), rare stri-



Figure 10. Examples of where boulder pavement in till can be used as an ice-flow indicator. **A)** A horizon of boulders (indicated by arrows) in the wall of a roadside borrow pit. **B)** Ideal boulders will have faceted or planed upper surfaces created by glacial erosion of the lodged boulder. **C)** Striations measured from several boulders should have similar trends and, if so, represent an erosional ice-flow indicator similar to a striated outcrop (Brunton compass for scale).

ated boulder pavements, clast orientation fabrics, and bullet-shaped boulders.

Striated boulder pavements are usually only observed in natural sections such as those exposed along rivers or in man-made exposures such as road-cuts and borrow pits. These can form as polished armoured surfaces from glacial overriding of gravel deposits (Krüger, 1984; Paulen and McClenaghan, 2015) or as an erosional surface within a till sequence where they are typically one clast thick and clasts can either be in contact with each other or separated by enclosing sediment (Clark, 1991; Hicock, 1991). The clasts in these pavements are faceted (planed tops) and striated on their upper surfaces, indicating an erosive ice bed (Fig. 10). Care has to be exercised when interpreting boulder pavements, as clasts could have been faceted by earlier entrainment at the base of an ice sheet and simply reworked into a boulder pavement by successive ice flow (McMartin and Paulen 2009).

Clast orientation analysis (i.e. till fabrics) can be conducted within till deposits. Information about ice-flow direction is preserved in the arrangement of elongated clasts in till deposited under ice sheets. As tills are accreted and deform (i.e. active or deforming bed), prolate clasts (i.e. clasts having an a-axis or length-to-width ratio of 2:1, or greater) within the active layer

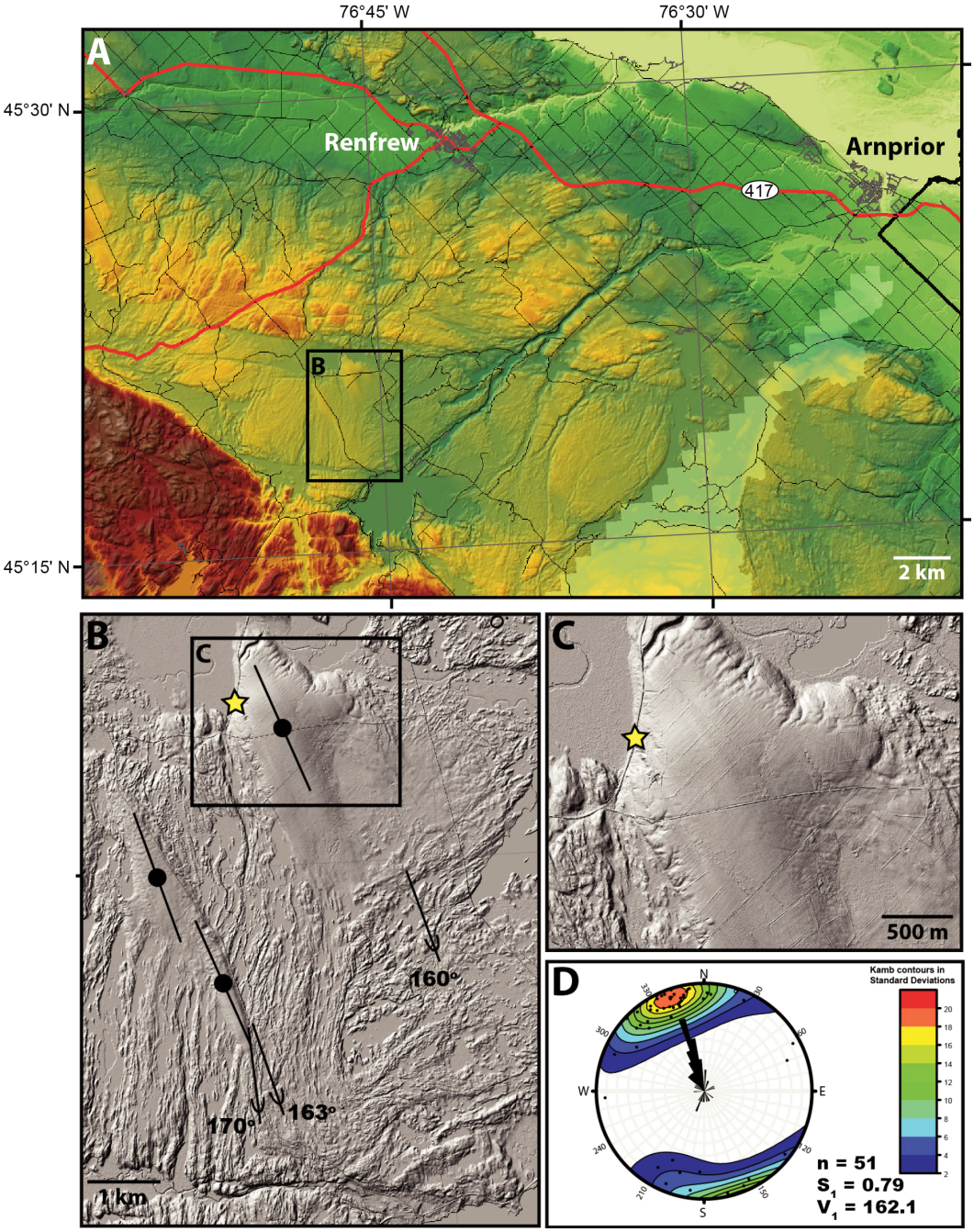


Figure 11. An example of a till fabric site in eastern Ontario with inset maps. **A)** Coloured DEM (Ministry of Natural Resources and Forestry, 2018) and 0.5 m LiDAR hillshade relief maps (Ministry of Natural Resources and Forestry, 2022a,b) of Grenville Province terrain between the Ottawa-Bonnechere Graben to the northeast (Ottawa Valley) and the Madawaska Highlands to the southwest. The white sawtooth mask represents a region with no LiDAR coverage. **B)** A hillshade DEM showing details of streamlined landforms not readily seen on the provincial DEM. The yellow star represents a till fabric site and locations and orientations of selected striae measurements are plotted. **C)** A detailed hillshade image showing the till fabric site (yellow star) in a roadcut exposing till along the up-ice nose of the streamlined glacial landform. **D)** Results of the measured clasts plotted as both a bidirectional rose plot and an equal area stereonet projection, illustrating how the till clasts are parallel to the landform and the regional striation measurements seen in photograph B (rose and stereonet plots created by Stereonet; Allmendinger et al., 2013; Cardozo and Allmendinger, 2013).

tend to rotate into a stable, flow-parallel position as long as the stress direction remains uniform (Larsen and Piotrowski, 2003). Once clasts become aligned, they tend to stay aligned parallel to the shear direction when exposed to high-strain rates, giving a high fabric strength (Hooyer and Iverson, 2000). However, stone-rich tills tend to have lower fabric strength because of more frequent clast collisions (Ildefonse et al., 1992). This is a statistical exercise, and a minimum of 50 clast measurements is required to reduce statistical variance

and to calculate the relative strength (eigenvalues) by using an Equal Area Stereonet (Fig. 11). Careful interpretation of till fabric data is necessary as this is a statistical method, and consequently not every till fabric analysis will yield the true direction of glacial flow, or indeed any direction at all. This means that little weight can be attached to the results of a single till fabric analysis unless it is backed up by observations of other ice-flow indicators.

Conclusions based on till fabric evidence alone require a number of analyses to be made in the same area. A till clast fabric may represent an amalgam of several previous glacial flow directions involving initial transport, differential stresses at or near the glacier sole, deformation, reorientation during deposition, and subsequent modification by deglacial processes. Local variations in subglacial topography, ice temperature and ductility, and debris concentrations produce differing stress fields, ice-flow directions, and fabric alignments (Krüger, 1970; Dreimanis, 1999). Large sculpted clasts, sometimes referred to as 'bullet-shaped boulders' (McMartin and Paulen, 2009) may have a different alignment than smaller ones, as ice and fine debris transported along the glacier's base flow around the boulders and cobbles (cf. Kjær and Krüger, 1998). Modification can be expected during deposition around drumlins, flutings, and crag-and-tail structures as ice flows from high-pressure regimes to low-pressure 'shadows' down-ice of the obstacle.

There are extensive discussions with detailed field methodologies and statistical analysis for till fabrics in McMartin and Paulen (2009), Paulen and McClenaghan (2015), and Benn and Lukas (2021), and references therein. To summarize, tills deposited subglacially (Ross, 2024) are characterized by strong fabrics, with primary eigenvalues (E1) in excess of 0.6, aligned in the direction of glacial transport, and tertiary (E3) eigenvalues of less than 0.15. Modal plunge angles should be low, with pebbles plunging in the direction of the source (McMartin and Paulen, 2009).

SUMMARY

Recognition and identification of ice-flow indicators, regional landform analysis of remotely sensed data sets, small erosional features on bedrock surfaces, and till fabric analysis are essential components for developing an understanding of past glacial trajectories and the relative ages of discrete ice-flow phases (glacial erosion history) that collectively lead to the net glacial sediment transport recorded in dispersal trains. These notes provide a broad overview of ice-flow indicators with a focus on those most commonly used in Canada. Successful drift prospecting relies on incorporating observations of local ice-flow indicators into regional ice-flow interpretations. Local ice flows can have varying effects on the dispersion of ore indicators from regional ice flows. Often, elongated glacial landforms will indicate one dominant flow direction and striae and till fabric indicators reveal a more complicated glacial history. Furthermore, although the dominant direction of ice-flow indicators tends to represent the last flow stage, some bedforms, or the tills into which they are carved/formed/eroded, may have developed during older flow stages, particularly under former ice divides or in areas once covered by sluggish, non-erosive ice.

Consultation of published survey maps and reports or analysis of increasingly high-resolution regional data sets, such as satellite imagery and terrain data, provide a preliminary working model for glacial dispersal in a regional perspective or at a nearby property. However, site-specific work is still necessary to either confirm the existing interpretations of ice-flow directions or to establish local deviations so that one prospects in all the up-ice directions, or exploration vector, of the mineralization indicators.

ACKNOWLEDGEMENTS

This summary of ice-flow indicators is an output of the GSC's Geomapping for Energy and Minerals Program, (GEM-GeoNorth), under the *Geological Evolution and Mineral Potential of the Hopedale Block Sub-activity (2022–2025)* and also with contributions from the GSC's Critical Minerals Geoscience and Data Initiative (CMGD) under the *Ice Stream Paradigm and Search for Critical Minerals in Canada: Exploiting the Power of Automated Geospatial Mapping Techniques Sub-activity (2023–2027)*.

REFERENCES

Allmendinger, R.W., Cardozo, N.C., and Fisher, D., 2013. Structural geology algorithms: vectors and tensors; Cambridge University Press, Cambridge, England. https://doi.org/10.2138/am.2013.607

Benn, D.I. and Evans, D.J.A., 1998. Glaciers and Glaciation; Oxford University Press, New York. https://doi.org/10.4324/9780203785010

Benn D.I. and Lukas, S., 2021. Macrofabric; *in* A Practical Guide to the Study of Glacial Sediments, Second Edition, (ed.) D.J.A. Evans and D.I. Benn; Quaternary Research Association, London, p. 125–154.

Bobrowsky, P.T., Sibbick, S.J., Newell, J.H., and Matesek, P.F. (ed.), 1995. Drift Exploration in the Canadian Cordillera; British Columbia Ministry of Energy, Mines and Petroleum Resources, Paper 1995-2. https://cmscontent.nrs.gov.bc.ca/geoscience/publicationcatalogue/Paper/BCGS_P1995-02.pdf

Cardozo, N.C. and Allmendinger, R.W., 2013. Spherical projections with OSXStereonet; Computers and Geosciences, v. 51, p. 193–205. https://doi.org/10.1016/j.cageo.2012.07.021

Clark, C.D., 1994. Large-scale ice-moulding: a discussion of genesis and glaciological significance; Sedimentary Geology, v. 91, p. 253–268. https://doi.org/10.1016/0037-0738(94)90133-3

Clark, P.U., 1991. Striated clast pavements: products of deforming subglacial sediment? Geology, v. 19, p. 530–533. https://doi.org/10.1130/0091-7613(1991)019<0530:SCPPOD>2.3.CO;2

DiLabio, R.N.W., 1990. Glacial dispersal trains; *in* Glacial Indicator Tracing (1st Edition), (ed.) R. Kujansuu and M. Saarnisto; CRC Press, p. 109–122.

DiLabio, R.N.W. and Coker, W.B. (ed.), 1989. Drift Prospecting; Geological Survey of Canada, Paper 89-20. https://doi.org/10.4095/127357

Dreimanis, A., 1999. Need for three-dimensional analysis of structural elements in glacial deposits for determination of direction of glacier movement; *in* Glacial Processes, Past and Present, (ed.) D.M. Mickelson and J.W. Attig; Geological Society of America, Special Paper 337, p. 59–67. https://doi.org/10.1130/0-8137-2337-X.59

Ferbey, T., Plouffe, A., and Hicken, A.S. (ed.), 2017. Indicator Minerals in Till and Stream Sediments of the Canadian Cordillera;. Geological Association of Canada, Special Paper Volume 50.

Glasser, N.F. and Warren, C.R., 1990. Medium scale landforms of glacial erosion in south Greenland: process and form; Geografiska Annaler, Series A, Physical Geography, v. 72, p. 211–215. https://doi.org/10.2307/521149

Hicock, S.R., 1991. On subglacial stone pavements in till; Journal of Geology, v. 99, p. 607–619. https://doi.org/10.1086/629520

Hirvas, H. and Nenonen, K., 1990. Field methods for glacial indicator tracing; in Glacial Indicator Tracing (1st Edition), (ed.) R. Kujansuu and M. Saarnisto; CRC Press, p. 217–248.

Hooyer, T.S. and Iverson, N.R., 2000. Clast-fabric development in a shearing granular material: implications for subglacial till and fault gouge; Geological Society of America, Bulletin 112, p. 683–692. https://doi.org/10.1130/0016-7606(2000)112<683:CDIASG>2.0.CO;2

Ildefonse, B., Launeau, P., Bouchez, J.L., and Fernandez, A., 1992. Effects on mechanical interactions on the development of preferred orientations: a two-dimensional experimental approach; Journal of Structural Geology, v. 14, p. 73–83. https://doi.org/10.1016/0191-8141(92)90146-N

Kjær, K.H. and Krüger, J., 1998. Does clast size influence fabric strength?; Journal of Sedimentary Petrology, v. 68, p. 746–749. https://doi.org/10.2110/jsr.68.746

Klassen, R.A., 2001. A Quaternary geological perspective on geochemical exploration in glaciated terrain; *in* Drift Exploration in Glaciated Terrain, (ed.) M.B. McClenaghan, P.T. Bobrowsky, G.E.M. Hall, and S.J. Cook; Association of Exploration Geochemistry, Geological Society of London, Canada, Special Publication 185, p. 1–17.

Krabbendam, M., Eyles, N., Putkinen, N., Bradwell, T., and Arbelaez-Moreno, L., 2016. Streamlined hard beds formed by palaeo-ice streams: A review; Sedimentary Geology, v. 338, p. 24–50. https://doi.org/10.1016/j.sedgeo.2015.12.007

Krüger, J., 1970. Till fabric in relation to direction of ice movement, a study from the Fakse Banke, Denmark; Geografisk Tidsskrift, v. 69, p. 133–170.

Krüger, J., 1984. Clasts with stoss-lee form in lodgement tills: a discussion; Journal of Glaciology, v. 30, p. 241–243. https://doi.org/10.3189/S0022143000006006

Kujansuu, R., 1990. Glacial flow indicators in air photographs; *in* Glacial Indicator Tracing (1st Edition), (ed.) R. Kujansuu and M. Saarnisto; CRC Press, p. 71–86.

Kujansuu, R. and Saarnisto, S.M. (ed.), 1990. Glacial Indicator Tracing (1st Edition); CRC Press. https://doi.org/10.1201/9781003079415

Larsen, N.K. and Piotrowski, J.A., 2003. Fabric pattern in a basal till succession and its significance for reconstructing subglacial processes; Journal of Sedimentary Research, v. 73, p. 725–734. https://doi.org/10.2110/jsr.2005.024

Lundqvist, J., 1990. Glacial morphology as an indicator of the direction of glacial transport; in Glacial Indicator Tracing (1st Edition), (ed.) R. Kujansuu and M. Saarnisto; CRC Press, p. 61–70.

McClenaghan, M.B. and Paulen, R.C., 2018. Mineral exploration in glaciated terrain; Chapter 20 *in* Past Glacial Environments (Sediments, Forms and Techniques) A new & revised edition, (ed.) J. Menzies and J.J-M. van der Meer; Elsevier, p. 689–751. https://doi.org/10.1016/B978-0-08-100524-8.00022-1

McClenaghan, M.B., Bobrowsky, P.T., Hall, G.E.M., and Cook, S.J. (ed.), 2001. Drift Exploration in Glaciated Terrain; Geological Society, London, Special Publication No. 185. https://doi.org/10.1144/GSL.SP.2001.185

McMartin, I. and Henderson, P.J., 2004. Evidence from Keewatin (central Nunavut) for paleo-ice divide migration; Géographie physique et Quaternaire, v. 58, p. 163–186. https://doi.org/10.7202/013137ar

McMartin, I. and Paulen, R.C., 2009. Ice-flow indicators and the importance of ice-flow mapping for drift prospecting; *in* Application of Till and Stream Sediment Heavy Mineral and Geochemical Methods to Mineral Exploration in Western and Northern Canada, (ed.) R.C. Paulen and I. McMartin; Geological Association of Canada, Short Course Notes 18, p. 153–166.

Ministry of Natural Resources and Forestry, 2018. Provincial Digital elevation Model, version 3; Ministry of Natural Resources and Forestry, Provincial Mapping Unit, Peterborough, Ontario, available on Ontario GeoHub. https://ws.geoservices.lrc.gov.on.ca/arcgis5/rest/services/Elevation

Ministry of Natural Resources and Forestry, 2022a. Ontario digital terrain model (Lidar-derived) – Eastern Ontario DTM; Ministry of Natural Resources and Forestry, Provincial Mapping Unit, Peterborough, Ontario, available on Ontario GeoHub. https://ws.geoservices.lrc.gov.on.ca/arcgis5/rest/services/Elevation

Ministry of Natural Resources and Forestry, 2022b. Forest Resource Inventory Term 2 Lidar; Ministry of Natural Resources and Forestry, Provincial Mapping Unit, Peterborough, Ontario, available on Ontario GeoHub. https://geohub.lio.gov.on.ca/maps/lio::forest-resources-inventory-leaf-on-lidar/about

Mollard, J.D., 1996. Landforms and surface materials of Canada: a stereoscopic airphoto atlas and glossary, 8th Edition; Printwest, Regina.

Paulen, R.C. and McClenaghan, M.B., 2015. Late Wisconsin ice-flow history in the Buffalo Head Hills kimberlite field, north-central Alberta; Canadian Journal of Earth Sciences, v. 52, p. 1–17. http://dx.doi.org/10.1139/cjes-2014-0109

Paulen, R.C. and McMartin, I. (ed.), 2009. Application of till and stream sediment heavy mineral and geochemical methods to mineral exploration in western and northern Canada; Geological Association of Canada, Short Course Notes 18. https://gac.ca/product/application-of-till-and-stream-sediment-heavy-mineral-and-geochemical-methods/

Paulen, R.C., Rice, J.M., and Ross, M., 2022. Surficial geology, Lac aux Goélands, Quebec, NTS 23 P southeast; Geological Survey of Canada, Canadian Geoscience Map 429, 1:100,000. https://doi.org/10.4095/328291

Plouffe, A., Bednarski, J.M., Huscroft, C.A., and McCuaig, S.J., 2009. Gold grain content of till in the Bonaparte Lake map area, south central British Columbia (NTS 92P); Geological Survey of Canada, Open File 6047. https://doi.org/10.4095/226247

Prest, V.K., 1983. Canada's heritage of glacial features; Geological Survey of Canada, Miscellaneous Report 28. https://doi.org/10.4095/109273

Puranen, R., 1990. Modelling of glacial transport in tills; *in* Glacial Indicator Tracing (1st Edition), (ed.) R. Kujansuu and M. Saarnisto; CRC Press, p. 15–34.

Rea, B.R., 2013. Micro- to macroscale forms; *in* Encyclopedia of Quaternary Science (Second Edition), (ed.) R. Kujansuu and M. Saarnisto; Elsevier, p. 865–876. https://doi.org/10.1016/B978-0-444-53643-3.00076-5

Rice, J.M., Ross, M., Paulen, R.C., Kelley, S.E., Briner, J.P., Neudorf, C.M., and Lian, O.B., 2019. Refining the ice flow chronology and subglacial dynamics across the migrating Labrador Divide of the Laurentide Ice Sheet with age constraints on deglaciation; Journal of Quaternary Science, v. 347, p. 519–535. https://doi.org/10.1002/jqs.3138

Rice, J.M., Paulen, R.C., Campbell, H.E., and Ross M., 2024. The surficial geology record of ice stream catchment dynamics and ice-divide migration in the Quebec-Labrador sector of the Laurentide Ice Sheet; Quaternary Science Advances, v. 13, 100123. https://doi.org/10.1016/j.qsa.2023.100123

Ross, M., 2024. Glacial dynamics and glacial sediment dispersal explained; *in* Till Geochemistry and Indicator Mineral Methods for Exploration in Glaciated Terrains, (ed.) R.C. Paulen and M.B. McClenaghan; Geological Survey of Canada, Open File 9210, p. 4–9. https://doi.org/10.4095/pbmy2d03m0

Ryder, J.M., 1995. Recognition and interpretation of flow direction indicators for former glaciers and meltwater streams; *in* Drift Exploration in the Canadian Cordillera, (ed.) P.T. Bobrowsky, S.J. Sibbick, J.H. Newell, and P.F. Matesek; British Columbia Ministry of Energy, Mines and Petroleum Resources, Paper 1995-2, p. 1–22.

Sauer, E.K. and Elder, L., 1982. Airphoto interpretation for terrain analysis; Extension Division, University of Saskatchewan, Saskatoon.

Smith M.J. and Clark, C.D., 2005. Methods for the visualization of digital elevation models for landform mapping; Earth Surface Processes and Landforms, v. 30, p. 885–900. https://doi.org/10.1002/esp.1210

Stea, R.R. and Brown, Y., 1989. Variation in drumlin orientation, form and stratigraphy relating to successive ice flows in southern and central Nova Scotia; Sedimentary Geology, v. 62, p. 223–240. https://doi.org/10.1016/0037-0738(89)90117-6

Stumpf, A.J., Broster, B.E., and Levson, V.M., 2000. Multi-phase flow of the Late Wisconsinan Cordilleran ice sheet in western Canada; Geological Society of America, Bulletin 112, p. 1850–1863. https://doi.org/10.1130/0016-7606(2000)112<1850:MFOTLW>2.0.CO;2

Dirt detectives: Unravelling buried mineral potential with advanced till sampling techniques

Jessey Rice and M. Beth McClenaghan

Geological Survey of Canada, 601 Booth Street, Ottawa, Ontario K1A 0E8

ABSTRACT

Arguably the most critical step in any drift prospecting program is collecting high-quality samples for laboratory analysis, as interpretation and exploration decisions rely on the quality of these samples. Every till sampling survey for mineral exploration will be unique in terms of its operation and setting, however, the goal will remain the same: detecting and determining the bedrock provenance of the lithological, mineralogical, or geochemical constituents of the till. From even the most basic mineral exploration approach to the use of groundbreaking artificial intelligence, the collection of high-quality till samples is essential for proper data interpretation. This paper reviews survey design, various methods for collecting till samples, the benefits and limitations of the different methods, best practices, and other considerations for carrying out till sampling to improve mineral exploration success.

INTRODUCTION

In glaciated terrains, drift prospecting has increasingly become an integral part of any mineral exploration program, with till being the optimal sample medium (Coker and DiLabio, 1989; Kujansuu and Saarnistro, 1990; McMartin and Campbell, 2009; Paulen, 2009; McClenaghan et al., 2023). Sample collection is one of the most critical aspects of a drift exploration program for data collection. Additionally, till sampling is often one of the most expensive parts of the initial exploration phases, which reinforces the importance of proper till sampling for any successful drift exploration campaign. Developing an effective till sampling survey, correctly collecting till samples using the appropriate techniques and equipment, and practicing proper quality assurance and quality control (QA/QC) procedures are key to maximizing drift exploration success. Overall, till sampling surveys are an effective method for locating buried mineralization in regions that have been glaciated, which includes most of Canada.

This paper reviews the methods used to collect till for both geochemical and indicator mineral surveys that are carried out to detect mineralized bedrock. It provides an overview of methods for till sampling survey design, sample site selection, methods and equipment for till sampling, and quality control considerations during sample collection. Material presented here is summarized from papers by McClenaghan and Paulen (2018), McClenaghan et al. (2023), and Sarala (2015a, b) that discuss till sampling methods, together with the more detailed and descriptive till sampling and analysis protocol manual that has been published by the Geological Survey of Canada (GSC) (McClenaghan et al., 2020). However, the major focus of this chapter is collecting till at surface. Refer to Sacco (2024) for information about collecting till samples at depth.

TILL SURVEY DESIGN

A successful till sampling program is built upon a foundation of planning and creating an appropriate till sampling design. To start, all sources of available information should be collected and evaluated. These sources should include digital topographic maps, digital elevation models such as ArcticDEM (e.g. Porter et al., 2018), light detection and ranging (LiDAR) imagery (e.g. Johnson et al., 2015; Eyles et al., 2022), satellite imagery, surficial geology maps, and previous work contained in geological reports, industry assessment reports, and published literature. Once existing resources have been evaluated, the initial survey design can commence. A number of logistical and geological factors will control the type and amount of till sampling that will be conducted under any exploration program. Logistically, the design of a till sampling survey will consider the purpose of the survey, size of the survey area, budget (both time and financial), land tenure, land use restrictions, accessibility, previous work, and sampling crew. Geological factors that will influence the till sampling survey are the nature and size of the mineralization target, type and distribution of till within the study area, the ice-flow history of the region, environmental factors, and the geomorphology of the study area (see McClenaghan et al., 2023). The type of survey being conducted is broadly categorized by the overall goal of the project. For example, samples may

Recommended citation:

Rice, J. and McClenaghan, M.B., 2024. Dirt detectives: Unravelling buried mineral potential with advanced till sampling techniques; *in* Till Geochemistry and Indicator Mineral Methods for Exploration in Glaciated Terrains, (ed.) R.C. Paulen and M.B. McClenaghan; Geological Survey of Canada, Open File 9210, p. 24–34. https://doi.org/10.4095/pbmy2d03m0

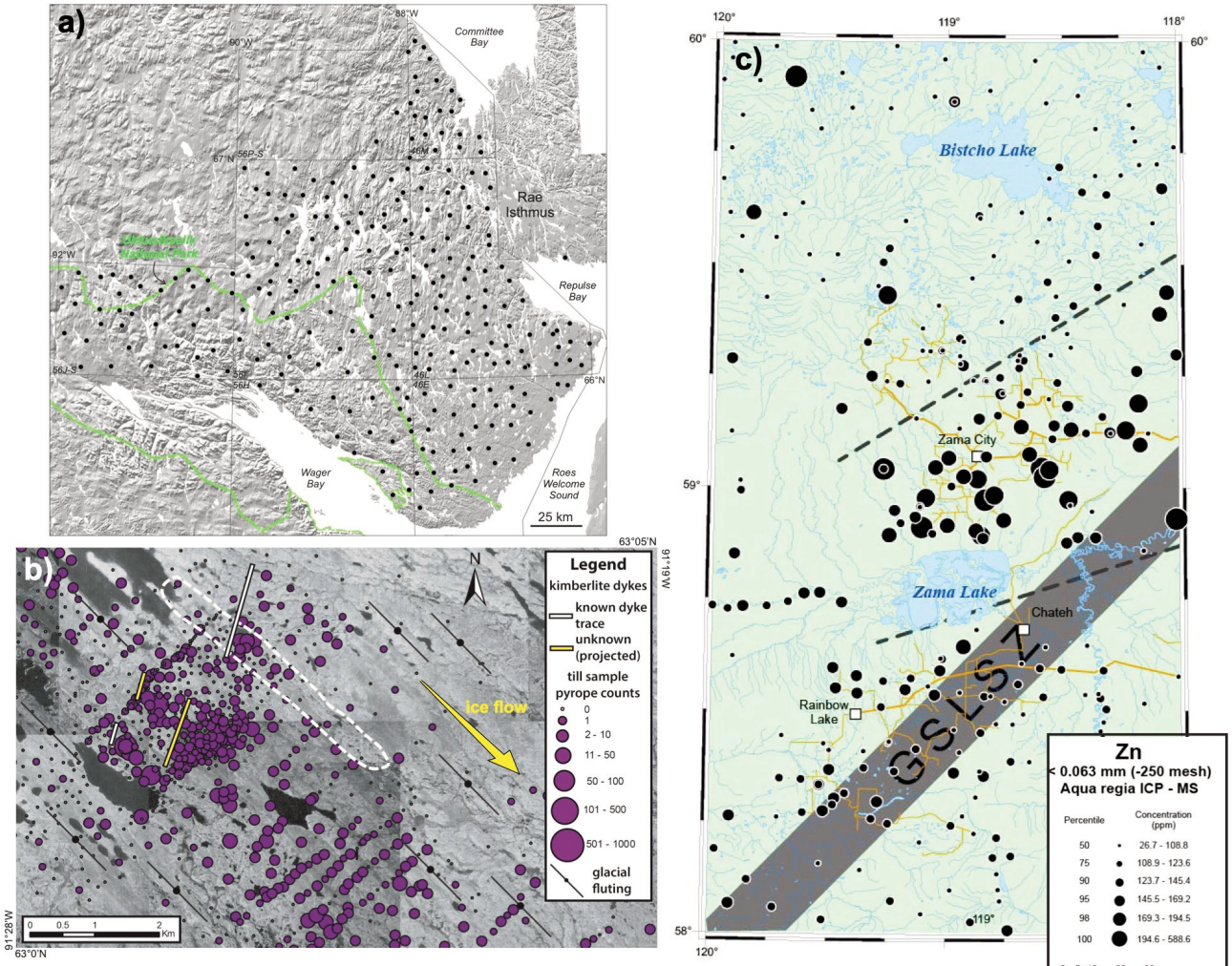


Figure 1. Examples of different sample spacing strategies used to collect surface till samples: **a)** sample sites (black dots) over a regularly spaced grid for a regional-scale survey (modified *from* McMartin et al., 2015); **b)** sample sites (purple dots) collected at regularly spaced intervals along lines perpendicular to the known ice-flow direction (yellow arrow) with subsequent higher density infill sampling focused on corridors of interest (*from* Paulen et al., 2019); **c)** sample sites (black dots) collected along roads and waterways guided by access. The orange lines indicate roads; GSLSZ = Great Slave Lake shear zone (modified *from* Plouffe et al., 2006).

be collected at a reconnaissance scale to evaluate the prospectivity of a geological province, at a regional scale to evaluate a mineral district or belt, and at regional to local scale to discover individual or clusters of deposits (e.g. Salminen, 1992; McMartin and McClenaghan, 2001; McMartin and Campbell, 2009; Sorjonen-Ward et al., 2015). The number of samples that will be collected for any till sampling campaign will likely be dictated by the overall project budget.

When designing the distribution pattern of till sample sites, which is an important step in the planning stages of the survey, three distribution patterns are most commonly used (McClenaghan et al., 2020):

i) grid sampling (Fig. 1a) in which a specific sample density is maintained (e.g. 1 sample /10 km^2). This sampling pattern is often used where ice-flow directions are not known or where multi-phased ice-flow directions are significantly different;

ii) parallel line sampling in which sample spacing along lines is closer than spacing between lines (Fig. 1b). This sample distribution is often used perpendicular to known ice-flow directions, geophysical conductors, or known bedrock structures; and

iii) random sampling (Fig. 1c) where spacing is dictated by access along roads and waterways as well as the local availability of till in areas of extensive bedrock outcrop, discontinuous sediment cover, and/or thick non-till cover sediments.

SAMPLE SITE SELECTION

Once a till sampling survey has been designed, till collection can commence, ensuring that the material sampled is truly till. Indeed, one of the most challenging aspects of till sampling campaigns can be the correct identification and classification of the till collected.

Where possible, till samples should be collected from till veneers overlying bedrock. These are areas where till is <1 m thick and the bedrock structure is generally still visible on aerial photographs or LiDAR images. Where the till is thicker, samples should be collected vertically throughout the till blankets. Till blankets are areas where till is >1 m thick and blankets the underlying bedrock. See Deblonde et al. (2019) for examples and explanations of the terms "till veneer" and "till blanket" as well as other till units that appear on surficial geology maps published by the GSC and the provincial and territorial agencies in Canada.

The general assumption is that the till closest to the bedrock, except within paleo-ice streams, has the highest probability of being derived from the local bedrock (e.g. Bird and Coker, 1987). Aario and Peuraniemi (1992), Proudfoot et al. (1995), and McClenaghan et al. (2020) provide overviews of selected glacial landforms, their characteristics, and the preferred location for till sampling sites on the landforms. Sarala et al. (1998, 2007), Sarala and Rossi (2000), Sarala and Neonen (2005), and Sarala and Ojala (2008) report till sampling considerations and examples specifically for areas covered by drumlins or transverse moraine ridges, also known as Rogen or ribbed moraines. For regional-scale sampling in areas with varying glacial landforms, it is a good practice to document the glacial landforms from which the till samples are collected. This documentation will help to identify any biases that specific landforms could introduce, as well as highlight any multi-phase generation (e.g. Stea and Brown, 1989) or modification (Eyles et al., 2022) of till landforms. Considerations for till sampling in different physiographic settings are summarized below. The reader is referred to McClenaghan et al. (2020) for more detailed explanations for each setting described.

MOUNTAINOUS TERRAINS

Mountainous terrains are those with rugged topography, including steep mountain slopes, peaks, and arêtes separated by highlands, plateaus, and incised valleys (e.g. Hicken et al., 2017). In mountainous terrains, till is often covered by colluvium, or soil and sediments that have been deposited on top of the till through gravitational processes. This material can often resemble till, as it is composed of a spectrum of grain sizes from cobbles and boulders to fine silts and clays. The composition of colluvium depends on the source material and can vary in texture from bedrock rubble to diamicton, and it can have a stratified to massive structure. Where colluvium is derived from till, differentiating between the colluvium and the till can be challenging (Bond, 2001; Levson, 2001; Paulen, 2009; Lian and Hickin, 2017). Colluviated diamicton can be sampled if the downslope movement of the sediment is considered when tracing the source of mineralized debris, however, all dispersal patterns will be distorted in the downslope direction (e.g. Paulen, 2001).

In mountainous areas with active alpine glaciers, the glaciers are routinely affected by avalanches, rockfalls, and other slope processes, which leads to accumulations of debris on top of the glacier (i.e. supraglacial deposition). This supraglacial debris is transported down ice and deposited and is often very stony, with angular clasts and a loose sandy till-like matrix. Once the supraglacial debris is carried downice, it can be subsequently deposited as supraglacial gravity flow deposits. The main difference between a supraglacial deposit and a supraglacial gravity flow deposit is that a gravity flow deposit is composed predominantly of far-travelled debris, although it may be deposited on top of a subglacial till of more local provenance. Ultimately, understanding the genesis of the sediment being collected is paramount.

Additionally, in mountainous terrain, till can be sampled from veneers and blankets at the top and on the sides of valley walls. In some mountainous regions, thick till units may be exposed along road cuts and streams where it can be collected in vertical sections in order to assess compositional variability with depth and to increase the chances of intersecting a dispersal train. The thickest till units are usually found in valleys, which may also contain glacial, glaciofluvial, glaciolacustrine, alluvial, colluvial, and eolian sediments; again, this means proper identification and collection of actual till is critical.

ROLLING TERRAINS

In areas of flat, gently undulating, or rolling topography, till may occur at surface and/or may be deeply buried and may be part of a complicated thick stratigraphy (e.g. Bird and Coker, 1987; Bajc, 1991; Smith, 1992; Thorleifson and Garrett, 2000). Surficial geology maps, 3-D models, LiDAR imagery, and literature reviews are especially important in this terrain and should be examined before designing a till survey in these areas.

In lower lying parts of rolling terrains where surface drainage is poor, glacial sediments may be overlain by organic bog or fen deposits. In these areas, till samples may be collected at low-lying depressions within a bog, at the base of tree wells, near modern streams where the streambed is till or bedrock, or at the base of fens, which are often wet but have thin organic cover. In the winter when the landscape is frozen, till can be collected at depth using deep sampling techniques. No matter where the sample is collected, specific notes should be taken to ensure the context of the sample site is recorded.

AREAS ONCE COVERED BY POST-GLACIAL SEAS OR GLACIAL LAKES

Broad regions of Canada were once covered by marine waters or proglacial lakes, however, as a consequence of glacial-isostatic rebound, ice-margin retreat, and/or outlet incision, these regions are now subaerially exposed. Referring to existing resources and sources of information will assist in determining the areal extent inundated by post-glacial marine or lacustrine incursion. When sampling in these terrains, typically till from topographically higher elevations, at or just below the limit of submergence, will have only been weakly reworked by the postglacial sea or glacial lake, and therefore is suitable for sampling (e.g. Strand et al., 2009; Randour et al., 2016; McMartin et al., 2022). In contrast, till topographically lower than the upper marine/lacustrine limit may be significantly reworked and winnowed by waves and currents, which can form bouldery mantles or beaches of poorly sorted debris (i.e. washed till). In these situations, samples have to be collected from holes dug below the depth of reworking. Raised beaches and spits derived from winnowed till should be avoided because of the significant reworking of the till, loss of fine material, and significant transport distances entailed by longshore currents along the coastlines of former seas or lakes. Where deposits of glaciomarine or glaciolacustrine sediments are thick (e.g. >5 m in the Abitibi Greenstone Belt), sampling till at surface may not be possible, thus trenching or drilling methods will need to be used (McClenaghan et al., 2020; Sacco, 2024).

PERMAFROST AREAS

Permafrost underlies the northern half of Canada, much of Alaska, and most of the exposed land surface in Greenland and northern Russia (Heginbottom et al., 1995; Brown et al., 2002). In these areas, physical weathering is the dominant process in the near-surface environment. Cryoturbation, caused by perennial freeze-thaw processes within the active layer above the permafrost, mixes soil horizons and can be identified by earth hummocks and patterned ground features such as sorted and unsorted nets, circles, polygons, and stripes.

In these regions, frost boils (Fig. 2a) are ubiquitous in till and are the preferred till sampling sites (Shilts, 1973, 1977, 1978; Laurus and Fletcher, 1999; McMartin and McClenaghan, 2001; McMartin and Campbell, 2009). A frost boil is characterized by barren to lichen-covered oval patches that are commonly surrounded by a ridge of vegetation (Fig. 2b). Within a frost boil, material is extruded to the surface as the result of high-water pressure that has built up in the active layer due to the freeze-thaw process during the summer (McMartin and Campbell, 2009). Repeated frost heaving and frost churning further homogenizes the till. Frost boils are thus easy to identify in the field and are efficient places to dig a hole for sampling. The depth of sampling is restricted by the thickness of the active layer, which, during the summer (i.e. the maximum thaw period), can extend up to 2 m in the southern areas of continuous permafrost to <0.5 m in more northerly areas (e.g. Shilts, 1978; Dyke and Zoltai, 1980; Dredge, 2002; French, 2007). Frost boils can also form on silt- or clay-rich glaciomarine or glaciolacustrine sediments. which can be distinguished from till frost boils by the lack of rock fragments on the surface (Fig. 2c) and the presence of marine shells (Figs. 2d).

In areas that experienced sustained cold-based glaciation and there is little till production, the unconsolidated sediments tend to be very thin, or discontinuous, and can include older glacial sediments composed of oxidized rock fragments, secondary clay minerals, and deeply weathered bedrock (regolith and felsenmeer). In these areas, till samples can be collected from rare frost boils (Fig. 2e), cryogenic sediments pushed into the centre of boulder rings (sorted circles), or between boulders in felsenmeer terrain (e.g. Dredge, 2001; Tremblay and Paulen, 2012).

AREAS OF ANTHROPOGENIC DISTURBANCE OR CONTAMINATION

Till can be modified by human (anthropogenic) activities such that its original physical properties (e.g. structure, cohesion, composition, and compaction) have been significantly altered. This type of till should not be sampled for mineral exploration or research purposes for obvious reasons; its composition is not related to local geology and has been modified to unknown extents. Anthropogenic contamination of till can occur at, and downwind of, 1) present- and past-producing mines (DiLabio et al., 1988), mills, smelters, refineries, and tailings ponds; 2) present- and past-producing granular aggregate and rock quarries, or borrow pits; 3) man-made structures (e.g. dams) and signs; 4) transportation corridors (e.g. roads, railways, bridges); 5) electrical or hydrocarbon infrastructure and corridors (e.g. hydroelectric structures, pipelines, drill sites, pumping stations); 6) areas affected by forest harvesting; 7) agricultural areas; and 8) populated regions. Regional till surveys that have been conducted in mining districts that have detected anthropogenic contamination in till samples have been reported by McMartin et al. (1999, 2002), Bajc and Hall (2000), and McClenaghan et al. (2013, *see* their Fig. 8). Till recovered by diamond drilling may also anthropogenic contamination from drill wastewater and fluids, cuttings, mud, grease, or diamonds from drill bits (e.g. McClenaghan et al., 2014).

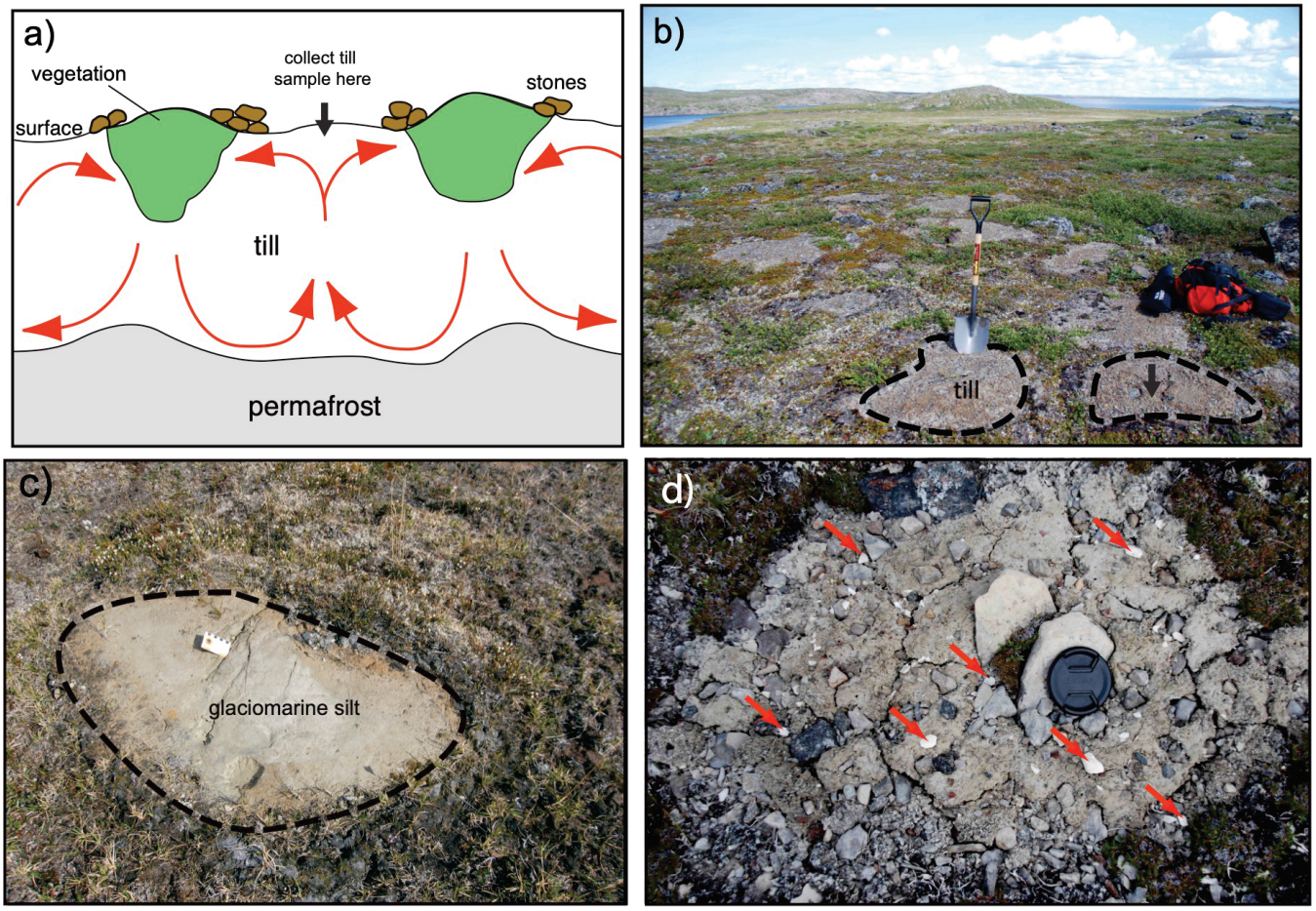


Figure 2. a) Illustration demonstrating frost boil formation, emphasizing the mixing and frost heaving due to cryoturbation and hydrostatic pressure during each summer thaw period (modified from Hornbrook and Allan, 1970). Photographs of **b)** active frost boils (outlined by black dashed lines) on a till plain with fresh material exposed at the surface in the centre for easy till sampling (photo by Roger Paulen, NRCan photo 2023-026); **c)** a frost boil developed in marine silt can be identified by the absence of clasts on the surface — these are not suitable for till sampling (photo by Isabelle McMartin, NRCan photo 2023-027); **d)** white shell fragments (indicated by red arrows) on the surface of a frost boil in marine sediments mixed with till —these are not suitable for till sampling (camera lens cap for scale) (photo by Roger Paulen. NRCan photo 2023-28); and **e)** a rare frost boil in the foreground (outlined by a white dashed line, rock hammer for scale) amongst a field of frost-shattered bedrock fragments that is a suitable sample site in cold-based ice terrain (photo by Roger Paulen, NRCan photo 2023-029).

TILL SAMPLING

Sample size

Matrix geochemistry

The amount of till to collect during a sampling campaign is a function of the type of analysis that will be conducted on the sample and the grain size of the matrix that makes up the bulk of the till sample. The recommended sample mass to collect for till matrix geochemical analysis is 2 kg (Fig. 3a, middle bag, Fig. 3b small bag). If additional physical determinations (grain size, colour, carbon content, etc.) and archiving are also required, at least 3 kg should be collected. If larger samples are collected for heavy mineral separation (described below, samples for geochemical analyses of the matrix should be collected from the same hole). Large, obvious clasts (>2 cm) should not be included when filling the geochemical sample bag. For tills containing abundant clasts or that have a coarse sandy matrix, the mass collected may need to be



Figure 3. a) Three till samples collected from the same site: (left) a large 10–15 kg sample of sandy till for the recovery of heavy minerals; (middle) a 3 kg sample for matrix geochemical analyses, determination of physical properties, and archiving; and (right) a 300 g sample for pXRF analyses (photo by Beth McClenaghan, NRCan photo 2023-030); **b)** a 20–30 kg sample of clay-rich till in a 19 litre (5 plastic gallon) pail and a 3 kg sample (bag) for matrix geochemical analyses (photo by Rod Smith, NRCan photo 2023-031); **c)** a section of highly compact till recovered during a drilling program (photo by Beth McClenaghan).

increased to allow for the recovery of a sufficient volume of the finer grained material (<0.063 mm) needed for analysis. In areas underlain by quartzite or sandstone (e.g. Athabasca and Thelon basins in Canada), till will be extremely sandy and quartz-rich, and till samples for geochemistry will have to be larger than usual in order to recover sufficient fine-grained material for geochemical analysis. For all till types, a separate smaller (~200 g) sample can also be collected if portable XRF measurements are to be used in the field to guide sample collection (Fig. 3a, small bag).

Heavy minerals

How much sample material to collect for heavy mineral separation and identification is largely dependent on the matrix texture of the till (i.e. dominant grain size of the till matrix). In regions where the till matrix is silty to sandy (e.g. Canadian Shield, Appalachians, Cordillera in Canada), a 10 litre (2.5 gallon) pail or large sample bag (10 to 20 kg) of till should be collected (Fig. 3a, pail). In regions where the till is clay-rich (e.g. Western Canada Sedimentary Basin), commonly a full 20 litre (5 gallon) pail or 20 to 40 kg sample in a large bag should be collected (Fig. 3b, pail). As these regions are characterized by clay-rich till, a larger amount of sample material is required to recover sufficient sand-size material for heavy mineral analysis.

Samples for heavy mineral analysis can also be collected using a coarse, stainless steel sieve (i.e. 2.5 cm) to screen out pebble-sized clasts. However, caution should be used as sieves can be a significant source of contamination if not cleaned thoroughly with water between sample sites. Additionally, if the sieves are made of other metals (i.e. brass) or contain solder, these could also be a source of contamination. Pebbles sieved or picked from the till during sampling, or separated during subsequent sample processing in a lab, should be retained for lithological examination, which can aid in provenance determination (e.g. Rice et al., 2024).

Sample depth

Surface sampling

In reconnaissance- and regional-scale surveys, till samples are collected at surface whenever possible. Examples of regional-scale surface till sampling surveys include Klassen and Thompson (1993), Plouffe and Ballantyne (1993), McMartin et al. (1996), Paulen and Lett (2005), Ward et al. (2011), and Rice et al. (2017, 2024).

When collecting surface till samples, soil formation is an important factor that influences sample depth. Oxidation and weathering caused by soil formation destroy labile minerals, such as sulphides and carbonates in the upper horizons (A and B) (Fig. 4a-c) and the soil forming process alters the chemical and mineralogical composition of till (e.g. Shilts, 1975; Hoffman and Woods, 1991; Levson, 2001; Lett and Jackaman, 2002; McMartin and Campbell, 2009). Sampling B-horizon soil, regardless of the substrate, is not recommended for mineral exploration or publicly funded surveys as the nature of the till is significantly affected by the underlying sediments, which may not be till (i.e. could be glaciomarine or glaciolacustrine sediments) and due to soil formation, the "soil" samples may include other glacial or non-glacial sediment types (e.g. regolith, colluvium, glaciofluvial, glaciolacustrine, glaciomarine, alluvial, or eolian sediments, or loess).

The C-horizon (Fig. 4c) is ideal for surface till sampling programs in order to obtain a relatively unaltered geochemical and mineralogical signal of clastic glacial dispersal that is least affected by weathering and hydromorphic dispersion. Often the division between the C-horizon and overlying B-horizon is gradational

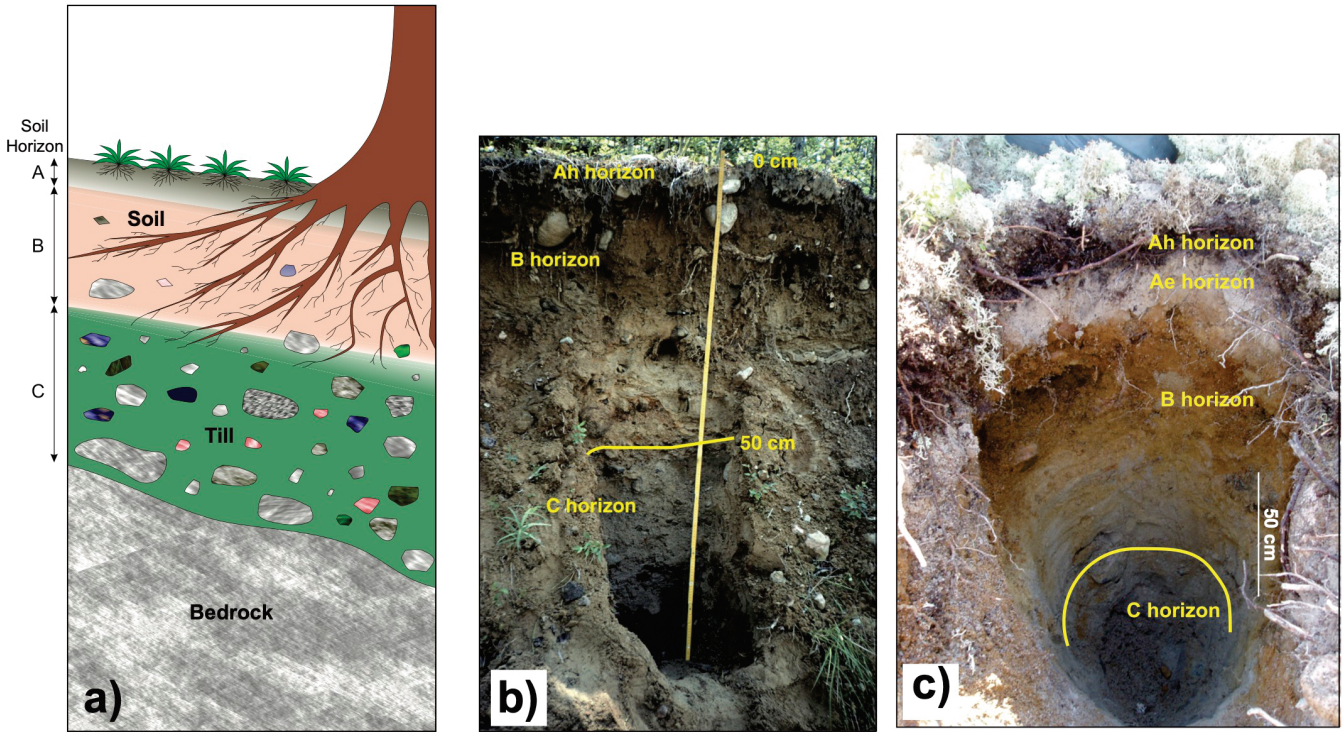


Figure 4. a) A schematic diagram of a soil profile formed on till showing the B- and C- horizons and the underlying bedrock. The C-horizon is the optimal sampling medium (from Hicken and Plouffe, 2017). Photographs of soil horizons developed on till and the ideal sample depths below the B-horizons: **b)** soil developed on sandy-silt till near Flin Flon, central Canada (photo by Penny Henderson, NRCan photo 2023-024); **c)** soil developed on sandy till near Reindeer Lake, central Canada (from McMartin and Campbell (2009), photo by Janet Campbell, NRCan photo 2023-025).

(Fig. 4c), thus it is standard practice to collect till samples from a depth of ≥1 m to ensure that only the C-horizon is being sampled.

Subsurface sampling

Where till is thick (>3 m) and where it is logistically possible, regional till sampling surveys should include samples collected at different depths (0.3–0.5 m intervals) to characterize compositional variations related to till stratigraphy and complex ice-flow patterns. Samples can be collected at depth in natural or human-made sections and open pits, excavator trenches, and overburden drill holes (Fig. 3c; *see* Sacco, 2024).

Multiple till samples should be systematically collected throughout thick till sequences across regions using overburden drilling because dispersal trains may be intersected at any depth and can be detectable in more than one till unit (e.g. Bird and Coker, 1987; Bajc, 1991; Paulen, 2009). Generally, the top part of a till sequence reflects a more distal and diluted source in comparison to sediments lower in the till sequence (e.g. Bond, 2001; Reyes and Clague, 2004). Ultimately, when conducting deep till sampling, having a Quaternary expert as part of the field sampling crew as well as part of the data interpretation team is essential.

Areas with thick drift, where overburden drilling has been used to sample till, include the Abitibi Greenstone Belt (Bird and Coker, 1987; Harron et al., 1987; Sauerbrei et al., 1987; Smith, 1992; McClenaghan, 1994, 2001), northern Manitoba (Brereton et al., 1988), Athabasca Basin (e.g. Geddes, 1982; Campbell, 2007), kimberlite fields in the Northwest Territories (Kelley et al., 2019), the Western Canada Sedimentary Basin (e.g. Thorleifson and Garrett, 2000), the central Interior Plateau of the Canadian Cordillera (Ferbey and Levson, 2009; Averill, 2017), and New Brunswick (Lamothe, 1992).

Field data and notes

Although logistical and geological constraints mentioned above will dictate the methodology and tools used for till collection, the choice of field gear and methods of data collection are also important considerations for any till sampling campaign. Increasingly, field computers, tablets, or smaller hand-held devices are used to capture field data. However, notebooks and handheld GPS devices are also commonly utilized. In addition to using a GPS, the sample location may also be recorded on an air photo, topographic map, or in a field notebook. Drones equipped with high-resolution cameras can assist with the identification of appropriate sample site locations, although a license to operate a drone may be required. Photographs should be taken of each sample site to show the sampling method, asso-

ciated glacial landforms, nearby anthropogenic influences, and local vegetation. A suggested list of the minimum field data to record for till samples collected for heavy mineral and geochemical analyses is included in McClenaghan et al. (2020).

Methods and equipment for collecting till samples

Most scientific and exploration till sampling programs have field-safety guidelines (e.g. Hirvas and Nenonen, 1990) that are dictated by the type of sampling program and by regulatory and legislative requirements (e.g. Alpay and Paulen, 2014; McClenaghan et al., 2020). Field equipment for surface (0–2 m) till sampling may include hand-held shovels, hoe picks, Dutch augers, and small portable drills. Till samples collected at depth may use excavators, and truck- or track-mounted drills. The following references provide overviews of sampling equipment that can be used to collect till samples in thin and thick till settings: Coker and DiLabio (1989), Averill (1990), Hirvas and Nenonen (1990), Coker (1991), Kauranne et al. (1992), Salminen (1992), Plouffe (1995), Levson (2001), McMartin and McClenaghan (2001), McMartin and Campbell (2009), Paulen (2009), Sarala (2005, 2015a), and McClenaghan et al. (2020). The sampling equipment chosen depends on the objectives and type of survey as well as the till sample density and depth, as well as field logistics (e.g. access, land tenure, field crew size, and budget).

It is important to ensure that till sampling equipment is not covered with paint, coatings, or rust that could contaminate the sample (Plouffe et al., 2017). All equipment and gear should be inspected before fieldwork begins to ensure it is in good working condition. The reader is referred to McClenaghan et al. (2020) for a detailed list of recommended sampling equipment and to Sarala (2015a-c) and McClenaghan et al. (2020) for detailed descriptions of till sampling methods.

Quality assurance in the field

QA/QC preparation begins at the planning stages of the sampling survey to ensure an appropriate portion of the budget will be assigned to include field duplicate samples, blank samples, and standards (certified reference material). A significant source of variability in till geochemical or mineralogy data can be due to poorly defined field protocols (e.g. Hoffman and Woods, 1991), therefore, having a strong QA/QC plan in place is essential.

Tools used for sample collection must be thoroughly cleaned between sample sites by rinsing the tools in water. If water is not available, a hard plastic bristle brush and a clean cloth could be used to ensure that no material adheres to the sampling tools between sites. Metal flakes or shavings may break off drill bits, machinery, picks, or shovels and end up contaminating the sample. It is good practice to monitor tools for their wear, to know the metallic composition of sampling tools, and to never wear hand jewellery during sample collection (Kontas, 1991).

Field duplicates should be collected from a second hole or from sediments exposed in a section up to 5 m away from the original sample site to assess homogeneity and variability. Ideally, the amount collected for a geochemical sample should be two times larger (e.g. 4 kg) than the routine sample size (e.g. 2 kg) because it will be split to create a laboratory duplicate (blind) after the entire field duplicate sample has been prepared in the laboratory for geochemical analysis. The field duplicate sample must not be homogenized with the original sample. The original and field duplicate samples should be collected using separate bags that are labelled with unique sample numbers.

For a detailed description of the QA/QC protocols used by the GSC samples, refer to McClenaghan et al. (2020).

CONCLUSIONS

This paper provides an overview of till sampling survey design, sample site selection, methods and equipment for till sampling, and quality control procedures to use during sample collection. This chapter, which focuses on collecting sample material at surface, is summarized from papers by Sarala (2015a) and McClenaghan et al. (2020, 2023), which contain more detailed descriptions of till sampling methods. Refer to Sacco (2024) for information about collecting till samples at depth. There are numerous logistical and geological considerations and constraints in planning a successful till sampling program, but proper preparation sets the foundation for sampling success. The ultimate goal of all till sampling programs is to collect sediment that best reflects the source bedrock of the till to aid in mineral exploration, and as such, till sampling is one of the most important initial steps during the drift prospecting journey.

ACKNOWLEDGMENTS

This summary of till sampling methods and protocols in glaciated terrain was largely derived from an output of the GSC's Geomapping for Energy and Minerals Program (GEM-GeoNorth), under the Geological Evolution and Mineral Potential of the Hopedale Block Subactivity. Roger Paulen is thanked for providing feedback on an earlier version of this summary.

REFERENCES

Aario, R. and Peuraniemi, V., 1992. Glacial dispersal of till constituents in moraine landforms of different types; Geomorphology, v. 6, p. 9–25.

Alpay, S. and Paulen, R.C., 2014. Field Safety: Principles, practice, culture; *in* Geomorphological Fieldwork, Developments in Earth Surface Processes 18, (ed.) M.J. Thornbush, C.D. Allen, and F. Fitzpatrick; Elsevier, p. 65–90.

Averill, S.A., 1990. Drilling and sample process methods for deep till geochemistry surveys: making the right choices; *in* Application de la géologie du Quaternaire à l'exploration minérale, Association Professionnelle des géologues et des géophysiciens du Québec, p. 139–173.

Averill, S.A., 2017. The Blackwater gold-spessartine-pyrolusite dispersal trains, British Columbia, Canada; influence of sampling depth on indicator mineralogy and geochemistry; Geochemistry: Exploration, Environment, Analysis, v. 17, p. 43– 60.

Bajc, A.F., 1991. Till sampling survey, Fort Frances area, results and interpretation; Ontario Geological Survey, Study 56.

Bajc, A.F. and Hall, G.E.M., 2000. Geochemical responses of surficial media, North and East ranges, Sudbury Basin; Ontario Geological Survey, Open File Report 6033.

Bird, D.J. and Coker, W.B., 1987. Quaternary stratigraphy and geochemistry at the Owl Creek gold mine, Timmins, Ontario, Canada; Journal of Geochemical Exploration, v. 28, p. 267–284.

Bond, J.D., 2001. Quaternary geology and till geochemistry of the Anvil district (parts of 105K/2, 3, 5, 6 and 7), central Yukon Territory; Exploration and Geological Services Division, Yukon, Indian and Northern Affairs Canada, Bulletin 11.

Brereton, W.E., Briggs, D.N., and Rollinson, J.P., 1988. Till prospecting in the area of the Farley Lake gold deposit, northwestern Manitoba, Canada; *in* Prospecting in Areas of Glaciated Terrain-1988, (ed.) D.R. MacDonald and K.A. Mills; Canadian Institute of Mining and Metallurgy, p. 225–239.

Brown, J., Ferrians, O., Heginbottom, J.A., and Melnikov, E., 2002. Circum-Arctic map of permafrost and ground-ice conditions, Version 2 [Data Set]; Boulder, Colorado USA, National Snow and Ice Data Center. https://doi.org/10.7265/skbg-kf16

Campbell, J.E., 2007. Quaternary geology of the eastern Athabasca Basin, Saskatchewan; *in* EXTECH IV: Geology and Uranium EXploration TECHnology of the Proterozoic Athabasca Basin, Saskatchewan and Alberta, (ed.) C.W. Jefferson and G. Delaney; Geological Survey of Canada, Bulletin 588, p. 211–228.

Coker, W.B., 1991. Overburden geochemistry in mineral exploration; *in* Exploration Geochemistry Workshop, (ed.) J.M. Franklin, J.M. Duke, W.W. Shilts, W.B. Coker, P.W.B. Friske, Y.T. Maurice, S.B. Ballantyne, C.E. Dunn, G.E.M. Hall, and R.G. Garrett; Geological Survey of Canada, Open File 2390, p. 3-1 to 3-60.

Coker, W.B. and DiLabio, R.N.W., 1989. Geochemical exploration in glaciated terrain: geochemical responses; *in* Proceedings of Exploration '87 (ed.) G.D. Garland; Ontario Ministry of Northern Development and Mines, Special Volume 3, p. 336–383.

Deblonde, C., Cocking, R.B., Kerr, D.E., Campbell, J.E., Eagles, S., Everett, D., Huntley, D.H., Inglis, E., Parent, M., Plouffe, A., Robertson, L., Smith, I.R., and Weatherston, A., 2019. Surficial data model: the science language of the integrated Geological Survey of Canada data model for surficial geology maps; Geological Survey of Canada, Open File 8236.

DiLabio, R.N.W., Newsome, J.W., McIvor, D.F., and Lowenstein, P.L., 1988. The spherical form of gold: man-made or secondary; Economic Geology, v. 83, p. 153–162.

Dredge, L.A., 2001. Late Pleistocene and Holocene glaciation and deglaciation of Melville Peninsula, northern Laurentide ice sheet; Géographie physique et Quaternaire, v. 55, p. 159–170.

Dredge, L.A., 2002. Quaternary geology of southern Melville Peninsula, Nunavut; Geological Survey of Canada, Bulletin 561.

Dyke, A.S. and Zoltai, S.C., 1980. Radiocarbon dated mudboils, central Canadian Arctic; Geological Survey of Canada, Scientific and Technical Notes, Current Research, Part B, Paper 80-1B, p. 271–275.

Eyles, N., Bukhari, S., Sookhan, S., Ruscica, P., and Paulen, R., 2022. LiDAR-based semi-automated mapping of drumlins and mega-scale glacial lineations of the Green Bay Lobe, Wisconsin, USA: Ice sheet beds as glaciotribological systems; Earth Surface Processes and Landforms. http://doi.org/10.1002/esp.5486

Ferbey, T. and Levson, V.M., 2009. The influence of ice-flow reversals on the vertical and horizontal distribution of trace element values in tills, Huckleberry Mine area, west-central British Columbia; *in* Application of Till and Stream Sediment Heavy Mineral and Geochemical Methods to Mineral Exploration in Western and Northern Canada, (ed.) R.C. Paulen and I. McMartin; Geological Association of Canada, Short Course Notes 18, p. 177–183.

French, H.M., 2007. The Periglacial Environment; John Wiley and Sons, West Sussex, England.

Geddes, R.S., 1982. The Vixen Lake indicator train, northern Saskatchewan; *in* Prospecting in Areas of Glaciated Terrain, (ed.) P.H. Davenport; Canadian Institute Mining Metallurgy, p. 264–283.

Harron, G.A., Middleton, R.S., Durham, R.B., and Philipp, A., 1987. Geochemical and geophysical gold exploration in the Timmins area, Ontario; a case history; Canadian Institute of Mining and Metallurgy, Bulletin, v. 80, p. 52–57.

Heginbottom, J.A., Dubrreuil, M.A. and Haker, P.T., 1995. Canada, permafrost; The National Atlas of Canada, Natural Resources Canada, MCR Series No. 4177. https://doi.org/10.4095/294672

Hicken, A.S., Ward, B.C., Plouffe, A., and Nelson, J., 2017. Introduction to the geology, physiography and glacial history of the Canadian Cordillera; *in* Indicator Minerals in Till and Stream Sediments of the Canadian Cordillera, (ed.) T. Ferbey, A. Plouffe, and A.S. Hicken; Geological Association of Canada, Special Paper Volume 50, p. 27–51.

Hirvas, H. and Nenonen, K., 1990. Field methods for glacial indicator tracing; *in* Glacial Indicator Tracing, (ed.) R. Kujansuu and M. Saarnisto; A.A. Balkema, Rotterdam, p. 217–248.

Hoffman, S.J. and Woods, G.A., 1991. Multidisciplinary exploration of the BOG volcanogenic massive-sulphide prospect, Bathurst, New Brunswick, Canada; Journal of Geochemical Exploration, v. 41, p. 85–101.

Hornbrook, E.H.W. and Allan, R.J., 1970. Geochemical exploration feasibility study within the zone of continuous permafrost, Coppermine River Region, Northwest Territories; Geological Survey of Canada, Paper 70-36.

Johnson, M.D., Fredin, O., Ojala, A.E.K., and Peterson, G., 2015. Unraveling Scandinavian geomorphology: the LiDAR revolution; Journal of the Geological Society of Sweden, v. 137, p. 245–251.

Kauranne, K., Salminen, R., and Eriksson, K., 1992. Regolith exploration geochemistry in arctic and temperate terrains; Handbook of Exploration Geochemistry, Elsevier, Amsterdam, Volume 5.

Kelley, S.E., Ross, M., Elliott, B., and Normandeau, P.X., 2019. Effect of shifting ice flow and basal topography in shaping three-dimensional dispersal patterns, Lac de Gras region, Northwest Territories, Canada; Journal of Geochemical

Exploration, v. 199, p. 105–127. https://doi.org/10.1016/j.gexplo.2019.01.012

Klassen, R.A. and Thompson, F.J., 1993. Glacial history, drift composition, and mineral exploration, central Labrador; Geological Survey of Canada, Bulletin 435.

Kontas, E., 1991. Gold contamination of the fine fraction of till during sampling and sample preparation; Journal of Geochemical Exploration, v. 39, p. 289–284.

Kujansuu, R. and Saarnisto, M. (ed.), 1990. Glacial indicator tracing; A.A. Balkema, Rotterdam.

Lamothe, M., 1992. Pleistocene stratigraphy and till geochemistry of the Miramichi Zone, New Brunswick; Geological Survey of Canada, Bulletin 433.

Laurus, K.A. and Fletcher, W.K., 1999. Gold distribution in glacial sediments and soils at Boston Property, Nunavut, Canada; Journal of Geochemical Exploration, v. 67, p. 271–285.

Lett, R.E. and Jackaman, W., 2002. Geochemical exploration models, Volume 1. VMS deposits in south-central British Columbia (NTS 82L/13, L/14, 82M/4. M/5, M/6 and 92P/1E); British Columbia Ministry of Energy, Mines and Petroleum Resources, Open File 2000-31.

Levson, V.M., 2001. Regional till geochemical surveys in the Canadian Cordillera: sample media, methods and anomaly evaluation; *in* Drift Exploration in Glaciated Terrain, (ed.) M.B. McClenaghan, P.T. Bobrowsky, G.E.M. Hall, and S. Cook; Geological Society of London, Special Publication 185, p. 45–68.

Lian, O.B. and Hicken, A.S., 2017. Origin and character of till and other diamicton and their applicability to mineral prospecting; *in* Indicator Minerals in Till and Stream Sediments of the Canadian Cordillera, (ed.) T. Ferbey, A. Plouffe, and A.S. Hicken; Geological Association of Canada, Special Paper 50, p. 109–127.

McClenaghan, M.B., 1994. Till geochemistry in areas of thick drift and its application to gold exploration, Matheson area, northeastern Ontario; Exploration and Mining Geology, v. 3, p. 17–30.

McClenaghan, M.B., 2001. Regional and local-scale gold grain till geochemical signatures of lode Au deposits in the western Abitibi Greenstone Belt, central Canada; *in* Drift Exploration in Glaciated Terrain, (ed.) M.B. McClenaghan, P.T. Bobrowsky, G.E.M. Hall, and S. Cook; Geological Society of London, Special Publication 185, p. 201–223.

McClenaghan, M.B. and Paulen, R.C., 2018. Mineral Exploration in Glaciated Terrain; Chapter 20 *in* Past Glacial Environments (Sediments, Forms and Techniques) A new & revised edition, (ed.) J. Menzies, and J.J-M. van der Meer; Elsevier, p. 689–751.

McClenaghan, M.B., Kjarsgaard, I.M., Averill, S.A., Layton-Matthews, D., Crabtree, D., Matile, G., McMartin, I., and Pyne, M., 2013. Indicator mineral signatures of magmatic Ni-Cu deposits, Thompson Nickel Belt, Manitoba: Part 2 – till data; Geological Survey of Canada, Open File 7200.

McClenaghan, M.B. Parkhill, M.A., Seaman, A.A., Pronk, A.G., Averill, S.A., Rice, J.M., and Pyne, M., 2014. Indicator mineral signatures of the Sisson W-Mo deposit, New Brunswick, Part 2 till; Geological Survey of Canada, Open File 7467.

McClenaghan, M.B., Spirito, W.A., Plouffe, A., McMartin, I., Campbell, J.E., Paulen, R.C., Garrett, R.G., Hall, G.E.M., Pelchat, P., and Gauthier, M.S., 2020. Geological Survey of Canada till-sampling and analytical protocols: from field to archive, 2020 update; Geological Survey of Canada, Open File 8591. https://doi.org/10.4095/326162

McClenaghan, M.B., Paulen, R.C., Smith, I.R., Rice, J.M., Plouffe, A. McMartin, M., Campbell, J.E., Lehtonen, M., Parsasadr, M., and Beckett-Brown, C.E., 2023. Review of till geochemistry and indicator mineral methods for mineral exploration in glaciated terrain; Geochemistry: Exploration, Environment, Analysis, v. 23. https://doi.org/10.1144/geochem2023-013

McMartin, I. and Campbell J.E., 2009. Near-surface till sampling protocols in shield terrain, with examples from western and northern Canada; *in* Application of Till and Stream Sediment Heavy Mineral and Geochemical Methods to Mineral Exploration in Western and Northern Canada, (ed.) R.C. Paulen and I. McMartin; Geological Association of Canada, Short Course Notes 18, p. 75–95.

McMartin, I. and McClenaghan, M.B., 2001. Till geochemistry and sampling techniques in glaciated shield terrain: a review; *in* Drift Exploration in Glaciated Terrain, (ed.) M.B. McClenaghan, P.T. Bobrowsky, G.E.M. Hall, and S.J. Cook; Geological Society of London, Special Publication 185, p. 19–43.

McMartin, I., Henderson, P.J., Nielsen, E., and Campbell, J.E., 1996. Surficial geology, till and humus composition across the Shield margin, north-central Manitoba Saskatchewan: geospatial analysis of a glaciated environment; Geological Survey of Canada, Open File 3277.

McMartin, I., Henderson, P.J., and Nielsen, E., 1999. Impact of a base metal smelter on the geochemistry of soils of the Flin Flon region, Manitoba and Saskatchewan; Canadian Journal of Earth Sciences, v. 36, p. 141–160.

McMartin, I., Henderson, P.J., Plouffe, A., and Knight, R.D., 2002. Comparison of Cu-Hg-Ni-Pb concentrations in soils adjacent to anthropogenic point sources: examples from four Canadian sites; Geochemistry: Exploration, Environment, Analysis, v. 2, p. 57–73.

McMartin, I., Campbell, J.E., Dredge, L.A., LeCheminant, A.N., McCurdy, M.W. and Scromeda, N., 2015. Quaternary geology and till composition north of Wager Bay, Nunavut: results from the GEM Wager Bay Surficial Geology Project; Geological Survey of Canada, Open File 7748.

McMartin, I., Gauthier, M.S., and Page, A.V., 2022. Updated postglacial marine limits along western Hudson Bay, central mainland Nunavut and northern Manitoba; Geological Survey of Canada, Open File 8921.

Paulen, R.C., 2001. Glacial transport and secondary hydromorphic metal mobilization: examples from the southern interior of British Columbia, Canada; *in* Drift Exploration in Glaciated Terrain, (ed.) M.B. McClenaghan, P.T. Bobrowsky, G.E.M. Hall, and S.J. Cook; Geological Society of London, Special Publication 185, p. 323–337.

Paulen, R.C., 2009. Sampling techniques in the Western Canada Sedimentary Basin and the Cordillera; *in* Application of Till and Stream Sediment Heavy Mineral and Geochemical Methods to Mineral Exploration in Western and Northern Canada, (ed.) R.C. Paulen and I. McMartin; Geological Association of Canada, Short Course Notes 18, p. 49–74.

Paulen, R.C. and Lett, R.E., 2005. Till geochemistry: a viable tool for polymetallic mineral exploration in British Columbia's southern interior; British Columbia Geological Survey, GEOFILE 2005-18.

Paulen, R.C., Stokes, C., and McClenaghan, M.B., 2019. Mineral dispersal trains as products of hard-bedded ice streams in northern Canada; 20th Congress of the International Union for Quaternary Research (INQUA), Abstract P-4840.

Plouffe, A., 1995. Drift-prospecting sampling methods; *in* Drift Exploration in the Canadian Cordillera, British Columbia, (ed.) P.T. Bobrowsky, S.J. Sibbick, J.M. Newell, and P.F. Matysek; British Columbia Ministry of Energy, Mines and Petroleum Resources, Paper 1995-2, p. 43–52.

Plouffe, A. and Ballantyne, S.B., 1993. Regional till geochemistry, Manson River and Fort Fraser area, British Columbia [93K, 93N], silt plus clay and clay size fractions; Geological Survey of Canada, Open File 2593.

Plouffe, A., Paulen, R.C., and Smith, I.R., 2006. Indicator mineral content and geochemistry of glacial sediments from northwest Alberta (NTS 84L, M): new opportunities for mineral exploration; Geological Survey of Canada, Open File 5121, Alberta Energy and Utilities Board, Special Report 77.

Plouffe, A., McClenaghan, M.B., Paulen, R.C., McMartin, I., Campbell, J.E., and Spirito, W., 2017. QA/QC measures applied to indicator mineral studies at the GSC; *in* New Frontiers for Exploration in Glaciated Terrain; Geological Survey of Canada, Open File 7374 (revised). https://doi.org/0.4095/300282

Porter, C., Morin, P., Howat, I., Noh, M.-J, Bates, B., et al., 2018. ArcticDEM, version 3; Harvard Dataverse, V1. https://doi.org/10.7910/DVN/OHHUKH

Proudfoot, D.N., Bobrowsky, P.T., and Meldrum, D.G., 1995. Drift exploration potential maps derived from terrain geology maps; *in* Drift Exploration in the Canadian Cordillera, (ed.) P.T. Bobrowsky, S.J. Sibbick, J.M. Newell, and P.F. Matysek; British Columbia Ministry of Energy, Mines and Petroleum Resources, Paper 1995-2, p. 43–52.

Randour, I., McMartin, I., and Roy, M., 2016. Study of the post-glacial marine limit between Wager Bay and Chesterfield Inlet, western Hudson Bay, Nunavut; *in* Summary of Activities 2016; Canada-Nunavut Geoscience Office, p. 51–60.

Reyes, A.V. and Clague, J.J., 2004. Stratigraphic evidence for multiple Holocene advances of Lillooet Glacier, southern Coast Mountains, British Columbia; Canadian Journal of Earth Sciences, v. 41, p. 903–918.

Rice, J.M., McClenaghan, M.B., Paulen, R.C., Pyne, M.D., and Ross, M., 2017. Till geochemical data for the southern Core Zone, Quebec and Newfoundland and Labrador (NTS 23-P and 23-I): samples collected in 2015 and 2016; Geological Survey of Canada, Open File 8219.

Rice, J.M., Ross, M., Campbell, H.E., Paulen, R.C., and McClenaghan, M.B., 2024. Net evolution of subglacial sediment transport in the Quebec-Labrador sector of the Laurentide Ice Sheet; Canadian Journal of Earth Sciences. https://doi.org/10.1139/cjes-2023-0050

Sacco, D., 2024. Strategic applications of shallow overburden drilling for drift prospecting; *in* Till Geochemistry and Indicator Mineral Methods for Exploration in Glaciated Terrains, (ed.) R.C. Paulen and M.B. McClenaghan; Geological Survey of Canada, Open File 9210, p. 35–40. https://doi.org/10.4095/pbmy2d03m0

Salminen, R., 1992. Scale of geochemical surveys; Chapter 7 *in* Regolith Exploration Geochemistry in Arctic and Temperate Terrains, (ed.) K. Kauranne, R. Salminen, and K. Eriksson; Handbook of Exploration Geochemistry, Volume 5; Elsevier, Amsterdam, p. 165–183.

Sarala, P., 2005. Till geochemistry in the ribbed moraine area of Peräpohjola, Finland; Applied Geochemistry, v. 20, p. 1714–1736.

Sarala, P. 2015a. Surficial geochemical exploration methods; Chapter 10.1 *in* Mineral Deposits of Finland, (ed.) W.D. Maier, R. Lahtinen, and H. O'Brien; Elsevier, Amsterdam, p. 711–731.

Sarala, P., 2015b. New Technologies for greenfield exploration; Geological Survey of Finland, Paper 57.

Sarala, P., 2015c. Comparison of different techniques for basal till sampling in mineral exploration; *in* New Technologies for Greenfield Exploration, (ed.) P. Sarala; Geological Survey of Finland, Paper 57, p. 11–22.

Sarala, P. and Ojala, J.V., 2008. Implications of complex glacial deposits for till geochemical exploration: examples from the central Fennoscandian Ice Sheet; *in* Geochemistry Research Advances, (ed.) O. Stefánsson; Nova Science Publishers, New York, p. 1–29.

Sarala, P. and Neonen, J., 2005. Ore prospecting in the ribbed moraine area of Misi, northern Finland; *in* Current Research 2003–2004 (ed.) S. Autio; Geological Survey of Finland, Special Paper 38, p. 25–29.

Sarala, P. and Rossi, S., 2000. The application of till geochemistry in exploration in the Rogen moraine at Petäjävaara, northern Finland; Journal of Geochemical Exploration, v. 8, p. 87–104.

Sarala, P., Peuraniemi, V. and Aario, R., 1998. Glacial geology and till geochemistry in ore exploration in the Tervola area, southern Finnish Lapland; Bulletin of the Geological Society of Finland, v. 70, p. 19–41.

Sarala, P., Rossi, S., Peuraniemi, V., and Ojala, V.J., 2007. Distinguishing glaciogenic deposits in northern Finnish Lapland: implications for exploration; Applied Earth Science, Transactions of Institute of Mining and Metallurgy, Section B, v. 116, p. 22–36.

Sauerbrei, J.A., Pattison, E.F., and Averill, S.A., 1987. Till sampling in the Casa-Berardi gold area, Quebec: a case history in orientation and discovery (Canada); Journal of Geochemical Exploration, v. 28, p. 297–314.

Shilts, W.W., 1973. Drift prospecting: Geochemistry of eskers and till in permanently frozen terrain, District of Keewatin, Northwest Territories; Geological Survey of Canada, Paper 72–45.

Shilts, W.W., 1975. Principles of geochemical exploration for sulphide deposits using shallow samples of glacial drift; Canadian Mining and Metallurgical Bulletin, v. 68, p. 73–80.

Shilts, W.W., 1977. Geochemistry of till in perennially frozen terrain of the Canadian Shield - application to prospecting; Boreas, v. 6, p. 203–212.

Shilts, W.W., 1978. Nature and genesis of mudboils, central Keewatin, Canada; Canadian Journal of Earth Sciences, v. 5, p. 1053–1068.

Smith, S.L., 1992. Quaternary stratigraphic drilling transect, Timmins to the Moose River Basin, Ontario; Geological Survey of Canada, Bulletin 415.

Sorjonen-Ward, P.B., Hartikainen, A., Nurmi, P.A., Rasilainen, K., Schaubs, P., Zhang, Y., and Liikanen, J., 2015. Exploration targeting and geological context of gold mineralization in the Neoarchean Ilomantsi greenstone belt in eastern Finland; *in* Mineral Deposits of Finland, (ed.) W.D. Maier, R. Lahtinen, and H. O'Brien; Elsevier, Amsterdam, p. 435–466.

Stea, R.R. and Brown, Y., 1989. Variation in drumlin orientation, form and stratigraphy relating to successive ice flows in southern and central Nova Scotia; Sedimentary Geology, v. 62, p. 223–240.

Strand, P., Banas, A., Baumgartner, M., and Burgess, J., 2009. Tracing kimberlite indicator mineral dispersal trains: an example from the Churchill Diamond Project, Kivalliq region, Nunavut; *in* Application of Till and Stream Sediment Heavy Mineral and Geochemical Methods to Mineral Exploration in Western and Northern Canada, (ed.) R.C. Paulen and I. McMartin; Geological Association of Canada, Short Course Notes 18, p. 167–175.

Thorleifson, L.H. and Garrett, R.G., 2000. Lithology, mineralogy, and geochemistry of glacial sediments overlying kimberlite at Smeaton, Saskatchewan; Geological Survey of Canada, Bulletin 551.

Tremblay, T. and Paulen, R.C., 2012. Glacial geomorphology and till geochemistry of Central Melville Peninsula, Nunavut; Geological Survey of Canada, Open File 7115.

Ward, B.C., Leybourne, M.I., and Sacco, D.N., 2011. Drift prospecting within the QUEST Project area, central British Columbia (NTS 093J): potential for porphyry copper-gold, volcanogenic massive sulphide mineralization and gold-copper veins; *in* Summary of Activities 2010; Geoscience BC, Report 2011-1, p. 73–96.

Strategic applications of shallow overburden drilling for drift prospecting

Dave Sacco

Principal, Surficial Geology and Exploration, Palmer, 470 Granville Street, Suite 630, Vancouver, British Columbia V6C 1V5

The aim of drift prospecting is to determine the bedrock source of transported lithological, mineralogical, or geochemical constituents in glaciated terrain (McClenaghan et al., 2020). Till is a common sample medium that is typically collected from the surface; however, there are numerous benefits to collecting subsurface till in support of mineral exploration. Shallow-drilling technology is beneficial for both surface and subsurface till sampling, but to ensure the efficient collection of reliable data, it is essential to understand where to sample and which drilling method is most appropriate for the survey goals and surficial setting.

Fundamentally, the concept of drift prospecting is simple; locate material that indicates mineralization (e.g. mineralized boulders, indicator minerals, sediment geochemistry) and use geomorphological sediment transport models to trace those materials back to their bedrock source. Till sampling is a proven method for mineral exploration under cover in previously glaciated terrain (McClenaghan et al., 2023), and subglacial traction till is widely considered the optimal till facies to sample (Shilts, 1993; Levson, 2001; McClenaghan et al., 2023). It is predominantly a first derivative of bedrock, it has predictable transport vectors that are related to the local ice-flow history, and it provides a detectible anomaly footprint that is areally more extensive and consistent than other sample media. Till sampling can be three-dimensional and is scalable, so the same method can be applied at any stage of exploration and continued at a higher resolution to develop and refine exploration targets for diamond drill testing. Optimal till sampling protocols and survey design considerations are provided in McClenaghan et al. (2020, 2023).

Regional-scale till surveys have been completed for decades by federal and provincial geological surveys and through government-funded programs because of their effectiveness in characterizing geology and prospectivity (e.g. Plouffe, 1995; Kerr and Knight, 2005; Fenton et al., 2006; Brushett, 2012; Sacco et al., 2022a, 2023). Despite this proven effectiveness, till sampling is commonly overlooked as a method for exploration in property- to target-scale initiatives. This is at least partially because it is difficult to reach the required sampling depths by hand in most subglacial traction till due to its compactness and clast content. Additionally, opportunistic sampling locations (e.g. road or stream cuts or frost boils) typically targeted for regional programs are too sporadic to support property- or target-scale programs. The difficulty in obtaining suitable till samples by hand fosters the use of more convenient exploration methods that are less effective in glaciated environments, such as B-Horizon soil sampling. Fortunately, drill-supported till sampling is becoming recognized as a practical approach, leading to more successful mineral exploration programs.

Drill-supported till surveys can provide reliable, high-density data required to support property- and target-scale exploration programs. It has been tested and adopted as the primary method for exploration under cover in Scandinavian countries for many years due to road networks that make this feasible (e.g. Sarala, 2015). This method of sampling has also been used successfully in Canada (e.g. Averill, 2013), and the advancements in drilling technology specifically for till sampling have furthered its utilization (e.g. Paulen, 2009; Sacco et al., 2022b, 2023). Drill-supported till sampling provides a means of collecting till samples wherever till occurs, even if not readily exposed or accessible at surface, and at various depths within the sediment column (e.g. beneath reworked till or other materials). Furthermore, more comprehensive survey methods, such as profile sampling or base-of-till and top-of-bedrock (BoT-ToB) sampling, can be completed with drill support. These advanced methods not only provide reliable data but can reveal specific zones of mineralization for diamond-drill testing in areas of thick drift over much shorter timeframes than other options.

Numerous drilling solutions are available for sampling till. The most appropriate equipment and survey design depend on a variety of factors, such as the purpose or scale of the survey; access to the area(s) of interest; budget; timing (length of program and seasonality); analytical methods; distribution of till; stratigraphy, and overburden thickness. Smaller drills are easily

Recommended citation:

Sacco, D., 2024. Strategic applications of shallow overburden drilling for drift prospecting; *in* Till Geochemistry and Indicator Mineral Methods for Exploration in Glaciated Terrains, (ed.) R.C. Paulen and M.B. McClenaghan; Geological Survey of Canada, Open File 9210, p. 35–40. https://doi.org/10.4095/pbmy2d03m0

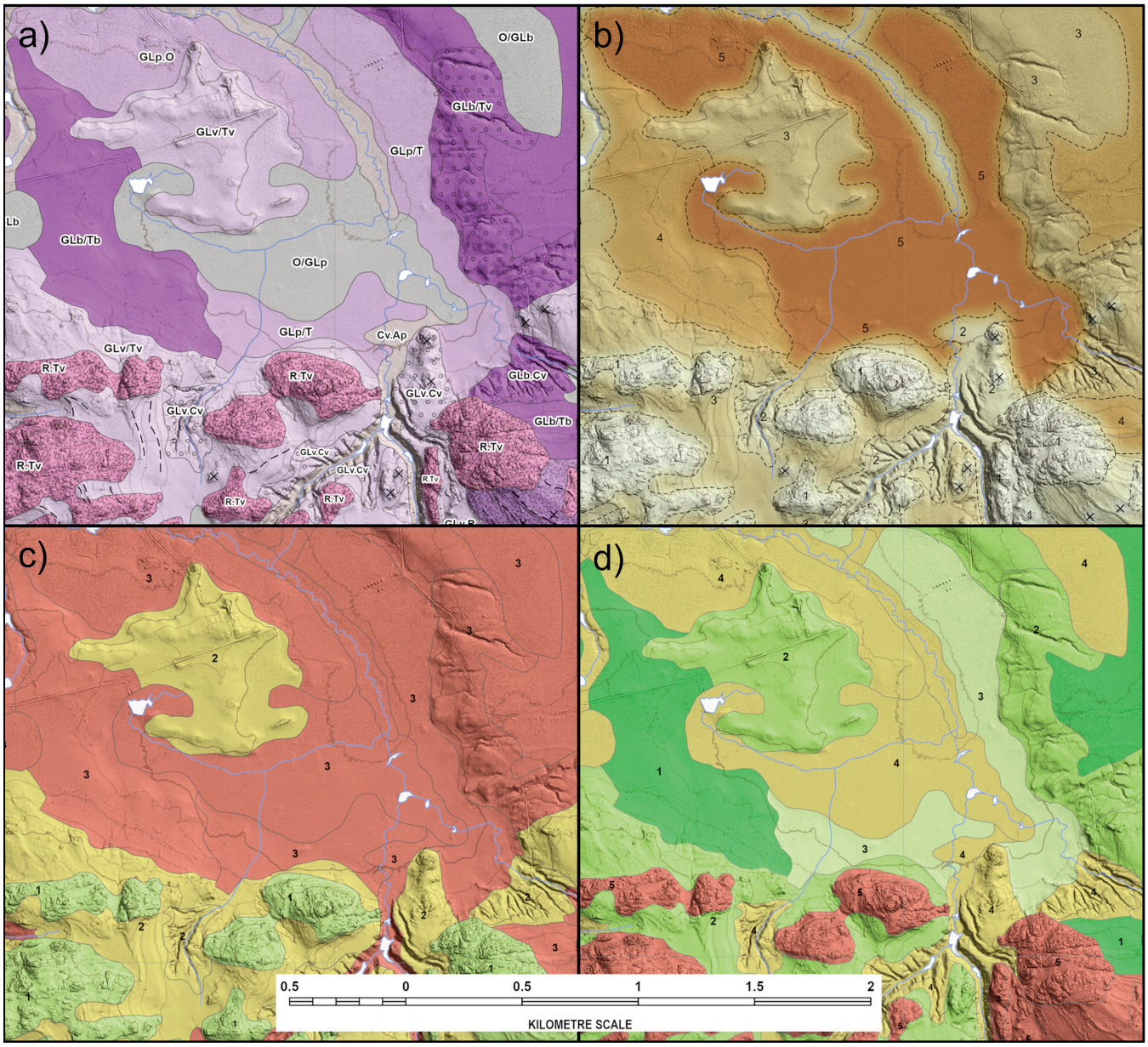


Figure 1. An example of detailed surficial geology and derived thematic maps produced in support of mineral exploration. **a)** A surficial geology map (C = colluvium; GL = glaciolacustrine; O = organics; R = rock; T = till). **b)** A drift thickness map (darker colours represent thicker drift). **c)** A map indicating the suitability for till sampling at surface (green to red indicates a relative decrease in sampling suitability). **d)** A map indicating the suitability for till sampling at subsurface (dark green to yellow to red indicates decreasing sampling suitability).

moved and may not require a drill permit to be acquired but have shallower operational depths and retrieve smaller sample volumes. Larger drills can provide large-volume samples from greater depths but require a permit and significant resources and expenditures to establish access and drill pads and move equipment between sites. The capabilities and limitations of available drilling systems must be known before selecting one for field deployment. It is common for the most efficient strategy to include more than one drilling system and for different systems to be used at different stages of exploration.

A detailed understanding of the surficial geology in the survey area is critical for till survey design and equipment selection. Relevant information includes the distribution of suitable till for sampling, where it occurs in the stratigraphic sequence, how thick it is, and vectors of displacement from the bedrock source. This information is optimally attained through field-verified surficial geology mapping, during which the till can be adequately characterized and sampling suitability and drift thickness maps can be derived to support survey strategy development (e.g. Ferbey, 2014; Sacco et al., 2014, 2022c) (Fig. 1). These maps differ-

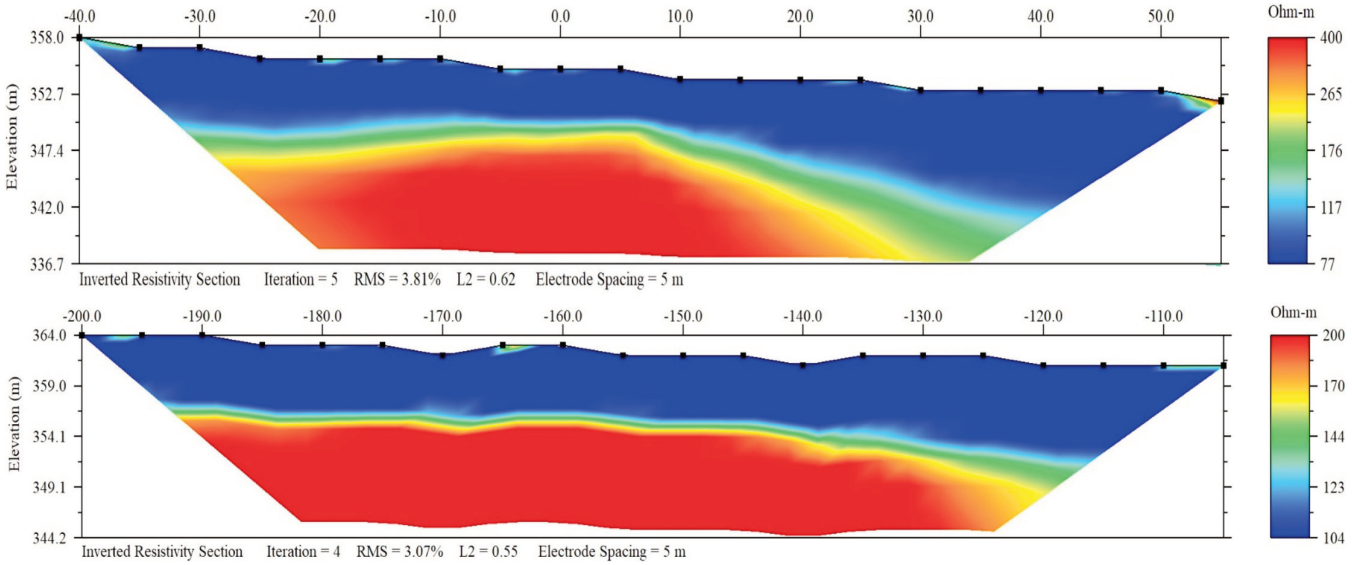


Figure 2. Electrical resistivity tomography (ERT) profiles showing sediment stratigraphy and the depth to bedrock near Red Lake, Ontario. These results were verified through subsequent drilling. Blue represents glaciolacustrine silt and clay, green represents till, and red represents bedrock.

entiate areas where till occurs at surface and smaller drills will be sufficient from areas where drift is thicker and larger drills may be required to reach buried till or the base of till. Where sediment thickness is difficult to determine through remote interpretations, ground-based geophysics, such as ground penetrating radar or electrical resistivity tomography, can be used in representative landscape settings to rapidly image the subsurface sedimentary unit thicknesses and depths to bedrock (e.g. Sibul et al., 2017) (Fig. 2). This information can be extrapolated to similar landscape assemblages to inform appropriate survey design and equipment selection. Applying this type of data-driven strategy to program planning ensures that reliable, high-quality data are efficiently collected.

The smallest drills used for till sampling are human-portable and are optimal for sampling in the shallow subsurface (<4 m). Most of these "ultra-lightweight" drilling systems were originally designed for construction; however, they are not all suitable for all tills. Most hammer drills (e.g. Cobra) and rotary drills (e.g. Sipre) are effective in tills with low clast contents but can have difficulty with advancing or sample retrieval in tills with a high clast content. The Talon drilling system™ uses a rotary-percussion drill head that has purpose-built interchangeable tooling (Fig. 3). Hammer auger bits can be used to drill through or pulverize clasts and custom flow-through samplers can be attached to collect in situ till matrix for analysis. Ultra-lightweight drills can be effective up to 10 m depth, or even greater in optimal conditions, but drill advancement and sample production rates decrease significantly when working at depths greater than 4 m. These drills are best suited to areas where till is at or near surface. Typically not requiring a permit, these drills provide the means to fill gaps in regional surveys where opportunistic exposures are rare (e.g. Sacco et al., 2022b). They are also optimal for high-resolution property- to target-scale surveys where till thicknesses are generally less than 5 m. The main limitation of human-portable drills is the small individual sample size, though suitable for geochemical analysis, is too small for mineralogical analysis.

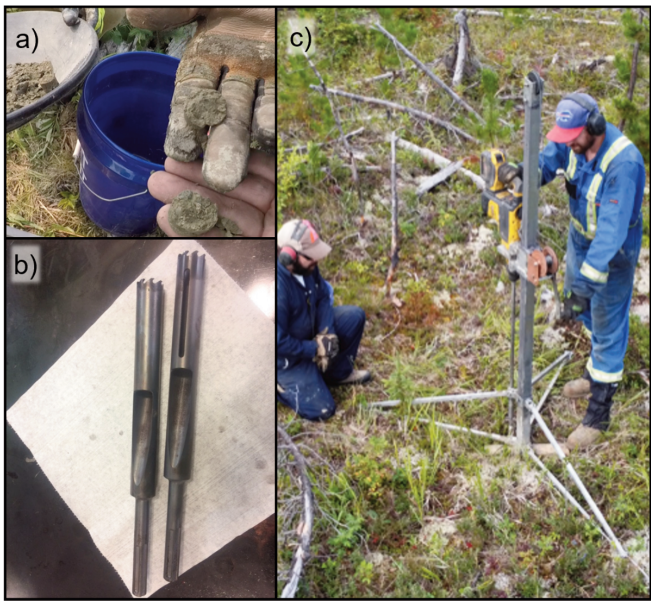


Figure 3. Talon ultra-lightweight drilling system™ that has been custom tooled to collect C-horizon till samples for geochemical analysis at depths less than 4 m. **a)** Till buttons that formed through parting along fissility planes after being extracted from the flow-through sampler. **b)** Flow-through samplers. **c)** Talon drilling system™ in use in the field.



Figure 4. Photographs of the ShockAuger lightweight drilling system configured with tracks (left) and without tracks (right) being used to collect in situ till core (centre) and top-of-bedrock samples at depths up to 20 m for geochemical and mineralogical analysis.

Lightweight or semi-portable drills are generally effective for sample depths in the tens of metres. Similar to ultra-lightweight drills, operating near the high end of depth capabilities will slow the rate of sample production and increase the potential for equipment to break or become stuck down-hole. Operating in the 5–20 m range is ideal for high sample production rates; operating at greater depths should be reserved for specific situations where the risks are understood and there is sufficient time to overcome complications without risking survey completion. Lightweight drills are optimal for profile sampling in thick till and for BoT-ToB sampling, which provides an indication of proximal bedrock composition and higher anomaly-to-background contrast in till, and a bedrock sample. Lightweight drills are also excellent for sampling till beneath a thick (2–20 m) mantle of other material (e.g. glaciolacustrine). These drills can collect samples suitable for geochemical and mineralogical analysis and are typically mounted on tracks or on a vehicle (e.g. a truck or a small loader).

Semi-portable power-augers have been effectively used for sampling in tills with very low clast content (e.g. Canadian prairies), but are impeded by cobbles and boulders and cannot sample bedrock. These units are generally truck-mounted and are most effective for road-accessible sampling during regional surveys where the till is thick or potentially buried beneath other fine-grained materials. There are several track-mounted options, such as the Geoprobe™ 6011DT, which is versatile and can navigate relatively narrow trails and uneven surfaces, making it more suitable for higher resolution surveys. This unit is optimal for property- or target-scale surveys where closely spaced sampling along transects is ideal. Its roughly 2,150 kg weight, however, limits its air-supported portability, so it is best suited for sampling along trails that are road accessible. The ShockAuger is a recently designed drilling system that was purpose-built to support property- to target-scale till sampling programs (Fig. 4). It can be configured with or without tracks and weighs about 815 kg and 1200 kg, respectively. The ShockAuger uses a rotary-percussion drilling system and provides similar sampling capabilities as the 6011DT but is transportable in one helicopter sling load. Maximum sampling depths are shallower than those of the 6011DT, but the custom tooling and chain-driven pull-back system increases the speed of drilling and sampling, and the increased portability makes it suitable for regional- to target-scale surveys (e.g. Sacco et al., 2023).

Larger drilling systems should be considered when sampling depths are greater than 20 m (McMartin and McClenaghan, 2001). Although some lightweight drills will boast this capability in optimal conditions, the complications associated with unknown sediment composition and saturated sediments will inevitably cause problems for smaller drills at these depths. These larger drilling systems require more access preparations, pad building, and significant effort when moving between

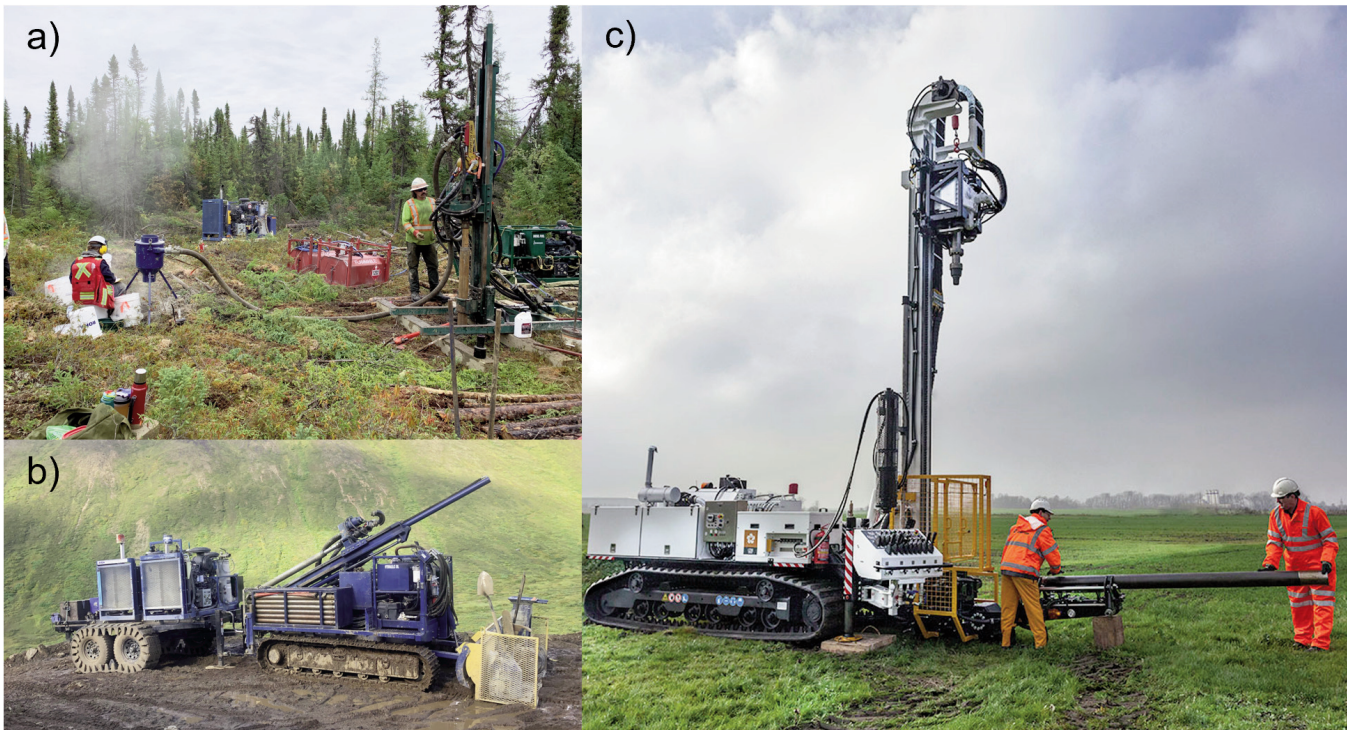


Figure 5. Drilling system options for till sampling at depths greater than 20 m. **a)** Multi-Power's Hornet reverse circulation drilling system configured for helicopter transport. **b)** Multi-Power's Grasshopper reverse circulation drilling system (photo credit: Ryan Babala, Ascent Exploration and Consulting Ltd.). **c)** Boart Longyear's LS™ MiniSonic™ drilling system (photo source: https://www.boartlongyear.com/product/ls250).

sample sites, so it is best to reserve their use for deeper applications where lighter weight rigs are inadequate. An additional consideration is that larger drills will require a separate drilling crew, whereas ultralightweight, and some lightweight, drills can be operated by Quaternary geologists. Typically, reverse circulation (RC) or sonic drills are recommended for till and bedrock sampling below a depth of 20 m. RC rigs, such as Multi-Power's Hornet and its track-mounted counterpart, the Grasshopper, use compressed air to move drill cuttings and they can be disassembled into several helicopter-portable sling loads (Fig. 5a,b). The increased operational depth and reasonable portability are advantageous. The downside of RC drilling for till sampling is its destructive nature, which disturbs the sample and makes it difficult to differentiate subglacial traction till from other materials and to discern sediment stratigraphy. Furthermore, the circulation of sediments causes unavoidable cross-contamination between samples. Sonic drills (Fig. 5c) collect an in situ sediment core, allowing for genetic discrimination and precise sampling. These drills provide the most reliable results, but they are relatively large and expensive. Typically requiring road or trail access, the use of a sonic drill is most applicable to more advanced projects, or projects with exceptionally good road access.

Geochemical and mineralogical data from till sampling have been a fundamental component of regional exploration in Canada. However, the difficulties associated with collecting suitable till for sampling with hand tools has resulted in it being underutilized during property- to target-scale programs, despite its effectiveness. As most mineralized systems exposed at surface in glaciated terrain have been discovered, the new frontier for exploration is under the cover of glacial sediments. Drill-supported till sampling provides the means to effectively collect till samples at optimal locations and from anywhere within the sediment stratigraphy. This, in turn, allows for more comprehensive three-dimensional surveys and BoT-ToB surveys that can map bedrock lithology and identify mineralization in areas completely covered by glacial sediments. There are numerous factors to consider when designing a strategy for drill-supported till sampling, with significant importance on understanding the surficial geology, access, and survey goals. An appropriately planned drill-supported till survey can be a key component to the development and prioritization of reliable exploration targets for diamond drill testing over shorter timelines.

REFERENCES

Averill, S.A., 2013. Discovery and delineation of the Rainy River gold deposit using glacially dispersed gold grains sampled by deep overburden drilling; *in* New Frontiers for Exploration in Glaciated Terrain, (ed.) R.C. Paulen and M.B. McClenaghan; Geological Survey of Canada, Open File 7347, p. 37–46.

Brushett, D., 2012. Till geochemistry of northeast Newfoundland (NTS map areas 2C/13, 2D/15, 2D/16, 2E/01, 2E/08, 2F/04 and 2 F/05); Government of Newfoundland and Labrador, Department of Natural Resources, Geological Survey, Open File NFLD/3174, 161 p.

Fenton, M.M., Pawlowicz, J.G., Paulen, R.C., and Prior, G.J., 2006. Quaternary stratigraphy and till geochemistry of the southern Buffalo Head Hills, Alberta: results of an auger coring program; Alberta Energy and Utilities Board, EUB/AGS Geo-Note 2005-10, 30 p.

Ferbey, T., 2014. Basal till potential of the Nadina River map area (NTS 093E/15), British Columbia; British Columbia Geological Survey, Open File 2014-02, scale 1:50 000.

Kerr, D.E. and Knight, R.D., 2005. Till geochemistry, Slave Province, Northwest Territories and Nunavut; Geological Survey of Canada, Open File 5015, 8 p.

Levson, V.M., 2001. Regional till geochemical surveys in the Canadian Cordillera: sample media, methods, and anomaly evaluation; *in* Drift Exploration in Glaciated Terrain, (ed.) M.B. McClenaghan, P.T. Bobrowsky, G.E.M. Hall, and S.J. Cook; Geological Society of London, Special Publication No.185, p. 45–68.

McClenaghan, M.B., Spirito, W.A., Plouffe, A., McMartin, I., Campbell, J.E., Paulen, R.C., Garrett, R.G., Hall, G.E.M., Pelchat, P., and Gauthier, M.S., 2020. Geological Survey of Canada till-sampling and analytical protocols: from field to archive, 2020 update; Geological Survey of Canada, Open File 8591, 1 zip file. https://doi.org/10.4095/326162

McClenaghan, M.B., Paulen, R.C., Smith, I.R., Rice, J.M., Plouffe, A. McMartin, M., Campbell, J.E., Lehtonen, M., Parsasadr, M., and Beckett-Brown, C.E., 2023. Review of till geochemistry and indicator mineral methods for mineral exploration in glaciated terrain; Geochemistry: Exploration, Environment, Analysis, v. 23. https://doi.org/10.1144/geochem2023-013

McMartin, I. and McClenaghan, M.B., 2001. Till geochemistry and sampling techniques in glaciated shield terrain: a review; *in* Drift Exploration in Glaciated Terrain, (ed.) M.B. McClenaghan, P.T. Bobrowsky, G.E.M. Hall, and S. J. Cook; Geological Society of London, Special Publication 185, p. 19–44.

Paulen, R.C., 2009. Sampling techniques in the Western Canada Sedimentary Basin and the Cordillera; *in* Application of Till and Stream Sediment Heavy Mineral and Geochemical Methods to Mineral Exploration in Western and Northern Canada, (ed.) R.C. Paulen and I. McMartin; Geological Association of Canada, GAC Short Course Notes 18, p. 49–73.

Plouffe, A., 1995. Geochemistry, lithology, mineralogy and visible gold grain content of till in the Manson River and Fort Fraser map areas, central British Columbia (NTS 93K and N); Geological Survey of Canada, Open File 3194, 119 p.

Sacco, D., Ferbey, T., and Jackaman, W., 2014. Basal till potential of the Clusko River map area (NTS 093C/09), British Columbia; British Columbia Geological Survey, Open File 2014-06, Geoscience BC Map 2014-06-01, scale 1:50 000.

Sacco, D.A., Jackaman, W., and Janzen, B., 2022a. Drift prospecting in the central interior copper-gold research projects area (parts of NTS 093A, B, G, J, K, O): Minerals; Geoscience BC, Report 2023-03.

Sacco, D.A., Janzen, B., and Jackaman, W., 2022b. Mineral exploration in the Central Interior Copper-Gold Research projects area, central British Columbia (parts of NTS 093A, B, G, J, K, O): new tools for a proven approach to exploration under cover; *in* Geoscience BC Summary of Activities 2021: Minerals; Geoscience BC, Report 2022-01, p. 1–10.

Sacco, D., McGregor, C., Janzen, B., Knox, C., and Wolter, A., 2022c. Surficial geology, drift thickness and till sampling suitability maps (NTS 093A/13; 093G/01, 07, 09, 10, 16), British Columbia; Geoscience BC Report 2022-08, scale 1:50 000.

Sacco, D., Howitt, L., Knox, C., DesRosiers, P., Whitney, J., Janzen, B., McCuaig, S., McKillop, R., and Meek, D.M., 2023. Regional till and stream sediment sampling to support the evaluation of critical mineral potential in Alberta; Alberta Energy Regulator / Alberta Geological Survey, AER/AGS Special Report 115.

Sarala, P., 2015. Comparison of different techniques for basal till sampling in mineral exploration; Geological Survey of Finland, Special Paper 57, p. 11−22.

Shilts, W., 1993. Geological Survey of Canada's contributions to understanding the composition of glacial sediments; Canadian Journal of Earth Sciences, v. 30, p. 333–353.

Sibul, I., Plado, J., and Joeleht, A., 2017. Ground-penetrating radar and electrical resistivity tomography for mapping bedrock topography and fracture zones: a case study in Viru-Nigula, NE Estonia; Estonian Journal of Earth Sciences, v. 66 (3), p. 142–151.

Till geochemistry and indicator mineral laboratory methods

Christopher E. Beckett-Brown[1,2] and M. Beth McClenaghan[3]

[1]Ontario Geological Survey, Ministry of Mines, 933 Ramsey Lake Road, Sudbury, Ontario P3E 6B5
[2]Harquail School of Earth Sciences, Laurentian University, Sudbury, Ontario P3E 2C6
[3]Geological Survey of Canada, 601 Booth Street, Ottawa, Ontario K1A 0E8

ABSTRACT

Using till for mineral exploration has undergone significant advancement since boulder tracing was first used in the 1700s (Sauramo, 1924). With the development of various lab and field geochemical techniques, there are now various tools to aid exploration for many types of mineral deposits (e.g. gold, base metals, platinum group element deposits, porphyry Cu-Mo-Au, rare-earth elements, lithium, etc.). In glaciated terrain, clastic glacial sediments (till) are sampled and analyzed to detect direct or indirect indicators of mineral systems. Exploration methods for different types of commodities have changed over time; there was a mid-1980s boom in gold exploration followed by an explosion in diamond exploration in the early 1990s to a surge in lithium exploration in the late 2010s until today. Significant advancements in the availability of analytes at low cost, increased precision and accuracy of results, and drastically lower detection limits across the board have aided the uptake of till geochemical and indicator mineral methods. As these exploration methods evolve, we need to remember the importance of data quality, QA-QC protocols, and proper data treatment as these tool sets are applied for successful exploration. Regional till geochemical surveys have been completed for over 40% of Canada and almost all of Fennoscandia, and provide an excellent starting point to identify areas of interest for mineral exploration.

INTRODUCTION

Indicator minerals are mineral species recovered from till samples that, based on their physical or chemical characteristics, are indicative of mineralization type, alteration, and/or bedrock lithology. Till geochemistry and/or indicator mineral surveys are effective methods to detect mineralized bedrock in glaciated terrain (e.g. Ferbey et al., 2017; McClenaghan et al., 2000). Nearly all of Fennoscandia and over 40% of Canada have been sampled as part of regional-scale till geochemical surveys (Fig. 1). In glaciated terrains of Canada, Fennoscandia, and mountainous areas of South America, till geochemical and indicator mineral methods have been used with success since the 1970s (McClenaghan et al., 2023a).

This chapter presents a summary of till geochemical and indicator mineral laboratory methods that have been developed through years of dedicated work in this field. This summary is based largely on material published in McClenaghan et al. (2020) and McClenaghan et al. (2023a). Refer to these publications for more details and references about the material presented here.

The analyses and interpretation of till matrix geochemistry and indicator minerals should not be undertaken unless appropriate till sampling methods and strategies have been employed (Rice and McClenaghan, 2024) with an understanding of glacial

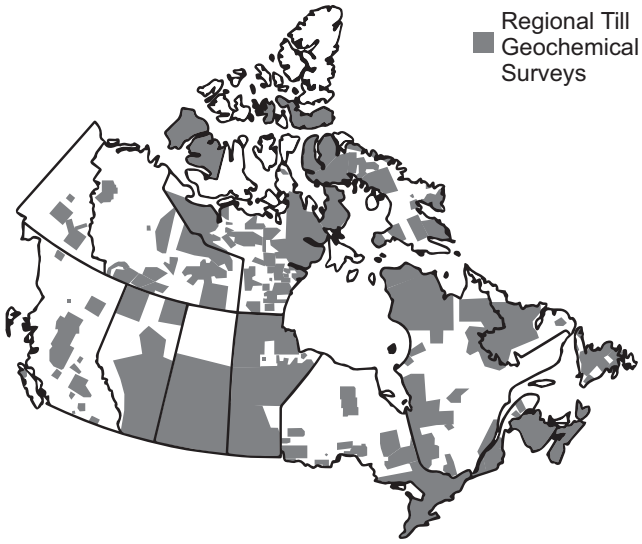


Figure 1. Map showing a compilation of the spatial coverage of till geochemical surveys across Canada conducted by provincial and territorial surveys as well as the Geological Survey of Canada. Data compiled from McClenaghan et al. (2000), CDoGS (https://geochem.nrcan.gc.ca/cdogs/content/main/home_en.htm), Bustard et al. (2017), SIGEOM geochemical database – Quebec (https://gq.mines.gouv.qc.ca/documents/SIGEOM/TOUTQC/FRA/CSV/SIGEOM_QC_Geochimie_CSV.zip).

Recommended citation:

Beckett-Brown, C.E. and McClenaghan, M.B., 2024. Till geochemistry and indicator mineral laboratory methods; *in* Till Geochemistry and Indicator Mineral Methods for Exploration in Glaciated Terrains, (ed.) R.C. Paulen and M.B. McClenaghan; Geological Survey of Canada, Open File 9210, p. 41–57. https://doi.org/10.4095/pbmy2d03m0

Table 1. List of deposit types and their associated geochemical pathfinders in till that are used to explore glaciated terrains (modified *from* McClenaghan et al., 2023a).

Deposit type	Ore elements	Indicator/ Pathfinder elements	Selected till geochemistry reviews and examples
Gold	Au, Ag	Ag, As, Au, B, Ba, Bi, Cu, Co, Fe, Hg, Mn, Pb, S, Sb, Se, Te, U, W, Zn	Lestinen et al. (1991); Hartikainen and Nurmi (1993); McClenaghan (2001); Plouffe (2001); Sarala (2005); Sarala et al. (2009); Sarapää and Sarala (2013); de Bronac de Vazelhes et al. (2021)
Intrusion-related Sn or W	Sn, W, Mo	As, Ag, Be, Bi, Cd, Cu, F, In, Mo, Pb, S, Te, W, Zn	Snow and Coker (1987); Coker et al. (1988); McClenaghan et al. (2014a, 2017a)
Iron oxide-copper-gold	Fe, Cu, Au, U	Au, As, Bi, Cd, Co, Cu, Fe, Mo, Ni, Sb, Th, U, W	McMartin et al. (2009, 2011); Normandeau (2018)
Kimberlite-hosted diamonds	C	Ba, Cr, K, LREE, Mg, Nb, Ni, P, Rb, Sr, Ta, Ti	McClenaghan et al. (1996, 1999a,b); McClenaghan and Kjarsgaard (2007)
Li-Cs-Ta (LCT) pegmatite	Li, Cs, Ta, Nb	Li, Sn, W, Cs, Ta, Be, Nb, F	Ahtola et al. (2015); Brushett et al. (2024)
Magmatic Ni-Cu-PGE	Ni, Cu, PGE	As, Au, Cr, Co, Cu, Mg, Ni, PGE, S	Bajc and Hall (2000); Barnett (2007); McClenaghan et al. (2011); Brownscombe et al. (2015); Hashmi et al. (2021)
Outokumpo-type	Ag, Au, Co, Cu, Ni, Zn	Ag, Au, Co, Cr, Cu, Ni, Zn	Salminen and Hartikainen (1985)
Porphyry Cu-Au-Mo	Cu, Mo, Au, Ag	Cu, Mo, Au, Ag, As, Ba, Pb, S, Sb, Zn, Al_2O_3, K_2O	Sibbick et al. (1997); Bobrowsky and Sibbick (1996); Hashmi et al. (2015); Plouffe et al. (2016, 2022)
REE in carbonatites, peralkaline granites	REE	Ba, Be, Ce, Cl, F, Li, Nb, U, P, REE, Ta,Th, Y, Zr	Ford et al. (1988); Batterson (1989); Batterson and Taylor (2009); Sarapää and Sarala (2013)
Sediment-hosted Zn-Pb	Ag, Cu, Pb, Zn	Ag, Cu, Pb, S, Zn	Bond (2001); Paulen et al. (2011); McClenaghan et al. (2018)
Uranium	U	As, Ba, Cu, F, La, Ni, P, Pb, Th ,Ti, U, Y, Zn, Zr	Boyle (1982); Geddes (1982); Simpson and Sopuck (1983); Campbell (2009)
Volcanogenic massive sulphide	Cu, Pb, Zn, Ag, Au	Ag, As, Au, Ba, Bi, Cd, Cu, Hg, In, Pb, S, Sb, Tl, Zn	Kaszycki et al. (1996); Lett (2001); Lett and Jackaman (2002); Parkhill and Doiron (2003); McClenaghan and Peter (2013, 2016); McClenaghan et al. (2015b)

Note: LREE = Light Rare Earth Elements; PGE = Platinum Group Elements; PGM = Platinum Group Minerals; REE = Rare Earth Elements

dynamics and glacial dispersal (Ross, 2024), and glacial transport (Paulen et al., 2024). Glacial comminution processes are complex (Ross, 2024, and references therein) and greatly affect the geochemical and indicator mineral signatures in till. Mineral hardness (i.e. Mohs hardness scale), which is a direct reflection of bond strength, is the major factor influencing the abrasion and crushing of mineral grains. Minerals with weaker bonds, such as sulphide ore minerals, will be comminuted significantly faster than silicate minerals, which is subsequently reflected in the till geochemical and indicator mineral anomalies.

Shilts (1993, 1996) reported that the mineralogy of the size fractions of a till matrix can differ and that this difference will inherently affect the chemistry of these fractions. Base metals, gold, and platinum group elements best highlight these differences as they are dominantly concentrated in the fine fraction (DiLabio, 1988; Nevalainen, 1989). Physically robust minerals, such as chromite (Cr), scheelite (W), and cassiterite (Sn), tend to occur in the coarser sand-size fraction (Shilts 1993, 1995). Various mineral systems including gold, intrusion-related Sn-W, iron oxide-copper-gold (IOCG), kimberlite-hosted diamond, Li-Cs-Ta pegmatite, magmatic Ni-Cu-PGE (platinum group element), Outokumpu-type Cu-Ni, porphyry Cu-Mo-Au, rare earth element (REE) deposits, sediment-hosted Zn-Pb, uranium, and volcanogenic massive sulphide deposits can be detected using various till geochemical signatures (Table 1).

Most mineral systems also have characteristic indicator mineral suites (Table 2). Much of the application of indicator mineral methods to date has been focused on optical/visual characterization and abundance anomalies but over the last few decades, research has increasingly focused on developing additional features

Table 2. List of deposit type and their associated indicator minerals in till that are used to explore in glaciated terrains, divided into the type 1 and type 2 minerals (modified *from* McClenaghan et al., 2023a). Type 1 are minerals that directly identify the presence of mineralization (e.g. gold, chalcopyrite, sphalerite, spodumene), and type 2 are those that can be found in mineralized systems but require additional information (e.g. mineral chemistry) to identify their link to a specific system (e.g. apatite, epidote, tourmaline).

Deposit type	Type 1 Indicator Minerals	Type 2 Indicator Minerals	Selected indicator mineral reviews and examples
Gold	gold, pyrite, arsenopyrite, tellurides, PGM, cinnabar	scheelite, tourmaline, rutile, barite	Averill and Zimmerman (1986); Averill (2001, 2013, 2017); McClenaghan (2001); Plouffe (2001); Sarala et al. (2009); McClenaghan and Cabri (2011); Sarapää and Sarala (2013); Manéglia et al. (2018); de Bronac de Vazelhes et al. (2021)
Intrusion-related Sn or W	cassiterite, scheelite, wolframite, molybdenite, chalcopyrite, Bi sulphides, sulphides	fluorite, topaz, tourmaline	Nikkarinen and Bjorklund (1976); Snow and Coker (1987); McClenaghan et al. (2014b, 2016, 2017a); Poulin et al. (2016, 2018)
Iron oxide-copper-gold	gold, arsenopyrite, Bi sulphides, chalcopyrite, pyrite	magnetite, apatite	McMartin et al. (2011); Lypaczewski et al. (2013); Sappin et al. (2014); Normandeau et al. (2018)
Kimberlite-hosted diamonds	diamond	Cr-pyrope, Cr-diopside, eclogitic garnet, Mg-ilmenite, chromite	Fipke et al. (1995); McClenaghan et al. (1996, 1999a,b, 2002); McClenaghan and Kjarsgaard (2001, 2007); Lehtonen et al. (2005); Averill (2009); Pell et al. (2013)
Li-Cs-Ta (LCT) pegmatite	spodumene, tantalite, columbite	tourmaline, beryl, apatite, cassiterite, scheelite, uraninite	Nikkarinen and Bjorklund (1975); McClenaghan et al. (2023c)
Magmatic Ni-Cu-PGE	pentlandite, chalcopyrite, pyrite, millerite, PGM, chromite	chromite, Cr-diopside, enstatite, olivine, Cr-andradite	Averill (2009, 2011); Barnett and Averill (2010); McClenaghan and Cabri (2011); McClenaghan et al. (2013); Hashmi et al. (2021); Makvandi et al. (2021)
Outokumpo type	uvarovite		Aumo and Salonen (1986)
Porphyry Cu-Au-Mo	chalocopyrite, chalcocite, pyrite, molybdenite, gold, silver, jarosite, malachite	epidote, tourmaline, apatite, andradite, barite, monazite, rutile, titanite, zircon, pyrolusite	Averill (2011); Kelley et al. (2011); Plouffe et al. (2016, 2022); Pisiak et al. (2017); Lee et al. (2021); Beckett-Brown et al. (2023a,b)
REE in carbonatites, peralkaline granites	pyrochlore, columbite, Ta-minerals, monazite, fluorite, rhabdophane	allanite, zircono-silicates, apatite, arfvedsonite	Lehtonen et al. (2011, 2015); Sarapää and Sarala (2013); Mackay and Simandl (2015); Mao et al. (2017); McClenaghan et al. (2019)
Sediment-hosted Zn-Pb	chalcopyrite, sphalerite, galena, pyrite, smithsonite, anglesite, cerussite	barite, spessartine	Paulen et al. (2011); Oviatt et al. (2015);
Uranium	uraninite (*pitchblende), thorianite, sulphides, niccolite, U-Th anatase, U-Th rutile, brannerite	tourmaline, monazite, allanite, zircon, baddelyite, magnetite	Boyle (1982); Geddes (1982)
Volcanogenic massive sulphide	chalcopyrite, sphalerite, galena, pyrrhotite, gold, pyrite, beaudantite, jarosite	gahnite, staurolite, spessartine, sillimanite, andalusite, barite, cassiterite, tourmaline	Morris et al. (1997); Averill (2001); McClenaghan et al. (2015a,b, 2017b); Makvandi et al. (2015, 2016)

Note: PGE = Platinum Group Elements; PGM = Platinum Group Minerals; REE = Rare Earth Elements; *pitchblende = brown or black pitchy massive form of uraninite

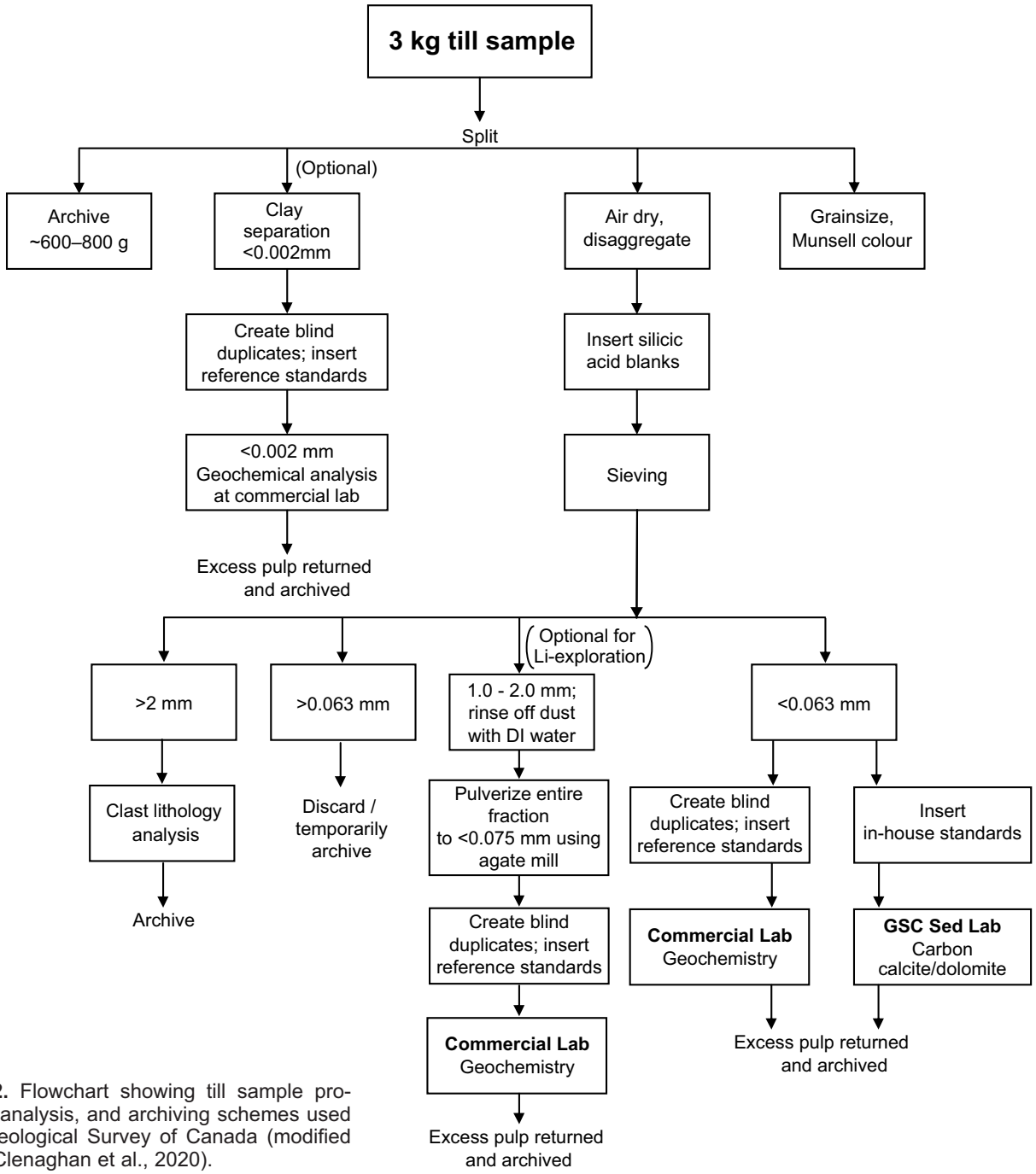


Figure 2. Flowchart showing till sample processing, analysis, and archiving schemes used at the Geological Survey of Canada (modified *from* McClenaghan et al., 2020).

(e.g. major-minor-trace element chemistry; grain shape) to aid in mineral system targeting. One of the most significant advancements, although not yet mainstream, is the automated counting of heavy minerals. Likely, it will replace optical counting as automated counting is expected to be less expensive and faster. Traditionally, indicator mineral investigation has been focused around the 0.25–0.50 mm size fraction, but with the introduction of automated methods, researchers have begun to investigate the silt- to fine-sand-sized (<0.25 mm) heavy mineral fraction due to the ability to accurately characterize the small grains.

SAMPLE PROCESSING/PREPARATION

Drying and disaggregation

Sample preparation for till matrix geochemical analyses is described below and illustrated in Figure 2. Following sample collection, the entire sample should be air dried at <40°C in a dust-free space/room. When the samples have been dried, a split of unprocessed material should be separated for archiving. Depending on the level of compaction and wetness, some samples may need to be disaggregated before sieving using a rubber mallet while the sample is inside a thick plastic bag. To monitor

potential contamination during sample preparation, processing, and analyses, silicic acid blank samples should be inserted into a batch before sample sieving.

Sieving

For geochemical analysis, samples should be sieved using stainless steel sieves that have no tears, holes, or solder (which can be a source of Sn contamination). Between each sample, the sieve(s) should be cleaned using a stiff plastic brush and then blown with compressed air in a fume hood, then wiped with distilled/de-ionized water and visually inspected. This sequence of steps has been shown to sufficiently clean sieves (Grenier et al., 2015). An ultrasonic cleaning method should also be used at regular intervals (e.g. every 10th sample). Due to minerals having a wide range of densities, the entire sample should be sieved to completion because high-density materials (e.g. gold, specific gravity 16–19), will preferentially pass through the sieve first (Grenier et al., 2015).

<0.063 mm (-230 mesh) fraction

The <0.063 mm (clay + silt) fraction is the most common size fraction of till used for geochemical analysis (Koljonen et al., 1992a,b; Edén and Bjorklund, 1995; Friske et al., 2001; McClenaghan et al., 2011, 2014a; Brushett et al., 2024a). Key factors supporting the use of the <0.063 mm fraction include the following:

1) it can be prepared rapidly and inexpensively (Lett, 1995);
2) gold, base metals, and precious metal minerals are easily comminuted to the <0.063 mm fraction due to their low hardness and weak bonding and as such are enriched in this size fraction (Coker and DiLabio, 1989; Nevalainen,1989; Shilts, 1995, 1996);
3) in published studies, gold is most abundant in the silt-sized (<0.063 mm) fraction of till (DiLabio, 1982; Tarvainen, 1995; McMartin, 2009);
4) a smaller sample is collected for the <0.063 mm fraction versus the <0.002 mm fraction;
5) phyllosilicates are abundant in the <0.063 mm fraction and these will scavenge cations released during weathering (Shilts, 1993, 1995).

1.0–2.0 mm fraction

The 1.0–2.0 mm (coarse to very coarse sand) fraction of till has not received much attention due to the focus on base and precious metal exploration using the <0.063 mm fine fraction. Some environmental researchers and soil scientists historically analyzed the <2.0 mm till fraction (e.g. Olsson et al., 1993). During glacial erosion, transport, and deposition, rock can be broken down into two components: 1) clast-size rock fragments (>1 mm) and 2) till matrix (<2 mm) that is dominated by mineral fragments. In the till matrix, minerals have reached their terminal mode, which is determined by a mineral's original grain size, cleavage, hardness, grain boundaries, and crystallization history (Shilts, 1995). Physically robust minerals, such as quartz and feldspar in the fine-sand-size fractions and greater, are thought to comprise up to 95% of the till matrix (Dreimanis and Vagners, 1971; Shilts, 1977). However, a study in Finland showed that the normative abundance of quartz between the coarse (<2.0 mm) and fine (<0.063 mm) fractions was 10% or less, depending on the bedrock source (Tarvainen, 1995). Recent analysis of the 1.0–2.0 mm fraction of till proved it to be more effective than the <0.063 mm fraction in delineating Li anomalies for LCT pegmatite exploration (Brushett et al., 2024a,b). A disadvantage of using the coarse (1.0–2.0 mm) fraction is the requirement to crush the material to <0.074 mm before chemical digestion, which increases the cost and time for sample preparation (Brushett et al., 2024a).

<0.002 mm fraction

The <0.002 mm (clay) fraction of till has also been of interest to some explorationists and researchers (e.g. Simpson and Sopuck, 1983; Campbell, 2009; Plouffe et al., 2016). Analysis of this fraction is significantly less common due to the higher cost and greater time required to centrifuge samples to recover the clay-sized material. The benefit of using this fraction is that a greater abundance of clay minerals, which are known to adsorb large ions that have been released during weathering. This <0.002 mm fraction also avoids the potential for textural bias in matrix geochemistry (Shilts, 1995). However, a larger sample size (~800 g) is required and the clay fraction has a higher potential for hydromorphic influence.

Indicator Minerals

Indicator mineral separation of till samples is routinely conducted at commercial laboratories. Canadian labs that offer this service (listed in alphabetical order) include C.F. Mineral Research Ltd., Microlithics Laboratories Inc., IOS Services Geoscientifiques Inc., Overburden Drilling Management Ltd., and Saskatchewan Research Council. Although the laboratories have slightly different separation methods/techniques, they generally follow preparation schemes similar to what is used by the Geological Survey of Canada (Fig. 3) and described in detail in McClenaghan et al. (2020).

ANALYTICAL METHODS

Till Matrix Geochemistry

Aqua regia

Aqua regia is a widely employed method for the strong partial digestion of unconsolidated sediments in the

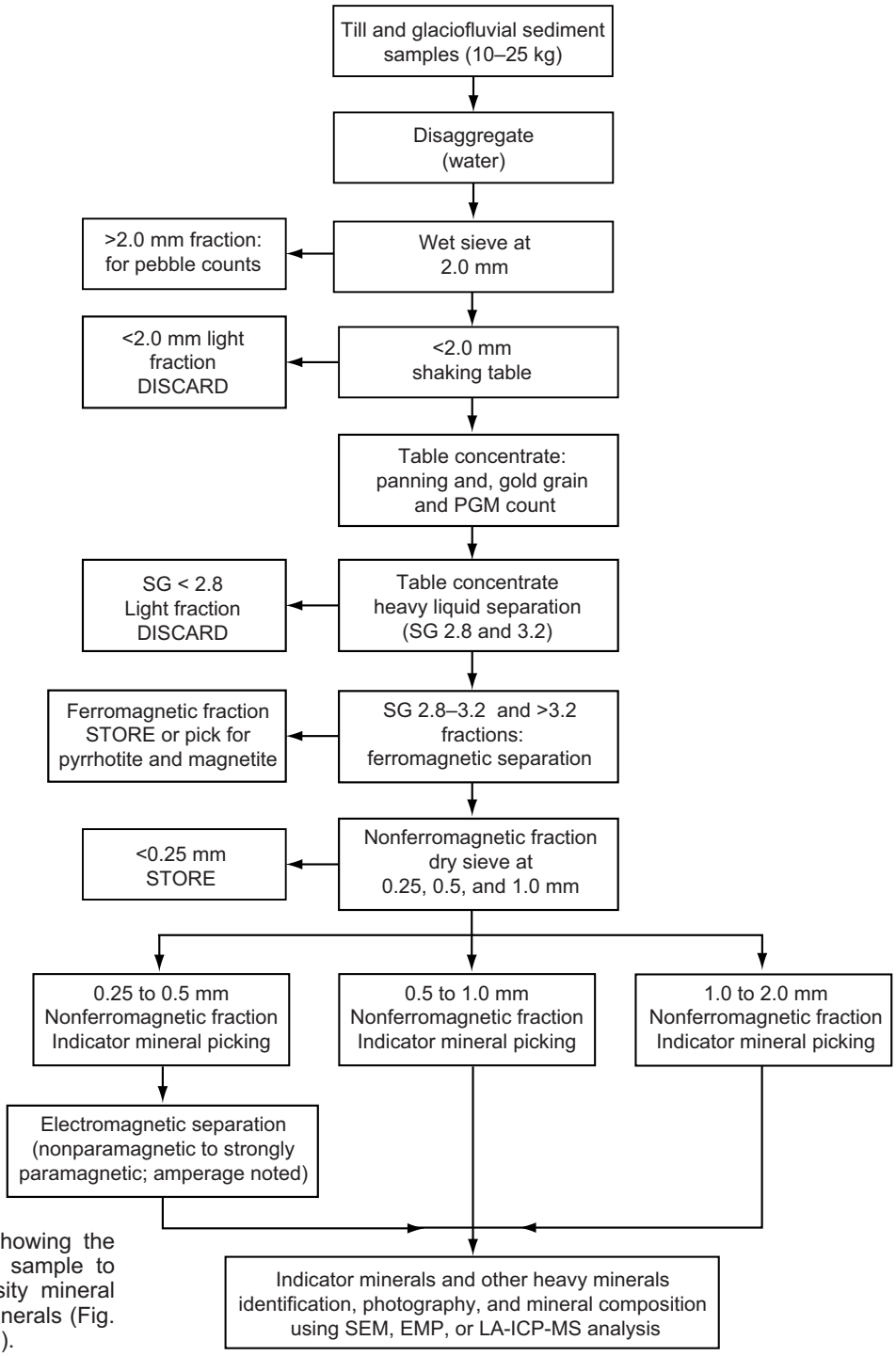


Figure 3. Schematic flowchart showing the main stages of processing a till sample to recover the heavy and mid-density mineral fractions and to count indicator minerals (Fig. 49 *from* McClenaghan et al., 2020).

exploration of base metals and gold (Marsden and House, 2006; McClenaghan et al., 2023a). Traditional aqua regia consists of 1 part nitric acid to 3 parts hydrochloric acid (HNO_3:HCl 1:3), with modified aqua regia consisting of 1 part nitric acid to 1 part hydrochloric acid to 1 part water (HNO_3:HCl:H_2O 1:1:1) (Lett and Rukhlov, 2017). Aqua regia digestion is used effectively on a small 0.5–1 g aliquot for most elements, but a 30 g aliquot should be used for Au, Pt, and Pd for reproducible results. Aqua regia is a leach that targets sulphides, sulphates, and some secondary oxides without significant dissolution of silicates (Gaudino et al., 2007).

Lithium metaborate/tetraborate fusion

Considered a 'total' technique, lithium metaborate/tetraborate fusion is useful for identifying bedrock lithological signatures (Koljonen et al., 1992b). This fusion technique can determine concentrations of elements tied up in robust silicates and oxides that are not

readily dissolved using aqua regia. Lithium metaborate/tetraborate fusion, which is most commonly used to determine the 'total' concentrations of REEs and other high-field-strength elements (HFSEs; e.g. Nb, Ta), has been used to identify provenance and even map underlying bedrock in areas of thick till cover (e.g. Graves et al., 1988; Lahtinen et al., 1993; Tarvainen et al., 1996; Stea and Pe Piper, 1999; Klassen, 2003; Plouffe et al., 2006; Lett, 2008; Lett and Rukhlov, 2017). Many refractory mineral phases that are not dissolved by aqua regia can be adequately determined by a total method. Such phases include barite (Ba), chromite (Cr: Cook and Fletcher, 1992, 1994; McClenaghan et al., 2011), scheelite (W: McClenaghan et al., 2014a), cassiterite (Sn: McClenaghan et al., 2016), columbite and tantalite (Nb, Ta: Brushett et al., 2024a). Characteristic REE patterns can be determined using this total method for kimberlites (e.g. McClenaghan et al., 2001, 2002; McClenaghan and Kjarsgaard, 2007), carbonatites, and peralkaline granite (Kjarsgaard et al., 2013a,b). One downside of this method is that it cannot analyze lithium and boron content as these elements are added to the sample prior to fusion, thus excluding this technique for Li exploration.

Sodium peroxide fusion

Another less common 'total' technique, sodium peroxide fusion, is useful for the digestion of refractory phases (similar to lithium metaborate/tetraborate fusion) but allows for the analyses of lithium. This is the most effective method for determining the 'total' lithium concentration in a till sample as sodium peroxide can digest lithium tied up in spodumene (McClenaghan et al., 2023a; Brushett et al., 2024a). However, this method requires a slightly larger sample mass (5 g), has higher detection limits than aqua regia, and cannot be used for determining some elements (e.g. sodium and zirconium).

Four-acid digestion

Four-acid digestion is a 'near total' method for till analyses that can provide information on till provenance (Klassen, 2003; Parkhill and Doiron, 2003; Batterson and Taylor, 2009; Kjarsgaard et al., 2013a,b; McMartin et al., 2019; Campbell et al., 2021; Brushett et al., 2024a). It is appropriate for determining total Cu, Ni, Co, Pb, Zn, Mo, and Ag but is not suitable for REEs, Cr, Ba, Al, Fe, Hf, Mn, Sn, Ta, and Zr. The Geological Survey of Finland has used four-acid digestion to aid bedrock mapping at various scales as part of the Geochemical Atlas of Finland-Part 2 (till) (Nikkarinen et al., 1984; Koljonen et al., 1992a,b). This method requires a 0.25 to 0.5 g aliquot for analyses.

Instrumental neutron activation analysis

Instrumental neutron activation analysis (INAA) is one of a few quantitative 'total' analytical methods that is non-destructive, i.e., does not require digestion of the sample (Lett and Rukhlov, 2017). Challenges with INAA include the need for a neutron source and a cooling period to reduce radioactivity before samples can be returned to the client. INAA is often the preferred method for determining REE, HFSE, Th, U, and Au content (Lett and Rukhlov, 2017). INAA has even been used to determine the concentration of elements in a heavy mineral fraction of till samples prior to optical indicator mineral picking (McClenaghan et al., 1996, 1999a,b). This method requires a 30 g aliquot for analyses.

Fire assay determination of Au, Pt and Pd

Lead or nickel fire assay methods are used to determine the total concentrations of Au, Pt, Pd, and other PGEs in till samples when exploring for gold or PGE deposits (e.g. Bajc and Hall, 2000; McClenaghan et al., 2009, 2011, 2020; McMartin et al., 2011; Hashmi et al., 2021). This method only determines the elements listed above and also requires a 30 g aliquot for analyses.

Isotopic studies (Pb, Hf, Nd, Sr)

Lead isotopic studies of till matrix have been undertaken to identify Pb sourced from volcanogenic massive sulphide mineralization (Bell and Franklin, 1993; Bell and Murton, 1995; Simonetti et al., 1996; Hussein et al., 2003; van Geffen et al., 2013; Rukhlov and Ferbey, 2015). This has been most effectively applied to till samples that display a volcanogenic massive sulphide (VMS) geochemical signature (i.e. Cu, Pb, Zn).

Hafnium, neodymium, and strontium isotopes have been investigated to understand the provenance and transport process of glacial sediments (Wittkop et al., 2020). These radiogenic isotopes were successfully used to discern samples from crystalline rocks from those from sedimentary basin rocks. However, analyzing for these isotopes has not yet been applied in a mineral exploration context.

Portable field analyses

Portable field analytical methods have become commonplace in many exploration programs due to the small size of the equipment and real-time detection, allowing for instant feedback on exploration success. Although these methods are still rapidly developing, they can provide significant information while in the field and are used appropriately.

Portable X-ray fluorescence (pXRF) spectrometers can be used to determine element concentrations in 2 to 5 g of pebble-free unsieved or sieved till. They have

been used in field camps to guide sampling and/or exploration (Arne et al., 2014; Sarala et al., 2015; Côté-Mantha et al., 2017). This method can be particularly useful in remote sampling areas that would be costly to return for follow-up sampling (Lemière, 2018). Certified reference materials (CRM) are an essential part of any pXRF analytical program (Knight et al., 2021). Several public agencies have published reports outlining pXRF protocols to analyze till samples (e.g. Sarala, 2016; McClenaghan et al., 2020; Knight et al., 2021).

To the authors' knowledge, there has not been a published report of laser-induced breakdown spectroscopy (LIBS) applied to till matrix samples. Several advantages of LIBS are that it can detect light elements that pXRF cannot (e.g. Li, Be, B), the required materials are portable, little to no sample preparation is required, and it has quick analytical times (Villas-Boas et al., 2020). Similar to pXRF, LIBS analyses could be conducted on either unsieved or sieved pebble-free till samples. LIBS can also be used to indirectly determine sample pH as well as sand-silt-clay proportions (Villas-Boas et al., 2019). However, LIBS is known to have challenges with matrix effects and rigorous studies on till matrix material will be needed to refine this method.

Indicator Minerals

Identifying indicator minerals is a well defined method that can aid in the exploration of various mineral deposit types in glaciated terrain (McClenaghan et al., 2023a). Indicator minerals can be grouped into two categories (Table 2): type 1 are minerals that directly identify the presence of mineralization (e.g. gold, chalcopyrite, sphalerite, spodumene), and type 2 are those that can be found in mineralized systems but require additional information (e.g. mineral chemistry) to identify their link to a specific system (e.g. apatite, epidote, tourmaline).

Optical counting and characterization

The >3.2 specific gravity (SG) non-ferromagnetic heavy mineral fraction of till is most commonly examined and the indicator minerals counted, although more recently the mid-density 2.8–3.2 SG fraction has also been utilized. Three size fractions of the mid- and/or high-density fractions are commonly counted: 0.25–0.5 mm, 0.5–1.0 mm, and 1.0–2.0 mm. Various mineral species can be readily and easily identified and counted by commercial labs and, depending on clients' requests, minerals can be set aside in individual vials for subsequent chemical analyses. In some cases, magnetite may be of interest and the ferromagnetic fraction can also be isolated and examined (Makvandi et al., 2015, 2016; Pisiak et al., 2017).

Physical and/or visual characteristics of indicator minerals, including crystal shape, surface textures, interlocked minerals, colour, and inclusions, not only aid in mineral identification but also can provide information about the bedrock source and distance of glacial transport. These features can be optically observed and noted during the counting stage. One visual characteristic commonly used is the shape of gold grains (i.e. pristine, reshaped, and modified), which can be correlated to the transport distance (DiLabio, 1990). Soft kelyphite reaction rims on Cr-pyrope indicate a kimberlitic source and that the Cr-pyrope's transport history has been limited (Garvie and Robinson, 1984; McCandless, 1990). Chromite grains with resorbed octahedral crystal faces are also indicative of being sourced from a kimberlite, in contrast, sharp angular faces are indicative of magmatic or hydrothermal sources (McClenaghan and Kjarsgaard, 2001, 2007; Averill, 2011). Large inclusion-free forsteritic olivine crystals are indicative of a kimberlitic source but smaller colourless olivine with inclusions of oxides is indicative of magmatic sources (Averill, 2009). Tourmaline occurring as radiating crystal clusters can be indicative of being derived from porphyry Cu mineralization (Beckett-Brown et al., 2023a; McClenaghan et al., 2023b).

Rapid energy dispersive spectroscopy counting techniques

Rapid energy dispersive spectroscopy (rapid EDS) scanning with automated counting is a quickly advancing technique for investigating indicator minerals and heavy mineral fractions (Layton-Matthews and McClenaghan, 2022). Various versions of "automated mineralogy" exist, including mineral liberation analyses (MLA), particle and feature analyses with Aztec Feature, TESCAN integrated mineral analyzer (TIMA), advanced mineral identification and characterization (AMICS), and quantitative evaluation of minerals by scanning electron microscopy (QEMSCAN). Data that can be collected include major and minor element chemistry, grain size and shape, mineral associations, mineral inclusions, and grain roundness. Currently, most applications of automated mineralogy are used for the fine (<0.25 mm) heavy mineral fraction. A detailed description of automated methods applied to indicator minerals can be found in Layton-Matthews and McClenaghan (2022). Examples of automated mineralogy methods applied to till samples have been reported in Lehtonen et al. (2015), Mackay et al. (2016), Lougheed et al. (2020, 2021), McClenaghan et al. (2020), Girard et al. (2021a,b), Makvandi et al. (2021), Plouffe et al. (2022), and Gao et al. (2023).

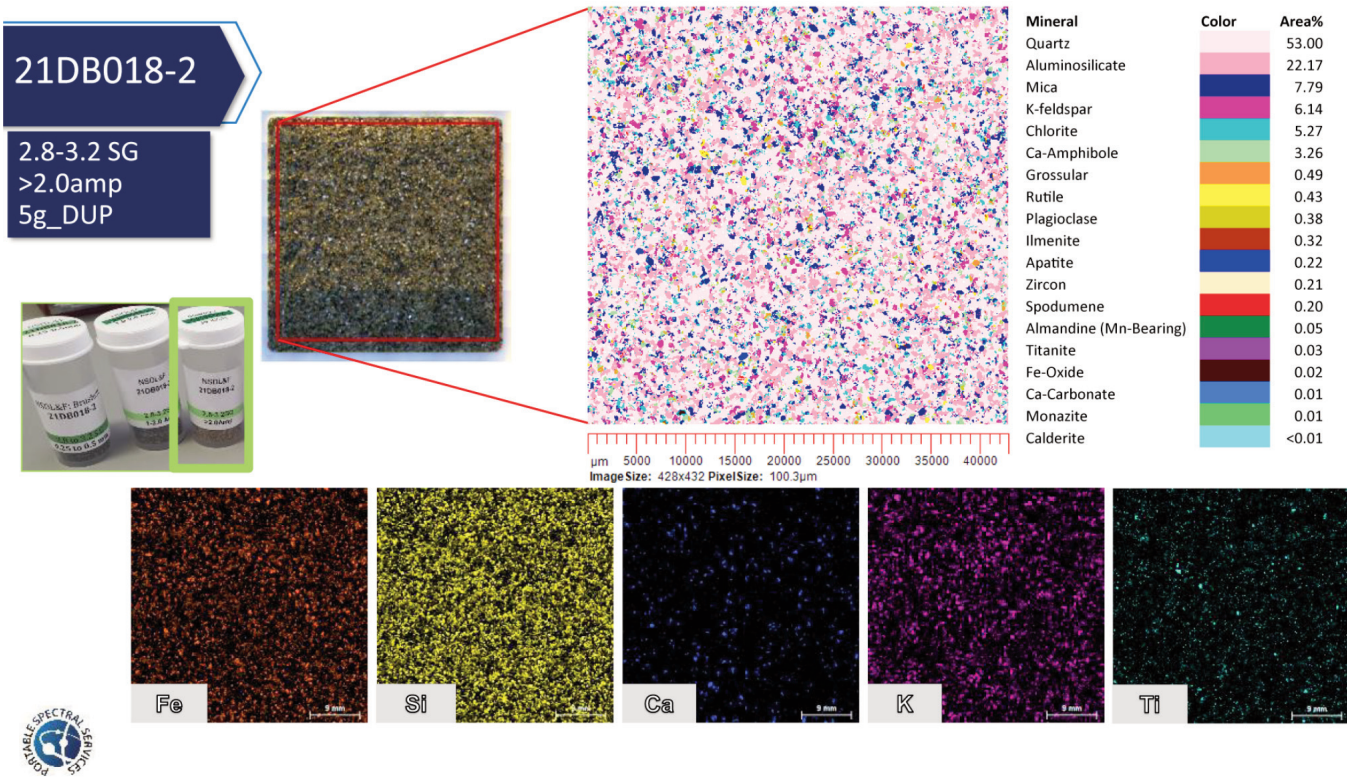


Figure 4. Scan of a till heavy mineral concentrate sample from the Brazil Lake pegmatite area, Nova Scotia using µXRF setup of Portable Spectral Services – Australia. Spodumene grains were classified based on the proportion of Si:Al.

Rapid µXRF counting techniques

An additional rapid scanning mineral characterization technique is emerging, micro-X-ray fluorescence (µXRF). This method is similar to EDS techniques and uses similar software to classify and bin the minerals, the difference being that it uses XRF to detect element concentrations. A benefit of µXRF is the ability to report lower detection limits (ppm for some elements) than EDS (which generally has limits around 100s of ppm). Samples do not need to be polished or carbon-coated, which can speed up sample preparation time. Loose, unpicked heavy mineral concentrates can be loaded onto trays and placed in the µXRF for rapid scanning (Fig. 4). Some challenges for this approach are the current spatial resolution (i.e. pixel analyses size), surface sensitivity (if examining unpolished samples, i.e., edge effects), and the inability to detect internal chemical information (e.g. zoning or mineral inclusions). Similar to EDS methods, µXRF can only detect elements heavier than carbon (i.e. Z>11), making it challenging to analyze Li, Be, and B minerals. Testing by the Geological Survey of Canada to assess the accuracy of µXRF mineral counting is currently ongoing.

Mineral Chemistry

Electron microprobe analyzer techniques

Electron microprobe analyzer (EPMA) methods (i.e. energy-dispersive X-ray spectroscopy (EDS), wavelength-dispersive X-ray spectroscopy (WDS), micro-Xray fluorescence (µXRF)) are commonly used to determine major and minor elements if detection limits of 0.01 wt.% (100 ppm) or lower are required (Layton-Matthews and McClenaghan, 2022). In general, these techniques are used to confirm the visual identification of indicator minerals but have also been used to apply some kimberlite discrimination schemes (e.g. Grütter et al., 2004).

Laser ablation-inductively coupled plasma-mass spectrometry

Laser ablation inductively coupled plasma mass spectrometry (LA-ICP-MS) can measure significantly lower concentrations (ppb to ppm) as well as isotopic measurements. For a review of LA-ICP-MS, readers are referred to Sylvester and Jackson (2016) and references therein. This method is significantly more expensive and time-consuming than microprobe techniques and is also destructive whereby material is ablated during analyses. Similar to microprobe techniques, LA-ICP-MS techniques can collect chemical data about individual grains and apply classification schemes to identify prospective mineral grains. In addition to trace-element data, LA-ICP-MS can also be used to collect isotopic ratios and measure various radiogenic isotopic systems to determine mineral age constraints

(discussed further in Beckett-Brown and McClenaghan, 2004).

Mineral chemistry examples

Numerous chemical discrimination schemes and isotopic fertility indexes developed for bedrock samples can easily be applied to indicator minerals recovered from till (McClenaghan et al., 2023a). The most recognizable application of indicator mineral chemistry is classifications related to diamond fertility (McClenaghan and Kjarsgaard, 2001, 2007 and references therein). Some of the authors that have demonstrated the application of discrimination diagrams for mineral grains recovered from till and other unconsolidated sediments include the following: i) gahnite, magnetite, cassiterite, and rutile from VMS deposits (Makvandi et al., 2015, 2016; Salama et al., 2018; Layton-Matthews and McClenaghan, 2022), ii) gahnite, garnet, and magnetite from sedimentary exhalative (SEDEX) deposits (Lisboa et al., 2023), iii) apatite, epidote, magnetite, rutile, tourmaline, and zircon from porphyry Cu deposits (Scott, 2005; Mao et al., 2016; Pisiak et al., 2017; Plouffe et al., 2022; Beckett-Brown et al., 2023a,b; Pizarro et al., 2024), iv) tourmaline and scheelite from orogenic Au deposits (Manéglia et al., 2018), v) chromite and magnetite from magmatic Ni-Cu-PGE deposits (Peltonen et al., 1992; McClenaghan et al., 2013; Ward et al., 2018; Layton-Matthews and McClenaghan, 2022), vi) chromite from Alaska-type PGE deposits (Cook and Fletcher, 1992), chalcopyrite and pyrite from magmatic or hydrothermal deposits (Duran et al., 2019), and vii) fluorite from intrusion-hosted REE deposits (Makin et al., 2014). A classification scheme that shows promise for analyzing till samples uses gold grain chemistry combined with mineral inclusion assemblages to identify deposit type (Chapman and Mortensen, 2007; Chapman et al., 2018, 2021, 2022).

Additional discrimination diagrams, which have not yet been tested, use detrital grains in till: i) rutile from Sn-deposits (Clark and Williams-Jones, 2004), ii) rutile, scheelite, and tourmaline from orogenic Au deposits (Sciuba et al., 2020, 2021; Sciuba and Beaudoin, 2021), iii) apatite and fluorite from IOCG deposits (Normandeau et al., 2018; Schlegel et al., 2020), v) fluorite and scheelite from various deposit types (Mao et al., 2017; Poulin et al., 2016, 2018).

QUALITY ASSURANCE AND QUALITY CONTROL

Quality assurance and quality control (QA/QC) evaluation can be carried out using various software and or statistical packages. Till matrix geochemistry, indicator mineral picking, and mineral chemistry analysis and should report QA/QC results for all field duplicates, laboratory duplicates, in-house reference materials, certified reference materials, and blanks. Fit-for-purpose criteria generally are defined by the user and their specific data application, but some general guidelines include ≤5% relative variation for major elements, 5–10 % for trace elements, and 5–15% for elements difficult to analyze (e.g. Sb, W). Horwitz and Albert (2006) determined acceptable precision can be calculated $PRSD_R$ (%) = $2C^{-0.15}$, where C is the concentration found or added, expressed as a mass fraction.

SUMMARY

Till geochemical and indicator mineral lab methods have undergone and continue to undergo rapid advancements in our ability to collect, visualize, and understand data. Large publicly available regional-scale datasets can be used for project generation and early stage targeting. Till matrix geochemistry has well defined analysis protocols that can be used as a template for mineral exploration programs (Fig. 2). The most widely used approach for mineral exploration is aqua regia digestion of the <0.063 μm size fraction, which can detect a wide range of mineral systems. Total digestion and analyzing other size fractions can be useful in specific cases. As automated indicator mineral counting techniques continue to advance, inevitably costs and turnaround time will be reduced and mineral identification accuracy will improve, making the use of mineral chemistry more widely available. Continued advancement and reduced costs are still required for greater uptake in the application of type 2 indicator minerals as well as more streamlined heavy mineral processing, counting, and grain picking. As the search for critical minerals continues, there is a need for more/new matrix-appropriate certified reference materials for partial digestion methods. Some excellent case studies and examples are presented in this volume and should be referred to for commodity-specific exploration strategies (see Averill for a discussion of gold, Brushett for lithium, McClenaghan for VMS, Layton-Matthews for Ni-Cu-PGE, Beckett-Brown for porphyry Cu-Mo-Au).

REFERENCES

Ahtola, T., Kuusela, J., Käpyaho, A., and Kontoniemi, O., 2015. Overview of lithium pegmatite exploration in the Kaustinen area in 2003–2012; *in* Report of Investigation, (ed.) T. Ahtola; Geological Survey of Finland, v. 220, 28 p.

Arne, D.C., Mackie, R.A., and Jones, S.A., 2014. The use of property-scale portable X-ray fluorescence data in gold exploration: advantages and limitations; Geochemistry: Exploration, Environment, Analysis, v. 14, p. 233–244.

Aumo, R. and Salonen, V.-P., 1986. Uvarovite and glacial transportation distance as provenance indicators of ore mineralization in the southern part of the Outokumpu district, north Karelia, Finland; *in* Prospecting in Areas of Glaciated Terrain-1986; The Institution of Mining and Metallurgy, London, p. 17–23.

Averill, S.A., 2001. The application of heavy indicator minerals in mineral exploration with emphasis on base metal indicators in glaciated metamorphic and plutonic terrain; Geological Society, London, Special Publications, v. 185, p. 69–82.

Averill, S.A., 2009. Useful Ni-Cu-PGE versus kimberlite indicators in surficial sediments: similarities and differences; *in* Application of Till and Stream Sediment Heavy Mineral and Geochemical Methods to Mineral Exploration in Western and Northern Canada. (ed.) R.C. Paulen and I. McMartin; Geological Association of Canada, Short Course Notes, v. 18, p. 125–139.

Averill, S.A., 2011. Viable indicators in surficial sediments for two major base metal deposit types: Ni-Cu-PGE and porphyry Cu; Geochemistry: Exploration, Environment, Analysis, v. 11, p. 279–291.

Averill, S.A. 2013. Discovery and delineation of the Rainy River gold deposit using glacially dispersed gold grains sampled by deep overburden drilling. *in* New Frontiers for Exploration in Glaciated Terrain, (ed.) R.C. Paulen and M.B. McClenaghan, M.B; Geological Survey of Canada, Open File 7374, p. 37–46.

Averill, S.A., 2017. The Blackwater gold-spessartine-pyrolusite dispersal trains, British Columbia, Canada; influence of sampling depth on indicator mineralogy and geochemistry; Geochemistry: Exploration, Environment, Analysis, v. 17, p. 43–60.

Averill, S.A. and Zimmerman, J.R. 1986. The Riddle resolved: the discovery of the Partridge gold zone using sonic drilling in glacial overburden at Waddy Lake, Saskatchewan. Canadian Geology Journal of the Canadian Institute of Mining and Metallurgy, v. 1, p. 14–20.

Bajc, A.F. and Hall, G.E.M., 2000. Geochemical responses of surficial media, North and East ranges, Sudbury Basin; Ontario Geological Survey, Open File Report 6033.

Barnett, P.J., 2007. Overburden geochemical signature of the Lac des Iles platinum group element deposit, northwestern Ontario, Canada; Canadian Journal of Earth Sciences, v. 44, p. 1151–1168.

Barnett, P.J. and Averill, S. 2010. Heavy mineral dispersal trains in till in the area of the Lac des Iles PGE deposit, northwestern Ontario, Canada; Geochemistry: Exploration, Environment, Analysis, v. 10, p. 391-399.

Batterson, M.J., 1989. Glacial dispersal from the Strange Lake alkalic complex, northern Labrador; *in* Drift Prospecting, (ed.) R.N.W. DiLabio and W.B. Coker; Geological Survey of Canada, Paper 89-20, p. 31–40.

Batterson, M.J. and Taylor, D.M., 2009. Geochemical Re-Analysis of Till Samples From the Strange Lake Area, Labrador (NTS Map Sheets 14D/5 and 24A/8); Government of Newfoundland and Labrador, Department of Natural Resources, Geological Survey, Open File LAB/1479.

Beckett-Brown, C.E. and McClenaghan, M.B., 2024. Using indicator minerals to explore for porphyry Cu deposits and their related critical minerals; *in* Till Geochemistry and Indicator Mineral Methods for Exploration in Glaciated Terrains, (ed.) R.C. Paulen and M.B. McClenaghan; Geological Survey of Canada, Open File 9210, p. 147–156. https://doi.org/10.4095/pbmy2d03m0

Beckett-Brown, C.E., McDonald, A.M., and McClenaghan, M.B., 2023a. Recognizing tourmaline in mineralized porphyry copper systems: textures and major-element chemistry; The Canadian Journal of Mineralogy and Petrology, v. 61, p. 3–29.

Beckett-Brown, C.E., McDonald, A.M., and McClenaghan, M.B., 2023b. Trace element characteristics of tourmaline in porphyry copper systems: development and application to discrimination; The Canadian Journal of Mineralogy and Petrology, v. 61, p. 31–60.

Bell, K. and Franklin, J.M., 1993. Application of Pb isotopes to mineral exploration in glacial terrains; Geology, v. 21, p. 1143–1146.

Bell, K. and Murton, J.B., 1995. A new indicator of glacial dispersal: lead isotopes; Quaternary Science Reviews, v. 14, p. 275–287,

Bobrowsky, P.T. and Sibbick, S.J., 1996. Till geochemistry of northern Vancouver Island area. British Columbia Geological Survey Branch, Open File 1996-7.

Bond, J.D., 2001. Quaternary Geology and Till Geochemistry of the Anvil District (parts of 105 K/2, 3, 5, 6 and 7), Central Yukon Territory; Exploration and Geological Services Division, Yukon, Indian and Northern Affairs Canada, Bulletin, 11 p.

Boyle, R.W., 1982. Geochemical prospecting for thorium and uranium deposits; Developments in Economic Geology; Elsevier, New York, 16 p.

Brownscombe, W., Ihlenfeld, C., Coppard, J., Hartshorne, C., Klatt, S., Siikaluoma, J.K., and Herrington, R.J., 2015. The Sakatti Cu-Ni-PGE sulfide deposit in northern Finland; *in* Mineral Deposits of Finland, (ed.) W.D. Maier, R. Lahtinen, and H. O'Brien; Elsevier, Amsterdam, p. 211–252.

Brushett, D.M., Beckett-Brown, C.E., McClenaghan, M.B., Paulen, R.C., Rice, J.M., Haji Egeh, A., and Pelchat, P., 2024a. Till geochemical data for the Brazil Lake pegmatite area, southwest Nova Scotia (NTS 21A/04, 20-O/16 and 20P/13): samples collected in 2020, 2021, and 2022; Geological Survey of Canada, Open File 9148, p. 1 zip file.

Brushett, D.M., Beckett-Brown, C.E., McClenaghan, M.B., Paulen, R.C., and Rice, J.M., 2024b. Lithium signatures in till at the Brazil Lake lithium-cesium-tantalum pegmatites, Nova Scotia; *in* Till Geochemistry and Indicator Mineral Methods for Exploration in Glaciated Terrains, (ed.) R.C. Paulen and M.B. McClenaghan; Geological Survey of Canada, Open File 9210, p. 99–109. https://doi.org/10.4095/pbmy2d03m0

Bustard, A.L., Han, T., and Ferbey, T., 2017. Compiled till geochemical data for British Columbia; British Columbia Ministry of Energy and Mines, British Columbia Geological Survey GeoFile 2017-9, 7 p.

Campbell, J.E., 2009. Drift prospecting for uranium in the Athabasca Basin, Saskatchewan; *in* Application of Till and Stream Sediment Heavy Mineral and Geochemical Methods to Mineral Exploration in Western and Northern Canada, (ed.) R.C. Paulen and I. McMartin; Geological Association of Canada, Short Course Notes 18, p. 207–214.

Campbell, J.E., McMartin, I., McCurdy, M.W., Godbout, P-M., Tremblay, T., and Normandeau, P.X., 2021. Field Data and Till Composition in the GEM-2 Rae Glacial Synthesis Activity Field Areas, Nunavut and Northwest Territories; Geological Survey of Canada, Open File 8808.

Chapman, R.J. and Mortensen, J.K., 2007. Application of microchemical characterization of placer gold grains to exploration for epithermal gold mineralization in regions of poor exposure; Journal of Geochemical Exploration, v. 91, p. 1–26.

Chapman, R.J., Allen, M.M., Mortensen, J.K., Wrighton, T.M., and Grimshaw, M.R., 2018. A new indicator mineral methodology based on a generic Bi-Pb-Te-S mineral inclusion signature in detrital gold from porphyry and epithermal environments in Yukon Territory, Canada; Mineralium Deposita, v. 53, p. 815–834.

Chapman, R.J., Banks, D.A., Styles, M.T., Walshaw, R.D., Piazolo, S., Morgan, D.J., Grimshaw, M.R., Spence-Jones, C.P., Matthews, T.J., and Borovinskaya, O., 2021. Chemical and physical heterogeneity within native gold: implications for the design of gold particle studies; Mineralium Deposita, v. 56, p. 1563–1588.

Chapman, R.J., Mortensen, J.K., Allan, M.M., Walshaw, R.D., Bond, J., and MacWilliam, K., 2022. A new approach to characterizing deposit type using mineral inclusion assemblages in gold particles; Economic Geology, v. 117, p. 361–381.

Clark, J.R. and Williams-Jones, A.E., 2004. Rutile as a potential indicator mineral for metamorphosed metallic ore deposits. Rapport Final de DIVEX, Sous-projet SC2, Montréal, Canada, 17 p.

Coker, W.B. and DiLabio, R.N.W., 1989. Geochemical exploration in glaciated terrain: geochemical responses; *in* Proceedings of Exploration '87, (ed.) G.D. Garland; Ontario Ministry of Northern Development and Mines, Special Volume 3, p. 336–383.

Coker, W.B., Robertson J., and Snow, R.J., 1988. Till geochemistry at the Great Gull scheelite prospects, Newfoundland, Canada: a case history in orientation and discovery; *in* Prospecting in Areas of Glaciated Terrain-1988; Canadian Institute of Mining and Metallurgy, p. 587–598.

Cook, S.J. and Fletcher, W.K., 1992. Distribution and Behavior of Platinum in Soils of the Tulameen Ultramafic Complex, Southern British Columbia; Province of British Columbia, Geological Survey Branch, Paper, 1992-6.

Cook, S.J. and Fletcher, W.K., 1994. Platinum distribution in soil profiles of the Tulameen ultramafic complex, southern British Columbia; Journal of Geochemical Exploration, v. 51, p. 161–191.

Côté-Mantha, O., Gosselin, G., Vaillancourt, D., and Blackburn, A., 2017. The Amaruq deposits – building a customized toolset and using a flexible geomodel: optimization from discovery to mine development; *in* Proceedings of Exploration 17, (ed.) V. Tschirhart and M.D. Thomas; Sixth Decennial International Conference on Mineral Exploration, Toronto, p. 553–567.

de Bronac de Vazelhes, V., Beaudoin, G., McMartin, I., Côté-Mantha, O., and Boulianne-Verschelden, N., 2021. Assessment of the Amaruq gold deposit signature in glacial sediments using multivariate geochemical data analysis and indicator minerals; Journal of Geochemical Exploration, v. 228, p. 1–17.

DiLabio, R.N.W., 1982. Gold and tungsten abundance vs. grain size in till at Waverley, Nova Scotia; *in* Current Research, Part B; Geological Survey of Canada, Paper 82-1B, p. 57–62.

DiLabio, R.N.W. 1988. Residence sites of gold, PGE and rare lithophile elements in till. *in* Prospecting in Areas of Glaciated Terrain-1988, (ed.) D.R. MacDonald and K.A. Mills; Canadian Institute of Mining and Metallurgy, 121–140.

DiLabio, R.N.W., 1990. Classification and interpretation of the shapes and surface textures of gold grains from till on the Canadian Shield; *in* Current Research, Part C; Geological Survey of Canada, Paper, 90-1C, p. 323–329.

Dreimanis, A. and Vagners, U.J., 1971. Bimodal distribution of rock and mineral fragments in basal tills; *in* Till – A Symposium, (ed.) R.P. Goldthwait; Ohio State University Press, p. 237–250.

Duran, C.J., Dubé-Loubert, H., Pagé, P., Barnes, S.J., Roy, M., Savard, D., Cave, B.J., Arguin, J.P., and Mansur, E.T., 2019. Applications of trace element chemistry of pyrite and chalcopyrite in glacial sediments to mineral exploration targeting: Example from the Churchill Province, northern Quebec, Canada; Journal of Geochemical Exploration, v. 196, p. 105–130.

Edén, P. and Björklund, A., 1995. Geochemistry of till in Fennoscandia from ultra-low density sampling; Journal of Geochemical Exploration, v. 52, p. 285–302.

Ferbey, T., Plouffe, A., and Hicken, A.S. (ed.), 2017. Indicator Minerals in Till and Stream Sediments of the Canadian Cordillera; Geological Association of Canada Special Paper Volume, p. 50.

Fipke, C.E., Gurney, J.J., and Moore, R.O., 1995. Diamond exploration techniques emphasising indicator mineral geochemistry and Canadian examples. Geological Survey of Canada, Bulletin 423, 86 p.

Ford, K.L., DiLabio, R.N.W., and Rencz, A.N., 1988. Geological, geophysical and geochemical studies around the Allan Lake carbonatite, Algonquin Park, Ontario; Journal of Geochemical Exploration, 30, p. 99–121.

Friske, P.W.B., McCurdy, M.W., Day, S.J.A., and McNeil, R.J., 2001. Evaluation of partial and selective leach data from humus, B-horizon and till: a case study from the Clarence Stream gold property, southern New Brunswick; Geological Survey of Canada, Current Research 2000, Mineral Resource Report 2001-4, p. 25–45.

Gao, C., Hagedorn, G.W., Crabtree, D.C., Clarke, S.A., Hastie, E.C.G., Launay, G., and Beckett-Brown, C.E., 2023. Determination of indicator minerals in archived fine-fraction non-magnetic heavy mineral concentrate samples using scanning electron microscope energy dispersive spectrometry; *in* Summary of Field Work and Other Activities, 2023; Ontario Geological Survey, Open File Report 6405, p. 21–1 to 21–8.

Garvie, O.G. and Robinson, D.N., 1984. The formation of kelyphite and associated subkelyphitic and sculpted surfaces on pyrope from kimberlite; *in* Proceedings of the Third International Kimberlite Conference, Volume 1, Kimberlites and Related Rocks, Clermont-Ferrand, (ed.) J. Kornprobst; Elsevier, Amsterdam, p. 371–382.

Gaudino, S., Galas, C., Belli, M., Barbizzi, S., de Zorzi, P., Jaćimović, R., Zvonka Jeran, Z., Pati, A., and Sansone, U., 2007. The role of different soil sample digestion methods on trace elements analysis: a comparison of ICP-MS and INAA measurement results; Accreditation and Quality Assurance, v. 12, p. 84–93.

Geddes, R.S., 1982. The Vixen Lake indicator train, northern Saskatchewan; *in* Prospecting in Areas of Glaciated Terrain, (ed.) P.H. Davenport; Canadian Institute Mining Metallurgy, p. 264–283.

Girard, R., Tremblay, J., Néron, A., and Longuépée, H., 2021a. Automated gold grain counting. Part 1: why counts matter!; Minerals, v. 11, p. 337.

Girard, R., Tremblay, J., Néron, A., Longuépée, H., and Makvandi, S., 2021b. Automated gold grain counting, Part 2: what a gold grain size and shape can tell!; Minerals, v. 11, p. 379.

Graves, R.M., MacDonald, M.A., Finck, P.W., and Boner, F.J., 1988. A comparison of the clast composition and geochemistry of granite tills to underlying bedrock in the Halifax Pluton, central Nova Scotia; *in* Prospecting in Areas of Glaciated Terrain-1988, (ed.) D.R. MacDonald; Canadian Institute of Mining and Metallurgy, p. 21–39.

Grenier, A., Connell-Madore, S., McClenaghan, M.B., Wygergangs, M., and Moore, C.S., 2015. Study of cleaning methods for electro-welded sieves to reduce/eliminate carry-over contamination between till samples; Geological Survey of Canada, Open File 7769.

Grütter, H.S., Gurney, J.J., Menzies, A.H., and Winter, F., 2004. An updated classification scheme for mantle-derived garnet, for use by diamond explorers; Lithos, v. 77, p. 841–857.

Hartikainen, A. and Nurmi, P.A., 1993. Till geochemistry in gold exploration in the Late Archean Hattu schist belt, Ilomantsi, eastern Finland; Geological Survey of Finland, Special Paper, v. 17, p. 323–352.

Hashmi, S., Ward, B.C., Plouffe, A., Leybourne, M.I., and Ferbey, T., 2015. Geochemical and mineralogical dispersal in till form the Mount Polley Cu-Au porphyry deposit, central British Columbia, Canada; Geochemistry: Exploration, Environment, Analysis, v. 15, p. 234–249.

Hashmi, S., Leybourne, M.I., Layton-Matthews, D., Hamilton, S., McClenaghan, M.B., and Voinot, A., 2021. Surficial geochemical and mineralogical signatures of Ni-Cu-PGE deposits in glaciated terrain examples from the South Range of the Sudbury Igneous Complex, Ontario, Canada; Ore Geology Reviews, v. 137, p. 104301.

Horwitz, W. and Albert, R., 2006. The Horwitz ratio (HorRat): a useful index of method performance with respect to precision. Journal of AOAC International, v. 89, p.1095–1109.

Hussein, A.A., Lochner, C., and Bell, K., 2003. Application of Pb isotopes to mineral exploration in the Halfmile Lake area, Bathurst, New Brunswick; *in* Massive Sulfide Deposits of the Bathurst Mining Camp, New Brunswick, and Northern Maine, (ed.) W.D. Goodfellow, S.R. McCutcheon, and J.M. Peter; Society of Economic Geologists, Monograph, v. 11, p. 679–688.

Kaszycki, C.A., Nielsen, E., and Gobert, G., 1996. Surficial geochemistry and response to volcanic-hosted massive sulphide mineralization in the Snow Lake region; *in* EXTECH I: A Multidisciplinary Approach to Massive Sulphide Research in the Rusty Lake-Snow Lake Greenstone Belts, Manitoba, (ed.) G.F. Bonham-Carter, A.G. Galley, and G.E.M. Hall; Geological Survey of Canada, Bulletin 426, p. 139–154.

Kelley, K.D., Eppinger, R.G., Lang, J., Smith, S.M., and Fey, D.L., 2011. Porphyry Cu indicator minerals in till as an exploration tool: example from the giant Pebble porphyry Cu-Au-Mo deposit, Alaska, USA; Geochemistry: Exploration, Environment, Analysis, v. 11, p. 321–334.

Kjarsgaard, B.A, Knight, R.D., Grunsky, E.C., Kerr, D.E., Sharpe, D.R., Cummings, D.I., Russell, H.A.J., Kerswill, J.A., and Wright, D.F., 2013a. Till geochemistry studies of the Thaidene Nene MERA study area; Chapter 10 *in* Mineral and Energy Resources Assessment for the Proposed Thaidene Nene National Park Reserve in the Area of the East Arm of Great Slave Lake, Northwest Territories, (ed.) D.F. Wright, E.J. Ambrose, D. Lemkow, and G.F. Bonham-Carter; Geological Survey of Canada, Open File 7196, p. 313–337.

Kjarsgaard, B.A., Knight, R.D., Plourde, A.P., Sharpe D.R., and Lesemann J-E., 2013b. Geochemistry of till samples, NTS 75-I, 75-J, 75-O, 75-P (Mary Frances Lake – Whitefish Lake – Thelon River area) Northwest Territories; Geological Survey of Canada, Open File 7351.

Klassen, R.W., 2003. The geochemical and physical properties of till, Bathurst Mining Camp, New Brunswick, Canada; *in* Massive Sulfide Deposits of the Bathurst Mining Camp, New Brunswick, and Northern Maine, (ed.) W.D. Goodfellow, S.R. McCutcheon, and J.M. Peter; Society of Economic Geologists, Monograph 11, p. 661–678.

Knight, R.D., Kjarsgaard, B.A., and Russell, H.A.J., 2021. An analytical protocol for determining the elemental chemistry of Quaternary sediments using a portable X-ray fluorescence spectrometer; Applied Geochemistry, v. 131, p. 105026.

Koljonen, T., Gustavsson, N., Noras, P., and Tanskanen, H., 1992a. Description of elements and geochemical maps; *in* The Geochemical Atlas of Finland, Part 2: Till, (ed.) T. Koljonen; Geological Survey of Finland, Espoo, p. 143–216.

Koljonen, T., Gustavsson, N., Noras, P., and Tanskanen, H., 1992b. Sampling, analysis, and data processing; *in* The Geochemical Atlas of Finland Part 2: Till, (ed.) T. Koljonen; Geological Survey of Finland, Espoo, p. 15–28.

Lahtinen, R., Lestinen, P., and Savolainen, H., 1993. The use of total and partial dissolution till geochemical data in delineating favorable areas for Ni prospects: an example from the Tampere-Hämeenlinna area, southern Finland; Geological Survey of Finland, Special Paper 18, p. 107–111.

Layton-Matthews, D., and McClenaghan, M.B., 2022. Current techniques and applications of mineral chemistry to mineral exploration; Minerals, v. 12, p. 59.

Lee, R.G., Plouffe, A., Ferbey, T. Hart, C.J.R., Hollings, P. and Gleeson, S.A., 2021. Recognizing porphyry copper potential from till zircon composition: a case study from the Highland Valley porphyry district, south-central British Columbia. Economic Geology, v. 116, p. 1035–1045.

Lehtonen, M.L., Marmo, J.S., Nissinen, A.J., Johanson, B.S., and Pakkanen, L.K., 2005. Glacial dispersal studies using indicator minerals and till geochemistry around two eastern Finland kimberlites; Journal of Geochemical Exploration, v. 87, p. 19–43.

Lehtonen, M., Laukkanen, J., and Sarala, P., 2011. Exploring RE and REE mineralization using indicator minerals; *in* Indicator Mineral Methods in Mineral Exploration, Workshop 3; Association of Applied Geochemists, Rovaniemi, Finland, p. 13–18.

Lehtonen, M.L., Lahaye, Y., O'Brien, H., Lukkari, S., Marmo, J.S., and Sarala, P., 2015. Novel technologies for indicator mineral-based exploration; Geological Survey of Finland, Special Paper 57, p. 23–62.

Lemière, B., 2018. A review of pXRF (field portable X-ray fluorescence) applications for applied geochemistry; Journal of Geochemical Exploration, v. 188, p. 350–363.

Lestinen, P., Kontas, E., Niskavaara, H., and Virtasalo, J., 1991. Till geochemistry of gold, arsenic and antimony in the Seinäjoki district, western Finland; Journal of Geochemical Exploration, v. 39, p. 343–361.

Lett, R.E., 1995. Analytical methods for drift; *in* Drift Exploration in the Canadian Cordillera, British Columbia, (ed.) P.T. Bobrowsky, S.J. Sibbick, J.M. Newell, and P.F. Matysek; British Columbia Ministry of Energy, Mines and Petroleum Resources, Paper 1995-2, p. 215–228.

Lett, R.E., 2001. Geochemical signatures around massive sulphide deposits in southern British Columbia, Canada; *in* Drift Exploration in Glaciated Terrain, (ed.) M.B. McClenaghan, P.T. Bobrowsky, G.E.M. Hall, and S.J. Cook; Geological Society of London, Special Publication 185, p. 301–322.

Lett, R.E., 2008. British Columbia till geochemical survey data; British Columbia Ministry of Energy, Mines and Housing, Open File 2008-13.

Lett, R.E. and Jackaman, W., 2002. Geochemical Exploration Models, Volume 1. VMS Deposits in South-Central British Columbia (NTS 82L/13, L/14, 82 M/4. M/5, M/6 and 92P/1E); British Columbia Ministry of Energy, Mines and Petroleum Resources, Open File 2000-31.

Lett, R.E. and Rukhlov, A.S., 2017. Review of analytical methods for regional geochemical (RGS) programs in the Canadian Cordillera; *in* Indicator Minerals in Till and Stream Sediments of the Canadian Cordillera, (ed.) T. Ferbey, A. Plouffe, and A.S. Hicken; Geological Association of Canada, Special Paper Volume 50, p. 53–108.

Lisboa, L.H.D., Ferreira Filho, C.F., Monteiro, L.V.S., and Mansur, E.T., 2023. Gahnite, garnet and magnetite compositions of metamorphosed sediment-hosted Zn-Pb-(CuAg) deposits of the Mesoproterozoic Nova Brasilândia Group: Vectors for SEDEX deposits with Broken Hill-type affinities in the western Amazonian Craton, Brazil; Journal of Geochemical Exploration, v. 249, p. 107210.

Lougheed, H.D., McClenaghan, M.B., Layton-Matthews, D., and Leybourne, M., 2020. Exploration potential of fine-fraction heavy mineral concentrates from till using automated mineralogy: a case study from the Izok Lake Cu–Zn–Pb–Ag VMS Deposit, Nunavut, Canada; Minerals, v. 10, p. 310.

Lougheed, D., McClenaghan, M.B., Layton-Matthews, D., Leybourne, M.I., and Dobosz, A.N., 2021. Automated indicator

mineral analysis of fine-grained till associated with the Sisson W-Mo Deposit, New Brunswick, Canada; Minerals, v. 11, p. 103.

Lypaczewski, P., Normandeau, P.X., Paquette, J., and McMartin, I., 2013. Petrographic and cathodoluminescence characterization of apatite from the Sue-Dianne and Brooke IOCG mineralization systems, Great Bear magmatic zone, Northwest Territories; Geological Survey of Canada, Open File 7319.

Mackay, D.A.R. and Simandl, G.J. 2015. Pyrochlore and columbite-tantalite as indicator minerals for specialty metal deposits. Geochemistry: Exploration, Environment, Analysis, v. 15, p. 167–178.

Mackay, D.A.R., Simandl, G.J., Ma, W., Redfearn, J., and Gravel, J., 2016. Indicator mineral-based exploration for carbonatites and related specialty metal deposits – A QEMSCAN® orientation survey, British Columbia, Canada; Journal of Geochemical Exploration, v. 165, p. 159–173.

Makin, S.A., Simandl, G.J., and Marshall, D., 2014. Fluorite and its potential as an indicator mineral for carbonatite-related rare earth element deposits; *in* Geological Fieldwork 2013; British Columbia Ministry of Energy and Mines, British Columbia Geological Survey Paper, 2014-1, p. 207–212.

Makvandi, S., Beaudoin, G., McClenaghan, M.B., and Layton-Matthews, D., 2015. The surface texture and morphology of magnetite from the Izok Lake volcanogenic massive sulfide deposit and local glacial sediments, Nunavut, Canada: application to mineral exploration; Journal of Geochemical Exploration, v. 150, p. 84–103.

Makvandi, S., Ghasemzadeh-Barvarz, M., Beaudoin, G., Grunsky, E.C., McClenaghan, M.B., and Duchesne, C., 2016. Principal component analysis of magnetite composition from volcanogenic massive sulphide deposits: case studies from the Izok Lake (Nunavut, Canada) and Halfmile Lake (New Brunswick, Canada) deposits; Ore Geology Reviews, v. 72, p. 60–85.

Makvandi, S., Pagé, P., Tremblay, J., and Girard, R., 2021. Exploration for Platinum-Group Minerals in till: a new approach to the recovery, counting, mineral identification and chemical characterization; Minerals, v. 11, p. 264.

Manéglia, N., Beaudoin, G., and Simard, M., 2018. Indicator minerals of the Meliadine orogenic gold deposits, Nunavut (Canada), and application to till surveys; Geochemistry: Exploration, Environment, Analysis, v. 18, p. 241–251.

Mao, M., Rukhlov, A.S., Rowins, S.M., Spence, J., and Coogan, L.A., 2016. Apatite trace element compositions: A robust new tool for mineral exploration; Economic Geology, v. 111(5), p. 1187–1222.

Mao, M., Rukhlov, A.S., Rowins, S.M., Hickin, A.S., Ferbey, T., Bustard, A., Spence, J. and Coogan, L.A., 2017. A novel approach using detrital apatite and till geochemistry to identify covered mineralization in the TREK areas of the Nechako Plateau, British Columbia; *in* Indicator Minerals in Till and Stream Sediments of the Canadian Cordillera, (ed.) T. Ferbey, A. Plouffe, and A.S. Hicken; Geological Association of Canada, Special Paper 50, p. 191–243.

Marsden, J. and House, I. 2006. The chemistry of gold extraction; Society for Mining, Metallurgy, and Exploration, Inc. 680 p.

McCandless, T.E., 1990. Kimberlite xenocryst wear in high-energy fluvial systems: experimental studies; Journal of Geochemical Exploration, v. 37, p. 323–331.

McClenaghan, M.B. 2001. Regional and local-scale gold grain till geochemical signatures of lode Au deposits in the western Abitibi Greenstone Belt, central Canada. *in* Drift Exploration in Glaciated Terrain, (ed.) M.B. McClenaghan, P.T. Bobrowsky, G.E.M. Hall, and S. Cook; Geological Society of London, Special Publication 185, p. 201–223.

McClenaghan, M.B. and Cabri, L.J., 2011. Gold and platinum group element indicator minerals in surficial sediments; Geochemistry: Exploration, Environment, Analysis, v. 11, p. 251–263.

McClenaghan, M.B. and Kjarsgaard, B.A., 2001. Indicator mineral and geochemical methods for diamond exploration in glaciated terrain in Canada; Geological Society, London, Special Publication 185, p. 83–123,

McClenaghan, M.B. and Kjarsgaard, B.A., 2007. Indicator mineral and surficial geochemical exploration methods for kimberlite in glaciated terrain: examples from Canada; *in* Mineral Deposits of Canada: A Synthesis of Major Deposit Types, District Metallogeny, the Evolution of Geological Provinces, and Exploration Methods, (ed.) W.D. Goodfellow; Geological Association of Canada, Mineral Deposits Division, Special Publication 5, p. 983–1006.

McClenaghan, M.B. and Peter, J.M., 2013. Till geochemical signatures of volcanogenic massive sulphide deposits in glaciated terrain: a summary of Canadian examples; Geological Survey of Canada, Open File 7354.

McClenaghan, M.B. and Peter, J.M., 2016. Till geochemical signatures of volcanogenic massive sulfide deposits: an overview of Canadian examples; Geochemistry: Exploration, Environment, Analysis, v. 16, p. 27–47.

McClenaghan, M.B., Kjarsgaard, I.M., Schulze, D.J., Stirling, J.A.R., Pringle, G., and Berger, B.R., 1996. Mineralogy and geochemistry of the B30 kimberlite and overlying glacial sediments, Kirkland Lake, Ontario; Geological Survey of Canada, Open File 3295.

McClenaghan, M.B., Kjarsgaard, I.M., Stirling, J.A.R., Pringle, G., Kjarsgaard, B.A., and Berger, B.R., 1999a. Mineralogy and geochemistry of the C14 kimberlite and associated glacial sediments, Kirkland Lake, Ontario; Geological Survey of Canada, Open File 3719.

McClenaghan, M.B., Kjarsgaard, I.M., Kjarsgaard, B.A., Stirling, J.A.R., Pringle, G., and Berger, B.R., 1999b. Mineralogy and geochemistry of the A4 kimberlite and associated glacial sediments, Kirkland Lake, Ontario; Geological Survey of Canada, Open File 3769.

McClenaghan, M.B., Thorleifson, L.H., and DiLabio, R.N.W., 2000. Till geochemical and indicator mineral methods in mineral exploration; Ore Geology Reviews, v. 16, p. 145–166.

McClenaghan, M.B., Bobrowsky, P.T., Hall, G.E.M., and Cook, S.J. (ed.), 2001. Drift Exploration in Glaciated Terrain; Geological Society, London, Special Publications, v. 185.

McClenaghan, M.B., Ward, B.C., Kjarsgaard, I.M., Kjarsgaard, B.A., Kerr, D.E., and Dredge, L.A., 2002. Indicator mineral and till geochemical dispersal patterns associated with the Ranch Lake kimberlite, Lac de Gras region, NWT, Canada; Geochemistry: Exploration, Environment, Analysis, v. 2, p. 299–320.

McClenaghan, M.B., Matile, G., Layton-Matthews, D., and Pyne, M., 2009. Till Geochemical Signatures of Magmatic Ni-Cu Deposits and Regional Till Geochemistry, Thompson Nickel Belt, Manitoba; Geological Survey of Canada, Open File 6005.

McClenaghan, M.B., Layton-Matthews, D., and Matile, G., 2011. Till geochemical signatures of magmatic Ni-Cu deposits, Thompson Nickel Belt, Manitoba, Canada; Geochemistry: Exploration, Environment, Analysis, v. 11, p. 145–159.

McClenaghan, M.B., Kjarsgaard, I.M., Averill, S.A., Layton-Matthews, D., Crabtree, D., Matile, G., McMartin, I., and Pyne, M., 2013. Indicator Mineral Signatures of Magmatic Ni-Cu Deposits, Thompson Nickel Belt, Manitoba Part 2– Till Data; Geological Survey of Canada, Open File 7200.

McClenaghan, M.B., Seaman, A.A., Parkhill, M. A., and Pronk, A.G., 2014a. Till geochemical signatures associated with the

Sisson W-Mo deposit, New Brunswick, Canada; Atlantic Geology, v. 50, p. 116–137.

McClenaghan, M.B., Parkhill, M.A., Seaman, A.A., Pronk, A.G., Averill, S.A., Rice, J.M., and Pyne, M., 2014b. Indicator Mineral Signatures of the Sisson W-Mo Deposit, New Brunswick, Part 2 Till; Geological Survey of Canada, Open File 7467.

McClenaghan, M.B., Paulen, R.C., Layton-Matthews, D., Hicken, A.K., and Averill, S.A., 2015a. Glacial dispersal of gahnite from the Izok Lake Zn-Cu-Pb-Ag VMS deposit, northern Canada; Geochemistry: Exploration, Environment, Analysis, v. 15, p. 333–349.

McClenaghan, M.B., Peter, J.M., and Layton-Matthews, D., 2015b. Overview of VMS exploration in glaciated terrain using indicator minerals, till geochemistry and boulder tracing: a Canadian perspective; *in* Targeted Geoscience Initiative 4: Contributions to the understanding of volcanogenic massive sulphide deposit genesis and exploration methods development, (ed.) J.M. Peter and P. Mercier-Langevin; Geological Survey of Canada, Open File 7853, p. 81–89.

McClenaghan, M.B., Parkhill, M.A., Pronk, A.G., and Sinclair, W.D., 2016. Indicator mineral signatures of Sn-W deposits: examples from the Mount Pleasant Sn-W-Mo-Bi-In deposit, New Brunswick, Canada; Journal of Geochemical Exploration, v. 172, p. 151–166.

McClenaghan, M.B., Parkhill, M.A., Pronk, A.G., Seaman, A.A., McCurdy, M., and Leybourne, M.I., 2017a. Indicator mineral and geochemical signatures associated with the Sisson W-Mo deposit, New Brunswick, Canada; Geochemistry: Exploration, Environment, Analysis, v. 17, p. 297–313.

McClenaghan, M.B., Budulan, G., Parkhill, M.A., Layton-Matthews, D., and Crabtree, D., 2017b. Indicator Mineral Signatures of the Halfmile Lake Zn-Pb-Cu Volcanogenic Massive Sulphide Deposit, Bathurst, New Brunswick: Part 2 – Till Data; Geological Survey of Canada, Open File 8111.

McClenaghan, M.B., Paulen, R.C., and Oviatt, N.M., 2018. Geometry of indicator mineral and till geochemistry dispersal fans from the Pine Point Mississippi Valley-type Pb-Zn district, Northwest Territories, Canada; Journal of Geochemical Exploration, v. 190, p. 69–86.

McClenaghan, M.B., Paulen, R.C., and Kjarsgaard, I.M., 2019. Rare metal indicator minerals in bedrock and till at the Strange Lake peralkaline complex, Quebec and Labrador, Canada; Canadian Journal of Earth Sciences, v. 56, p. 857–869.

McClenaghan, M.B., Spirito, W.A., Plouffe, A., McMartin, I., Campbell, J.E., Paulen, R.C., Garrett, R.G., Hall, G.E.M., Pelchat, P., and Gauthier, M.S., 2020. Geological Survey of Canada till-sampling and analytical protocols: from field to archive, 2020 update; Geological Survey of Canada, Open File 8591, 1 zip file.

McClenaghan, M.B., Paulen, R.C., Smith, I.R., Rice, J.M., Plouffe, A., McMartin, I., Campbell, J.E., Lehtonen, M., Parsasadr, M., and Beckett-Brown, C.E., 2023a. Review of till geochemistry and indicator mineral methods for mineral exploration in glaciated terrain; Geochemistry: Exploration, Environment, Analysis, v. 23, p. 1–43.

McClenaghan, M.B., Beckett-Brown, C.E., McCurdy, M.W., and Casselman, S.G., 2023b. Stream sediment indicator mineral signatures of the Casino porphyry Cu-Au-Mo deposit, Yukon, Canada; Economic Geology, v. 118, p. 411–431.

McClenaghan, M.B., Brushett, D.M., Beckett-Brown, C.E., Paulen, R.C., Rice, J.M., Haji Egeh, A., and Nissen, A., 2023c. Indicator mineral studies at the Brazil Lake LCT pegmatites, southwest Nova Scotia; Geological Survey of Canada, Scientific Presentation 157. https://doi.org/10.4095/331686

McMartin, I., 2009. Till composition along the Meliadine Trend near Rankin Inlet, Nunavut: applications to gold exploration in permafrost terrain; *in* Application of Till and Stream Sediment Heavy Mineral and Geochemical Methods to Mineral Exploration in Western and Northern Canada, (ed.) R.C. Paulen and I. McMartin; Geological Association of Canada, Short Course Notes 18, p. 153–166.

McMartin, I., Corriveau, L., and Beaudoin, G. 2009. Heavy mineral and till geochemical signatures of the NICO Co-Au-Bi deposit, Great Bear magmatic zone, Northwest Territories, Canada; *in* Proceedings, Volume II, (ed.) D.R. Lentz, KG. Thorne, and K.-L. Beal; 24th International Applied Geochemistry Symposium, Fredericton, New Brunswick, p. 573–576. https://www.appliedgeochemists.org/images/stories/IAGS_2009/24th_IAGS_Abstracts_Vol2_ALL_revised.pdf

McMartin, I., Corriveau, L., Beaudoin, G., Averill, S.A., and Kjarsgaard, I., 2011. Results from an Orientation Study of the Heavy Mineral and Till Geochemical Signatures of the NICO Au-Co-Bi Deposit, Great Bear Magmatic Zone, Northwest Territories, Canada; Geological Survey of Canada, Open File 6723.

McMartin, I., Randour, I. and Wodicka, N. 2019. Till composition across the Keewatin Ice Divide in the Tehery-Wager GEM-2 Rae project area, Nunavut; Geological Survey of Canada, Open File 8563.

Morris, T.F., Breaks, F.W., Averill, S.A., Crabtree, D.C., and McDonald, A., 1997. Gahnite composition: Implications for base metal and rare-element exploration; Exploration and Mining Geology, v. 6, p. 253–260.

Nevalainen, R., 1989. Lithology of Fine Till Fractions in the Kuhmo Greenstone Belt Area, Eastern Finland; Geological Survey of Finland, Special Paper 7, p. 59–65.

Nikkarinen, M. and Bjorklund, A., 1975. The use of till in spodumene exploration; Journal of Geochemical Exploration, v. 5, p. 212–214.

Nikkarinen, M. and Bjorklund, A., 1976. Kautinen: The use of till in tungsten prospecting; Journal of Geochemical Exploration, v. 5, p. 247–248.

Nikkarinen, M., Kallio, E., Lestinen, P., and Äyräs, M., 1984. Mode of occurrence of copper and zinc in till over three mineralized areas in Finland; Journal of Geochemical Exploration, v. 21, p. 239–247.

Normandeau, P., Harlov, D.E., Corriveau, L., Paquette, J., and McMartin, I., 2018. Characterization of fluorapatite within iron oxide alkali-calcic alteration systems of the Great Bear magmatic zone: a potential metasomatic process record; The Canadian Mineralogist, v. 56, p. 167–187.

Olsson, M., Rosén, K., and Melkerud, P.A., 1993. Regional modelling of base cation losses from Swedish forest soils due to whole-tree harvesting; Applied geochemistry, v. 8, p. 189–194.

Oviatt, N.M., Gleeson, S.A., Paulen, R.C., McClenaghan, M.B., and Paradis, S., 2015. Characterization and dispersal of indicator minerals associated with the Pine Point Mississippi Valley-type (MVT) district, Northwest Territories, Canada; Canadian Journal of Earth Sciences, v. 52, p. 776–794.

Parkhill, M.A., and Doiron, A., 2003. Quaternary geology of the Bathurst Mining Camp and implications for base metal exploration using drift prospecting; *in* Massive Sulfide Deposits of the Bathurst Mining Camp, New Brunswick and Northern Maine, (ed.) W.D. Goodfellow, S.R. McCutcheon, and J.M. Peter; Society of Economic Geologists, Monograph 11, p. 631–660.

Paulen, R.C., Paradis, S., Plouffe, A., and Smith, I.R., 2011. Pb and S isotopic composition of indicator minerals in glacial sediments from NW Alberta, Canada: implications for Zn-Pb base

metal exploration; Geochemistry: Exploration, Environment, Analysis, v. 11, p. 309–320.

Paulen, R.C., Mulligan, R.P.M., and Rice, J.M., 2024. Determination of glacial transport directions; *in* Till Geochemistry and Indicator Mineral Methods for Exploration in Glaciated Terrains, (ed.) R.C. Paulen and M.B. McClenaghan; Geological Survey of Canada, Open File 9210, p. 10–23. https://doi.org/10.4095/pbmy2d03m0

Pell, J., Grütter, H., Neilson, S., Lockhart, G., Dempsey, S. and Grenon, H., 2013. Exploration and discovery of the Chidliak Kimberlite Province, Baffin Island, Nunavut: Canada's newest diamond district; *in* Proceedings of 10th International Kimberlite Conference, v. 2, (ed.) D.G. Pearson et al.; Special Issue of the Journal of the Geological Society of India, p. 209–227.

Peltonen, P., Huhta, P., and Korsman, K., 1992. Occurrence and Mineral Chemistry of Chrome Spinel in Till- Implications for Prospecting for Magmatic Ni-Cu Sulfide Ores in Svecofennian Terrain; Geological Survey of Finland, Report of Investigation 111.

Pisiak, L.K., Canil, D., Lacourse, T., Plouffe, A. and Ferbey, T. 2017.Magnetite as an indicator mineral in the exploration of porphyry deposits: a case study in till near the Mount Polley Cu-Au deposit, British Columbia, Canada; Economic Geology, v. 112, p. 919–940.

Pizarro, H., Rousse, S., Bouzari, F., Bissig, T., Gregoire, M., Riquelme, R., Carretier, S., Townley, B., Hoareau, G., and Mpodozis, C., 2024. Use of porphyry indicator zircons (PIZs) in the sedimentary record as an exploration tool for covered porphyry copper deposits in the Atacama Desert, Chile; Journal of Geochemical Exploration, v. 256, p.107351.

Plouffe, A. 2001. The glacial transport and physical partitioning of mercury and gold in till: implications for mineral exploration with examples from central British Columbia. *in* Drift Exploration in Glaciated Terrain, (ed.) M.B. McClenaghan, P.T. Bobrowsky, G.E.M. Hall, and S.J. Cook; The Geological Society, Special Publication No. 185, 287–299.

Plouffe, A., Paulen, R.C., and Smith, I.R., 2006. Indicator mineral content and geochemistry of glacial sediments from northwest Alberta (NTS 84L, M): new opportunities for mineral exploration; Geological Survey of Canada, Open File 5121, Alberta Energy and Utilities Board, Special Report 77, CD-ROM.

Plouffe, A., Ferbey, T., Hashmi. S., and Ward, B.C., 2016. Till geochemistry and mineralogy: vectoring towards Cu porphyry deposits in British Columbia, Canada; Geochemistry: Exploration, Environment, Analysis, v. 16, p. 213–232.

Plouffe, A., Kjarsgaard, I.M. Ferbey, T., Wilton, D.H.C., Petts, D.C., Percival, J.B., Kobylinski, C.H., and McNeil, R., 2022. Detecting buried porphyry Cu mineralization in a glaciated landscape: a case study from the Gibraltar Cu-Mo deposit, British Columbia, Canada; Economic Geology, v. 117, p. 777–799.

Poulin, R.S., McDonald, A.M., Kontak, D.J., and McClenaghan, M.B., 2016. On the relationship between cathodoluminescence and the chemical composition of scheelite from geologically diverse ore deposit discriminator using its trace element and REE chemistry; The Canadian Mineralogist, v. 56, p. 265–302.

Poulin, R.S., McDonald, A.M., Kontak, D.J., and McClenaghan, M.B., 2018. Assessing scheelite ore-deposit environments; The Canadian Mineralogist, v. 54, p. 1147–1173.

Rice, J. and McClenaghan, M.B., 2024. Dirt detectives: Unravelling buried mineral potential with advanced till sampling techniques; *in* Till Geochemistry and Indicator Mineral Methods for Exploration in Glaciated Terrains, (ed.) R.C. Paulen and M.B. McClenaghan; Geological Survey of Canada, Open File 9210, p. 24–34. https://doi.org/10.4095/pbmy2d03m0

Ross, M., 2024. Glacial dynamics and glacial sediment dispersal explained; *in* Till Geochemistry and Indicator Mineral Methods for Exploration in Glaciated Terrains, (ed.) R.C. Paulen and M.B. McClenaghan; Geological Survey of Canada, Open File 9210, p. 4–9. https://doi.org/10.4095/pbmy2d03m0

Rukhlov, A.S. and Ferbey, T., 2015. Application of Lead Isotopes in Till for Mineral Exploration: A Simplified Method Using ICP-MS; British Columbia Geological Survey, Paper, 2015-2.

Salminen, R. and Hartikainen, A. 1985. Glacial transport of till and its influence on interpretation of geochemical results in North Karelia, Finland; Geological Survey of Finland, Bulletin 335.

Sappin, A.-A., Dupuis, C., Beaudoin, G., McMartin, I., and McClenaghan, M.B., 2014. Optimal ferromagnetic fraction in till samples along ice-flow paths: case studies from the Sue-Dianne and Thompson deposits, Canada; Geochemistry: Exploration, Environment, Analysis, v. 14, p. 315–329.

Salama, W., Anand, R., and Roberts, M., 2018. Cassiterite and rutile as indicator minerals for exploring the VMS system; ASEG Extended Abstracts, 2018(1), p. 1–4.

Sarala, P., 2005. Till geochemistry in the ribbed moraine area of Peräpohjola, Finland; Applied Geochemistry, v. 20, p. 1714–1736.

Sarala, P., 2016. Comparison of different portable XRF methods for determining till geochemistry; Geochemistry: Exploration, Environment, Analysis, v. 16, p. 181–192.

Sarala, P., Pulkkinen, E., Ojala, J.V., and Peltoniemi-Taivalkoski, A., 2009. Gold exploration using till at Petäjälehto, northern Finland; Geochemistry: Exploration, Environment, Analysis, v. 9, p. 247–255.

Sarala, P., Taivalkoski, A., and Valkama, J., 2015. Portable XRF: an advanced on-site analysis method in till geochemical exploration; *in* New Technologies for Greenfield Exploration, (ed.) P. Sarala; Geological Survey of Finland, Paper, v. 57, p. 63–86.

Sarapää, O. and Sarala, P., 2013. Rare earth element and gold exploration in glaciated terrain: example from the Mäkärä area, northern Finland; Geochemistry: Exploration, Environment, Analysis, v. 13, p. 131–143.

Sauramo, M., 1924. Tracing of glacial boulders and its application in prospecting; Bulletin de la Commission géologique de Finlande, No. 67, p. 5–37.

Schlegel, T.U., Wagner, T., and Fusswinkel, T., 2020. Fluorite as indicator mineral in iron oxide-copper-gold systems: explaining the IOCG deposit diversity; Chemical Geology, v. 548, p.119674.

Sciuba, M. and Beaudoin, G., 2021. Texture and trace element composition of rutile in orogenic gold deposits; Economic Geology, v. 116, p. 1865–1892.

Sciuba, M., Beaudoin, G., Grzela, D., and Makvandi, S., 2020. Trace element composition of scheelite in orogenic gold deposits; Mineralium Deposita, v. 55, p.1149–1172.

Sciuba, M., Beaudoin, G., and Makvandi, S., 2021. Chemical composition of tourmaline in orogenic gold deposits; Mineralium Deposita, v. 56, p. 537–560.

Scott, K.M., 2005. Rutile geochemistry as a guide to porphyry Cu–Au mineralization, Northparkes, New South Wales, Australia. Geochemistry: Exploration, Environment, Analysis, v. 5, p. 247–253.

Shilts, W.W., 1977. Geochemistry of till in perennially frozen terrain of the Canadian Shield - application to prospecting; Boreas, v. 6, p. 203–212.

Shilts, W.W., 1993. Geological Survey of Canada's contributions to understanding the composition of glacial sediments; Canadian Journal of Earth Sciences, v. 30, p. 333–353.

Shilts, W.W., 1995. Geochemical partitioning in till; *in* Drift Exploration in the Canadian Cordillera, (ed.) P.T. Bobrowsky,

S.J. Sibbick, J.M. Newell, and P.F. Matysek; British Columbia Ministry of Energy, Mines and Petroleum Resources, Paper 1995-2, p. 149–163.

Shilts, W.W., 1996. Drift exploration; *in* Past Glacial Environments: Sediments, Forms and Techniques, (ed.) J. Menzies; Butterworth-Heinemann Ltd, Oxford, p. 411–439.

Sibbick, S.J., Balma, R.G., and Dunn, C.E., 1997. Till Geochemistry of the Mount Milligan Area (Parts of 93N/1 and 93O/4); British Columbia Geological Survey, Open File 1996–22.

Simonetti, A., Bell, K., and Hall, G.E.M., 1996. Pb isotopic ratios and elemental abundances for selective leachates from near-surface till: implications for mineral exploration; Applied Geochemistry, v. 11, p. 721–734.

Simpson, M.A. and Sopuck, V.J., 1983. Till geochemistry near the Midwest uranium deposit; in Uranium Exploration in the Athabasca Basin, (ed.) E.M. Cameron; Geological Survey of Canada, Paper 82-11, p. 207–214.

Snow, R.J. and Coker, W.B. 1987. Overburden geochemistry related to W-Cu-Mo mineralization at Sisson Brook, New Brunswick, Canada: an example of short- and long-distance glacial dispersal; *in* Geochemical Exploration 1985, (ed.) R.G. Garrett; Journal of Geochemical Exploration, v. 28, p. 353–368

Stea, R.R. and Pe Piper, G., 1999. Using whole rock geochemistry to locate the source of igneous erratics from drumlins on the Atlantic coast of Nova Scotia; Boreas, v. 28, p. 308–325.

Sylvester, P.J. and Jackson, S.E. (ed.), 2016. Studying the Earth with LA-ICP-MS; Elements Magazine, v.12(5).

Tarvainen, T., 1995. The geochemical correlation between coarse and fine fractions of till in southern Finland; Journal of Geochemical Exploration, v. 54, p. 187–198.

Tarvainen, T., Aatos, S., and Räisänen, M.-L., 1996. A method for determining the normative mineralogy of tills; Applied Geochemistry, v. 11, p. 117–120.

van Geffen, P.W.G., Kyser, T.K., Oates, C.J., and Ihlenfeld, C., 2013. Lead isotope ratios in till and vegetation over a VMS occurrence under significant allochthonous cover; Geochemistry: Exploration, Environment, Analysis, v. 13, p. 53–61.

Villas-Boas, P.R., Franco, M.A.D.M., Martin Neto, L., Gollany, H.T., and Milori, D.M.B.P., 2019. Applications of laser-induced breakdown spectroscopy for soil analysis, part II: Review of Elemental Analysis and Soil Classification; European Journal of Soil Science, p. 1–43.

Villas-Boas, P.R., Franco, M.A., Martin-Neto, L., Gollany, H.T., and Milori, D.M., 2020. Applications of laser-induced breakdown spectroscopy for soil analysis, part I: Review of fundamentals and chemical and physical properties; European Journal of Soil Science, v. 71, p. 789-804.

Ward, L.A., Holwell, D.A., Barry, T.L., Blanks, D.E. and Graham, S.D., 2018. The use of magnetite as a geochemical indicator in the exploration for magmatic Ni-Cu-PGE sulfide deposits: A case study from Munali, Zambia; Journal of Geochemical Exploration, v. 188, p.172–184.

Wittkop, C., Bartley, J.K., Krueger, R., Bouvier, A., Georg, R.B., Knaeble, A.R., Clair, K.S., Piper, C., and Breckenridge, A., 2020. Influence of provenance and transport process on the geochemistry and radiogenic (Hf, Nd, and Sr) isotopic composition of Pleistocene glacial sediments, Minnesota, USA; Chemical Geology, v. 532, p. 119390.

Tower Resources' rapid discovery from scratch, via glacially dispersed gold grains, of the Lightning and Thunder Au zones within the intensely explored Kamloops district: A recipe for effectively exploring the till-covered Interior Plateau of British Columbia

S.A. Averill

Overburden Drilling Management Limited, 15 Capella Court, Unit 107, Ottawa, ON, K2E 7X1

The Interior Plateau of the Canadian Cordillera in British Columbia (Fig. 1) is well endowed with mineral deposits, including world-class porphyry Cu±Mo±Au deposits such as Highland Valley and Gibraltar. However, bedrock on the plateau is extensively covered by glacial sediments, mostly till, left from the meltdown of the Cordilleran Ice Sheet ~10,000 years ago.

The terrain on the plateau is rolling, with rocky ridges separated by broader valleys. Historically, mineral exploration has focused on the ridges where the till cover is thin and the bedrock is well exposed. This practice has left many opportunities for discovering mineral deposits hidden beneath the till on the lower slopes and valley bottoms by applying modern exploration methods designed for this purpose. One method is to sample the till directly for anomalous concentrations of glacially dispersed, deposit-specific indicator mineral grains such as gold.

Till indicator mineral sampling has been applied successfully for decades in exploration programs in Precambrian terranes in other parts of Canada but only a few companies have utilized it in the Mesozoic porphyry belt in the B.C. interior despite its efficacy having been well documented by government demonstration surveys at several Late Triassic porphyry deposits (e.g. Plouffe and Ferbey, 2016; Plouffe et al., 2016) and a comprehensive exploration case history at the Early Cretaceous, volcanic-associated Blackwater Au-Ag deposit (Averill, 2017). One company that has successfully adopted till indicator mineral sampling is Tower Resources Ltd. ("Tower"), a junior B.C. exploration company that focuses specifically on till-covered lowlands below outcropping ridges with historical Au and/or Cu-Au showings suggestive of large mineralized systems that could extend into the lowlands. Tower has shown repeatedly that these prospective



Figure 1. Location of the Rabbit North property relative to the Interior Plateau and Kamloops mining district in southern British Columbia, Canada.

lowlands can be evaluated quickly, reliably, and cost-effectively by heavy mineral gold grain sampling (full disclosure: the author currently serves on Tower's Board of Directors and is Chairman of Overburden Drilling Management Limited ("ODM"), the contractor that plans and performs Tower's gold grain surveys).

This contribution describes how, in less than two years starting from scratch with a modest, reconnaissance-scale gold grain survey, Tower systematically discovered two significant, shear-hosted orogenic Au zones, Lightning and Thunder, on the entirely till covered and previously undrilled lower slope of a large

Recommended citation:

Averill, S.A., 2024. Tower Resources' rapid discovery from scratch, via glacially dispersed gold grains, of the Lightning and Thunder Au zones within the intensely explored Kamloops district: A recipe for effectively exploring the till-covered Interior Plateau of British Columbia; *in* Till Geochemistry and Indicator Mineral Methods for Exploration in Glaciated Terrains, (ed.) R.C. Paulen and M.B. McClenaghan; Geological Survey of Canada, Open File 9210, p. 58–65. https://doi.org/10.4095/pbmy2d03m0

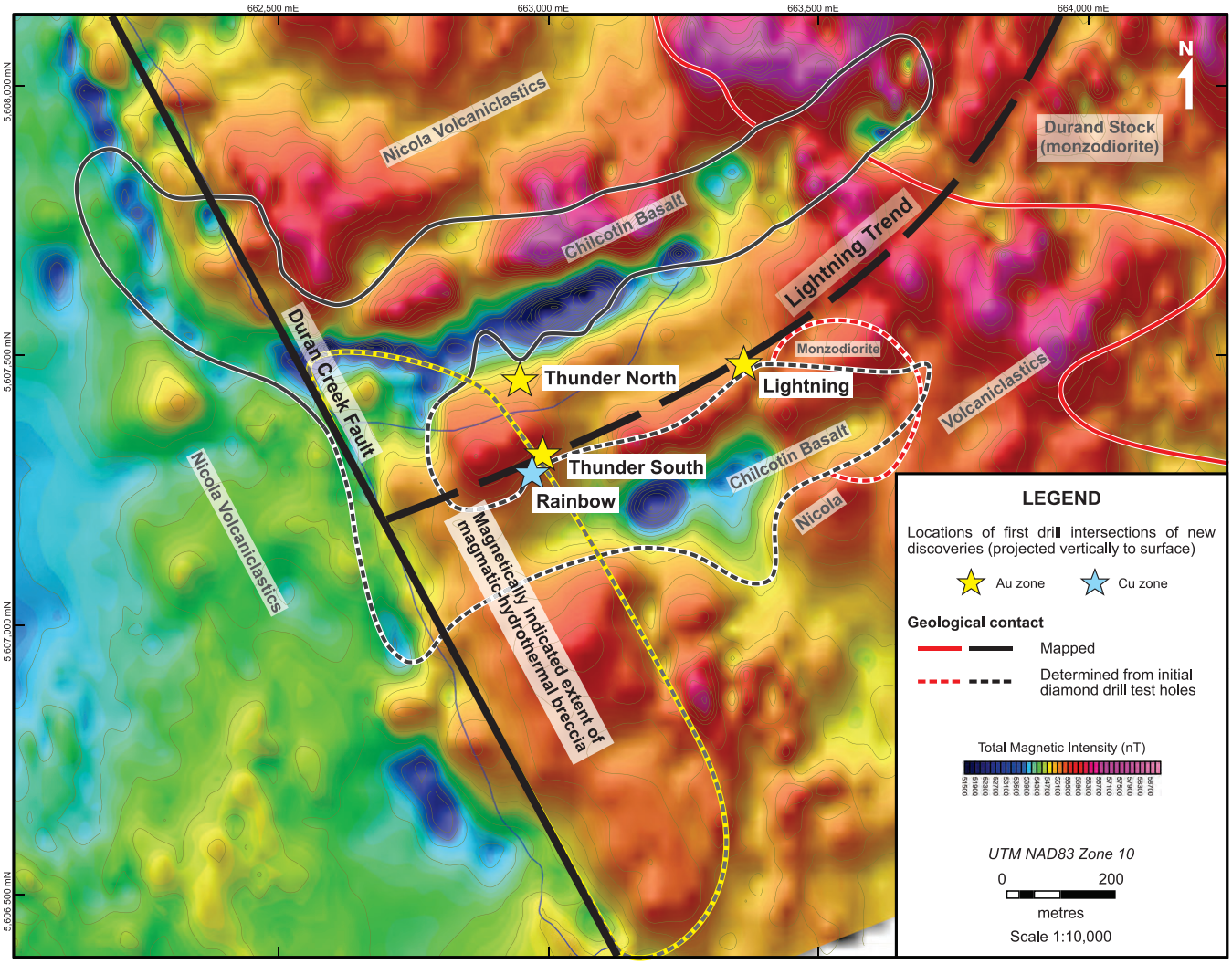


Figure 2. Ground magnetic map showing the principal lithologies in the discovery area and the locations of the first drill intercepts of the discoveries resulting from the till gold grain surveys.

bedrock ridge on the company's Rabbit North property in the heart of the Kamloops porphyry Cu±Au±Mo district, midway between the Highland Valley and New Afton mines (Fig. 1). These discoveries were made despite the gold zones being not only completely covered by Pleistocene till but also, unknowingly, partly covered by a band of Miocene basalt flows (Fig. 2). And as a bonus one of the discovery drill holes on the Thunder Zone also intersected a large new porphyry Cu-Au-Mo zone, Rainbow. In contrast, 50 years of historical exploration on the adjacent ridge produced only small porphyry Cu-Au showings with no associated Mo and found little evidence of the property's high potential for also hosting significant orogenic Au deposits.

The historical showings at Rabbit North are of the mildly alkalic porphyry type, similar to the mineralization at the nearby New Afton mine to the northeast (Fig. 1), and thus contain significant Au in addition to Cu. Mineralization is mainly in a monzodiorite intrusion known as the Durand Stock (Fig. 2, 3), which is physically resistant to weathering and forms a large ridge on the south-central part of the property. This Late Triassic stock was emplaced into thickly bedded Nicola alkalic andesite tuffs and breccias comprising a large, coeval stratovolcano that erupted in an island arc in the ancestral Pacific Ocean and was subsequently accreted to the Cordillera. Tower's initial intent was to use glacially dispersed gold grains from the Au component of the porphyry mineralization to determine whether any larger, economically significant deposits of this type might be present in the till-covered Nicola volcaniclastic rocks below the monzodiorite ridge, not to explore for orogenic Au deposits as no significant deposits of this type were known in the Kamloops district.

The company's initial reconnaissance-scale till sampling program, consisting of 137 samples, was performed in May 2021. It covered two areas (Fig. 3): the core claims around the Durand Stock and the southern tip of the property, which lies further down the ~150°

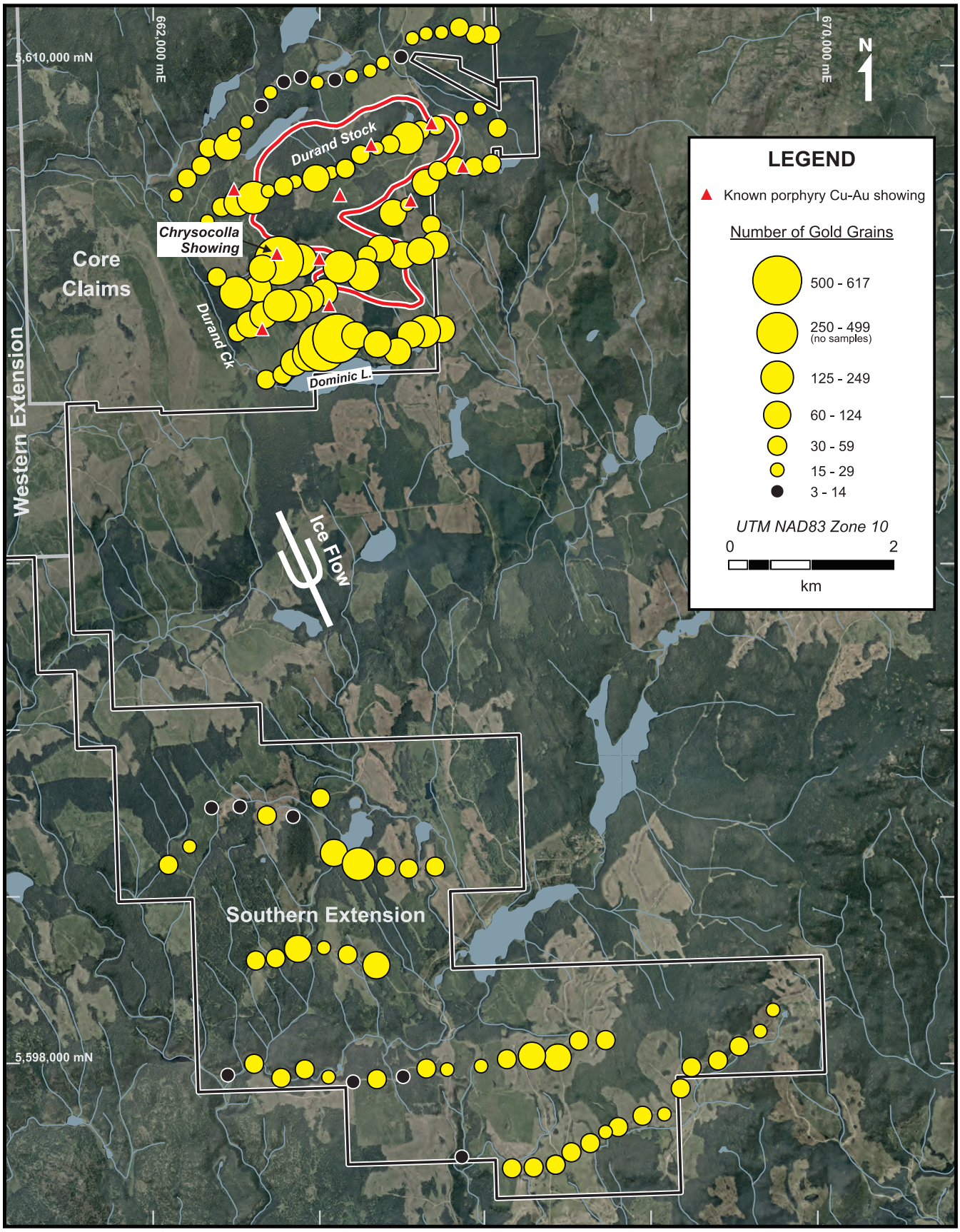


Figure 3. Gold grain results from May 2021 reconnaissance till survey. The average till sample weight was 10 kg.

glacial ice-flow path on the south side of a 4 km wide notch in the property boundary. The sampling traverses were oriented roughly orthogonal to the ice flow direction; however, their actual paths were determined systematically from stereo airphotos to ensure that they would cross till exposures of a suitable thickness for sampling. The traverse separation, sample spacing, and sampling density averaged approximately 1500 m, 250 m, and 2.7 samples per km^2, respectively, on the southern claims but were tightened to 1000 m, 200 m, and 5 samples per km^2 in the northern area due to the high frequency of porphyry Cu-Au showings in and near the Durand Stock. At each sample site, weakly oxidized but still very compact till from an average depth of 0.5 to 0.8 m within the upper part of the C horizon of the overprinted post-glacial soil profile was rubbed through an 8 mm sieve to obtain a 12 to 13 kg sample. Each sample was further sieved at ODM's heavy mineral laboratory to remove the smaller 2–8 mm clasts. Together these procedures consistently yielded approximately 10 kg of -2 mm silty sand matrix for gold grain extraction, eliminating any need to normalize the gold grain results for variations in sample size.

Most of the till samples collected in the eastern half of the southern survey area yielded 30 to 60 gold grains (Fig. 3), whereas the background gold level in the till in the Kamloops district, which was known from nearby projects (e.g. Plouffe et al., 2016), is only 0 to 10 grains per 10 kg sample. These weakly anomalous gold grain values were inferred to represent the distal tail of an amalgamated, 3 km wide dispersal train from the widespread but low-grade Cu-Au mineralization in the Durand Stock as the samples were collected 5 to 10 km directly down-ice from the stock. However, this inference could not be proven unequivocally due to the 4 km notch in the property up-ice from the weak anomaly. The gold grain content of the till over the stock itself was found to increase systematically from 20 to 40 grains per sample in the northern samples to 50 to 100 grains in the southern samples, in agreement with the known Cu-Au showings occurring toward the central and southern parts of the stock and the main ice-flow direction towards the southeast. However, the dispersal trains from the individual showings do not appear to be strong enough to be recognizable within the amalgamated train. This is probably due to a combination of the weakness of the mineralization and the subordinance of Au to Cu in alkalic porphyry deposits. One sample collected directly over the Chrysocolla showing did yield a strong gold anomaly of 609 grains but historical drilling had shown that the low-grade porphyry Cu-Au mineralization at this showing is cut by a shear zone that locally contains shallow, high-grade Au mineralization.

Though the strength of the gold grain anomaly from the Cu-Au mineralization in the Durand Stock is rather modest, two samples collected 200 m apart over Nicola pyroclastic rocks ~1 km to the southwest beside Dominic Lake yielded strong, matching gold responses of 514 and 617 grains (Fig. 4). The apparent continuity and uniform strength of this anomaly fulfilled the basic requirement of a dispersal train—systematic anomalism—and the anomaly was named the Dominic Lake Train. Importantly, the unusually high concentration of gold grains suggested, potentially, an economic source. In fact, the anomaly was much stronger than expected for a porphyry Cu-Au source, suggesting a different type of source mineralization; the highest gold values from samples of dispersal trains down-ice from the Mount Polley, B.C. (Plouffe et al., 2016) and giant Pebble, Alaska (Kelley et al., 2011) porphyry deposits were only 105 and 419 grains, respectively. Infill sampling was performed for 800 m up-ice (330°) in October 2021. Of the 22 samples collected, 21 yielded more than 200 gold grains (Fig. 4), with a peak value of 785 grains, establishing that the Dominic Lake Train was ~400 m wide but still open up-ice beyond 800 metres.

Essentially all of the gold grains in the dispersal train were silt-sized, with a modal diameter of just 15 µm. In all samples, irrespective of their position in the dispersal train, the gold grains were of mixed pristine to significantly modified (deformed) and even completely reshaped morphologies rather than showing progressive wear with increasing distance down the train. Together the small size and variable wear of the gold grains suggested that they originally occurred as inclusions within larger grains of a soluble mineral such as pyrite and that some were liberated from this mineral by physical comminution during glacial transport and others were liberated after deposition of the till by post-glacial oxidation, which extends to a depth of 2 to 3 m, well below the bottoms of the sample pits.

Normally, additional till sampling would have been performed to follow the train up-ice to its cut-off but this was not possible due to the onset of winter conditions. However, the source area was constrained sufficiently for a diamond drill test because the till-covered slope on which the dispersal train occurs ends 300 m up-ice at the foot of the ridge formed by the Durand Stock. Tower elected to probe progressively up-ice with the drill at 100 m intervals from the established part of the train (Fig. 5). The third hole, the 26th drilled since Tower acquired the Rabbit North property in 2013, was successful, discovering the Lightning Zone with a long, 95 m intersection that averaged 1.40 g/t Au.

The Lightning Zone occurs in a pyritized shear zone in Nicola volcaniclastic rocks. It is partly covered by an unexposed and previously unknown band of young

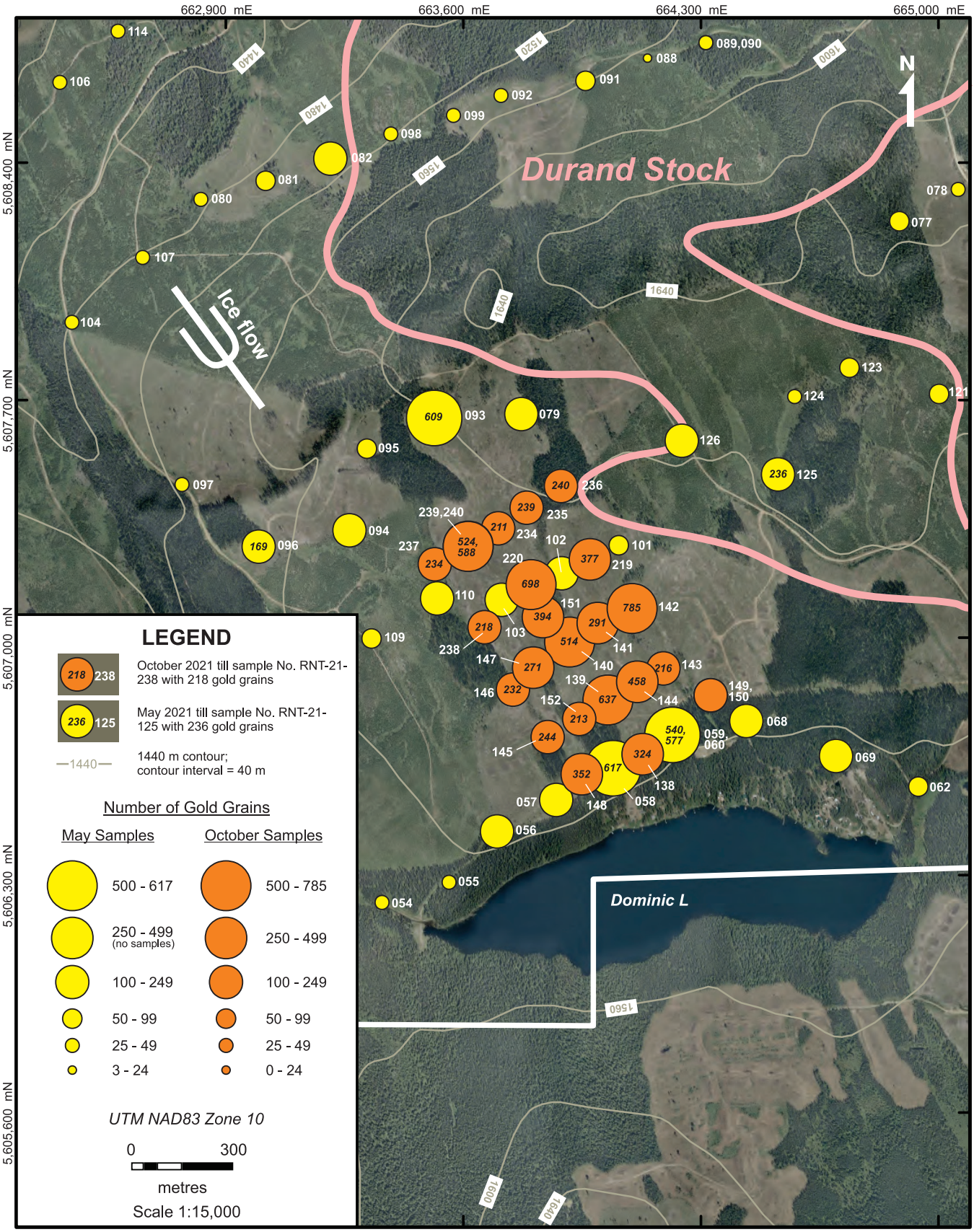


Figure 4. Gold-grain content of the till in the area of the Dominic Lake Train. The actual number of grains is included for samples with >200 grains and for sample 096 collected 400 m west of the train.

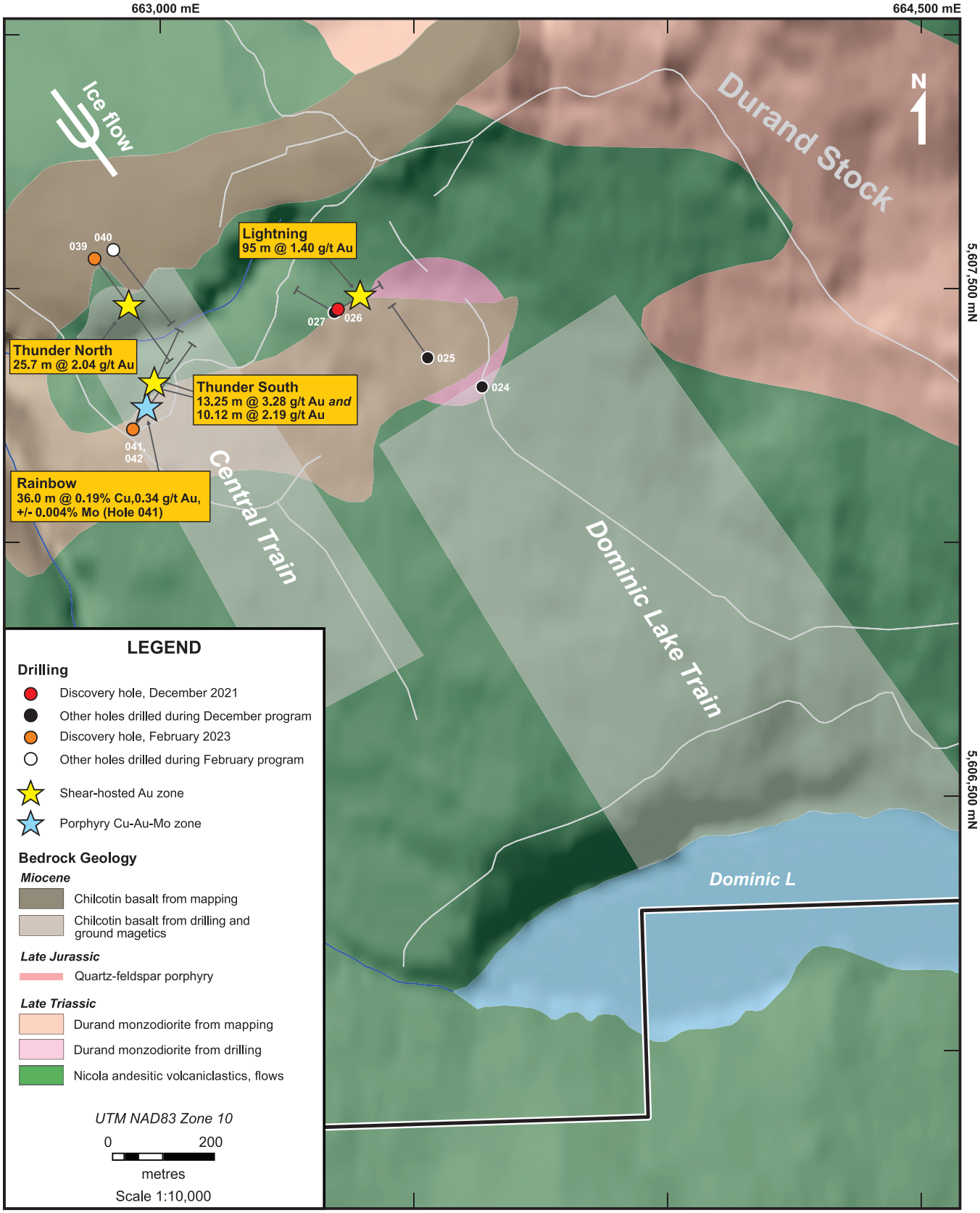


Figure 5. Locations of the mineralized zone discovery holes in relation to bedrock geology and the till-hosted gold grain dispersal trains that led to the discoveries.

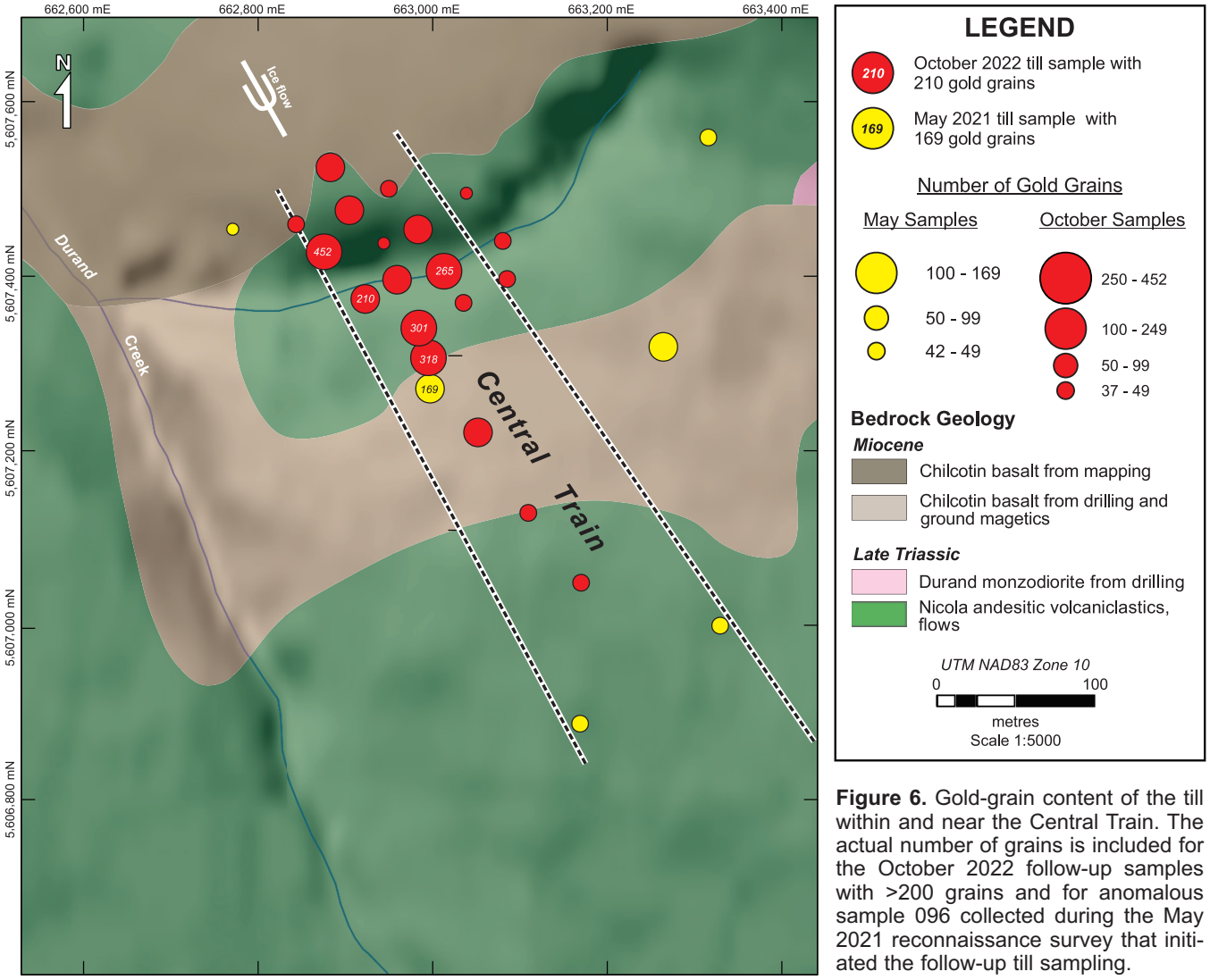


Figure 6. Gold-grain content of the till within and near the Central Train. The actual number of grains is included for the October 2022 follow-up samples with >200 grains and for anomalous sample 096 collected during the May 2021 reconnaissance survey that initiated the follow-up till sampling.

(Miocene) olivine basalt flows that lies 200 m south of and is parallel to another, well exposed band of these flows (Fig. 2, 5). Both bands erupted from local, underlying vents and the lava was constrained by the Miocene topography, following and filling in drainages that fed west-southwest into the deep valley of Durand Creek. This valley traces a major fault (Fig. 2) and appears to have been only minimally modified by glaciation. Although strongly magnetic, the basalt erupted during a reversal of Earth's magnetic poles. Thus the two bands are manifested as magnetic troughs (Fig. 2) rather than as highs. The basalt is unconformably underlain by brick-red lateritic saprolite produced by tropical Cretaceous to Paleogene weathering.

The Lightning Zone lacks coarse, visible gold grains, corroborating the inference from the minuteness of the gold grains in its dispersal train that the gold occurs as small inclusions in larger pyrite grains. The gold zone, unlike the nearby porphyry Cu-Au showings in the Durand Stock, is devoid of chalcopyrite. As well, the mineralization is closely associated both spatially and genetically with siliceous quartz-feldspar porphyry dykes rather than alkalic monzodiorite. Zircon from the porphyry has been dated as latest Jurassic (149 Ma), post-dating emplacement of the Durand Stock in the Late Triassic (ca. 215 Ma) by nearly 70 million years and accretion of the Cordillera in the Middle Jurassic by ca. 25 million years.

After recognizing the extent of the basalt cover and its potential for inhibiting gold grain dispersal during glaciation, Tower revisited and upgraded a modest and seemingly isolated, 169 grain gold anomaly identified in the first till survey ~400 m west of the Dominic Lake Train (Fig. 4), in the gap between the two basalt bands (Fig. 2, 5). Nineteen additional till samples were collected over this gap in October 2022, resulting in the delineation of a narrow but systematic gold grain anomaly, the Central Train (Fig. 6). The gold grains in this train were coarser than those in the Dominic Lake Train, suggesting a higher grade source. This was confirmed by a four-hole follow-up drilling program in February 2023, with the first hole, No. 039, which was

drilled southward from the exposed northern basalt band, intersecting a new mineralized shear zone—Thunder North—midway between the two bands (Fig. 5). This intersection contained rare specks of visible gold and averaged 2.04 g/t Au across 25.7 m. The third hole, No. 041, was drilled northward from the till-covered southern basalt band and intersected another, parallel gold zone—Thunder South—150 m to the south beneath the basalt, with two mineralized intervals 10 m apart averaging 3.28 g/t Au over 13.25 m and 2.19 g/t Au over 10.12 m. Thunder South appears to be hosted by the same shear structure as the Lightning Zone (Fig. 2).

Closer to surface, Hole 041 also clipped the eastern edge of a new zone of porphyry Cu-Au-Mo mineralization—Rainbow (Fig. 5)—with a 36.6 m intersection grading 0.19% Cu, 0.34 g/t Au, and 0.004% Mo. Hole 042, a steeper undercut from the same pad, obtained a longer 72.4 m intersection with a higher grade of 0.27% Cu, 0.40 g/t Au, and 0.01% Mo. The Rainbow mineralization is hosted by a zone of magmatic-hydrothermal breccia that contains 5 to 10% magnetite and appears to be responsible for a 350 m x 1200 m magnetic anomaly alongside the Durand Creek Fault (Fig. 2). The two reverse-polarized bands of Miocene cover basalt cut across this anomaly as magnetic troughs. Recent follow-up drilling on the Rainbow Zone suggests that the zone extends westward to the fault.

The total discovery cost from scratch for the Lightning and Thunder zones and the bonus Rainbow Zone, including the cost of the eight diamond drill test holes, was less than $1 million, ranking the discoveries among the most cost-effective in the Interior Plateau in decades. The low cost of discovery is due to the unique ability of till indicator mineral sampling to reliably discern from widely spaced samples any areas where significant mineralization is present beneath the till, and then with additional sampling accurately pinpoint the location of the mineralization, minimizing the number of drill holes required to intersect and evaluate it. Tower's Rabbit North property is just a pinpoint on the vast till-covered plateau (Fig. 1), leaving many opportunities for similar discoveries.

REFERENCES

Averill, S.A., 2017. The Blackwater gold-spessartine-pyrolusite glacial dispersal train, British Columbia, Canada: Influence of sampling depth on indicator mineralogy and geochemistry; Geochemistry: Exploration, Environment, Analysis, v. 17, p. 43–60.

Kelley, K., Eppinger, R.G., Lang, J., Smith, S.M., and Fey, D.L., 2011. Porphyry Cu indicator minerals in till as an exploration tool: example from the giant Pebble porphyry Cu-Au-Mo deposit, Alaska, USA; Geochemistry: Exploration, Environment, Analysis, v. 11, p. 321–334.

Plouffe, A., Ferbey, T., Hashmi, S., and Ward, B.C., 2016. Till geochemistry and mineralogy: vectoring towards Cu porphyry deposits in British Columbia, Canada; Geochemistry: Exploration, Environment, Analysis, v. 16, p. 213–232.

Plouffe, A. and Ferbey, T., 2016. Porphyry Cu indicator minerals in till: a method to discover buried mineralization; *in* Indicator Minerals in Till and Stream Sediments of the Canadian Cordillera, (ed.) T. Ferbey, A. Plouffe, and A.S. Hickin; Geological Association of Canada, Special Volume 50, p. 129–160.

Volcanogenic massive sulphide exploration in glaciated terrain: till geochemistry, indicator mineral, and boulder tracing methods

M. Beth McClenaghan and Jan M. Peter

Geological Survey of Canada, 601 Booth Street, Ottawa, Ontario K1A 0E8

INTRODUCTION

Volcanogenic massive sulphide (VMS) deposits are accumulations of Fe-, Cu-, Zn-, and Pb-sulphides that were precipitated on, or close to (in the shallow subsurface), the paleoseafloor from moderate- to high-temperature (up to ~350°C) fluids (predominantly modified seawater) circulating in the subsurface (Fig. 1). Convective fluid circulation is driven by the emplacement of magma to relatively shallow (~2 km) depths below the seafloor, with fluids traveling along faults and fractures. Host rocks are predominantly volcanic, with sedimentary rocks in some settings. The genetic model for VMS deposits, which had been formulated in the late 1950s, received validation with the discovery of active venting of high-temperature fluids from black smoker chimneys on the seafloor in a mid-ocean ridge setting in 1979 (Francheteau et al., 1979), and such deposits are widely considered to be modern analogues to VMS. Although such modern and ancient deposits can form in divergent (e.g. mid-ocean ridge) and convergent (arc and back-arc) tectonic settings, they are largely only preserved in the ancient record in the latter settings, by incorporation into accretionary orogens.

There are numerous classification schemes for VMS deposits, ranging from namesake monikers for classic deposits or districts, to metal (Cu, Zn, Pb) contents, to host succession rock types, with the latter currently receiving the widest general acceptance. There are over 1000 VMS deposits recognized globally, not including showings and prospects without reliable grade and tonnage data, and these deposits range in age from Paleoarchean (3.45 Ga) to present-day (modern seafloor massive sulphides).

VMS deposits are a significant exploration target in Canada (and elsewhere around the world). They accounted for 10.7% of Cu, 85.1% of Zn, 20.3% of Pb, 38.9% of Ag, and 17.8% of Au production in Canada in 2023 (calculated using S&P Capital IQ Pro database, accessed January 8, 2024). In addition to Cu, Zn, Ag, and Au, such deposits can be sources of byproduct critical minerals and other minor metals such as Bi, Co, Ge, In, Mn, Ni, Sn, Te, As, Cd, Ga, Sb, and Se.

Over 97% of Canada's land mass was covered by glaciers during the Quaternary Period (Nichol and Bjorklund, 1973). Glaciers eroded bedrock and deposited glacial sediments over large regions and as a result, till geochemistry, indicator mineral methods, and boulder tracing are important exploration methods for VMS deposits in Canada. This chapter provides an overview of best practices for applying these methods, including recommendations on appropriate size fractions to analyze, geochemical techniques, pathfinder elements, and indicator mineral methods.

Material for this chapter is largely summarized from a review of till geochemistry methods for VMS exploration by McClenaghan and Peter (2013, 2016) and a review of geochemical and indicator mineral methods for VMS exploration in GSC Open File 7853 (McClenaghan et al., 2015a). Numerous published reports and scientific papers describe surficial geochemical studies that have been carried out around VMS deposits in Canada; the key information for 25 of these deposits is summarized in Table 1.

SAMPLE MEDIA

Boulders

Mineralized boulder tracing is one of the oldest exploration methods in glaciated terrain (e.g. Grip, 1953; Dreimanis, 1958; Lee, 1971; Hyvarinen et al., 1973). Prospecting for massive sulphide boulders has contributed to the discoveries of the VMS deposits listed in Table 2, including deposits in the Bathurst Mining Camp in eastern Canada, the Mogador VMS deposit in the Val d'Or Mining Camp, and the Izok Lake VMS deposit, Nunavut. James and Perkins (1981) documented the presence of mineralized float down-ice of the Buchans VMS Mining District, Newfoundland that reflects the net result of ice flows to the southwest, southeast, and east-northeast. The finding of different massive sulphide boulder fields led to the exploration and discovery of the Kristineberg, Renström (PorterGeo database, 2024), Näsliden, and Rakkejaur deposits (Grip, 1953) between 1918 and 1926 in what was later to be named the Skellefte VMS District in northern Sweden.

Recommended citation:

McClenaghan, M.B. and Peter, J.M., 2024. Volcanogenic massive sulphide exploration in glaciated terrain: geochemistry, indicator mineral, and boulder tracing methods; *in* Till Geochemistry and Indicator Mineral Methods for Exploration in Glaciated Terrains, (ed.) R.C. Paulen and M.B. McClenaghan; Geological Survey of Canada, Open File 9210, p. 66–85. https://doi.org/10.4095/pbmy2d03m0

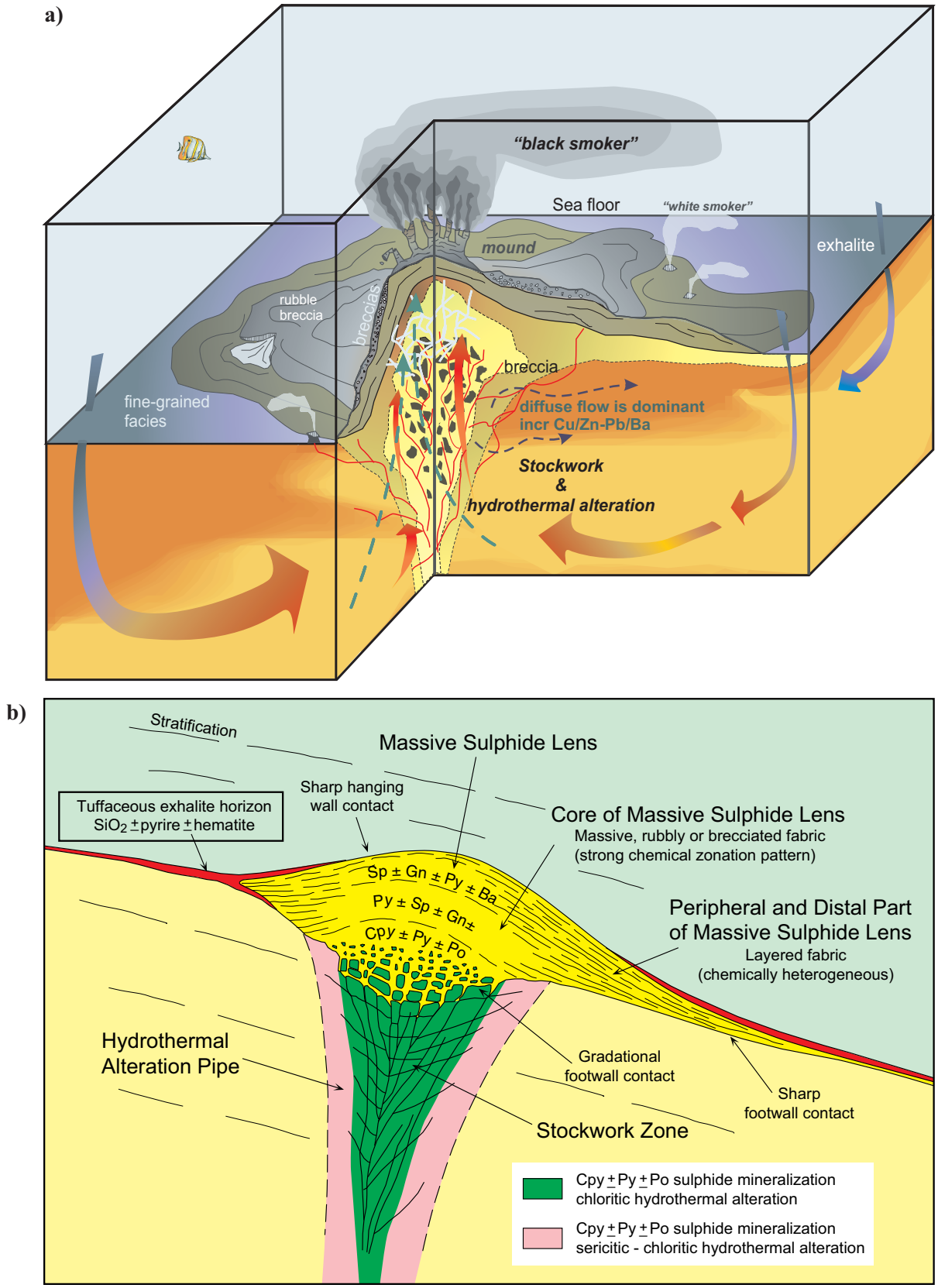


Figure 1. a) Block model schematic diagram of a mound-like volcanogenic massive sulphide system illustrating the relationships between the massive sulphide and the underlying stockwork. Red to purple arrows denote fluid circulation pathways. From Tornos et al. (2015). **b)** Idealized cross-section through a volcanogenic massive sulfide deposit, showing massive sulfide lens (deep yellow), alteration zones (green, pink), and exhalative horizon (red). Note mineralogical zoning within the lens. Ba = barite; Cpy = chalcopyrite; Gn = galena; Po = pyrrhotite; Py = pyrite; Sp = sphalerite. Modified *from* Lydon (1984).

Table 1. Case studies and examples that document the till geochemical signatures of VMS deposits across Canada (modified *from* McClenaghan and Peter, 2013).

Deposit/ occurrence	Location	Ore elements	Pathfinder elements	Size fraction(s) analyzed	Analytical method(s)	Source(s) of information for till geochemistry	Indicator minerals	Source(s) of information for indicator minerals
Halfmile Lake deposit, Bathurst, NB	Bathurst Mining Camp	Zn-Pb-Cu	Ag, As, Au, Bi, Cu, In, Sn, Sb, Pb	<0.063 mm	INAA + 4-acid/ ICP-ES,MS	Parkhill and Doiron (2003)		
Halfmile Lake deposit, Bathurst, NB	Bathurst Mining Camp	Zn-Pb-Cu	Ag, As, Au, Bi, Cu, Hg, Pb, Sb, Se, Sn, Zn	<0.063 mm	aqua regia + borate fusion/ICP-MS,ES	Budulan et al. (2013)	gold, chalcopyrite, pyrite, beudantite, goethite, jarosite, cinnabar	McClenaghan et al. (2017)
Restigouche deposit, Bathurst, NB	Bathurst Mining Camp	Zn-Pb-Cu-Ag	As, Au, Bi, Cu, In, Pb, Sb, Sn, Zn	<0.063 mm	INAA + 4-acid/ ICP-ES,MS	Parkhill and Doiron (2003)		
Mount Fronsac deposit, Bathurst, NB	Bathurst Mining Camp	Zn-Pb-Cu-Ag	Ag, Cd, Cu, Hg, Pb,	<0.063 mm	Aqua regia/ ICP-MS + CV-AAS	Campbell (2009)		
Bog deposit, Bathurst, NB	Bathurst Mining Camp	Pb-Zn-Cu-Ag	Ag, As, Cd, Cu, Pb, Sb, Zn	not reported	not reported	Hoffman and Woods (1991)		
CNE deposit, Bathurst, NB	Bathurst Mining Camp	Zn-Pb-Cu-Ag	Ag, As, Au, Cu, Hg, Pb, Sb, Zn	<0.063 mm	4-acid/ICP-ES + INAA + CV-AAS	Parkhill and Doiron (1995, 2003)		
Buchans, Oriental, Lucky Strike, NL	Buchans Mining Camp	Zn-Pb-Cu	Pb, Zn	<0.002 mm	LeForte/ICP-AES	Klassen and Murton (1996)		
Buchans, Oriental, Lucky Strike, NL	Buchans Mining Camp	Zn-Pb-Cu	Zn	<0.177 mm	nitric acid digestion	James and Perkins (1981)		
New Bay Pond, NL	central Newfoundland	Cu-Zn	As, Cu, Hg, Zn	<0.063 mm; 0.063–0.297 mm HMC (SG>2.96)	2-acid AAS, CV-AAS	Hornbrook et al. (1975)		
Kidd Creek deposit, Timmins, ON	Timmins Mining Camp	Zn-Cu-Pb-Ag	Cu, Zn	<0.0177 mm	3-acid/colourimetric	Fortescue and Hughes (1965)		
Kidd Creek deposit, Timmins, ON	Timmins Mining Camp	Zn-Cu-Pb-Ag	Cu, Zn	<0.0177 mm	total digestion	Fortescue and Hornbrook (1969); Hornbrook (1975)		
Kidd Creek deposit, Timmins, ON	Timmins Mining Camp	Zn-Cu-Pb-Ag	As, Cu, Zn	<1.7 mm HMC (SG>3.3)	aqua regia/ICP-ES	McClenaghan et al. (1998)		
Kam Kotia deposit, Timmins, ON	Timmins Mining Camp	Cu-Zn	Ag, Cd, Cu, Ga, Sb, Se, Ga, Tl, V, Zn	<0.002 mm; <0.063 mm HMC (SG>3.3)	aqua regia/ ICP-MS & ES	Smith (1990, 1992)		
Kam Kotia deposit, Timmins, ON	Timmins Mining Camp	Cu-Zn	Cu, Zn	<0.063 mm; <0.25–0.063 mm HMC (SG>3.3)	not reported	Skinner (1972); Shilts (1976)		
Jameland despoit, Tmmins, ON	Timmins Mining Camp	Cu-Zn-Au-Ag	Cu, Zn	<0.063 mm; <0.25–0.063 mm HMC (SG >3.3)	not reported	Skinner (1972); Shilts (1976)		
Currie deposit (Tillex)	Timmins Mining Camp	Cu	Cu	<0.177 mm; <2.0 mm HMC (SG>3.3)	not reported	Thompson (1979)	chalcopyrite, sphalerite	Thompson (1979)
Horne deposit, Noranda, QC	Noranda Mining Camp	Cu-Au-Ag	Cu, Pb, Zn	<0.0177 mm	not reported	Dreimanis (1958, 1960)		
MacDonald (Gallen) deposit, Noranda, QC	Noranda Mining Camp	Zn-Cu-Au-Ag	Cu, Pb, Zn	<0.177 mm	not reported	Dreimanis (1958, 1960)		
Magusi River deposit, Noranda, QC	Noranda Mining Camp	Zn-Cu	Cu, Ag, Hg, Zn	whole till; >0.177 mm HMC (SG >2.96); <0.177 mm	not reported	Gleeson (1975b)		
Iso deposit	Noranda Mining Camp	Cu-Zn	Ag, Cu, Zn	matrix and HMC fractions	not reported	Telford and Becker (1979)		
Mogador (Vendome) deposit, Val d'Or, QC	Val d'Or Mining Camp	Zn-Cu-Pb-Ag-Au	Ag, Cu, Zn	<0.177 mm; >0.177 mm HMC	not reported	Dreimanis (1958); Gleeson (1975a)		
Louvem deposit, Val D'Or, QC	Val d'Or Mining Camp	Zn-Cu-Ag-Au	Cu, Zn	<0.177 mm; >0.177 mm HMC (SG >2.96)	not reported	Gleeson and Cormier (1971)		
Louvem deposit, Val D'Or, QC	Val d'Or Mining Camp	Zn-Cu-Ag-Au	Cu, Zn	<0.177 mm; 0.064–0.177 mm HMC (SG>3.3)	pyrosulfate fusion + colourimetry	Garrett (1969,1971)		
Montauban deposit, QC	Montauban, QC	Zn-Pb-Au-Ag	As, Au, Cd, Co, Sb, Zn	<0.177 mm	AAS + INAA	Pelletier and Beaumier (1990)	gahnite	Lalonde et al. (1994)
Geco, Willroy, Nama Creek deposits, Manitouwadge, ON	Manitouwadge Mining Camp	Zn-Cu-Ag	Ag, Cu, Zn	<0.063 mm	aqua regia	Kettles et al. (1998)		
Chisel Lake, Lost Lake, Ghost Lake deposits, Snow Lake, MB	Snow Lake Mining Camp	Zn-Cu	As, Au, Cu, Hg, Pb, Sb	<0.002 mm; <0.063 mm	INAA + aqua regia AAS and ICP-ES	Kaszycki et al. (1996)		
Kudz Ze Kayah deposit, Finlayson Lake, YT	Canadian Cordillera	Zn-Pb-Cu-Ag-Au	Ag, Au, Pb, Zn	<0.063 mm	aqua regia/ ICP-MS	Bond and Plouffe (2002); Plouffe and Bond (2003, 2004)		
Southern Kootenay Terrane, multiple VMS occurrences	Canadian Cordillera	Cu-Pb-Zn-Ag	As, Au, Bi, Cu, Hg, Pb, Sb, Se, Zn	<0.063 mm	aqua regia/ICP-ES + INAA	Lett et al. (1998); Lett and Jackaman (2002)		
Samatosum and Rea deposits, Adams Lake, BC	Canadian Cordillera	Ag-Pb-Zn-Cu	Au, As, Hg, Pb, Sb, Zn	<0.063 mm	aqua regia/ICP-ES + INAA	Bobrowksy et al. (1997); Lett (2001); Paulen (2001)		
Lynx, Myra, H-W, Prince deposits, Myra Falls, BC	Canadian Cordillera	Cu-Zn-Pb-Au-Ag-Cd	Cu, Pb, Zn	<0.002 mm	total digestion/AAS	Hicock (1986)		
Yava (Agricola Lake) deposit, NU	Canadian Arctic	Zn-Cu-Pb-Ag-Au	Ag, Au, Cu, Hg, Pb, Zn	<0.177 mm	2-acid AAS + CV-AAS + FA-AAS	Cameron and Durham (1975); Cameron (1977)		
Hackett River deposit, NU	Canadian Arctic	Zn-Pb-Cu-Ag	Pb	<0.177 mm	2-acid AAS, CV-AAS	Miller (1979)		
Spi Lake occurrence, NU	Canadian Arctic	Zn, Pb,Cu	Cu, Zn	<0.002 mm	2-acid AAS	Shilts (1975)		
Izok Lake deposit, NU	Canadian Arctic	Zn-Cu-Pb-Ag	Ag, Bi, Cd, Cu, Fe, Hg, In, Pb, Sb, Se, Tl, Zn	<0.063 mm	aqua regia/ICP-MS + borate fusion/ ICP-MS	Hicken et al. (2012); McClenaghan et al.(2015b)	gahnite, chalcopyrite, sphalerlite, galena, pyrite	McClenaghan et al. (2015b)

Note: AAS = Atomic absorption spectrometry; CV-AAS = Cold vapour-atomic absorption spectrometry; FA-AAS = Fire assay - atomic absorption spectrometry; HMC = Heavy mineral concentrate; ICP-ES = Inductively coupled plasma - emission spectrometry; ICP-MS = Inductively coupled plasma - mass spectrometry; INAA = Instrumental Activation Analysis; SG = Specific gravity.

Table 2. Selected volcanogenic massive sulphide (VMS) deposits for which boulder tracing, till geochemistry, and/or indicator mineral methods have contributed to their discovery.

Deposit	Location	Deposit type	Commodity	Method contributing to deposit discovery	References
Taivaljärvi	eastern Finland	VMS-epithermal	Ag-Au-Zn	boulder tracing	Lindborg et al. (2015)
Kristineberg	Sweden	VMS	Cu-Pb-Zn	boulder tracing	PorterGeo database (2024)
Renström	Sweden	VMS	Cu-Pb-Zn	boulder tracing	PorterGeo database (2024)
Rakkejaur	Sweden	VMS	Cu-Pb-Zn	boulder tracing	Grip (1953)
Näsliden	Sweden	VMS	Cu-Pb-Zn	boulder tracing	Grip (1953)
Orvan Brook	New Brunswick, Canada	VMS	Cu-Pb-Zn	boulder tracing	Dreimans (1958); Walker et al. (2006)
Restigouche	New Brunswick, Canada	VMS	Pb, Zn	soil (till) geochemistry	McCutcheon et al. (2003)
Flat Landing Brook	New Brunswick, Canada	VMS	Pb, Zn	boulder tracing	McCutcheon et al. (2003)
Currie (Tillex)	Ontario, Canada	VMS	Cu-Pb-Zn	till geochemistry, indicator minerals	Thompson (1979)
Vendome (Mogador)	Quebec, Canada	VMS	Zn-Pb	boulder tracing	Dreimanis (1958)
Buchans	Newfoundland, Canada	VMS	Zn-Pb-Cu-Ag	boulder tracing	Neary (1981)
Newfoundland Zinc	Newfoundland, Canada	VMS	Zn	soil (till) geochemistry, boulders	Brummer et al. (1987)
Izok Lake	Nunavut, Canada	VMS	Zn-Pb-Cu	boulder tracing	Money and Heslop (1976)
Photo Lake	Manitoba, Canada	VMS	Zn-Cu-Au	till geochemistry	Kaszycki et al. (1996)
Fyre Lake	Yukon, Canada	VMS	Zn-Pb-Cu-Ag-Au	boulder tracing	Peter et al. (2007)
Louvem East	Quebec, Canada	VMS	Zn	till geochemistry	Gleeson and Cormier (1971); Brummer et al. (1987)

Till

Till is the optimal surficial sampling medium for exploration in glaciated terrain because of its ubiquity across a glaciated landscape and that it is directly derived from the erosion of bedrock, as compared to stream sediments and lake sediments that have undergone sorting and additional vectors of transport (Coker and Shilts, 1993; McClenaghan et al., 2023). Till geochemistry and indicator mineral methods have contributed to the discoveries of several of the VMS deposits listed in Table 2.

METHODS

Boulder Tracing

Exploration programs can include mapping the distribution of mineralized boulders on the surface and examining the composition of these boulders using geochemical, petrographic, mineralogical, and isotopic techniques (e.g. Day et al., 1987). These data are integrated with till geochemistry, indicator mineralogy, bedrock geology, and geophysical data to identify a mineral deposit type (i.e. VMS) and estimate glacial transport direction and distance from potential VMS source(s).

Till Geochemical Analysis

The use of modern inductively coupled plasma-mass spectrometry (ICP-MS) analytical instruments allows for the determination of 65 elements in till samples (e.g. McClenaghan and Peter, 2016). These elements can be used to document and delineate multi-element signatures in till down-ice of VMS deposits and determine if the eroded VMS mineralization is Ag- or Au-rich, and/or if it is enriched in any of the specific critical minerals (e.g. In) listed above.

Most current exploration programs and government surveys that utilize till geochemistry employ a strong partial digestion, such as 30 g aqua regia, to determine the contents of the major ore elements Cu, Pb, Zn, Au, and Ag, as well as the pathfinder elements As, Bi, Cd, Ga, Hg, In, Sb, Se, and Tl. "Total" digestions, such as borate fusion, or near total, such as 4-acid digestion, are optimal for determining elements such as Sn and Ba.

Size Fractions for Geochemical Analysis

The main VMS "ore" minerals chalcopyrite, galena, and sphalerite are relatively soft (hardness ≤ 4, Mohs hardness scale; Table 3) and, therefore, are readily comminuted during glacial transport to the fine fraction (silt+clay) of till over short distances (100s of m) (Kauranne, 1959; Salminen, 1980; Nikkarinen et al., 1984; Nevalainen, 1989). The -250 mesh (<0.063 mm) fraction of till is the most commonly analyzed size fraction for base metal exploration for the following reasons: 1) it is readily and quickly recovered by sieving, especially in till samples with only a minor (<2%) clay component and thus samples of this fraction are inexpensive to prepare; 2) it provides reasonable contrast between background and anomalous metal contents, and 3) it is less susceptible to hydromorphic dispersion effects (Pronk, 1987; McClenaghan et al., 2023).

Geochemical analysis of the -80 mesh (<0.177 mm) fraction is not recommended because this size fraction contains a significant component of sand-sized quartz and feldspar (Dreimanis and Vagners, 1972; Klassen, 2003). The abundant quartz and feldspar will mute (dilute) the geochemical signature of nearby VMS mineralization.

Table 3. Common indicator minerals of mineralization, hydrothermal alteration zones, and exhalites associated with metamorphosed VMS deposits in glaciated terrain (from McClenaghan et al., 2015a).

Indicator mineral	Zone	Chemical formula	Specific gravity	Hardness (Mohs)	Photo figure
Sillimanite	metmorphosed alteration	Al_2SiO_5	3.24	7.0	Appendix 2c
Kyanite	metamorphosed alteration	Al_2SiO_5	3.56–3.67	4.0-7.0	Appendix 2b
Corundum	metamorphosed alteration/alteration	Al_2O_3	4.0–4.1	9.0	Appendix 2a
Andalusite	metamorphosed alteration/alteration	Al_2SiO_5	3.15	6.5-7	
Mg-Spinel	metamorphosed alteration	$MgAl_2O_4$	3.64	8.0	
Staurolite	metamorphosed alteration	$(Fe,Mg,Zn)_2Al_9(Si,Al)_4O_{22}(OH)_2$	3.65–3.77	7.0-7.5	Appendix 2d
Topaz	metamorphosed alteration	$Al_2SiO_4(F,OH)_2$	3.5–3.6	8.0	
Mn-Epidote	alteration	$Ca_2(Al,Fe,Mn)_3Si_3O_{12}(OH)$	3.3–3.6	6.0-7.0	Appendix 2f
Anthophyllite	metamorphosed alteration/exhalite	$(Mg,Fe)_7Si_8O_{22}(OH)_2$	2.85–3.57	5.0-6.0	
Orthopyroxene	metamorphosed alteration/exhalite	$(Mg,Fe)_2Si2O_6$	3.4	5.0-6.0	
Tourmaline	alteration/exhalite	$(Na,Ca)(Mg,Fe)_3Al_6(BO_3)_3(Si_6O_{18})(OH)_4$	3.06	7.0-7.5	Appendix 2i,j
Spessartine	alteration/exhalite	$Mn_3Al_2Si_3O_{12}$	4.18	6.5-7.5	Appendix 2g
Magnetite	gangue/exhalite	Fe_3O_4	5.15	5.5-6.0	
Barite	gangue	$BaSO_4$	4.48	3.0-3.5	
Franklinite	metamorphosed mineralization/exhalite	$(Zn, Mn,Fe)(Fe,Mn)_2O_4$	5.14	5.5-6.0	Appendix 2h
Willemite	metamorphosed mineralization	Zn_2SiO_4	3.9–4.2	5.5	
Gahnite	metamorphosed mineralization	$ZnAl_2O_4$	4.0–4.6	7.5-8.0	Appendix 2k,l
Cinnabar	mineralization	HgS	8.1	2.0-2.5	
Loellingite	mineralization	$FeAs_2$	7.1–7.7	5.0-5.5	
Chalcopyrite	mineralization	$CuFeS_2$	4.1–4.3	3.5	Appendix 1a
Pyrite	mineralization	FeS_2	5–5.02	6.5	Appendix 1d
Galena	mineralization	PbS	7.2–7.6	2.5	Appendix 1c
Sphalerite	mineralization	(Zn,Fe)S	3.9–4.2	3.5-4.0	Appendix 1e,f
Native Gold	mineralization	Au	16.0–19.3	2.5-3.0	Appendix 1g
Electrum	mineralization	AuAg	16.0–19.3	2.5-3.0	
Pyrrhotite	mineralization	$Fe_{(1-x)}S$	4.58–4.65	3.5-4	Appendix 1b
Cassiterite	mineralization	SnO_2	6.8–7.0	6-7	Appendix 1h
Beudantite	gossan (preglacial oxidation of mineralization)	$PbFe_3(AsO_4)(SO_4)(OH)_6$	4.1–4.3	4.0	Appendix 3b
Jarosite	gossan (preglacial oxidation of mineralization)	$KFe_3(SO4)_2(OH)_6$	2.9–3.3	2.5-3.5	Appendix 3c
Goethite	gossan (preglacial oxidation of mineralization)	FeO(OH)	3.3–4.3	5.5	Appendix 3a

Field Portable X-Ray Fluorescence Analysis

Portable X-ray fluorescence spectrometry (pXRF) can be used in the field to actively guide till sampling programs and facilitate follow-up of geochemical anomalies during the same field season (McClenaghan et al., 2020 and references therein). General protocols recommended by public agencies for analyzing till samples using pXRF in Finland and Canada are reported in Sarala (2016), McClenaghan et al. (2020), and Knight et al. (2021).

The strong correlation between pXRF analytical values Cu, Pb, Zn in dry, unsieved bulk till (in open-ended pXRF cups covered by 4.0 µm Prolene® thin-film) with aqua regia/ICP-MS analyses of the <0.063 mm fraction till from around the Halfmile Lake VMS deposit in the Bathurst Mining Camp of eastern Canada (Fig. 1), illustrates the utility of pXRF analysis for quantitative determination of Cu, Pb, and Zn contents of till (Fig. 2).

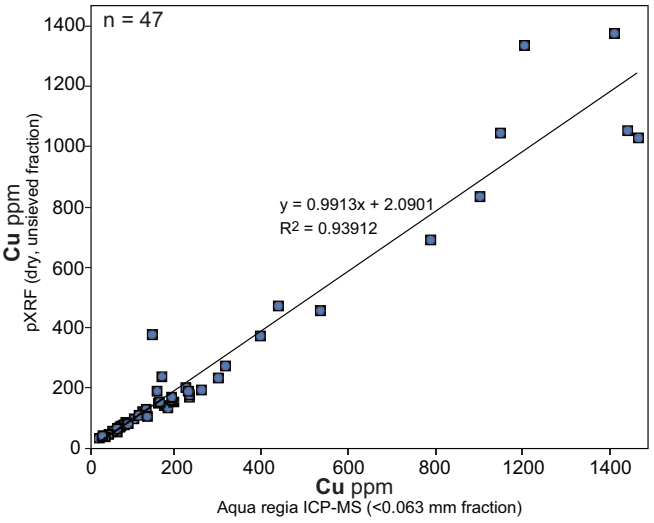


Figure 2. Comparison of Cu (ppm) content in till as determined by portable XRF (InnovX Delta with Ta tube) on dry, unsieved till versus dry, sieved (<0.063 mm) till analyzed using aqua regia/ICP-MS from the Halfmile Lake VMS deposit, New Brunswick, Canada (from McClenaghan et al., 2015a).

Table 4. Relative stabilities of Fe-sulphide minerals and gold grains that can be found in VMS deposits, and that may be present in surficial sediments that have endured weathering under temperate to humid tropical climatic conditions, as observed in heavy mineral concentrates by Overburden Drilling Management Ltd. (modified *from* Averill, 2011).

Mineral	Relative stability
pentlandite	very unstable
millerite	very unstable
pyrrhotite	very unstable
pyrite	unstable
chalcopyrite	marginally stable
FeNi-arsenides	stable
native Au	very stable

Indicator Mineral Methods

Indicator minerals of VMS deposits are routinely recovered from the heavy mineral concentrate (>3.2 specific gravity (SG)) fraction of till samples. Refer to Beckett-Brown and McClenaghan (2024) for a description of heavy mineral sample processing methods. The suite of VMS indicator minerals includes sulphide ore minerals and native gold (Table 3). Many of the metallic minerals are not resistant to chemical weathering and thus their usefulness is a function of the degree of weathering the till has undergone. Table 4 provides an indication of the relative stability of some of these minerals. Where VMS deposits are metamorphosed, the indicator mineral suite includes physically and chemically robust oxide and silicate minerals indicative of metamorphosed mineralization, hydrothermal alteration, or exhalite zones, including sillimanite, andalusite, gahnite, staurolite, and spessartine (Lalonde et al., 1994; Averill, 2001; Ghosh and Praveen, 2008; Heimann et al., 2005; McClenaghan et al., 2015a,b). Using magnetite as an indicator mineral, together with its mineral chemistry, may also be useful for VMS exploration (Makvandi et al., 2013, 2015). Where VMS mineralization has undergone preglacial weathering, secondary minerals, such as beudantite, jarosite, and goethite, may also be useful indicator minerals in till, however, these minerals are not physically robust, such that they may only indicate the local (< 2 km) presence of mineralization. Photographs of some of these minerals as they appear in the >3.2 specific gravity 0.25–2.0 mm fraction of heavy mineral concentrates are shown in Appendixes 1 to 3.

Lougheed et al.'s (2020) studies of Mineral Liberation Analysis (MLA) of till heavy mineral concentrates from the Izok Lake VMS deposit have documented the best practices when preparing and analyzing fine-grained heavy mineral fractions (<0.25 mm) using automated mineralogy and the indicators of metamorphosed VMS mineralization.

Laser ablation-inductively coupled mass spectrometry (LA-ICP-MS) can be used to measure very low abundances of elements and isotopes in individual indicator mineral grains. It uses a short-pulsed laser to ablate a small volume of a mineral for a duration of a few seconds, generally 5 to 30 s, during which the material is converted into vapour and aerosol components that are then continually transferred in a carrier gas to be ionized in an argon plasma and analyzed in either a triple quadrupole or magnetic-sector mass spectrometer (Layton-Matthews and McClenaghan, 2022). Several studies have documented the trace element signatures of minerals that are characteristic of VMS deposits (e.g. Genna and Gaboury, 2015; Dehnavi et al., 2018; Conde et al., 2021; Torró et al., 2022) and these methods and chemical characteristics can be applied to grains recovered from till samples to aid in tracing a bedrock source up ice.

Lead isotope methods

Lead is present mainly as galena in many VMS deposits. Since galena contains no U, there is no increase of radiogenic Pb (^{206}Pb or ^{207}Pb) subsequent to its formation. Thus, the Pb isotopic composition of galena gives the Pb isotopic composition of the fluid from which the mineral was precipitated. Typically, galena in VMS deposits is distinctly more primitive (less radiogenic) than the Pb isotopic composition(s) of the host rocks (e.g. Sangster et al., 2000; Huston and Champion, 2023). The recognition of galena with such primitive isotopic compositions can be used to identify (and vector toward) VMS mineralization by tracing the signature in the up-ice direction. Two different size fractions of the till can be analyzed, the <0.063 mm bulk till matrix or 0.25–2.0 mm sand-sized galena grains.

Several studies have demonstrated the utility of determining Pb isotope ratios for the till matrix (e.g. Bell and Franklin, 1993; Bell and Murton, 1995; Simonetti et al., 1996; Hussein et al., 2003; van Geffen et al., 2013; Rukhlov and Ferbey, 2015). This technique is best applied to till samples that display a VMS geochemical signature (i.e. anomalous concentrations of Cu, Pb, and Zn) in areas that are prospective for VMS mineralization.

Alternatively, Pb isotope ratios may be measured on single galena grains recovered from a heavy mineral concentrate using LA-ICP-MS (e.g. Paulen et al., 2011; Oviatt et al., 2015; King et al., 2018; Layton-Matthews and McClenaghan, 2022). LA-ICP-MS determinations may be faster, easier, and more cost-effective for the explorationist to use compared to traditional isotopic methods, and the service is readily available at commercial laboratories.

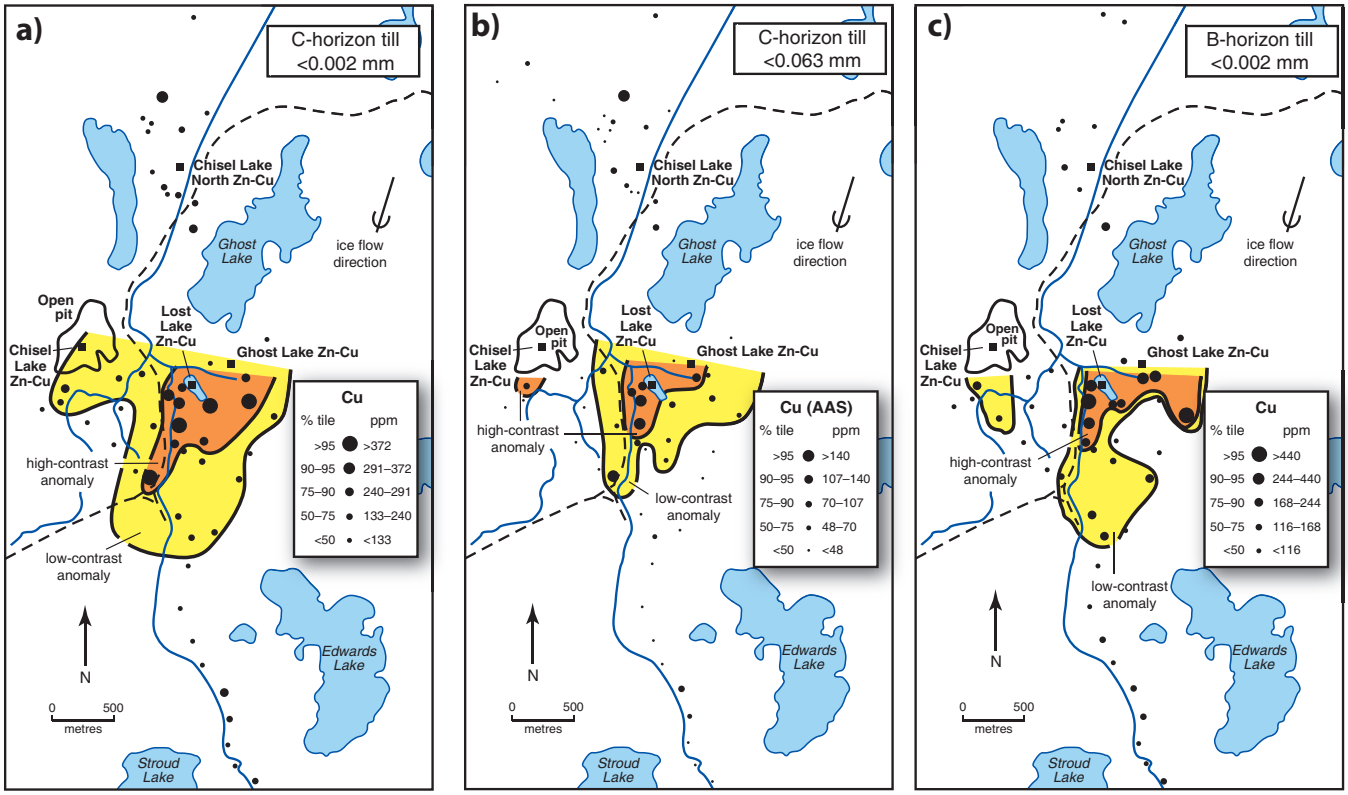


Figure 3. Till geochemistry maps of Cu (ppm) in surface till around the Chisel Lake, Lost Lake, and Ghost Lake Zn-Cu VMS deposits in the Snow Lake Camp: **a)** <0.002 mm fraction of C-horizon developed on till; **b)** <0.063 mm fraction of C-horizon developed on till; **c)** <0.002 mm fraction of B-horizon developed on till (modified *from* Kaszycki et al., 1996).

SELECTED CASE STUDIES ACROSS CANADA

Snow Lake Camp, central Canadian Shield

In the Snow Lake Camp of central Canada, detailed till sampling was used to outline south-southwest-trending glacial dispersal fans defined by Cu and Zn (Fig. 3) in two fractions of till around the Chisel Lake, Lost, and Ghost VMS deposits (Kaszycki et al., 1996). The contrast between background and anomalous Cu and Zn contents is greatest for the <0.002 mm fraction of till as compared to the <0.063 mm fraction. Glacial dispersal of these metals is detectable up to 1 km down-ice from the deposit. Areas of anomalous metal contents in the B-horizon soil developed on till are smaller in areal extent, indicating that the B-horizon contains less metals than the C-horizon in this area. Kaszycki et al. (1996) also identified a Cu, Hg, Pb, As, Au, and Sb multi-element anomaly in till north of the Chisel Lake deposit, an area where the Photo Lake VMS deposit was subsequently discovered. In addition to documenting the multi-element signatures of VMS deposits in till, Kaszycki et al. (1996) compared Cu/Zn ratios in till to those of underlying source rocks. They found that high Cu/Zn ratios in till closely match those in underlying felsic rocks that host Cu-rich VMS deposits, and that high Zn/Cu ratios in till closely reflect the ratios in VMS deposits hosted in mafic rocks in the area.

Adams Lake Area, Cordillera

Deposit-scale till, soil, and vegetation sampling carried out around the Samatosum and Rea Ag-Pb-Zn-Cu VMS deposits, in south-central British Columbia, was reported by Lett et al. (1998), Paulen (2001), and Lett (2001). These relatively small (each <1 Mt) VMS deposits occur in highly deformed and metamorphosed mafic volcanic and argillaceous sedimentary rocks of the Eagle Bay Assemblage (Bailey et al., 2000). Till and B-horizon soil (that has developed on the till) around and down-ice (southeast) of the deposits have anomalous Ag, As, Hg, Zn (Fig. 4), Sb, Au, and Pb contents in the <0.063 mm fraction of surface till (Paulen, 2001; Lett, 2001). The surface till geochemical anomalies can be traced up to 10 km down-ice to the southeast (Bobrowsky et al., 1997). Some clastic dispersal patterns in this mountainous region can be affected by subsequent downslope hydromorphic dispersion. These effects can be avoided by sampling till at greater depths (i.e. below the B horizon) (Paulen, 2001).

Halfmile Lake Deposit, Appalachians

The Halfmile Lake Zn-Pb-Cu VMS deposit, in northern New Brunswick, was discovered using soil (weathered till) geochemical and geophysical surveys (Adair, 1992; Parkhill and Doiron, 2003). The deposit is

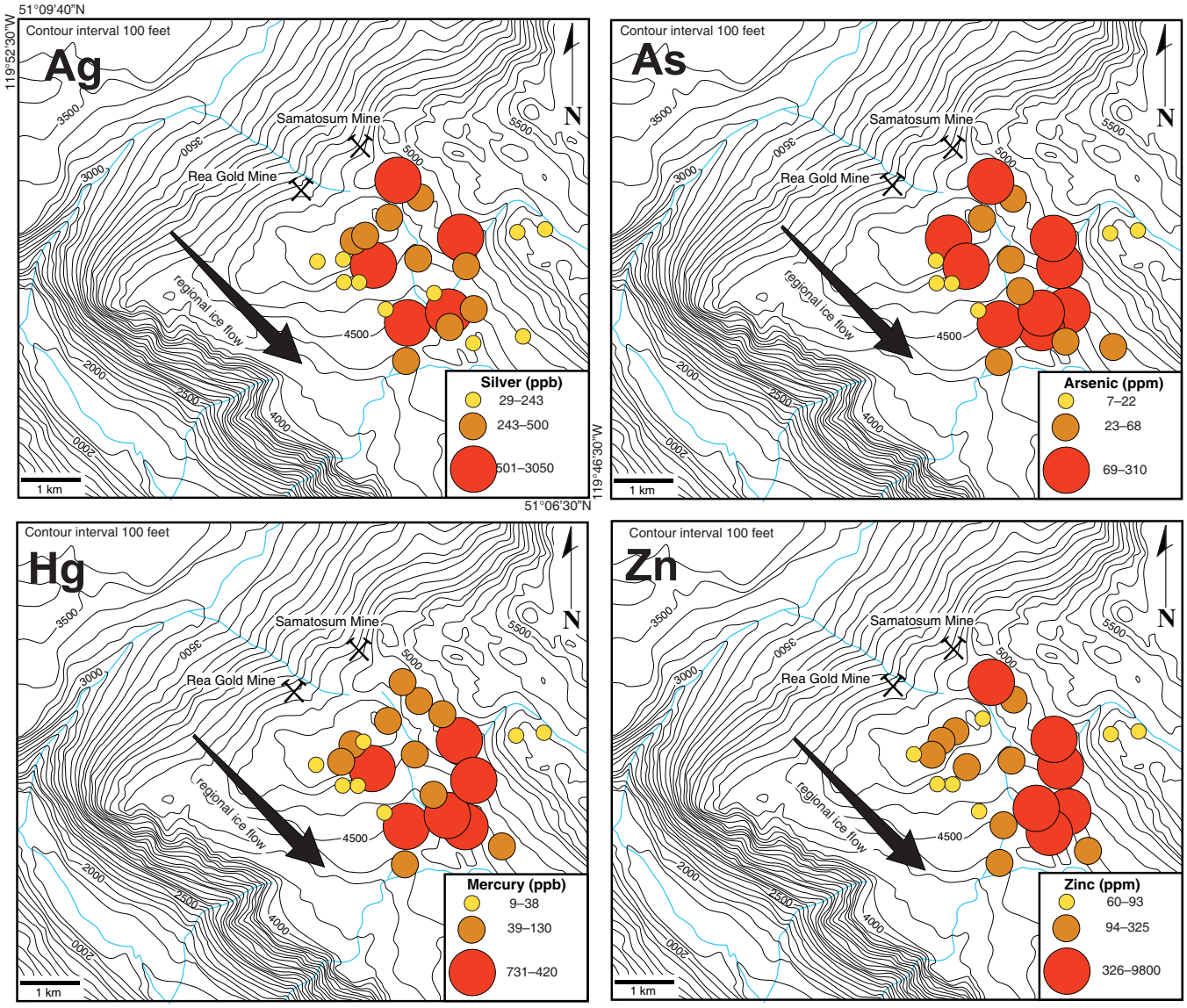


Figure 4. Till geochemistry maps for the <0.063 mm fraction of till down-ice (southeast) of the Rea Gold and Samatosum VMS deposits, British Columbia: **a)** Ag, **b)** As, **c)** Hg and **d)** Zn (modified *from* Paulen, 2001).

capped by a preglacial (Pliocene) massive sulphide gossan that is enriched in Pb, Cu, In, Au, Ag, Sn, As, Sb, Bi, and Se (Boyle, 2003). A well developed ribbon-shaped glacial dispersal train (Fig. 5) extends at least 1 km down-ice (east-northeast to east-southeast) and is best defined by Cu, Pb, In, Ag, As, Au, Sb, Bi, Hg, Sb, Se, and Sn in the <0.063 mm till fraction (Parkhill and Doiron, 2003; Budulan et al., 2013). Although Zn is the most abundant base metal in the deposit, it is not a pathfinder element in till immediately down-ice, likely due to Zn depletion in the preglacial gossan cap (Parkhill and Doiron, 2003). The broad multi-element signature in till around the Halfmile Lake deposit demonstrates significant glacial dispersal from this VMS deposit.

Indicator minerals recovered from till around the deposit include chalcopyrite, galena, sphalerite, pyrite, pyrrhotite, and goethite. Indicator minerals of the preglacial gossan cap include gold, beudantite ($PbFe_3(AsO_4)(SO_4)(OH)_6$), jarosite ($KFe_3(SO_4)_2(OH)_6$), and goethite (McClenaghan et al., 2012a; Budulan et al., 2015). Chalcopyrite and gold are the most useful of the indicator minerals identified, as they have survived glacial transport and post-glacial weathering of the till. This case study was one of the first to demonstrate the recovery and usefulness of the secondary minerals jarosite and beudantite in till.

Izok Lake Deposit, Arctic permafrost

The Izok Lake Zn-Cu-Pb-Ag VMS in the Point Lake Greenstone Belt, Nunavut is one of the largest undeveloped Zn-Cu resources in North America (Morrison, 2004). It was discovered in the 1970s by tracing mineralized boulders along the west shore of Izok Lake. Till

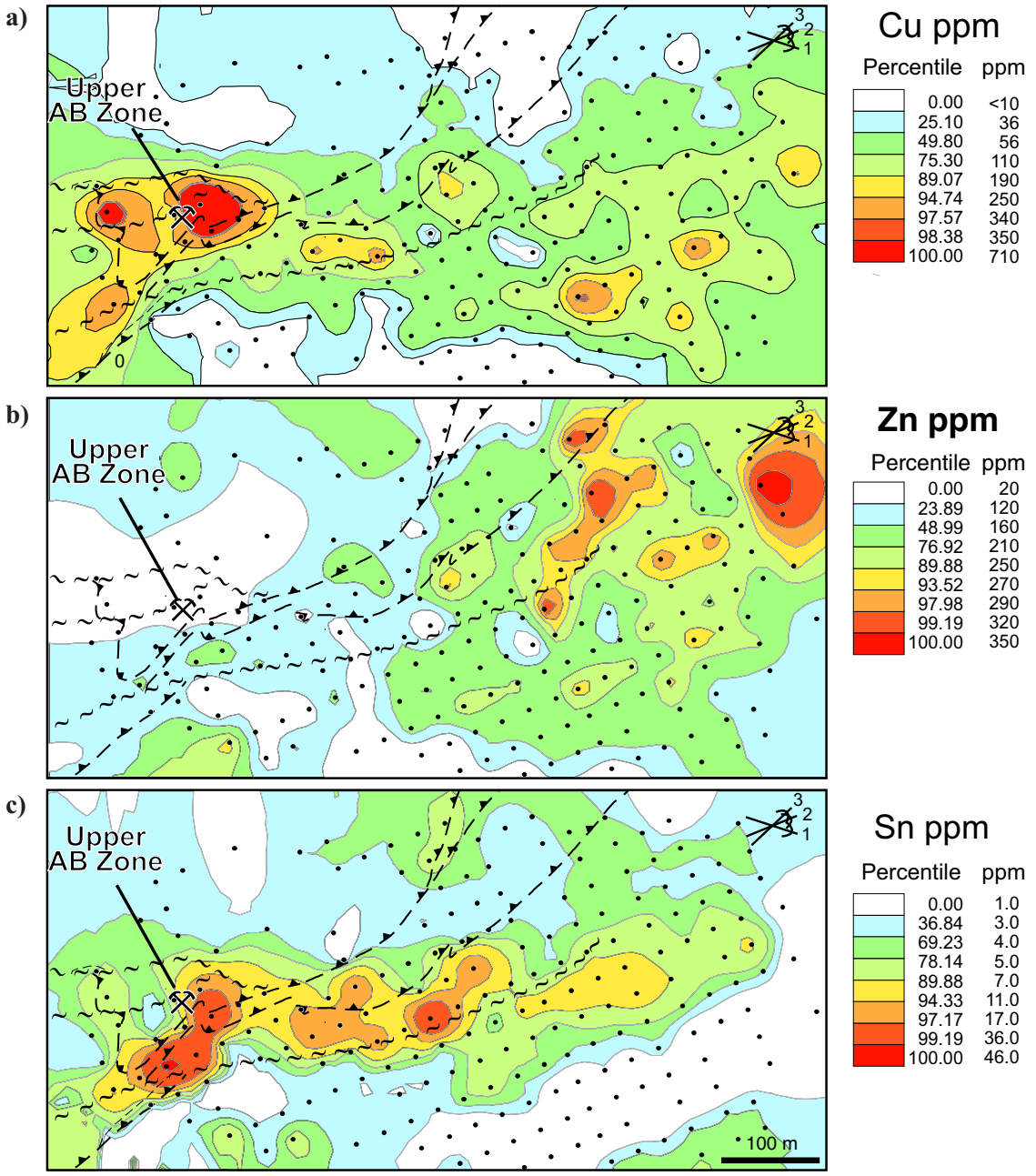


Figure 5. Till geochemistry maps for the <0.063 mm fraction of till around the Halfmile Lake VMS deposit, Bathurst Mining Camp, New Brunswick, showing a well developed northeast-trending glacial dispersal train: **a)** Cu, **b)** Zn, and **c)** Sn (modified *from* Parkhill and Doiron, 2003).

sampling in this region is best carried out using mud-boils in the permafrost terrain. Pathfinder elements of the deposit in till include Zn, Cu, Pb, Ag, Cd, and Bi and to a lesser extent Sb, Hg, Se, In, and Tl in the <0.063 mm fraction. Dispersed mineralization can be detected up to 1.3 km down-ice (northwest) using till geochemistry (Fig. 6a) (McClenaghan et al., 2015b).

Gahnite is the most useful indicator of glacial dispersal from this deposit (Paulen et al., 2013; McClenaghan et al., 2012b,c, 2015b) because of its physical robustness (hardness of 8, Mohs scale), visual distinctiveness (bluish green colour), and its high abundance in the deposit relative to its abundance in other rock types in the region. Till immediately down-ice of the deposit contains thousands of gahnite grains per 10 kg sample (Fig. 6b). The compositions of gahnite in the local till (Fig. 7) are consistent with a bedrock source that is a metamorphosed massive sulphide deposit in Fe-Al metasedimentary and metavolcanic rocks. Chalco-pyrite, sphalerite, galena, loellingite, pyrite, and axinite (calcium aluminum boro-silicate) are also useful indicator minerals in till down-ice, but they are much less abundant (10s to 100s of grains) (McClenaghan et al., 2015b; Lougheed et al., 2020).

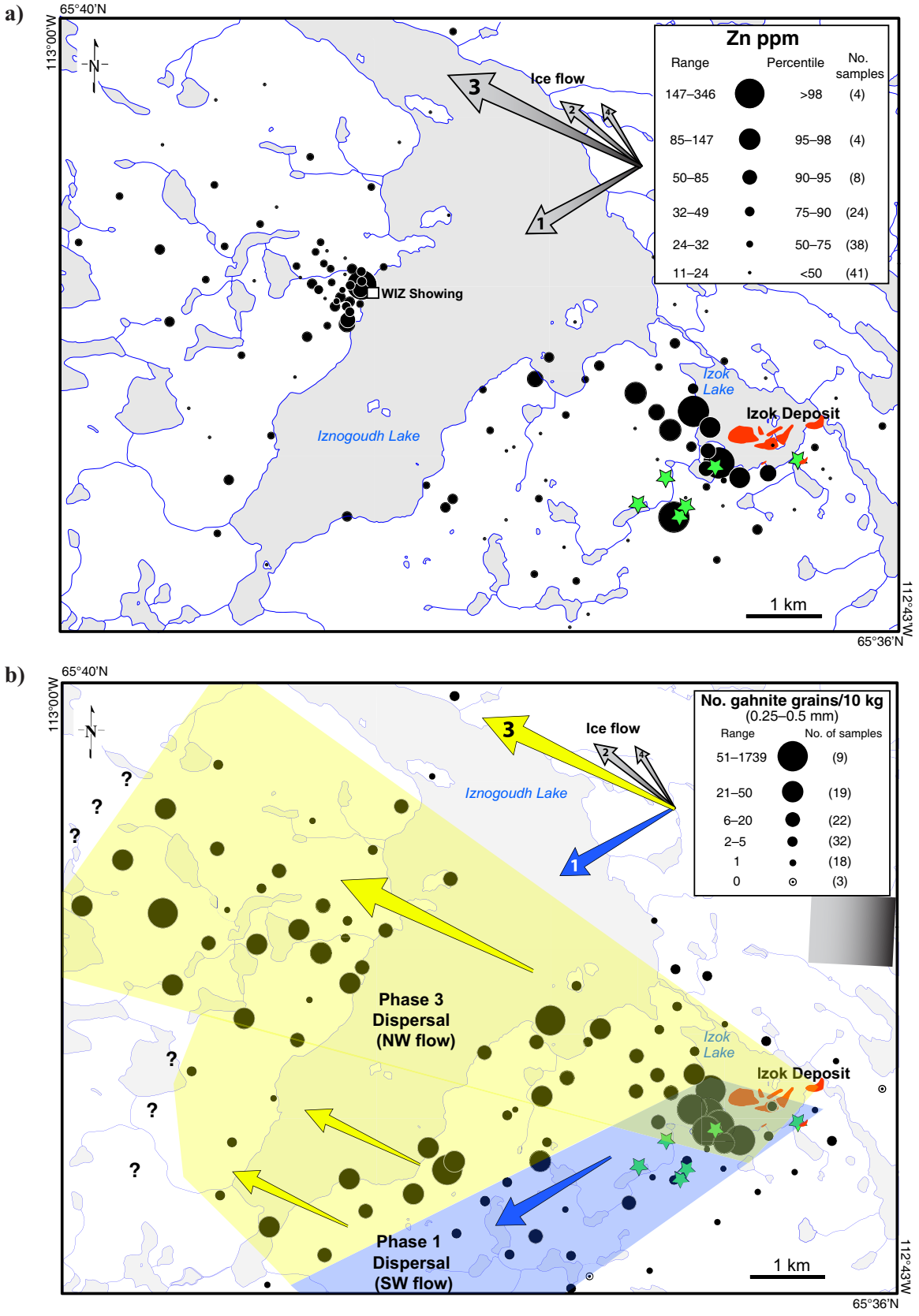
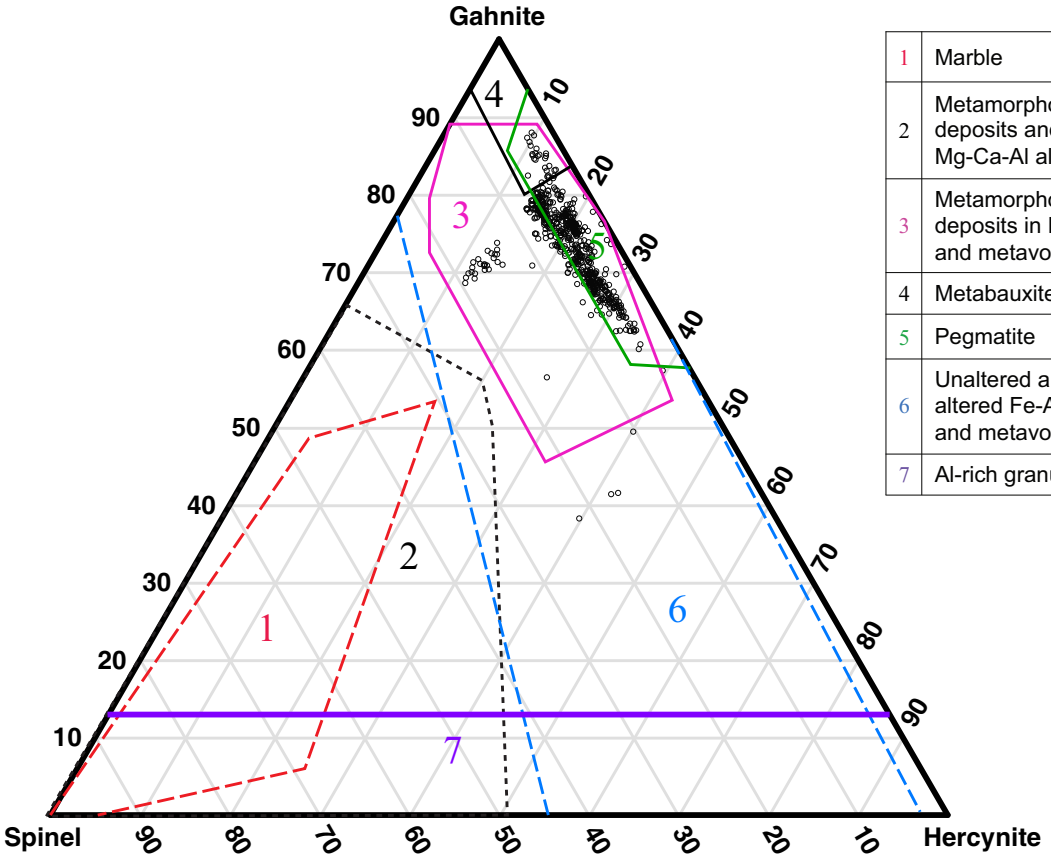


Figure 6. Distribution maps for till samples collected around the Izok Lake VMS deposit, Nunavut: **a)** Zn (ppm) in the <0.063 mm fraction of till; and **b)** gahnite in the 0.25–0.5 mm non-ferromagnetic heavy mineral fraction. Arrows indicate relative ice-flow chronology (1 = oldest) and vigor (arrow size) of flow events. The blue polygon represents dispersal by the southwest (Phase 1) ice flow and the yellow represents dispersal by northwest (Phase 3) ice flows. Modified *from* McClenaghan et al. (2015b).



1	Marble
2	Metamorphosed massive sulphide deposits and S-poor rocks in Mg-Ca-Al alteration zones
3	Metamorphosed massive sulphide deposits in Fe-Al metasedimentary and metavolcanic rocks
4	Metabauxite
5	Pegmatite
6	Unaltered and hydrothermally altered Fe-Al-rich metasedimentary and metavolcanic rocks
7	Al-rich granulite

Figure 7. Ternary plot of gahnite composition from bedrock and till samples from the Izok Lake VMS deposit, Nunavut in terms of the gahnite (Zn), hercynite (Fe), and spinel sensu stricto (Mg) spinel end members. Compositional fields are from Heimann et al. (2005). Modified *from* McClenaghan et al. (2015a).

At Izok Lake, debris has been glacially dispersed by two main ice flow phases, an older flow to the southwest and a younger flow to the northwest to produce a fan-shaped train (Fig. 6b). The gahnite dispersal fan can be detected at least 40 km down-ice (McClenaghan et al., 2012b; 2015b). At source, gahnite grains are intergrown with quartz, muscovite, and other minerals (Appendix 2, photo k). As the glacial transport distance down-ice increases, the proportion of quartz-gahnite (Appendix 2-photo l) and muscovite-gahnite intergrown grains decreases, the number of gahnite grains decreases, and the gahnite grain-size decreases (McClenaghan et al., 2014, 2015b).

DATA VISUALIZATION

Regional till surveys are conducted to assess mineral prospectivity and identify areas for further exploration. Ideally, regional till geochemical and indicator mineral data will be interpreted in combination with bedrock geology and metallogenic information, geophysical data, surficial geology, and ice-flow indicator data to assess VMS prospectivity. Parsa and McClenaghan (2024) present an example of how till geochemical data can be incorporated into the modelling of VMS prospectivity for the Bathurst Mining Camp of New Brunswick.

CONCLUSIONS

For additional details about the methods described here and more examples of the applications of these methods, the reader should refer to the reviews of till geochemistry methods for VMS exploration by McClenaghan and Peter (2013, 2016) and a review of geochemical and indicator mineral methods for VMS exploration in GSC Open File 7853 (McClenaghan et al., 2015a).

In summary, boulder tracing, till geochemistry, and indicator mineral methods have been used for more than 40 years to explore for VMS deposits in the glaciated terrain of Canada. Case studies conducted around VMS deposits demonstrate the types of geochemical and mineralogical signatures that may occur in till down-ice of VMS mineralization and how the analytical and indicator mineral methods can be applied. Four case studies from different physiographic regions have been highlighted here: Cordillera, Canadian Shield-Boreal forest, Canadian Shield-permafrost terrain, and the Appalachians. Refer to McClenaghan and Peter (2013, 2016) for explanations

of 25 of the VMS case studies or examples that have been documented from across Canada.

Other than the main ore elements (Cu, Pb, Zn), pathfinder elements of VMS deposits that are detected in till samples include other critical "minerals" (elements) and minor to trace elements that can be enriched in the sulphide and gangue minerals in mineralization and related hydrothermal products (exhalites and/or alteration), including one or more of the following (listed here alphabetically): Ag, As, Au, Ba, Bi, Cd, Co, Ga, F, Ge, Hg, In, Sb, Se, Sn, Te, and Tl. These elements are most commonly determined for the <0.063 mm (silt+clay, -250 mesh) fraction of till.

Indicator minerals of VMS deposits are recovered from the heavy mineral concentrate (>3.2 SG) fraction of till and an extensive list of potential minerals is listed in Table 3. These include the main ore minerals, galena, sphalerite, chalcopyrite, pyrite, and pyrrhotite, as well as accessory native gold, electrum, cassiterite, cinnabar, and gangue minerals magnetite and barite. Where VMS deposits have been metamorphosed, the indicator mineral suite includes physically and chemically robust oxide and silicate minerals, including sillimanite, andalusite, gahnite, staurolite, and spessartine, which indicate one or more of the following is likely present: mineralization, hydrothermal alteration, or exhalite zones. Where VMS mineralization has undergone preglacial weathering and oxidation, secondary minerals such as beudantite, jarosite, and goethite may also be useful VMS indicator minerals in till.

LA-ICP-MS is a useful tool to aid in the interpretation of indicator mineral results and to assess the fertility of potential bedrock sources up-ice.

ACKNOWLEDGEMENTS

This summary of drift exploration methods for VMS deposits in glaciated terrain is an output of the GSC's Targeted Geoscience Initiative 6 (TGI-6) Indicator Minerals for Critical Minerals and Controls on Critical Minerals in Volcanogenic Massive Sulfide Deposits sub-activities. The Izok Lake VMS case study was funded by the GSC's Geo-Mapping for Energy and Minerals Program (GEM-1) (2008–2013). The Halfmile Lake case studies were funded by the GSC's EXTECH II (1994–1999) and Targeted Geoscience Initiative 3 (TGI-3) (2005–2010) projects. We thank Don Wright (Minerals and Metals Statistics Division, Natural Resources Canada) for help with production statistics.

REFERENCES

Adair, R.N., 1992. Stratigraphy, structure, and geochemistry of the Halfmile Lake massive-sulfide deposit, New Brunswick; Exploration and Mining Geology, v. 1, p. 151–166.

Averill, S.A., 2001. The application of heavy indicator mineralogy in mineral exploration; *in* Drift Exploration in Glaciated Terrain, (ed) M.B. McClenaghan, P.T. Bobrowsky, G.E.M. Hall, and S. Cook; Geological Society of London, Special Publication 185, p. 69–81.

Averill, S.A., 2011. Viable indicators in surficial sediments for two major base metal deposit types: Ni-Cu-PGE and porphyry Cu; Geochemistry: Exploration, Environment, Analysis, v. 11, p. 279–291.

Bailey, S.L., Paradis, S., and Johnston, S., 2000. Geological setting of the Samatosum and Rea massive-sulphide deposits, Eagle Bay assemblage, south central British Columbia; Geological Survey of Canada, Current Research 2000-A15, 10 p.

Beckett-Brown, C.E. and McClenaghan, M.B., 2024. Using indicator minerals to explore for porphyry Cu deposits and their related critical minerals; *in* Till Geochemistry and Indicator Mineral Methods for Exploration in Glaciated Terrains, (ed.) R.C. Paulen and M.B. McClenaghan; Geological Survey of Canada, Open File 9210, p. 147–156. https://doi.org/10.4095/pbmy2d03m0

Bell, K. and Franklin, J.M., 1993. Application of Pb isotopes to mineral exploration in glacial terrains; Geology, v. 21, p. 1143–1146.

Bell, K. and Murton, J.B., 1995. A new indicator of glacial dispersal: lead isotopes; Quaternary Science Reviews, v. 14, p. 275–287.

Bobrowsky, P.T., Leboe, E.R., Dixon-Warren, A., Ledwon, A., MacDougall, D., and Sibbick, S.J., 1997. Till geochemistry of the Adams Plateau-North Barriere Lake area (82M/4 and 5); British Columbia Ministry of Employment and Investment, Open File 1997-9, 27 p.

Bond, J.D. and Plouffe, A. 2002. Finlayson Lake Geoscience Initiative (southeastern Yukon), Part 2: Quaternary geology and till geochemistry; *in* Yukon Exploration and Geology 2011, (ed.) D.S. Emond, L.H. Weston, and L.L. Lewis; Indian and Northern Affairs Canada, p. 209–228.

Boyle, D.R., 2003. Preglacial weathering of massive sulfide deposits in the Bathurst Mining Camp: Economic geology, geochemistry and exploration applications; *in* Massive Sulfide Deposits of the Bathurst Mining Camp, New Brunswick, and Northern Maine, (eds.) W.D. Goodfellow, S.R. McCutcheon, and J.M. Peter; Society of Economic Geologists, Economic Geology Monograph 11, p. 689–721.

Budulan, G., McClenaghan, M.B., Parkhill, M.A., Layton-Matthews, D., and Pyne, M., 2013. Till geochemical signatures of the Halfmile Lake Zn-Pb-Cu volcanogenic massive sulphide deposit, Bathurst Mining Camp, New Brunswick; Geological Survey of Canada, Open File 7174, 122 p.

Budulan, G., McClenaghan, M.B., Layton-Matthews, D., Crabtree, D., Pyne, M., and McClenaghan, S., 2015. Indicator mineral signatures of the Halfmile Lake Zn-Pb-Cu volcanogenic massive sulphide deposit, Bathurst Mining Camp, New Brunswick: Part 1-bedrock data; Geological Survey of Canada, Open File 7644, 75 p.

Brummer, J.J., Gleeson, C.F., and Hansuld, J.A. 1987. A historical perspective of exploration geochemistry in Canada-the first 30 years; Journal of Geochemical Exploration, v. 28, p. 1–39.

Cameron, E.M., 1977. Geochemical dispersion in mineralized soils of a permafrost environment; Journal of Geochemical Exploration, v. 7, p. 301–326.

Cameron, E.M. and Durham, C.C. 1975. Soil geochemistry of the Agricola Lake massive sulphide prospect; *in* Report of activities part A, April to October 1974; Geological Survey of Canada, Paper 75-1A, p. 199–202.

Campbell, H.E., 2009. Examination of glacial dispersal and use of cold vapor atomic fluorescence spectrometry at Mount Fronsac

North; M.Sc. thesis, University of New Brunswick, Fredericton, New Brunswick, 504 p.

Coker, W.B. and Shilts, W.W., 1993. Geochemical exploration for gold in glaciated terrain; Chapter 11 in: Gold Metallogeny and Exploration, (ed) R.P. Foster; Chapman & Hall., p. 336–359.

Conde, C., Tornos, F., Danyushevsky, L.V., and Large, R., 2021. Laser ablation-ICPMS analysis of trace elements in pyrite from the Tharsis massive sulphide deposit, Iberian Pyrite Belt (Spain); Journal of Iberian Geology, v. 47, p. 429–440.

Day, S.J., Broster, B.E., and Sinclair, A.J., 1987. Sulphide erratics applied to subglacial exploration: St. Elias Mountains, British Columbia; Canadian Journal of Earth Sciences, v. 24, p. 723–730.

Dehnavi, A., McFarlane, C., Lentz, D., and Walker, J.A., 2018. Assessment of pyrite composition by LA-ICP-MS techniques from massive sulfide deposits of the Bathurst Mining Camp, Canada: From textural and chemical evolution to its application as a vectoring tool for the exploration of VMS deposits; Ore Geology Reviews, v. 92, p. 656–671.

Dreimanis, A., 1958. Tracing ore boulders as a prospecting method; Canadian Institute of Mining and Metallurgy Bulletin, v. 5, p. 73–80.

Dreimanis, A., 1960. Geochemical prospecting for Cu, Pb and Zn in glaciated areas, eastern Canada; International Geological Congress XXI Session, Part II: p. 7–19.

Dreimanis, A. and Vagners, U.J., 1972. The effect of lithology upon the texture of till; *in* Research Methods in Pleistocene Geomorphology, (ed) E. Yatsu and A. Falconer; Proceedings of Second Guelph Symposium on Geomorphology 1971, p. 66–82.

Fortescue, J.A.C. and Hughes, O.L., 1965. Copper, zinc, nickel and lead in lower till material collected near a massive sulphide orebody in the Clay Belt of northern Ontario; *in* Report of Activities: Part II; Geological Survey of Canada, Paper 65-2, p. 23–27.

Fortescue, J.A.C. and Hornbrook, E.H.W., 1969. Two quick projects, one at a massive sulphide orebody near Timmins, Ontario and the other at a copper deposit in Gaspé Park, Quebec; *in* Progress report on biogeochemical research at the Geological Survey of Canada 1963-1966, (ed) J.A.C. Fortescue and E.H.W. Hornbrook; Geological Survey of Canada, Paper 67-23, Part II, p. 39–63.

Francheteau, J., Needham, H.D., Choukroune, P., Juteau, T., Seguret, M., Ballard, R.D., Fox, P. J., Normark, W., Carranza, A., Cordoba, D., Guerrero, J., Rangin, C., Bougault, P., Cambon, P., and Hekinian, R., 1979. Massive deep sea sulfide ore deposits discovered on the East Pacific Rise; Nature, v. 277, p. 523–528.

Garrett, R.G., 1969. Geochemical study, Louvicourt Township, Quebec (32C/4); *in* Report of Activities; Geological Survey of Canada, Paper 69-1 Part B, p. 18–19.

Garrett, R.G., 1971. The dispersion of copper and zinc in glacial overburden at the Louvem deposit, Val d'Or, Quebec; *in* Geochemical Exploration, Proceedings, 3rd International Geochemical Exploration Symposium, Toronto, April 16–18, 1970, (ed) R.W. Boyle; Canadian Institute of Mining and Metallurgy, Special Volume 11, p. 157–158.

Genna, D. and Gaboury, D., 2015. Deciphering the hydrothermal evolution of a VMS system by LA-ICP-MS using trace elements in pyrite: An example from the Bracemac-McLeod deposits, Abitibi, Canada, and implications for exploration; Economic Geology, v. 110, p. 2087–2108.

Ghosh, B. and Praveen, M.N., 2008. Indicator minerals as guides to base metal sulphide mineralization in Betul Belt, central India; Journal of Earth System Sciences, v. 117, p. 521–536.

Gleeson, C.F., 1975a. Magusi River Zn-Cu deposit, Quebec; *in* Conceptual Models in Exploration Geochemistry, The Canadian Cordillera and Canadian Shield, (ed) P.M.D. Bradshaw; Journal of Geochemical Exploration, v. 4, p. 172–174.

Gleeson, C.F., 1975b. Consolidated Mogador Cu-Pb-Zn-Ag-Au deposit, Quebec; *in* Conceptual Models in Exploration Geochemistry, The Canadian Cordillera and Canadian Shield, (ed) P.M.D. Bradshaw; Journal of Geochemical Exploration, v. 4, p. 158–159.

Gleeson, C.F. and Cormier, R., 1971. Evaluation by geochemistry of geophysical anomalies and geological targets using overburden sampling at depth; *in* Geochemical Exploration, Proceedings, 3rd International Geochemical Exploration Symposium, Toronto, April 16–18, 1970, (ed) R.W. Boyle; Canadian Institute of Mining and Metallurgy, Special Volume 11, p. 159–165.

Grip, E., 1953. Tracing of glacial boulders as an aid to ore prospecting in Sweden; Economic Geology, v. 48, p. 715–725.

Heimann, A., Spry, P.G., and Teale, G., 2005. Zincian spinel associated with metamorphosed Proterozoic base metal sulphide occurrences, Colorado: A re-evaluation of gahnite composition as a guide in exploration; The Canadian Mineralogist, v. 43, p. 601–622.

Hicock, S.R., 1986. Pleistocene glacial dispersal and history in Buttle Valley, Vancouver Island, British Columbia: a feasibility study for alpine drift prospecting; Canadian Journal of Earth Sciences, v. 23, p. 1867–1879.

Hicken, A.K., McClenaghan, M.B., Layton-Matthews, D., and Paulen, R.C., 2012. Till geochemical signatures of the Izok Lake Zn-Cu-Pb-Ag VMS deposit, Nunavut; Geological Survey of Canada, Open File 7046, 118 p.

Hoffman, S.J. and Woods, G.A., 1991. Multidisciplinary exploration of the BOG volcanogenic massive-sulphide prospect, Bathurst, New Brunswick, Canada; Journal of Geochemical Exploration, v. 41, p.85–101.

Hornbrook, E.H.W., 1975. Kidd Creek Cu-Zn-Ag deposit, Ontario; *in* Conceptual Models in Exploration Geochemistry, The Canadian Cordillera and Canadian Shield, (ed) P.M.D. Bradshaw; Journal of Geochemical Exploration, v. 4, p. 165–168.

Hornbrook, E.H.W., Davenport, P.H., and Grant, D.R., 1975. Regional and detailed geochemical exploration studies in glaciated terrain in Newfoundland; Newfoundland Department of Mines, Report 75-2, 116 p.

Hussein, A.A., Lochner, C., and Bell, K., 2003. Application of Pb isotopes to mineral exploration in the Halfmile Lake area, Bathurst, New Brunswick; *in* Massive Sulfide Deposits of the Bathurst Mining Camp, New Brunswick, and Northern Maine, (eds.) W.D. Goodfellow, S.R. McCutcheon, and J.M. Peter; Society of Economic Geologists, Economic Geology Monograph 11, p. 679–688.

Huston, D.L. and Champion, D.C., 2023. Applications of lead isotopes to ore geology, metallogenesis and exploration; *in* Isotopes in Economic Geology, Metallogenesis and Exploration, (ed) D. Huston and J. Gutzmer; Springer, Mineral Resource Reviews, p. 155–187.

Hyvarinen, L., Kauranne, K., and Yletyinen, V., 1973. Modern boulder tracing in prospecting; *in* Prospecting in Areas of Glaciated terrain-1973, (ed.) M.J. Jones; Institute of Mining and Metallurgy, p. 87-95.

James, L.D. and Perkins, E.W., 1981. Glacial dispersion from sulphide mineralization, Buchans area, Newfoundland; *in* The Buchans Orebodies: Fifty Years of Geology and Mining, (ed.) E.A. Swanson, D.F. Strong, and J.G. Thurlow; Geological Association of Canada, Special Paper 22, p. 269–283.

Kaszycki, C.A., Nielsen, E., and Gobert, G., 1996. Surficial geochemistry and response to volcanic-hosted massive sulphide mineralization in the Snow Lake region; *in* EXTECH I: A Multidisciplinary approach to massive sulphide research in the Rusty Lake-Snow Lake greenstone belts, Manitoba, (ed) G.F. Bonham-Carter, A.G. Galley, and G.E.M. Hall; Geological Survey of Canada, Bulletin 426, p.139–154.

Kauranne, K., 1959. Pedogeochemical prospecting in glaciated terrain; Geological Survey of Finland, Bulletin v. 184, p. 1–10.

Kettles, I.M., Garrett, R.G., and Bauke, S.T., 1998. Till, soil, and stream sediment geochemistry in the vicinity of the Manitouwadge greenstone belt; Geological Survey of Canada, Open File 3562, 210 p.

King, R.D., Piercey, S.J., and Paulen, R., 2018. In situ, microanalytical sulphur and lead isotopic compositions of sulphide indicator minerals from surficial sediments in southwestern Northwest Territories; Geological Survey of Canada, Open File 8449, p. 776–794.

Klassen, R.A., 2003. The geochemical and physical properties of till, Bathurst Mining Camp, New Brunswick, Canada; *in* Massive Sulfide Deposits of the Bathurst Mining Camp, New Brunswick and northern Maine, (ed) W.D. Goodfellow, S. McCutcheon, and J.M. Peter; Society of Economic Geologists, Economic Geology Monograph 11, p. 763-782.

Klassen, R.A. and Murton, J.B., 1996. Quaternary geology of the Buchans area, Newfoundland: implications for mineral exploration; Canadian Journal of Earth Sciences, v. 33, p. 363–377.

Knight, R.D., Kjarsgaard, B.A., and Russell, H.A.J., 2021. An analytical protocol for determining the elemental chemistry of Quaternary sediments using a portable X-ray fluorescence spectrometer; Applied Geochemistry, v. 131, 105026.

Lalonde, J.P., Bernier, L., Choinier, J., and Hebert, C., 1994. Dispersion of gahnite from the Montauban and Lac Dussault polymetallic deposits, Portneuf Township, Quebec; Quebec Ministère des Ressources Naturelles, Secteur des Mines, MB94-42, 39 p.

Layton-Matthews, D. and McClenaghan, M.B., 2022. Current techniques and applications of mineral chemistry to mineral exploration; Minerals, v. 12, 59. https://doi.org/10.3390/min12010059

Lee, H.A., 1971. Mineral discovery in the Canadian Shield using the physical aspects of overburden; The Canadian Institute of Mining, Bulletin 64, No. 715, p. 32–36.

Lett, R.E., 2001. Geochemical signatures around massive sulphide deposits in southern British Columbia, Canada; *in* Drift Exploration in Glaciated Terrain, (ed) M.B. McClenaghan, P.T. Bobrowsky, G.E.M. Hall, and S. Cook; Geological Society of London, Special Publication 185, p. 301–321.

Lett, R.E. and Jackaman, W., 2002. Geochemical exploration models, Volume 1. VMS deposits in south-central British Columbia (NTS 82L/13, L/14, 82M/4. M/5, M/6 and 92P/1E); British Columbia Ministry of Energy, Mines and Petroleum Resources, Open File 2000-31, 37 p.

Lett, R.E., Bobrowsky, P., Cathro, M., and Yeow, A., 1998. Geochemical pathfinders for massive sulphide deposits in the Southern Kootenay Terrane; *in* Geological Fieldwork 1997; British Columbia Geological Survey, Paper 1998-1, p. 15-1 – 15-10.

Lindborg, T., Papunen, H., Parkkinen, J., and Tuokko, I., 2015. The Taivaljärvi Ag-Au-Zn deposit in the Archean Tipasjärvi greenstone belt, eastern Finland; *in* Mineral Deposits of Finland, (ed) W. Maier, R. Lahtinen, and H. O'Brien; Elsevier, Amsterdam, p. 633–657.

Lougheed, H.D. McClenaghan, M.B., Layton-Matthews, D., and Leybourne, M., 2020. Exploration potential of fine-fraction heavy mineral concentrates from till using automated mineralogy: A case study from the Izok Lake Cu–Zn–Pb–Ag VMS Deposit, Nunavut, Canada; Minerals, v. 10, 310.

Lydon, J.W., 1984, Volcanogenic massive sulphide deposits. Part 1: a descriptive model; Geoscience Canada, v. 11, p. 195–202.

Makvandi, S., Beaudoin, G., Barvarz, M.G., and McClenaghan, B., 2013. Developing indicator mineral methods; application of iron oxides in discovery of VMS deposits; *in* Program with Abstracts; Geological Association of Canada-Mineralogical Association of Canada, Joint Annual Meeting, May 23, 2013, v. 36, p. 136.

Makvandi, S., Beaudoin, G., McClenaghan, B., and Layton-Matthews, D., 2015. The surface texture and morphology of magnetite from the Izok Lake volcanogenic massive sulfide deposit and local glacial sediments, Nunavut, Canada: application to mineral exploration; Journal of Geochemical Exploration, v. 150. p. 84–103.

McClenaghan, M.B. and Peter, J.M., 2013. Till geochemical signatures of Canadian volcanogenic massive sulphide deposits in glaciated terrain; Geological Survey of Canada, Open File 7354, 36 p.

McClenaghan, M.B. and Peter, J.M., 2016. Till geochemical signatures of volcanogenic massive sulfide deposits: an overview of Canadian examples; Geochemistry: Exploration, Environment, Analysis, v. 16, p. 27–47.

McClenaghan, M.B., Paulen, R.C., Ayer, J.A., Trowell, N.F., and Bauke, S.D., 1998. Regional till and humus geochemistry of the Timmins-Kamiskotia area, northeastern Ontario (NTS 42A/11, 12, 13, 14); Geological Survey of Canada, Open File 3675, 287 p. (1 sheet); 1 diskette.

McClenaghan, M.B., Budulan, G., Averill, S.A., Layton-Matthews, D., and Parkhill, M.A., 2012a. Indicator mineral abundance data for bedrock and till samples from the Halfmile Lake Zn-Pb-Cu volcanogenic massive sulphide deposit, Bathurst Mining Camp, New Brunswick; Geological Survey of Canada, Open File 7076, 10 p.

McClenaghan, M.B., Hicken, A.K., Paulen, R.C., and Layton-Matthews, D., 2012b. Indicator mineral counts for regional till samples around the Izok Lake Zn-Cu-Pb-Ag VMS deposit, Nunavut; Geological Survey of Canada, Open File 7029, 13 p.

McClenaghan, M.B., Hicken, A.K., Averill, S.A., Paulen, R.C., and Layton-Matthews, D., 2012c. Indicator mineral abundance data for bedrock and till samples from the Izok Lake Zn-Cu-Pb-Ag volcanogenic massive sulphide deposit, Nunavut; Geological Survey of Canada, Open File 7075, 11 p.

McClenaghan, M.B., Holmes, D.R.S., Averill, S.A., Paulen, R.C., and Layton-Matthews, D., 2014. Physical features indicating the glacial transport distance of gahnite from the Izok Lake Cu-Zn-Pb-Ag VMS deposit, Nunavut; Geological Survey of Canada, Open File 7603, 15 p.

McClenaghan, M.B., Peter, J.M., and Layton-Matthews, D., 2015a. Overview of VMS exploration in glaciated terrain using indicator minerals, till geochemistry, and boulder tracing: A Canadian perspective; *in* Targeted Geoscience Initiative 4 Contributions to the Understanding of Volcanogenic Massive Sulphide Genesis and Exploration Methods Development, (ed) J.M. Peter and P. Mercier-Langevin; Geological Survey of Canada, Open File 7853, p. 81–100.

McClenaghan, M.B., Paulen, R.C., Layton-Matthews, D., Hicken, A.K., and Averill, S.A. 2015b. Glacial dispersal of gahnite from the Izok Lake Zn-Cu-Pb-Ag VMS deposit, northern Canada; Geochemistry: Exploration, Environment, Analysis, v. 5, p. 333– 349.

McClenaghan, M.B., Budulan, G., Parkhill, M.A., Layton-Matthews, D., and Crabtree, D., 2017. Indicator mineral signatures of the Halfmile Lake Zn-Pb-Cu volcanogenic massive

sulphide deposit, Bathurst, New Brunswick: Part 2 – till data; Geological Survey of Canada, Open File 8111.

McClenaghan, M.B., Spirito, W.A., Plouffe, A., McMartin, I., Campbell, J.E., Paulen, R.C., Garrett, R.G., Hall, G.E.M., Pelchat, P., and Gauthier, M.S., 2020. Geological Survey of Canada till-sampling and analytical protocols: from field to archive, 2020 update; Geological Survey of Canada, Open File 8591, 73 p.

McClenaghan, M.B., Paulen, R.C., Smith, I.R., Rice, J.M., Plouffe, A., McMartin, I., Campbell, J.E., Lehtonen, M., Parsasadr, M., and Beckett-Brown, C.E., 2023. Review of till geochemistry and indicator mineral methods for mineral exploration in glaciated terrain; Geochemistry: Exploration, Environment, Analysis, v. 23 (4): geochem2023–013.

McCutcheon, S., Luff, W.M., and Boyle, R.W., 2003. The Bathurst Mining Camp, New Brunswick, Canada: History of the discovery and evolution of geological models. In: Massive Sulfide Deposits of the Bathurst Mining Camp, New Brunswick and Northern Maine, (ed) W.D. Goodfellow, S.B. McCutcheon, and J.M. Peter; Society of Economic Geologists, Economic Geology Monograph 11, p. 17–36.

Miller, J.K., 1979. Geochemical dispersion over massive sulphides within the continuous permafrost zone, Bathurst Norsemines, Canada; *in* Prospecting in Areas of Glaciated Terrain-1979; Institution of Mining and Metallurgy, London, p. 101–110.

Money, P.L. and Heslop, J.B., 1976. Geology of the Izok Lake massive sulphide deposit; Canadian Mining Journal, v. 97, p. 24–28.

Morrison, I.R., 2004. Geology of the Izok Lake massive sulphide deposit, Nunavut Territory, Canada; Exploration and Mining Geology. v. 13, p. 25–36.

Neary, G.N., 1981. Mining history of the Buchans area; *in* The Buchans Orebodies: Fifty Years of Geology and Mining, (ed) E.A. Swanson, D.F. Strong, and J.G. Thurlow; Geological Association of Canada, Canada, Special Paper 22, p. 1–64.

Nevalainen, R., 1989. Lithology of fine till fractions in the Kuhmo Greenstone Belt area, eastern Finland; Geological Survey of Finland, Special paper 7, p. 59–65.

Nichol, I. and Bjorklund, A., 1973. Glacial geology as a key to geochemical exploration in areas of glacial overburden with particular reference to Canada; Journal of Geochemical Exploration, v. 2, p. 133–170.

Nikkarinen, M., Kallio, E., Lestinen, P., and Äyräs, M., 1984. Mode of occurrence of copper and zinc in till over three mineralized areas in Finland; Journal of Geochemical Exploration, v. 21, p. 239–247.

Oviatt, N.M., Gleeson, S.A., Paulen, R.C., McClenaghan, M.B., and Paradis, S., 2015. Characterization and dispersal of indicator minerals associated with the Pine Point Mississippi Valley-type (MVT) district, Northwest Territories, Canada; Canadian Journal of Earth Sciences, v. 52, p. 776–794.

Parkhill, M.A. and Doiron, A., 1995. Surficial geology and till geochemistry near the Captain North Extension (CNE) massive sulphide deposit, northern New Brunswick; *in* Current Research 1994, (ed) S.A.A. Merlini; New Brunswick Department of Natural Resources and Energy, Miscellaneous Report 18, p. 165–203.

Parkhill, M.A. and Doiron, A., 2003. Quaternary geology of the Bathurst Mining Camp and implications for base metal exploration using drift prospecting; *in* Massive Sulfide Deposits of the Bathurst Mining Camp, New Brunswick, and Northern Maine, (ed) W.D. Goodfellow, S.R. McCutcheon, and J.M. Peter; Society of Economic Geologists, Economic Geology Monograph 11, p. 631–660.

Parsa, M. and McClenaghan, M.B., 2024. Application of machine learning to till geochemical data; *in* Till Geochemistry and Indicator Mineral Methods for Exploration in Glaciated Terrains, (ed.) R.C. Paulen and M.B. McClenaghan; Geological Survey of Canada, Open File 9210, p. 110–114. https://doi.org/10.4095/pbmy2d03m0

Paulen, R.C., 2001. Glacial transport and secondary hydromorphic metal mobilization: examples from the southern interior of British Columbia, Canada; *in* Drift Exploration in Glaciated Terrain, (ed) M.B. McClenaghan, P.T. Bobrowsky, G.E.M. Hall, and S. Cook; Geological Society of London, Special Publication 185, p. 323–337.

Paulen, R.C., Paradis, S., Plouffe, A., and Smith, I.R., 2011. Pb and S isotopic composition of indicator minerals in glacial sediments from NW Alberta. Canada: implications for Zn-Pb base metal exploration; Geochemistry: Exploration, Environment, Analysis, v. 11, p. 309–320.

Paulen, R.C., McClenaghan, M.B., and Hicken, A.K., 2013. Regional and local ice-flow history in the vicinity of the Izok Lake Zn-Cu-Pb-Ag VMS deposit, Nunavut; Canadian Journal of Earth Sciences, v. 50, p. 1209–1222.

Pelletier, M. and Beaumier, M., 1990. Géochemie du till de base (fraction fine-Région de Montauban; Gouvernement du Québec, Ministère de l'Energie et des Ressources, MB 90-20, 73 p.

Peter, J.M., Layton-Matthews, D., Piercey, S., Bradshaw, G., Paradis, S., and Boulton, A., 2007. Volcanic-hosted massive sulphide deposits of the Finlayson Lake District, Yukon; *in* Mineral Deposits of Canada: A Synthesis of Major Deposit Types, District Metallogeny, the Evolution of Geological Provinces, and Exploration Methods, (ed.) W.D. Goodfellow; Geological Association of Canada, Mineral Deposits Division, Special Publication 5, p. 471–508.

Plouffe, A. and Bond, J.D., 2003. Till geochemistry of the Finlayson Lake (105G), Glenlyon (105L) and east Carmacks (115I) map areas, Yukon Territory; Geological Survey of Canada, Open File 4479, Yukon Geological Survey Open File 2003-10(D).

Plouffe, A. and Bond, J.D., 2004. Drift prospecting in the region of the Yukon-Tanana Terrane, southern Yukon; *in* Yukon Exploration and Geology 2003, (ed) D.S. Emond and L.L. Lewis; Yukon Geological Survey, p. 221–257.

PorterGeo Database, accessed Jan19, 2024. https://portergeo.com.au/database/mineinfo.asp?mineid=mn247

Pronk, A.G., 1987. Pleistocene glacial dispersal and history in Buttle Valley, Vancouver Island, British Columbia: a feasibility study for alpine drift prospecting; Canadian Journal of Earth Sciences, v. 24, p.1504–1505.

Reed, L.E., 1977 . The discovery of the Lessard base metal deposit, Quebec; *in* Geophysics and Geochemistry in the Search for Metallic Ores; Geological Survey of Canada, Economic Geology Report 31, p. 631–639.

Rukhlov, A.S. and Ferbey, T., 2015. Application of lead isotopes in till for mineral exploration: a simplified method using ICP-MS; British Columbia Geological Survey, Paper 2015-2, 93 p.

Salminen, R., 1980. On the geochemistry of copper in the Quaternary deposits in the Kiihtelysvaara, area, north Karelia, Finland; Geological Survey of Finland, Bulletin 309, 48 p.

Sangster, D.F., Outridge, P.M., and Davis, W.J., 2000. Stable lead isotope characteristics of lead ore deposits of environmental significance; Environmental Reviews, v. 8, p.115–147.

Sarala, P., 2016. Comparison of different portable XRF methods for determining till geochemistry; Geochemistry: Exploration, Environment, Analysis, v. 16, p. 181–192.

Shilts, W.W., 1975. Principles of geochemical exploration for sulphide deposits using shallow samples of glacial drift; Canadian Institute of Mining and Metallurgy Bulletin, v. 68, p. 73–80.

Shilts, W.W., 1976. Glacial till and mineral exploration; *in* Glacial Till, (ed) R.F. Legget; Royal Society of Canada, Special Publication 12, p. 205–223.

Simonetti, A., Bell, K., and Hall, G.E.M., 1996. Pb isotopic ratios and elemental abundances for selective leachates from near-surface till: implications for mineral exploration; Applied Geochemistry, v. 11, p. 721–734.

Skinner, R.G., 1972. Overburden drilling and sampling and geological data compilation Timmins-Val d'Or area; *in* Report of Activities, Part B: November 1971 to March 1972; Geological Survey of Canada; Paper 72-01B; p. 122–123.

Smith, S., 1990. Geochemical and lithological data from overburden drill cores, with descriptive core logs, Timmins to Smoky Falls, Ontario; Geological Survey of Canada, Open File 2278, 214 p.

Smith, S.L., 1992. Quaternary stratigraphic drilling transect, Timmins to the Moose River Basin, Ontario; Geological Survey of Canada, Bulletin 415, 100 p.

Telford, W. M. and Becker, A., 1979. Exploration case histories of the Iso and New Insco orebodies; *in* Geophysics and Geochemistry in the Search for Metallic Ores, (ed) P.J. Hood; Geological Survey of Canada, Economic Geology Report 31, p. 605–629.

Thompson, I.S., 1979. Prospecting for sulphide ores in the Abitibi Clay Belt of Ontario; Canadian Institute of Mining and Metallurgy, Bulletin, v. 72, p. 65–66.

Tornos, F., Peter, J.M., Allen, R., and Conde, C., 2015. Controls on the siting and style of volcanogenic massive sulphide deposits; Ore Geology Reviews, v. 68, p. 142–163.

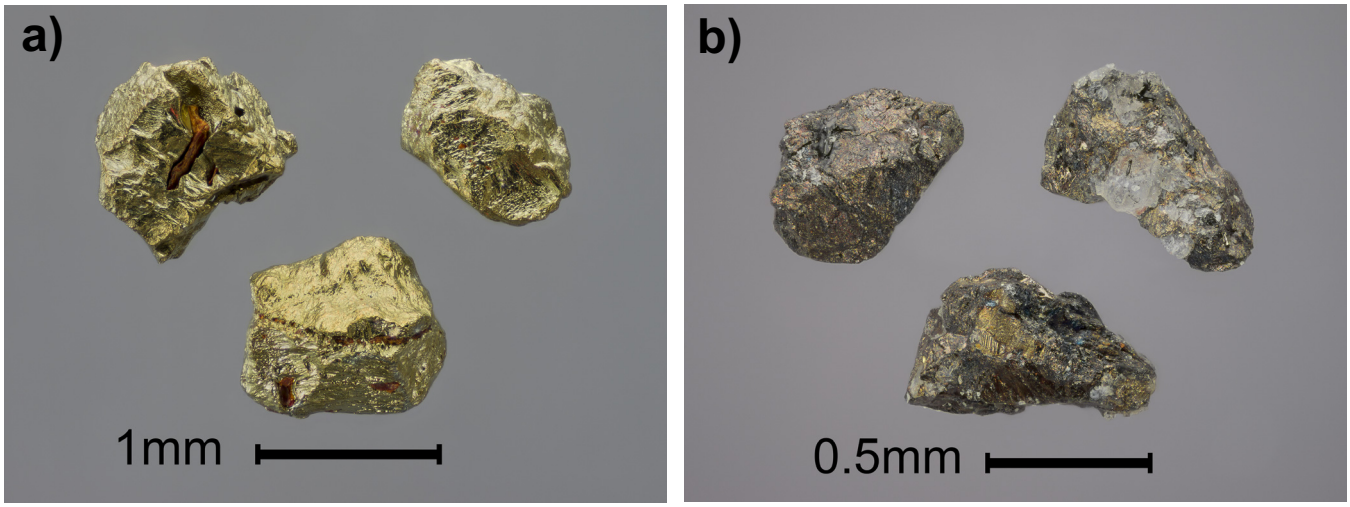
Torró, L., Benites, D., Vallance, J., Laurent, O., Ortiz-Benavente, B.A., Chelle-Michou, C., Proenza, J.A., and Fontboté, L., 2022. Trace element geochemistry of sphalerite and chalcopyrite in arc-hosted VMS deposits; Journal of Geochemical Exploration, v. 232, p. 106882.

van Geffen, P.W.G., Kyser, T.K., Oates, C.J., and Ihlenfeld, C., 2013. Lead isotope ratios in till and vegetation over a VMS occurrence under significant allochthonous cover; Geochemistry: Exploration, Environment, Analysis, v. 13, p. 53–61.

Walker, J.A., Lentz, D.R., and McClenaghan, S.H., 2006. The Orvan Brook volcanogenic massive sulphide deposit: Anatomy of a highly attenuated massive sulfide system, Bathurst Ming Camp, New Brunswick; Exploration and Mining Geology, v. 15, p.155–176.

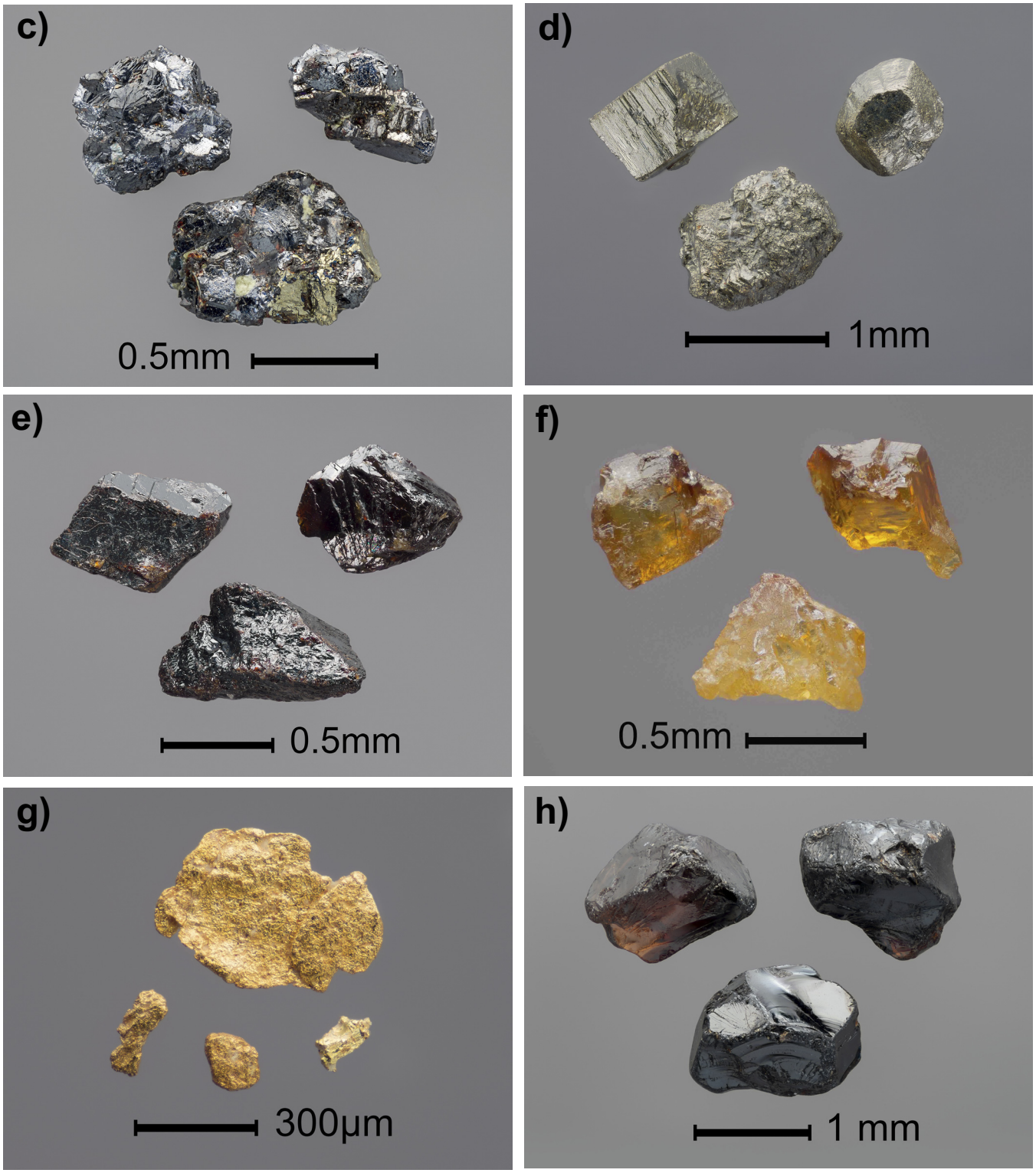
APPENDICES

Appendix 1. Photographs of volcanogenic massive sulphide indicator minerals in ore zones.



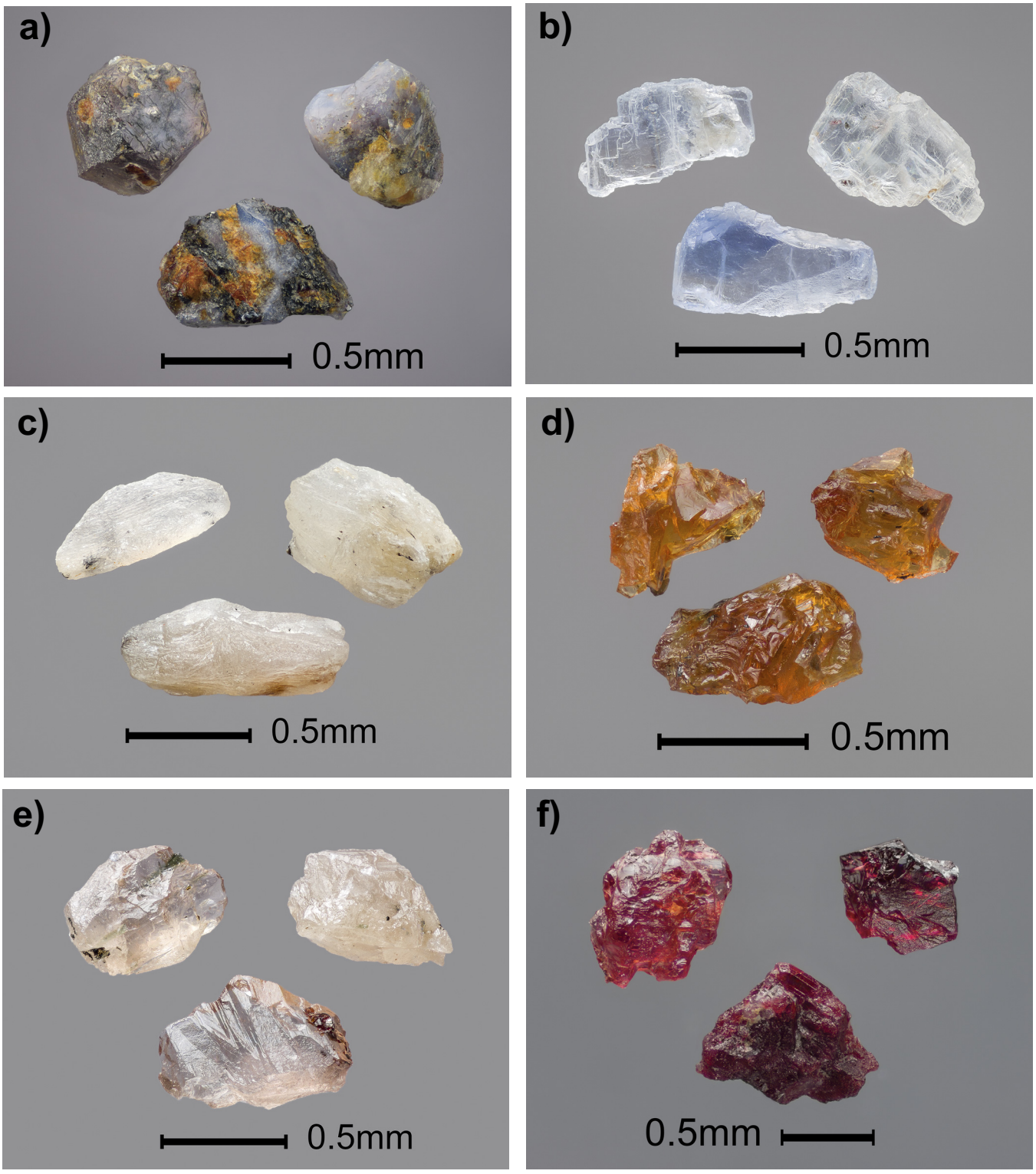
Appendix 1. Photographs of selected sand-sized VMS indicator minerals as they appear in ore zones: **a)** chalcopyrite and **b)** pyrrhotite, Appendix A1 is continued on the next page.

Appendix 1 continued.



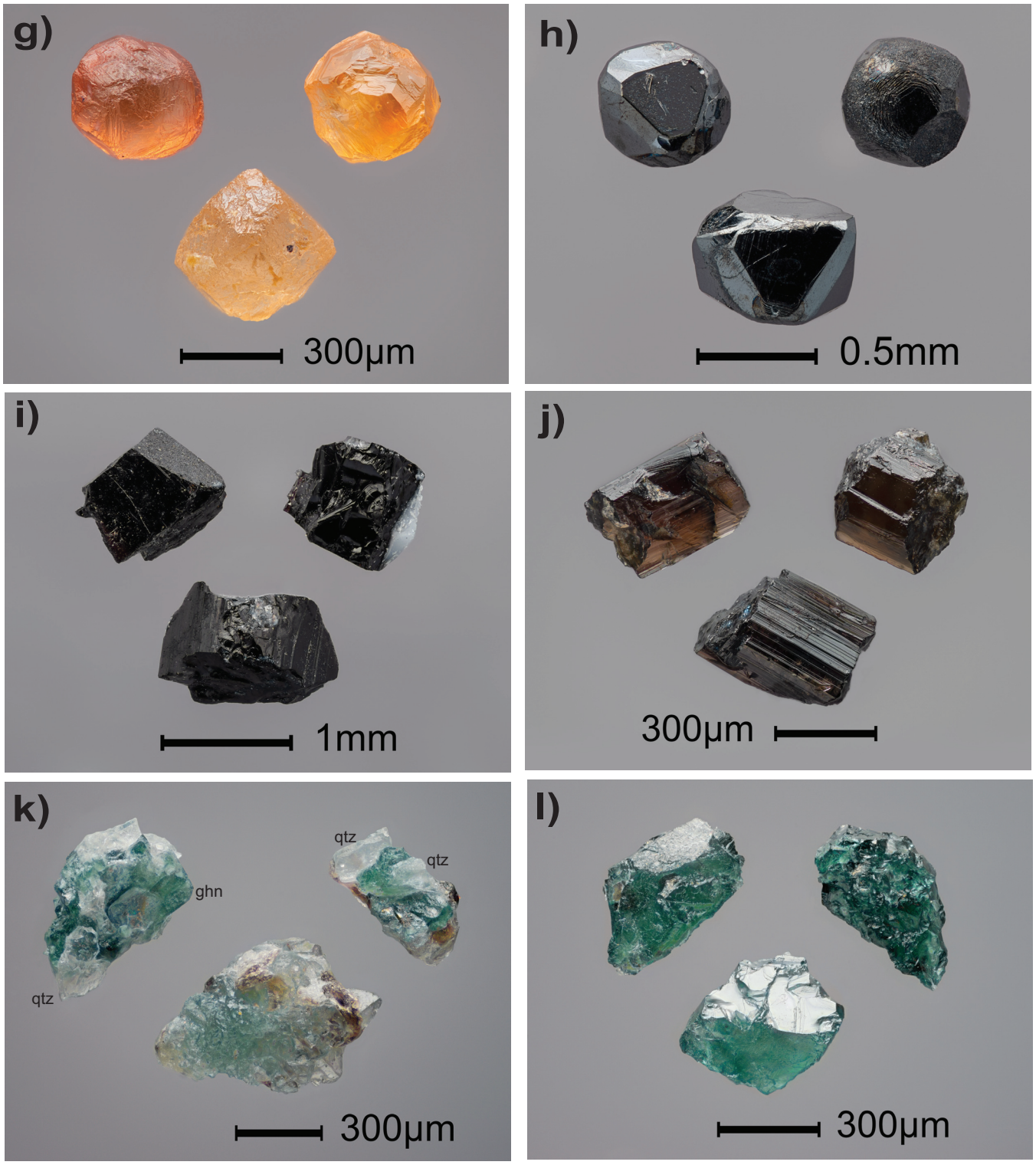
Appendix 1 continued. Photographs of selected sand-sized VMS indicator minerals as they appear in ore zones: **c)** galena, **d)** pyrite, **e)** black sphalerite (Fe-rich), **f)** honey sphalerite (Fe-poor), **g)** gold, and **h)** cassiterite. Photographs taken by Michael Bainbridge Photography.

Appendix 2. Photographs of volcanogenic massive sulphide indicator minerals in alteration or metamorphosed alteration zones.



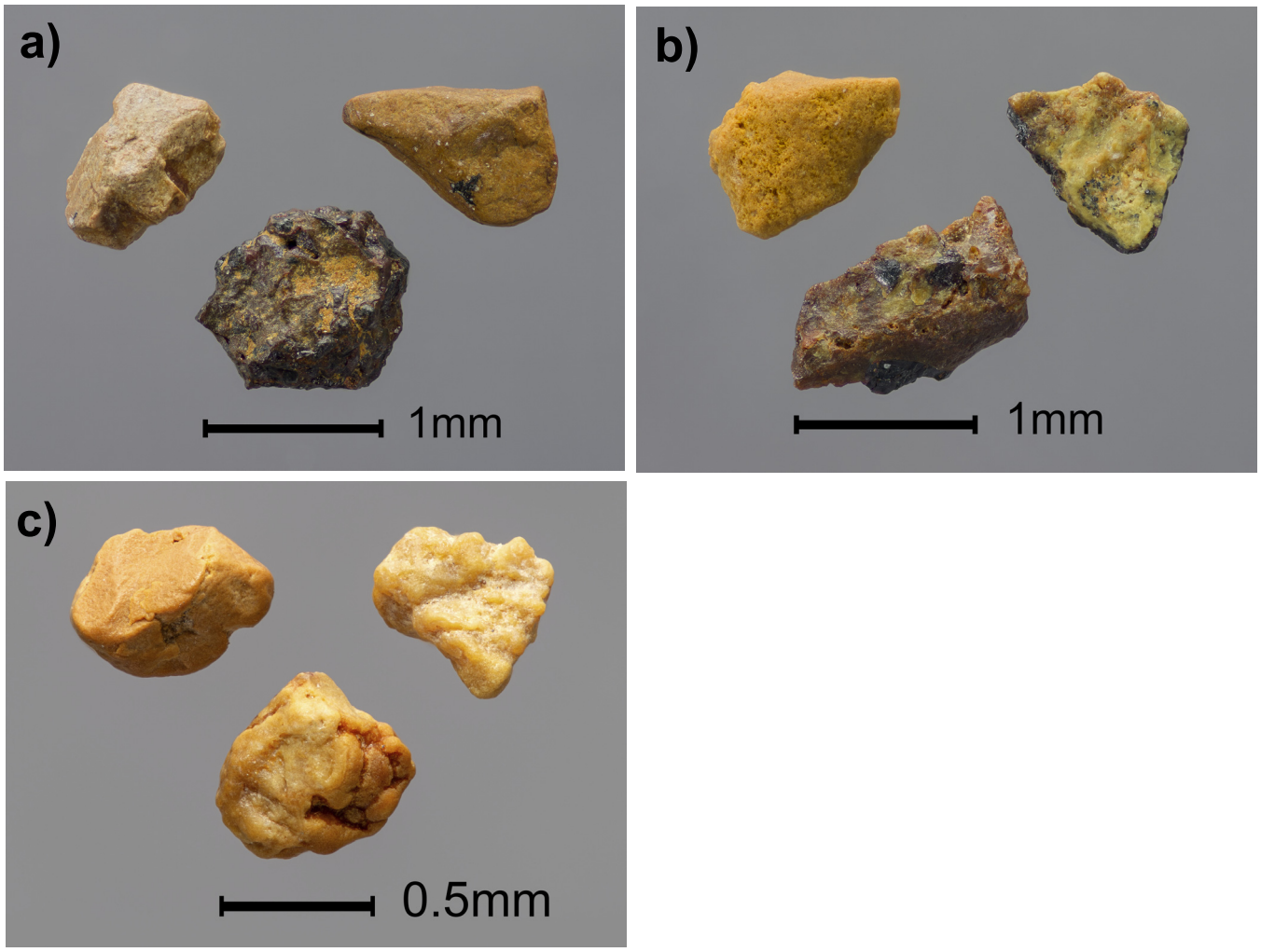
Appendix 2. Photographs of selected sand-sized VMS indicator minerals as they appear in alteration or metamorphosed alteration zones: **a)** corundum, **b)** kyanite, **c)** sillimanite, **d)** staurolite, **e)** axinite, and **f)** Mn-epidote. Appendix 2 is continued on the next page.

Appendix 2 continued.



Appendix 2 continued. Photographs of selected sand-sized VMS indicator minerals as they appear in ore zones: **g)** spessartine, and **h)** franklinite, **i)** black tourmaline, **j)** brown tourmaline, **k)** gahnite (ghn) interlocked with quartz (qtz), and **l)** gahnite. Photos taken by Michael Bainbridge Photography.

Appendix 3. Photographs of volcanogenic massive sulphide indicator minerals in gossan zones.



Appendix 3. Photographs of selected sand-sized VMS indicator minerals as they appear in gossan zones: **a)** goethite, **b)** beudanite, and **c)** jarosite. Photos taken by Michael Bainbridge Photography.

Exploring for magmatic Ni-Cu-PGE deposits in glaciated terrain: strategies and examples

Dan Layton-Matthews and M. Beth McClenaghan

Queen's University, 36 Union Street, Kingston, Ontario K7L 3N6
Geological Survey of Canada, 601 Booth Street, Ottawa, Ontario K1A 0E8

INTRODUCTION

In 2021, Canada was the sixth largest producer of nickel (Ni) globally (Natural Resources Canada, 2021). A significant proportion of Canada's Ni production is from Ni sulphides hosted in ultramafic and mafic rocks (Eckstrand and Hulbert, 2007; Lawley et al., 2021). In addition to Ni and Cu, magmatic Ni-Cu deposits can also host critical metals including Co, Bi, Au, IPGE's (Iridium-like PGEs: Iridium, Ir; Osmium, Os; and Ruthenium, Ru) and PPGE's (Palladium-like PGEs: Palladium, Pd; and Platinum, Pt).

Several books (Keays et al., 1999; Naldrett, 2004; Goldfarb et al., 2010), review chapters (Arndt et al., 2005; Eckstrand and Hulbert, 2007; Mungall, 2014) and countless journal articles (Barnes et al., 1997; Naldrett, 1999; Keays and Lightfoot, 2004; Hoatson et., 2006; Barnes et al., 2008, 2016) have outlined the genesis of the clan of Ni-Cu-PGE deposits. Fundamentally, these deposits form through a common series of steps and pathways that ultimately lead to a high concentration of these elements in a final ore deposit, including those dispersed by surficial processes. These include the following:

1) A high degree of partial melting in the mantle (Barnes and Lightfoot, 2005). To get the metal enrichments needed for optimally fertile Ni-Cu-PGE parental magmas a partial melting of >15% is required (~1000 ppm Ni, ~10 ppb Pt, ~1 ppb Ir and ~500 ppm S). Common mechanisms to achieve these high degrees of partial melting call on either mantle plumes (Hoatson et al., 2006; Arndt, 2011) or environments in a hotter and older Earth (Grove and Parman, 2004; Naldrett, 2005; Mole et al., 2014).
2) An ascent pathway that permits the rise of fertile ultramafic and mafic magmas without crustal influence (Lesher et al., 2001), substantial cooling, or crystallization (Mavrogenes and O'Neill, 1999). Pathways that are used in the genesis of these deposits include hot and softened crust through passive rifting associated with mantle plumes (Hoatson et al., 2006; Arndt, 2011) or extensional environments and active rifting related to near- and far-field tectonics (Naldrett, 2005).
3) The emplacement and crystallization environments can ultimately produce either high- or low-sulphide deposits (Naldrett, 1980; Maier, 2005) that are interpreted to be caused by differences in the timing of assimilation, crystallization, and sulphur saturation of fertile parental magmas.

3a) Fractional crystallization and immiscible sulphide segregation. If a fertile ultramafic magma is allowed to differentiate through significant crystallization of olivine then the resultant magma will be deficient in Ni (Hart and Davis, 1978), with little appreciable change to the other incompatible ore elements (Cu, Pd, S, etc.). Continued cooling and silicate crystallization would eventually cause sulphide saturation and the crystallization of chalcopyrite and platinum group minerals (PGM). These processes would create Cu-PGE deposits (Naldrett, 2004).

3b) Assimilation, immiscible sulphide segregation, and fractional crystallization. If a fertile ultramafic magma is allowed to assimilate a crustal source of S, i.e., i) coal measures, anhydrite or shales: Norilsk-Talnakh, Russia (Godlevsky and Grinenko, 1963; Li et al., 2003; Arndt, 2011); ii) iron formation: Thompson, Manitoba (Peredery, 1979; Paktunc, 1984; Layton-Matthews et al., 2010); iii) S-bearing gneisses: Voisey's Bay, Labrador (Li and Naldrett, 2000); or iv) interflow sediment or volcanic rocks: Kambalda, Western Australia (Lesher et al., 1981) or Raglan, Quebec (Lesher, 2007) then a magma may become sulphur-saturated allowing the partitioning of siderophile and chalcophile elements into an immiscible sulphide melt. This sulphide melt may then circulate through the remaining magma volume effectively scavenging additional siderophile and chalcophile elements (R-Factor; Campbell and Naldrett, 1979), turbulently flowing to other staging chambers (Lightfoot et al., 2012) or density segregating into keel (Ripley,

Recommended citation:
Layton-Matthews, D. and McClenaghan, M.B., 2024. Exploring for magmatic Ni-Cu-PGE deposits in glaciated terrain: strategies and examples; *in* Till Geochemistry and Indicator Mineral Methods for Exploration in Glaciated Terrains, (ed.) R.C. Paulen and M.B. McClenaghan; Geological Survey of Canada, Open File 9210, p. 86–98. https://doi.org/10.4095/pbmy2d03m0

Table 1. Ni-Cu-PGE deposits in glaciated terrains for which boulder tracing, till geochemistry, and/or indicator mineral methods have contributed to their discovery.

Deposit	Location	Deposit type	Commodity	Method contributing to deposit discovery	Reference
Lynn Lake	Manitoba, Canada	magmatic Ni-Cu	Ni-Cu	boulder tracing	Dreimanis (1958)
Hitura Mine	central Finland	magmatic Ni-Cu	Ni	boulder tracing	Isohanni et al. (1985)
Sakatti	northern Finland	magmatic Ni-Cu	Cu-Ni-PGE	till geochemistry	Brownscombe et al. (2015)
Kevista	northern Finland	magmatic Ni-Cu	Ni-Cu-PGE	till geochemistry	Santaguida et al. (2015)
Vammala	SW Finland	magmatic Ni-Cu	Ni-Cu	boulder tracing	Peltonen et al. (1992)
Mjövattnet	Sweden	magmatic Ni-Cu	Ni-Cu-Co	boulder tracing	Nilsson (1973)
Enonkoski (Laukunkangas)	eastern Finland	magmatic Ni-Cu	Ni-Cu	till geochemistry	Kokkola (1992)
Storbodsund	Sweden	magmatic Ni-Cu	Ni-Cu-Co	boulder tracing	Grip (1953)

2012), contact (Lesher, 2007) or footwall (Li et al., 2003; Layton-Matthews et al., 2007) deposits. Continued cooling would cause silicate and sulphide crystallization with platinum group minerals. These processes would create Ni-Cu-PGE deposits.

4) At magmatic temperatures greater than 1200ºC, an immiscible sulphide melt would contain dissolved PGEs, Au, and semimetals, plus Fe, Ni, and Cu (Howell and McDonald, 2010; and many other references). Cooling of this sulphide melt ultimately may result in the formation of a mono-sulphide saturation (MSS), commonly pyrrhotite ($Fe_{(1-x)}S$) composition, sequestering the IPGEs, Rh, and remaining Ni. The remaining liquid would be Cu-rich with the strong retention of Pt, Pd, and Au and semimetals. Continued cooling would allow the MSS to crystalize pentlandite, pyrrhotite, and PGM, whereas the Cu-rich melt would form an intermediate solid solution (ISS) and a semimetal-rich liquid before crystalizing chalcopyrite and PGM (Naldrett, 2004).

Lastly, there is increasing evidence for the variable involvement of late magmatic hydrothermal fluids in some PGE deposits (Boudreau et al., 1986, 2014; Boudreau and Meurer, 1999; Péntek et al., 2008; Tuba et al., 2014), including the Lac des Iles deposits and other low-S, high-Pd–Pt deposits. It is likely that these fluids partially dissolve already crystallized magmatic sulphide minerals, with Pd and, to a lesser degree, Pt being solubilized into the fluid (Barnes and Ripley, 2016). These fluids then move away from the original sulphide mineralization, and upon encountering changes in physical or chemical conditions, deposit Pd and Pt. This process can result in the formation of stratiform layers within intrusions or, in certain instances, transport palladium and platinum outside the intrusion, leading to the creation of low-S–high-Pd–Pt zones and veins around some intrusions (Boudreau and Meurer, 1999; Godel and Barnes, 2008; Hanley et al., 2008).

Regardless of the type of Ni-Cu-PGE system, till geochemistry, indicator mineral methods, and boulder tracing are important exploration methods for Ni-Cu-PGE deposits in Canada. In understanding the deposit models, this chapter provides an overview of best practices for applying these surficial exploration methods, including recommendations on appropriate geochemical techniques, pathfinder elements, and useful indicator minerals. The application of these surficial exploration methods has contributed to the discoveries of several Ni-Cu-PGE deposits in Canada, Sweden, and Finland, some of which are listed in Table 1. This chapter will indicate new methods for the future exploration of Ni-Cu-PGE deposits under sediment cover.

METHODS

Boulder tracing

Mineralized boulder tracing is one of the oldest exploration methods in glaciated terrain (e.g. Grip, 1953; Dreimanis, 1958; Lee, 1971; Hyvarinen et al., 1973). Prospecting for Ni-Cu-PGE by tracing mineralized boulders up-ice has contributed to the discoveries of Ni-Cu-PGE deposits, some of which are listed in Table 1. Exploration programs can include mapping the distribution of mineralized boulders and examining them using geochemical, petrographic, mineralogical, and isotopic techniques. The boulder data are integrated with till geochemistry, indicator mineralogy, bedrock geology, and geophysical data to identify mineralization style and estimate glacial transport distance and ice flow direction from potential Ni-Cu-PGE source(s).

Till geochemistry

Modern analytical methods allow for the determination of 65 elements in till samples (e.g. Brushett et al., 2024; *see* Beckett-Brown, *this volume*). These elements can delineate multi-element signatures in till down-ice of Ni-Cu-PGE deposits. Several studies have been successful in characterizing the geochemical signature of Ni-Cu-PGE deposits in surficial sediments. Research

on the soils and till around the Tulameen Complex (British Columbia, Canada) from low-sulphide, PGE-rich ultramafic rocks noted elevated levels of Pt (Cook and Fletcher, 1994). Others have reported elevated concentrations of Ni, Cu, Co, and Cr in till up to 5–7 km down-ice from the Lac des Iles low-sulphide PGE deposit (Ontario, Canada) and elevated Pt and Pd content in samples less than 1 km from sub-cropping mineralization (Barnett, 2007). In till samples collected near massive sulphide Ni-Cu-PGE deposits in the Thompson Nickel Belt (northern Manitoba, Canada) elevated ore elements Ni, Cu, Pd, Pt, and pathfinder elements Ag, As, Bi, Cd, Co, S, Sb, Se, and Te, were reported up to ~1 km away from known ore deposits (McClenaghan et al., 2011).

Given the success of till geochemistry, most current exploration programs and government surveys that utilize till geochemistry employ a strong partial digestion such as a 30-g aqua regia digestion to determine the contents of the ore elements Cu and Ni, and as well as the potential pathfinder elements Ag, Au, Bi, Cd, Co, Ni, S, Sb, Se, Te (Table 2). "Total" digestions such as lithium meta/tetraborate fusion or 4-acid digestion are optimal to determine the total contents of Cr, and other elements bound within acid-resistant minerals (oxides, zircon, etc.). Nickel sulphide fire assay followed by inductively coupled-plasma mass spectrometry (ICP-MS) on a 30 g aliquot is commonly used to determine Pt, Pd, Rh, Ru, Ir, and Au contents in the till matrix that produces a NiS button that is then digested in concentrated HCl with co-precipitation of PGEs with Te.

The main Ni-Cu-PGE "ore" minerals, chalcopyrite (H=3.5, Mohs scale), pentlandite (H=3.5–4), millerite (H=3–3.5), pyrrhotite (H=3.5–4), cubanite (H=3.5), heazlewoodite (H=4), bornite (H=3), polydymite (H=3.5–4), and violarite (H=3–4) are relatively soft and therefore are readily comminuted during glacial transport to the fine fraction (silt+clay) of till over short distances (Salminen, 1980; Nikarrinen et al., 1984; Nevalainen, 1989). Exceptions to transport size reduction are gersdorffite (H=5.5) nickeline (H=5–5.5), and sperrylite (H=6-7) due to their high hardness. The -250 mesh (<0.063 mm) fraction of till is the most commonly analyzed size fraction for Ni-Cu-PGE exploration because it: 1) is quickly and inexpensively prepared; 2) provides reasonable contrast between background and anomalous metal contents; and 3) is less susceptible to hydromorphic dispersion effects (Pronk, 1987; McClenaghan et al., 2023).

Geochemical analysis of the coarser, -80 mesh fraction (< 0.177 mm or 177 µm) of till is not recommended because many of the bedrock minerals resistant to abrasion (i.e. PGM) are smaller than 177 µm and this fraction contains a significant volume of sand-sized quartz and feldspar (Dreimanis and Vagners, 1971; Klassen, 2003). This large volume of quartz and feldspar will dilute, or mute, the geochemical signature of nearby Ni-Cu-PGE mineralization.

Indicator mineral methods

A suite of indicator minerals has been identified for Ni-Cu-PGE deposits (Tables 2, 3) that includes nickel, copper, and PGE-bearing sulphides, arsenides, and antimonides (Fig. 1), as well chromite, Cr-diopside, forsterite (Fig. 2), enstatite, and Cr-andradite (e.g. Averill, 2001, 2009, 2011; McClenaghan and Cabri, 2011; McClenaghan et al., 2020b). Sperrylite ($PtAs_2$) is the most common platinum group mineral recovered from till (Makvandi et al., 2021) down ice of Ni-Cu-PGE deposits because it is relatively stable in the surface weathering environment, physically robust (H=6–7, Mohs scale), and is visually distinct (tin white) (Fig. 1e). However, many other PGM minerals are common in till but require the use of smaller size fractions (i.e. <63 µm) and SEM-based automated mineralogical techniques (i.e. MLA, QEMSCAN, AZtecMineral, TIMA, etc.) for their use as indicator minerals. These PGM, in decreasing abundance in till (Makvandi et al., 2021), include cooperite (PtS, H=5), braggite ($PdPt_3S_4$, H=5), mertieite ($Pd_8Sb_{2.5}As_{0.5}$, H=6), laurite (RuS_2, H=7.5), erlichmanite (OsS_2, H=5), potarite (PdHg, H=3.5), isomertieite ($Pd_{11}Sb_2As_2$, H=5.5), irarsite ((Ir,Ru,Rh,Pt)AsS, H=6.5), platarsite ($Pt(As,S)_2$, H=7.5), keithconnite ($Pd_{20}Te_7$, H=5), stibiopalladinite (Pd_5Sb_2, H=4.5), stillwaterite (Pd_8As_3, H=4.5), and moncheite ($Pt(Te,Bi)_2$, H=2.5).

Olivine and chromite are indicators of both Ni-Cu-PGE and kimberlite deposits, and their physical characteristics can be used to distinguish between the two deposit types (Averill, 2009). For example, olivine grains in mineralized ultramafic rocks in the Thompson Nickel Belt and local till are smaller and colourless (Fig. 2a) compared to pale yellow to pale green olivine in kimberlites (Fig. 2b). Olivine grains in Thompson Nickel Belt rocks contain inclusions of Cr-magnetite or Fe-chromite which impart paramagnetism in contrast to kimberlitic olivine, which is nonparamagnetic. Chromite grains in Thompson Nickel Belt rocks and local till are sharp-edged (Fig. 2c) in contrast to kimberlitic chromite which commonly display resorbed surfaces (Fig. 2d).

The abundance of minerals, such as chromite and Cr-diopside, in till are particularly useful at broad reconnaissance scales to identify areas underlain by ultramafic rocks. Two examples of this are the (i) 100 km-long chromite dispersal fan down-ice (south) of favourable komatiitic rocks in the Western Abitibi Greenstone Belt (Fig. 7 *in* Averill, 2009); and (ii) 800 km long Cr-diopside dispersal fan down-ice (south-

Table 2. Case studies and examples that document the till geochemical and, in some cases, indicator mineral signatures of Ni-Cu-PGE deposits across Canada.

Deposit/occurrence	Location	Ore elements	Till geochemistry pathfinder elements	Till indicator minerals	Reference
Broken Hammer	Sudbury, Canada	Pt-Pd-Cu-Au	Ag, Au, Bi, Cd, Ni, Pd, Pt, S, Sb, Se,Te	sperrylite, chalcopyrite, gold	McClenaghan et al. (2020b)
Vermilion Mine	Sudbury, Canada	Ni-Cu-PGE	As, Bi, Co, Cu, In, Ir, Ni, Pd, Pt, Ru, Rh, Te, Tl	pentlandite, sperrylite, chalcopyrite, gold, pyrite	Hashmi (2018)
Surdbury South Range	Sudbury, Canada	Ni-Cu-PGE	As, Au, Bi, Co, Cr, Cu, Ni, Pd, Pt, Sb, Te	gold, chalcopyrite, sperrylite	Hashmi et al. (2021, 2022)
Sudbury North Range	Sudbury, Canada	Ni-Cu-Pt-Pd	Ni, Cu, Pd, Pt, Au, As, Se	gold	Coker et al. (1991); Bajc and Hall (2000)
Dana Lake, Azen Zones	northeastern Ontario	Pt-Pd-Rh	Au, Cu, Ni, Pd, Pt		Tardif (2000)
Thompson Ni Belt deposits	Manitoba, Canada	Ni-Cu	Cu, Ni, Pd, Pt	Cr-diopside, chromite, oivine, pyrrhotite, pentlandite, chalcopyrite, pyrite, arsenopyrite, gold, sperrylite	McClenaghan et al. (2009, 2011)
Lac des Isles	northwestern Ontario, Canada	Pd-Pt	Cr, Co, Cu, Mg, Ni, Pd, Pt	chromite, Cr-andradite, Pt and Pd arsenides, pyrite	Searcy (2001), Barnett (2007); Averill (2009); Barnet and Averill (2010)
Shebandowan	northwestern Ontario, Canada	Ni-Cu-PGE		Cr-diopside	Bajc (2000)
Ring of Fire/McFaulds Lake	northern Ontario	Ni-Cu, chromitite	Cr, Co, Cu, Ni	chromite	Gao and Crabtree (2016)
Tulameen ultramfic complex	British Columbia, Canada	PGE	Cr, Mg, Pt,	chromite, tulameenite, isoferroplatinum, magnetite	Cook and Fletcher (1993, 1994)
Rottenstone Lake	Saskatchewan, Canada	Ni-Cu	Ni, Cu, Pt, Pd, As, Sb		Coker et al. (1991)
Ferguson Lake	Nunavut, Canada	Cu-Ni	Au, Cu, Pd, Pt	Pd-rich minerals	Coker et al. (1991)
Rankin Inlet	Nunavut, Canada	Ni	Co, Cr, Cu, Ni		Rencz and Shilts (1980)
Voisey Bay (soil developed on till)	Labrador, Canada	Ni-Cu-Co	Cu, Ni, Pd, Pt		McConnell (2003)
Thetford Mines	Eastern Townships, Quebec, Canada	asbestos	Co, Cr, Ni		Shilts (1973); Rencz and Shilts (1980)
Sakatti	Finland	Cu-Ni-PGE	Cu, Ni, Pt		Brownscombe et al. (2015)
Enonkoski (Laukunkangas)	eastern Finland	Ni-Cu	Co, Cu, Ni		Kokkola (1992)
Talluskanava	central Finland	Ni-Cu	Co, Cu, Ni		Nurmi (1976)

Table 3. Common indicator minerals of magmatic Ni-Cu deposits that have been recovered from till samples in glaciated terrain (from Averill, 2009).

Metal Fertility indicators		Cumulus indicators		Hybrid indicators		Indicators of mineralization	
Mineral	Compostion	Mineral	Compostion	Mineral	Compostion	Mineral	Compostion
Enstatite	$(Mg,Fe)_2Si_2O_6$	Enstatite	$(Mg,Fe)_2Si_2O_6$	Ruby corundum	$(Al,Cr)_2O_3$	Chalcopyrite	$CuFeS_2$
Forsterite	$(Mg,Fe)SiO_4$	Forsterite	$(Mg,Fe)SiO_4$	Hercynite	$FeAl_2O_4$	Isoferroplatinum	Pt_3Fe
Low-Cr diopside	$Ca(Mg,Cr)Si_2O_6$	Low-Cr diopside	$Ca(Mg,Cr)Si_2O_6$	Cr-andradite	$Ca_3(Fe,Cr)_2(SiO_4)_3$	Native palladium	Pd
Chromite	$(Fe,Mg)(Cr,Al)_2O_4$	Chromite	$(Fe,Mg)(Cr,Al)_2O_4$	Cr-grossular	$Ca_3(Al,Cr)_2(SiO_4)_3$	Native gold	Au
				Uvarovite	$Ca_3Cr_2(SiO4)_3$	Sperrylite	$PtAs_2$
						Stillwaterite	Pd_8As_3
						Loellingite	$(Fe,Ni)As_2$
						Stibiopalladinite	Pd_5Sb_2

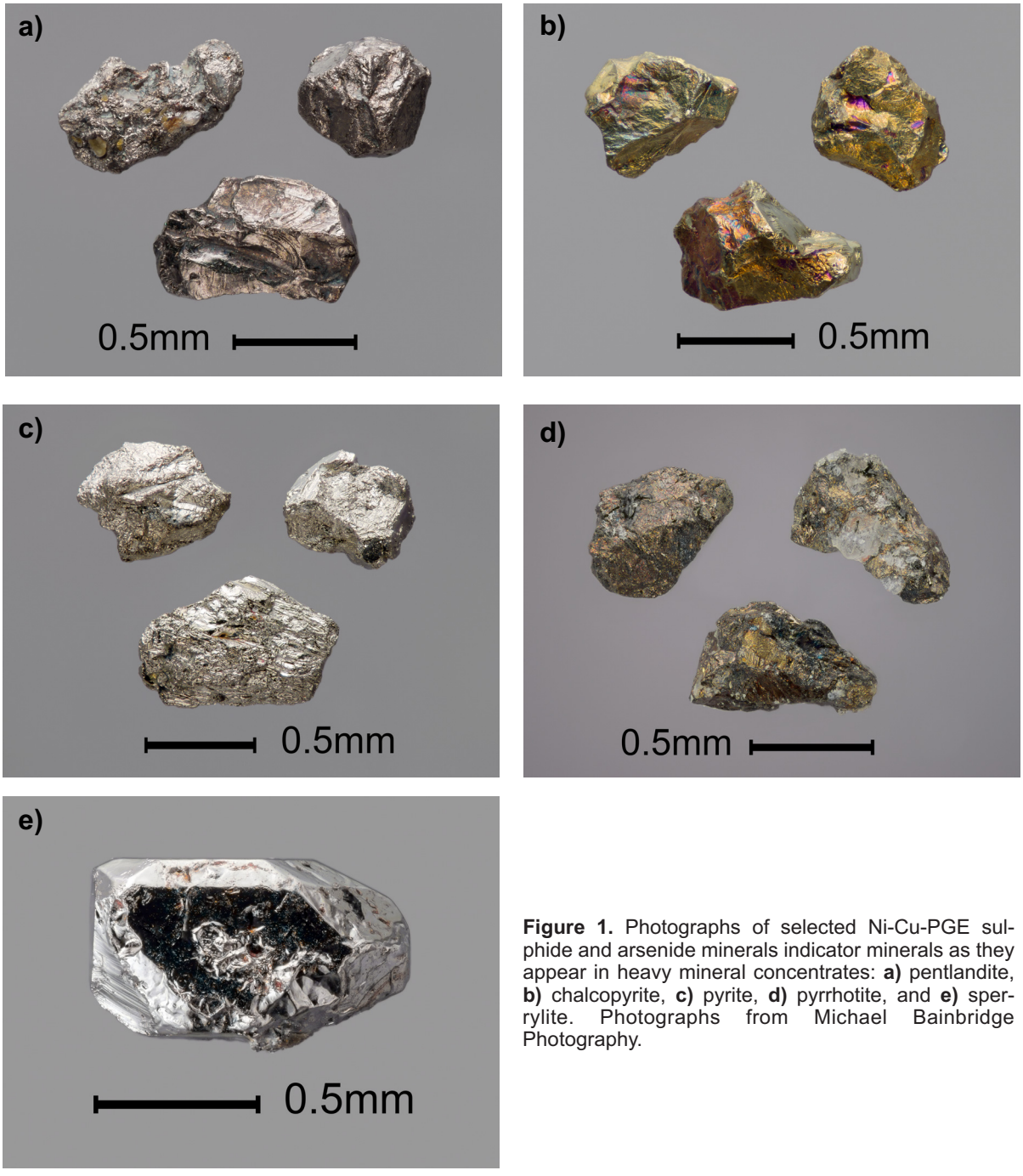


Figure 1. Photographs of selected Ni-Cu-PGE sulphide and arsenide minerals indicator minerals as they appear in heavy mineral concentrates: **a)** pentlandite, **b)** chalcopyrite, **c)** pyrite, **d)** pyrrhotite, and **e)** sperrylite. Photographs from Michael Bainbridge Photography.



Figure 2. Photographs of oxide and silicate Ni-Cu-PGE indicator minerals as they appear in heavy mineral concentrates and compared to grains from kimberlite: **a)** olivine from mineralized ultramafic rocks in the Thompson Nickel Belt, **b)** olivine from kimberlite, **c)** chromite from mineralized ultramafic rocks in the Thompson Nickel Belt, **d)** chromite from kimberlite, and **e)** Cr-diopside. Photographs from Michael Bainbridge Photography.

southwest) of the Thompson Ni Belt in northern Manitoba (Fig.6 *in* Averill, 2009).

The trace element contents of some, but not all, Ni-Cu-PGE indicator minerals have been measured, compiled and used to understand the genesis of many bedrock deposits: olivine (Li et al., 2003; Su et al., 2012; Foley et al., 2013; Mao et al., 2016; Barnes et al., 2023), chromite Economou-Eliopoulos, 1996; Melcher et al., 1999; Pagé and Barnes, 2009; Yudovskaya and Kinnaird, 2010; Mukherjee et al., 2015; Hu et al., 2022; Kang et al., 2022), pyroxene (Gao et al., 2017; Schoneveld et al., 2020), sulphides (Barnes et al., 2008; Godel and Barnes, 2008; Dare et al., 2010, 2011, 2014a; Piña et al., 2013, 2016; Duran et al., 2015; Mansur et al., 2021), Fe-Ti oxides (Dare et al., 2014b, Duran et al., 2016), and arsenides (Piña et al., 2015). The compilation of trace element contents and their distributions in minerals from bedrock ores can be used to piece together the history and progression of the geological processes that lead to ore formation. The trace element distribution patterns in minerals that exhibit specific spatial correlations on either a regional- or deposit-scale can be employed as direc-

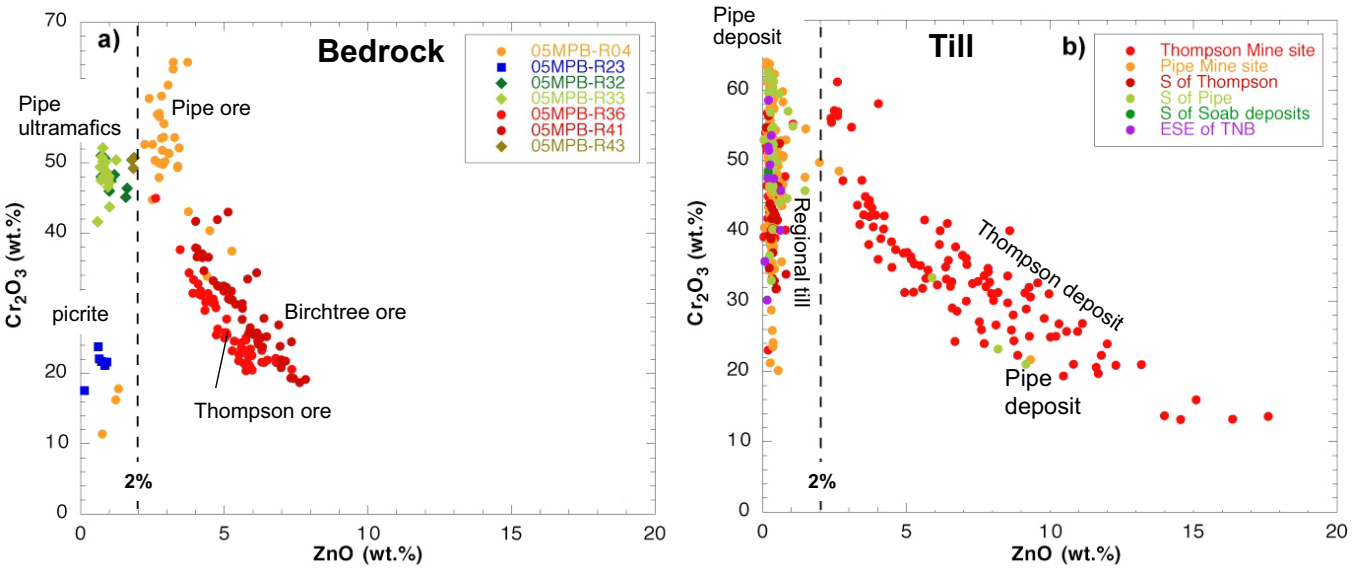


Figure 3. Cr_2O_3 versus ZnO in chromian spinels from **(a)** bedrock samples and **(b)** till samples from the Pipe, Birchtree, and Thompson mine sites. Sample colours in (a) correspond to deposit names in (b). Modified from McClenaghan et al. (2013).

tional indicators in mineral exploration strategies. Additionally, the detailed microanalysis of minerals that may contain economically valuable elements or elements that adversely affect metallurgical processes, is helping in our understanding of how certain elements or groups of elements are distributed and is also valuable for assessing their roles in element deportment studies and the broader field of geometallurgy.

These mineral chemical compilations can be readily applied to grains recovered from till samples to provide further insights and refinements of exploration targets. For example, Barnes et al. (2023) have recently reviewed the usefulness of Ni content in olivine as a fertility indicator of mafic and ultramafic intrusions. Magnetite chemistry may be useful for identifying the presence of nearby Ni-Cu-PGE mineralization and several discrimination schemes have been developed (e.g. Dupuis and Beaudoin, 2011; Dare et al., 2014b; Sappin et al., 2014; Ward et al., 2018). Duran et al. (2019) demonstrated how the trace element chemistry of chalcopyrite grains in till can be used to identify areas that have greater potential to host magmatic deposits.

CASE STUDIES

Numerous case studies have been conducted around Ni-Cu-PGE deposits in Canada and Finland (Table 2). These examples provide insights into the pathfinder elements, indicator minerals, and the nature of glacial dispersal (distance down-ice, dispersal train shape, etc.). The combined till geochemical and indicator mineral signatures of three Canadian deposits are highlighted below.

Thompson Nickel Belt, northern Manitoba

The Thompson Nickel Belt (TNB) is a 10 to 35 km wide belt of variably reworked Archean basement gneisses and Early Proterozoic cover rocks along the northwest margin of the Superior Craton (Zwanzig et al., 2007). It hosts several world-class magmatic Ni-Cu deposits that have been strongly structurally and metamorphically modified. Nickel sulphide mineralization is associated almost exclusively with, or localized within, ultramafic bodies within the lower part of the Proterozoic rocks (Bleeker and Macek, 1996). Primary ores are dominated by pyrrhotite, pentlandite, pyrite, and millerite. Chalcopyrite, magnetite, and ferrochromite are ubiquitous minor phases (Layton-Matthews et al., 2007, 2010)

Detailed till sampling was conducted in the northern part of the Belt around the Thompson, Birchtree, and Pipe deposits by the Geological Survey of Canada in 2005. Till proximal to these deposits contain 1000s ppm Ni and 100s ppm Cu. Pathfinder elements in till down ice of deposits include Pd, Pt, Co, As, Cd, Ag, Sb, Bi, Se, S, and Te. Using the geochemical signatures of the known deposits as a guide, new exploration targets were identified in the TNB that warrant further investigation (McClenaghan et al., 2009, 2011).

Indicator minerals in till down ice include chromite, Cr-diopside, olivine, enstatite, and Ni, Cu, and PGE sulphide and arsenide minerals. Chalcopyrite and sperrylite are the most useful metallic indicator minerals as they are the most likely to survive glacial transport and postglacial weathering. Chromite in strongly mineralized rocks contains elevated Zn contents (>2 wt.% ZnO; Fig. 3b) and this feature is a strong indicator of mineralization in the northern part of the belt where the

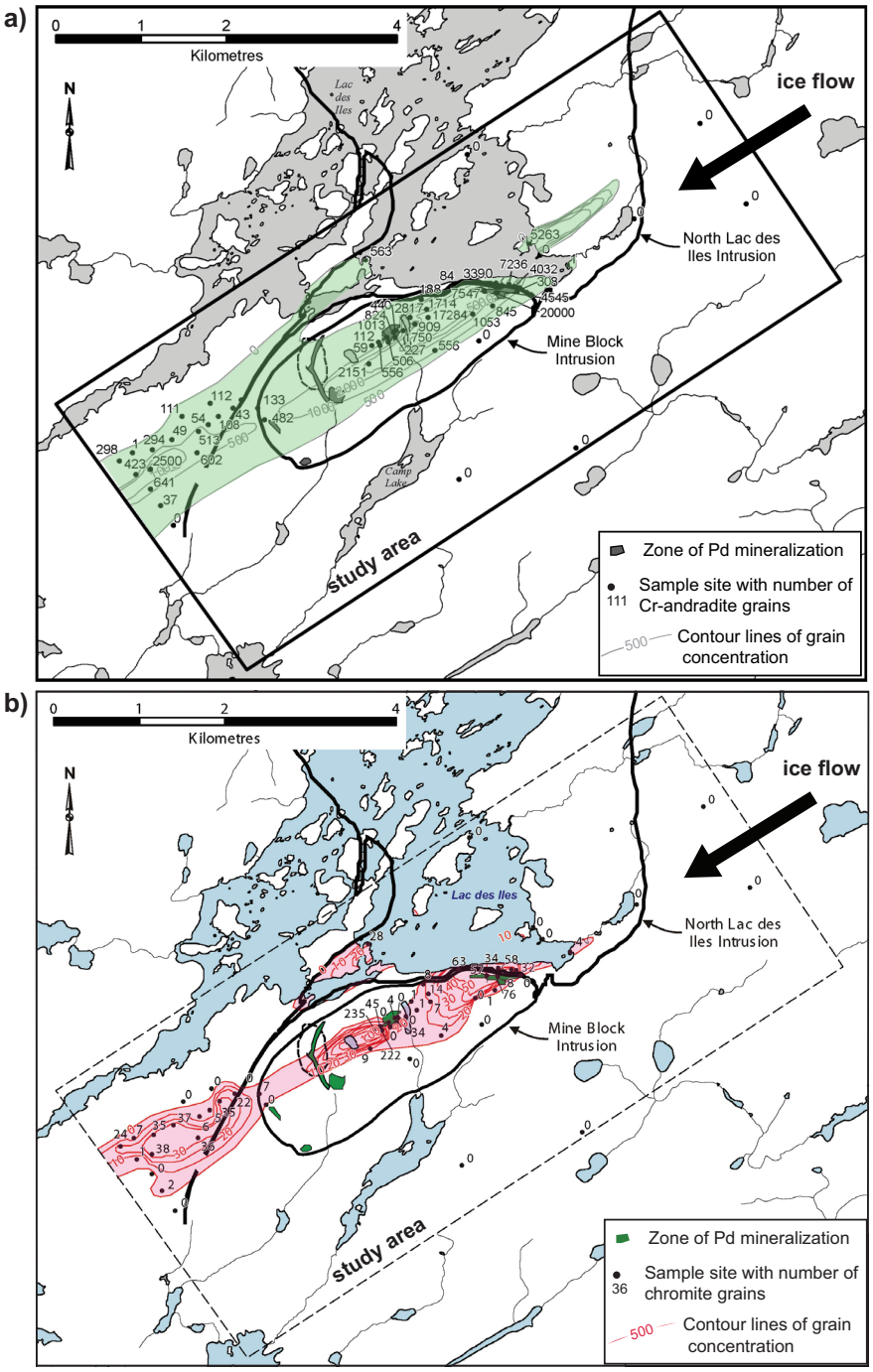


Figure 4. Distribution of indicator minerals in the 0.25–0.5 mm heavy mineral fraction of till around the Lac des Iles Pd mine: **a)** Cr-andradite dispersal with the disperal train highlighted in green. **b)** Chromite dispersal with the dispersal train highlighted in pink. Values have been normalized to a 10 kg sample weight. Modified *from* Barnett and Averill (2010).

metamorphic grade is high (McClenaghan et al., 2013). This same signature was found in chromite grains in till samples proximal to the deposits (Fig. 3b). Zinc content in chromite from Ni-deposits in the southern part of the belt with lower metamorphic grade might be considerably lower and thus the Zn enrichment does not have universal application along the belt.

Lac des Iles Pd deposit, northwestern Ontario

The Lac des Iles Pd deposit in northwestern Ontario is hosted in Archean mafic to ultramafic intrusive rocks that display complex magma mixing/mingling textures (Hinchey et al., 2005). Mineralization occurs mainly as Pd and Pt sulphides and bismuthinides (Lavigne et al., 2005; Duran et al., 2016). Till samples were collected around the deposit by the Ontario Geological Survey in 2005.

The deposit has a well developed, linear glacial dispersal train formed by a single phase of ice flow to the southwest. The train is easily detected using till geochemistry: a combination of Cr (100s ppm), Co, Cu, Mg, Ni, Pd (100s ppb), and Pt (10s ppb) at least 7 km down-ice (Barnett, 2007). Elevated concentrations of the pathfinder elements Cu and Ni are detectable far-

ther down ice than Pd and Pt due to their greater abundance and more widespread nature in local ultramafic rocks (Barnett, 2007). One of the best examples of glacial dispersal from the Pd deposit is the ribbon-shaped train defined by Cr-andradite (Fig. 4a; 1000s grains) extending at least 5 km down-ice (southwest) (Averill, 2009; Barnett and Averill, 2010). Chromite (Fig. 4b; 10s to 100s grains) displays a similar obvious and readily detectable ribbon-shaped dispersal train down ice.

A 15 km-long linear zone of anomalous Cr and Ni values in organic lake sediments along the same trend southwest of the deposit (Dyer and Russell, 2002) highlights the remarkable extent and influence of dispersed glacial debris from the ultramafic intrusive complex.

Broken Hammer Cu-Ni-PGE-Au deposit, Sudbury

The Broken Hammer deposit in the North Range of the Sudbury Structure (Sudbury, Ontario) formed in a primary magmatic-hydrothermal system that was created by the cooling Sudbury Igneous Complex. It has been suggested that a hot (>500°C) and high salinity (30 wt% NaCl equiv.) fluid, interacted with primary Ni-Cu-PGE mineralization and leached elements, transported and redeposited them in the structurally complex areas (Péntek et al., 2008). The Broken Hammer deposit consists of a shallow surface zone of vein and stockwork-hosted Cu-PGE mineralization within Sudbury breccia developed in the NeoArchean quartz monzonite Levack Gneiss Complex. Prior to mining, it consisted of a main 2–120 cm wide chalcopyrite vein and numerous smaller veins dominated by chalcopyrite-magnetite-millerite with trace gold, platinum group minerals, tellurides, bismuthides, and selenides (Péntek et al., 2008; Doran et al., 2012). Till samples were collected around the deposit by the Geological Survey of Canada in 2007.

McClenaghan et al. (2018, 2020b) reported that till down-ice contained sperrylite (100s of grains), chalcopyrite (1000s of grains), and gold (100s of grains) in the heavy mineral (>3.2 specific gravity) fraction. The <0.063 mm fraction of till displayed a strong geochemical signature of the mineralization, most notably for Pd (100s ppb), Pt (100s ppb), Au (10s ppb), and Cu (1000s ppm), but also for Ag, Cd, Ni, Sb, Bi, S, Se, and Te. Metal-rich till was encountered at least 125 m down-ice (south) of the main vein at the Broken Hammer. In contrast, the indicator minerals (sperrylite, gold, and chalcopyrite) in till were found at least 600 m down-ice of the main vein. This case study was one of the first to demonstrate the physical and chemical robustness of sperrylite during glacial erosion, transport and deposition in till and subsequent surficial weathering and the potential of indicator mineral methods to recover large numbers of sperrylite grains from till.

DATA VISUALIZATION

Regional till surveys are conducted to assess mineral prospectivity and identify areas for further exploration. Ideally, regional till geochemical and indicator mineral data will be interpreted in combination with bedrock geology and metallogenic information, geophysical data, surficial geology, and ice-flow indicator data to provide an assessment of Ni-Cu prospectivity. Parsa and McClenaghan (2024) describe an example of incorporating till geochemical data into the modelling volcanogenic massive sulphide prospectivity for the Bathurst Mining Camp of New Brunswick. Similar methodology could be used that incorporates both regional-scale till geochemical and mineralogical data for assessing Ni-Cu prospectivity in glaciated terrains.

CONCLUSIONS

In Canada, magmatic Ni-Cu-PGE deposits are important sources of the critical metals Ni, Co, Co, and PGE. Canada hosts a range of deposit types some of which contain Ni as the most valuable metal and others in which Cu and PGEs are the most important. Till geochemistry, indicator mineral methods, and boulder tracing are important exploration methods for these deposits. Pathfinder elements include the ore elements Ni, Cu, Pt, and Pd as well as a broad suite of other elements: Ag, As, Au, Cd, Co, Mg, Ni, Sb, Bi, S, Se, and Te. Useful indicator minerals include Ni-, Cu-, and PGE-bearing sulphide and arsenide minerals, as well as chromite, Cr-diopside, olivine, and pyroxene. The application of these methods in glaciated terrain has contributed to the discoveries of several Ni-Cu-PGE deposits in glaciated terrains globally (Canada, Alaska, Fennoscandia, and Russia).

ACKNOWLEDGEMENTS

This summary of drift exploration methods for Ni-Cu-PGE deposits in glaciated terrain is an output of the Geological Survey of Canada's Targeted Geoscience Initiative 6 (TGI-6) Indicator Minerals for Critical Minerals Project.

REFERENCES

Arndt, N.T., 2011. Insights into the geologic setting and origin of Ni-Cu-PGE sulfide deposits of the Norilsk-Talnakh region, Siberia; Reviews in Economic Geology, v. 17, p. 199–215.

Arndt, N.T., Lesher, C.M., and Czamanske, G.K., 2005. Mantle-derived magmas and magmatic Ni-Cu-(PGE) deposits; *in* One Hundredth Anniversary Volume, 1905–2005, (ed.) J.W. Hedenquist, J.F.H. Thompson, R.J. Goldfarb, and J.P. Richards; Economy Geology, p. 5–24.

Averill, S.A., 2001. The application of heavy indicator minerals in mineral exploration with emphasis on base metal indicators in glaciated metamorphic and plutonic terrain; *in* Drift

Exploration in Glaciated Terrain, (ed.) M.B. McClenaghan, P.T. Bobrowsky, G.E.M. Hall, and S. Cook; Geological Society of London, Special Volume 185, p. 69–82.

Averill, S.A., 2009. Useful Ni-Cu-PGE versus kimberlite indicators in surficial sediments: similarities and differences; *in* Application of Till and Stream Sediment Heavy Mineral and Geochemical Methods to Mineral Exploration in Western and Northern Canada, (eds) R.C. Paulen and I. McMartin; Geological Association of Canada, Short Course Notes 18, p. 125–139.

Averill, S.A., 2011. Viable indicators in surficial sediments for two major base metal deposit types: Ni-Cu-PGE and porphyry Cu; Geochemistry: Exploration, Environment, Analysis, v. 11, p. 279–291.

Bajc, A.F., 2000. Results of regional till sampling in the western part of the Shebandowan greenstone belt, northwestern Ontario; Ontario Geological Survey, Open File Report 6012.

Bajc, A.F. and Hall, G.E.M., 2000. Geochemical response of surficial media, north and east ranges, Sudbury Basin; Ontario Geological Survey, Open File Report 6033.

Barnes, S. and Lightfoot, P., 2005. Formation of magmatic nickel sulfide deposits and processes affecting their copper and platinum group element contents; *in* One Hundredth Anniversary Volume, 1905–2005, (ed.) J.W. Hedenquist, J.F.H. Thompson, R.J. Goldfarb, and J.P. Richards; Economy Geology, p. 179–213.

Barnes, S.-J. and Ripley, E.M., 2016. Highly Siderophile and Strongly Chalcophile Elements in Magmatic Ore Deposits; Reviews in Mineralogy and Geochemistry, v.81, p. 725–774.

Barnes, S.-J., Zientek, M.L., and Severson, M.J., 1997. Ni, Cu, Au, and platinum-group element contents of sulphides associated with intraplate magmatism; a synthesis; Canadian Journal of Earth Sciences, v. 34(4), p. 337-351.

Barnes, S-J., Prichard, H.M., Cox, R.A., Fisher, P.C., and Godel, B., 2008. The location of the chalcophile and siderophile elements in platinum-group element ore deposits (a textural, microbeam and whole rock geochemical study): Implications for the formation of the deposits; Chemical Geology, v. 248(3), p. 295–317.

Barnes, S,-J., Cruden, A.R., Arndt, N., Saumur, B.M., 2016. The mineral system approach applied to magmatic Ni-Cu-PGE sulphide deposits; Ore Geology Reviews, v. 76, p. 296-316.

Barnes, S.-J., Yao, Z-S, Mao, Y-J, Jesus, A.P., Yang, S., Taranovic, V., and Maier, W.D., 2023. Nickel in olivine as an exploration indicator for magmatic Ni-Cu sulfide deposits: A data review and re-evaluation; American Mineralogist, v. 108, p. 1-17.

Barnett, P.J., 2007. Overburden geochemical signature of the Lac des Iles platinum group element deposit, northwestern Ontario, Canada; Canadian Journal of Earth Sciences, v. 44, p. 1151–1168.

Barnett, P.J. and Averill, S., 2010. Heavy mineral trains in till in the area of the Lac des Iles PGE deposit, northwestern Ontario, Canada; Geochemistry: Exploration, Environment, Analysis, v. 10, p. 391-399.

Bleeker, W. and Macek, J., 1996. Evolution of the Thompson nickel belt, Manitoba: setting of Ni-Cu deposits in the western part of the Circum Superior Boundary zone; Geological Association of Canada–Mineralogical Association of Canada, Joint Annual Meeting, Field Trip Guidebook A1.

Boudreau, A.E. and Meurer, W.P., 1999. Concentration of platinum-group elements by magmatic fluids in layered intrusions; Economic Geology, v. 87, p. 1830–1848

Boudreau, A., Mathez, E., and McCallum, I., 1986. Halogen geochemistry of the Stillwater and Bushveld Complexes: Evidence for transport of the platinum-group elements by Cl-rich fluids; Journal of Petrology. v. 27, p. 967–986.

Boudreau, A., Djon, L., Tchalikian, A., and Corkery, J., 2014. The Lac Des Iles palladium deposit, Ontario, Canada part I: The effect of variable alteration on the offset zone; Mineralium Deposita, v. 49, p. 625–654.

Brownscombe, W., Ihlenfeld, C., Coppard, J., Hartshorne C., Klatt, S. Siikaluoma, J.K., and Herrington, R.J., 2015. The Sakatti Cu-Ni-PGE sulphide deposit in northern Finland; *in* Mineral Deposits of Finland, (ed.) W.D. Maier, R. Lahtinen, and H. O'Brien; Elsevier, p. 211–252.

Campbell, I.H. and Naldrett, A.J., 1979. The influence of silicate:sulfide ratios on the geochemistry of magmatic sulfides; Economic Geology, v. 74(6), p. 1503–1506.

Coker, W.B., Dunn, C.E., Hall, G.E.M., Rencz, A.N., DiLabio, R.N.W., Spirito, W.A., and Campbell, J.E., 1991. The behavior of platinum group elements in the surficial environment at Ferguson Lake, N.W.T., Rottenstone Lake, Sask., and Sudbury, Ont. Canada; Journal of Geochemical Exploration, v. 40, p. 165–192.

Cook, S.J. and Fletcher, W.K., 1993. Distribution and behavior of platinum in soils of the Tulameen ultramafic complex, southern British Columbia; Journal of Geochemical Exploration, v. 46, p. 279-308.

Cook, S.J. and Fletcher, W.K., 1994. Platinum distribution in soil profiles of the Tulameen ultramafic complex, southern British Columbia; Journal of Geochemical Exploration, v. 51, p. 161-191.

Dare, S.A.S., Barnes, S-J., and Prichard, H.M. 2010. The distribution of platinum group elements (PGE) and other chalcophile elements among sulfides from the Creighton Ni–Cu–PGE sulfide deposit, Sudbury, Canada, and the origin of palladium in pentlandite; Mineralium Deposita, v. 45(8), p. 765–793.

Dare, S.A.S., Barnes, S-J., Prichard, H.M., and Fisher, P.C., 2011. Chalcophile and platinum-group element (PGE) concentrations in the sulfide minerals from the McCreedy East deposit, Sudbury, Canada, and the origin of PGE in pyrite; Mineralium Deposita, v. 46(4), p. 381–407.

Dare, S.A.S., Barnes, S-J, Prichard, H.M., and Fisher, P.C., 2014a. Mineralogy and geochemistry of Cu-Rich ores from the McCreedy East Ni-Cu-PGE deposit (Sudbury, Canada): Implications for the behavior of Platinum Group and chalcophile elements at the end of crystallization of a sulfide liquid; Economic Geology, v. 109(2), p. 343–366.

Dare, S.A.S., Barnes, S-J., Beaudoin, G., Méric, J., Boutroy, E., and Potvin-Doucet, C., 2014b. Trace elements in magnetite as petrogenetic indicators; Mineralium Deposita, v. 49(7), p. 785–796.

Doran, R., Churchill, B.C., Cox, J.J., and McBride, T., 2012. Prefeasibility report on the Broken Hammer project, Sudbury, Ontario, Canada prepared for Wallbridge Mining Company Limited, Report for NI 43-101.

Dreimanis, A., 1958. Tracing ore boulders as a prospecting method in Canada; The Canadian Mining and Metallurgical Bulletin, v. 51, p. 73–79.

Dreimanis, A. and Vagners, U.J., 1971. Bimodal distribution of rock and mineral fragments in basal tills; *in* Till – A Symposium, (ed) R.P. Goldthwait; Ohio State University Press, p. 237–250.

Dupuis, C. and Beaudoin, G., 2011. Discriminant diagrams for iron oxide trace element fingerprinting of mineral deposit types; Mineralium Deposita, v. 46., p. 319–335.

Duran, C.J., Barnes, S-J., and Corkery, J.T., 2015. Chalcophile and platinum-group element distribution in pyrites from the sulfide-rich pods of the Lac des Iles Pd deposits, Western Ontario, Canada: Implications for post-cumulus re-equilibration of the ore and the use of pyrite compositions in exploration; Journal of Geochemical Exploration, v. 158, p. 223–242.

Duran, C.J., Barnes, S-J., and Cokery, J.T., 2016. Geology, petrography, geochemistry and genesis of sulfide-rich pods in the Lac des Iles palladium deposits, western Ontario; Mineralium Deposita, v. 51, p. 509–532.

Duran, C.J., Dubé-Loubert, H., Pagé, P., Barnes, S-J., Roy, M., Savard, D., Cave, B.J., Arguin, J-P., and Mansur, E.T., 2019. Applications of trace element chemistry of pyrite and chalcopyrite in glacial sediments to mineral exploration targeting: example from the Churchill Province, Northern Quebec, Canada; Journal of Geochemical Exploration, v. 196, p. 105–130.

Dyer, R.D. and Russell, D.F., 2002. Lac des Iles-Black Sturgeon River area lake sediment survey: Operation Treasure Hunt; Ontario Geological Survey, Open File Report 6096.

Eckstrand, O.R. and Hulbert, L., 2007. Magmatic nickel-copper-platinum group element deposits; *in* Mineral Deposits of Canada: A Synthesis of Major Deposit Types, District Metallogeny, the Evolution of Geological Provinces, and Exploration Methods (ed.) W.D. Goodfellow; Geological Association of Canada, Special Publication 5, Mineral Deposits Division, p. 205–222.

Economou-Eliopoulos, M., 1996. Platinum-group element distribution in chromite ores from ophiolite complexes: implications for their exploration; Ore Geology Reviews, v. 11(6), p. 363–381.

Foley, S.F., Prelevic, D., Rehfeldt, T., and Jacob, D.E., 2013. Minor and trace elements in olivines as probes into early igneous and mantle melting processes; Earth and Planetary Science Letters, v. 363 p. 181–91.

Gao, C. and Crabtree, D.C., 2016. Results of regional till and modern alluvium sampling in the McFaulds Lake ("Ring of Fire") area, northern Ontario; Ontario Geological Survey, Open File Report 6309.

Gao, W., Ciobanu, C.L., Cook, N.J., Huang, F., Meng, L., and Gao, S., 2017. Petrography and trace element signatures in silicates and Fe–Ti-oxides from the Lanjiahuoshan deposit, Panzhihua layered intrusion, Southwest China; Lithos, v. 294-295, p.164–183.

Godlevsky, M.N. and Grinenko, L.N., 1963. Some data on the isotopic composition of sulfur in the sulfides of the Noril'sk deposit; Geochemistry, v. 1, p. 335–341.

Goldfarb, R.J., Marsh, E.E., and Monecke, T., 2010. The Challenge of Finding New Mineral Resources: Global Metallogeny, Innovative Exploration, and New Discoveries; Society of Economic Geologists, Special Publication Number 15.

Godel, B. and Barnes, S-J., 2008. Platinum-group elements in sulfide minerals and the whole rock of the J-M Reef (Stillwater complex): Implication for the formation of the reef; Chemical Geology, v. 248, p. 272–294.

Grip, E., 1953. Tracing of glacial boulders as an aid to ore prospecting in Sweden; Economic Geology, v. 48, p. 715–725.

Grove, T.L. and Parman, S.W., 2004. Thermal evolution of the Earth as recorded by komatiites; Earth and Planetary Science Letters, v. 219(3), p. 173–187.

Hanley, J.J., Mungall, J.E., Pettke, T., Spooner, E.T.C., and Bray, C.J., 2008. Fluid and halide melt inclusions of magmatic origin in the Ultramafic and Lower Banded Series, Stillwater Complex, Montana, USA; Journal of Petrology, v. 49, p. 1133–1160.

Hart, S.R. and Davis, K.E., 1978. Nickel partitioning between olivine and silicate melt; Earth and Planetary Science Letters, v. 40(2), p. 203–219.

Hashmi, S., 2018. Quaternary geology and surficial media sampling in Drury and Denison townships, City of Greater Sudbury; Ontario Geological Survey, Open File Report 6342.

Hashmi, S., Leybourne, M.I., Layton-Matthews, D., Hamilton, S., McClenaghan, M.B., and Voinot, A., 2021. Surficial geochemical and mineralogical signatures of Ni-Cu-PGE deposits in glaciated terrain: Examples from the South Range of the Sudbury Igneous Complex, Ontario, Canada; Ore Geology Reviews, v. 137, 104301.

Hashmi, S., Leybourne, M.I., Hamilton, S., Layton-Matthews, D., and McClenaghan, M.B., 2022. Suitability of surficial media for Ni–Cu–PGE exploration in an established mining camp: a case study from the South Range of the Sudbury Igneous Complex, Canada; Geochemistry: Exploration, Environment, Analysis, v. 22, geochem2021–051. https://doi.org/10.1144/geochem2021-051

Hinchey, J.G., Hattori, K.H., and Lavigne, M.J., 2005. Geology, petrology and controls on PGE mineralization of the southern Roby and Twilight zones, Lac des Iles Mine, Canada; Economic Geology, v. 100, p. 43–61.

Hoatson, D.M., Jaireth, S., and Jaques, A.L., 2006. Nickel sulfide deposits in Australia; characteristics, resources, and potential; Ore Geology Reviews, v. 29 (3-4), p. 177–241.

Hu, W-J, Zhou, M-F, Yudovskaya, M.A., Vikentyev, I.V., Malpas, J., and Zhang, P-F., 2022. Trace Elements in chromite as indicators of the origin of the giant podiform chromite deposit at Kempirsai, Kazakhstan; Economic Geology, v. 117(7), p. 1629–1955.

Hyvarinen, L., Kauranne, K., and Yletyinen, V., 1973. Modern boulder tracing in prospecting; *in* Prospecting in Areas of Glaciated terrain-1973, (ed.) M.J. Jones; Institute of Mining and Metallurgy, p. 87–95.

Isohanni, M., Ohenoja, V., and Papunen, H., 1985. Geology and nickel-copper ores of the Nivala area; Geological Survey of Finland, Bulletin 333, p. 211–228.

Kang, J., Chen, L-M., Yu, S-Y., Zheng, W-Q., Dai, Z-H., Zhou, S-H., and Ai, Q-X., 2022. Chromite geochemistry of the Jinchuan Ni-Cu sulfide-bearing ultramafic intrusion (NW China) and its petrogenetic implications; Ore Geology Reviews, v. 141, p. 104644.

Keays, R.R. and Lightfoot, P.C., 2004. Formation of Ni–Cu–Platinum Group Element sulfide mineralization in the Sudbury Impact Melt Sheet; Mineralogy and Petrology, v. 82(3), p. 217–258.

Keays, R.R., Lesher, C.M., Lightfoot, P.C., and Farrow, C.E.G., 1999. Dynamic processes in magmatic ore deposits and their application to mineral exploration; Geological Association of Canada, Short Course Notes, v. 13.

Klassen, R.A., 2003. The geochemical and physical properties of till, Bathurst mining camp, New Brunswick, Canada; *in* Massive Sulfide Deposits of the Bathurst Mining Camp, New Brunswick, and Northern Maine, (ed.) W.D. Goodfellow, S.W. McCutcheon, D.R. Lentz, and J.M. Peter; Society of Economic Geologists, Monograph 11, p. 661–678.

Kokkola, M. 1992. Laukunkangas: Ni, Co and Cu concentrations of till at a Proterozoic mineralized mafic intrusion in humid plain terrain; *in* Regolith Exploration Geochemistry in Arctic and Temperate Terrains, (ed.) K. Kauranne; Handbook of Exploration Geochemistry, Elsevier, Amsterdam, v. 5, p. 293–295.

Lavigne, M.J, Michaud, M.J., and Rickard, J., 2005. Discovery and geology of the Lac des Iles palladium deposits; *in* Exploration for Platinum Group Elements Deposits, (ed.) J.E. Mungall; Mineralogical Association of Canada, Short Course 35, Oulu, Finland, p. 369–390.

Lawley, C.J.M., Tschirhart, V., Smith, J.W., Pehrsson, S.J., Schetselaar, E.M., Schaeffer, A.J., Houlé, M.G., and Eglington, B.M., 2021. Prospectivity modelling of Canadian magmatic Ni(±Cu±Co±PGE) sulphide mineral systems; Ore Geology Reviews, v. 132, 103985. https://doi.org/10.1016/ j.oregeorev.2021.103985

Layton-Matthews, D., Lesher, C.M., Burnham, O.M., Liwanag, J., Halden, N.M., Hulbert, L., and Peck, D., 2007. Magmatic Ni-Cu-platinum group element deposits of the Thompson Nickel Belt; *in* Mineral Deposits of Canada: A Synthesis of Major Deposit Types, District Metallogeny, the Evolution of Geological Provinces and Exploration Methods, (ed.) W. Goodfellow; Geological Association of Canada, Special Volume 5, p. 409–432

Layton-Matthews, D., Lesher, C.M., Burnham, O.M., Hulbert, L., Peck, D.C., Golightly, J.P., and Keays, R.R., 2010. Exploration for komatiite-associated Ni-Cu-(PGE) mineralization in the Thompson Nickel Belt, Manitoba; Economic Geology, Special Publication 15, p. 513–538.

Lee, H.A. 1971. Mineral discovery in the Canadian Shield using the physical aspects of overburden; Canadian Institute of Mining and Metallurgical Bulletin, v. 64, No. 715, p. 32–36.

Lesher, C.M., 2007. Ni-Cu-(PGE) deposits in the Raglan Area, Cape Smith belt, New Québec; *in* Mineral Deposits of Canada: A Synthesis of Major Deposit Types, District Metallogeny, the Evolution of Geological Provinces, and Exploration Methods, (ed.) W.D. Goodfellow; Mineral Deposits Division, Geological Association of Canada, Special Publication 5, p. 351–85.

Lesher, C.M., Lee, R.F., Groves, D.I., Bicklem M.J., and Donaldson, M.J., 1981. Geochemistry of komatiites from Kambalda, Western Australia; I, Chalcophile element depletion, a consequence of sulfide liquid separation from komatiitic magmas; Economic Geology, v. 1981, p. 1714–1728.

Lesher, C.M., Burnham, O.M., Keays, R.R., Barnes, S.J., and Hulbert, L., 2001. Trace-element geochemistry and petrogenesis of barren and ore-associated komatiites; The Canadian Mineralogist, v. 39, p. 673–696.

Li, C. and Naldrett, A.J., 2000. Melting reactions of gneissic inclusions with enclosing magma at Voisey's Bay: Implications with respect to ore genesis; Economic Geology, v. 95, p. 801–814.

Li, C., Ripley, E.M., and Naldrett, A.J., 2003. Compositional variations of olivine and sulfur isotopes in the Noril'sk and Talnakh intrusions, Siberia: Implications for ore-forming processes in dynamic magma conduits; Economic Geology, v. 98, p. 69–86.

Lightfoot, P.C., Keays, R.R., Evans-Lamswood, D., and Wheeler, R., 2012. S saturation history of Nain Plutonic Suite mafic intrusions: origin of the Voisey's Bay Ni–Cu–Co sulfide deposit, Labrador, Canada; Mineralium Deposita, v. 47(1), p. 23–50.

Maier, W., 2005. Platinum-group element (PGE) deposits and occurrences: Mineralization styles, genetic concepts, and exploration criteria; Journal of African Earth Sciences, v. 41, p. 165–191.

Mansur, E.T., Barnes, S-J., and Duran, C.J., 2021. An overview of chalcophile element contents of pyrrhotite, pentlandite, chalcopyrite, and pyrite from magmatic Ni-Cu-PGE sulfide deposits; Mineralium Deposita, v. 56, p. 179–204.

Mao, Y., Qin, K., Tang, D., Feng, H., and Xue, S., 2016. Crustal contamination and sulfide immiscibility history of the Permian Huangshannan magmatic Ni-Cu sulfide deposit, East Tianshan, NW China; Journal of Asian Earth Sciences; v. 129, p. 22–37.

Mavrogenes, J.A. and O'Neill, H.S.C., 1999. The relative effects of pressure, temperature and oxygen fugacity on the solubility of sulfide in mafic magmas; Geochimica et Cosmochimica Acta, v. 63(7), p. 173–1180.

McClenaghan, M.B. and Cabri, L.J., 2011. Gold and platinum group element indicator minerals in surficial sediments; Geochemistry: Exploration, Environment, Analysis, v. 11, p. 251–263.

McClenaghan, M.B., Matile, G. Layton-Matthews, D., and Pyne M., 2009. Till geochemical signatures of magmatic Ni-Cu deposits and regional till geochemistry, Thompson Nickel Belt, Manitoba; Geological Survey of Canada, Open File 6005.

McClenaghan, M.B., Layton-Matthews, D., and Matile, G., 2011. Till geochemical signatures of magmatic Ni-Cu deposits, Thompson Nickel Belt, Manitoba, Canada; Geochemistry Exploration, Environment, Analysis, v. 11, p. 145–159.

McClenaghan, M.B., Kjarsgaard, I.M., Averill, S.A., Layton-Matthews, D., Crabtree, D., Matile, G., McMartin, I., and Pyne, M., 2013. Indicator mineral signatures of magmatic Ni-Cu deposits, Thompson Nickel Belt, Manitoba: Part 2 – till data; Geological Survey of Canada, Open File 7200. https://doi.org/10.4095/292543

McClenaghan, M.B., Kjarsgaard, I.M., Ames, D.E., and Crabtree, D., 2018. Indicator mineral data for till samples from the Broken Hammer Cu-Ni-PGE-Au deposit, North Range, Sudbury Structure, Ontario; Geological Survey of Canada, Open File 8384. https://doi.org/10.4095/308118

McClenaghan, M.B., Spirito, W.A., Plouffe, A., McMartin, I., Campbell, J.E., Paulen, R.C., Garrett, R.G., Hall, G.E.M., Pelchat, P., and Gauthier, M.S., 2020a. Geological Survey of Canada till-sampling and analytical protocols: from field to archive, 2020 update; Geological Survey of Canada, Open File 8591.

McClenaghan, M.B., Ames, D.E., and Cabri, L.J., 2020b. Indicator mineral and till geochemical signatures of the Broken Hammer Cu-Ni-PGE-Au deposit, North Range, Sudbury structure, Ontario, Canada; Geochemistry: Exploration, Environment, Analysis, v. 20, p. 337–356.

McClenaghan, M.B., Brushett, D.M., Beckett-Brown, C.E., Paulen, R.C., Rice, J.M., Haji Egeh, A., and Nissen, A., 2023. Indicator mineral studies at the Brazil Lake LCT pegmatites, southwest Nova Scotia; Geological Survey of Canada, Scientific Presentation 157. https://doi.org/10.4095/331686

McConnell, J.W., 2003. Lake-sediment and soil surveys for Platinum-Group Metals in central Labrador and the Voisey's Bay area; Newfoundland Department of Energy and Mines, Current Research 2003, Report 03-1, p. 179–192.

Melcher, F., Grum, W., Thalhammer, T.V., and Thalhammer, O.A.R., 1999. The giant chromite deposits at Kempirsai, Urals: constraints from trace element (PGE, REE) and isotope data; Mineralium Deposita, v. 34(3), p. 250–272.

Mole, D.R., Fiorentini M.L., Thebaud N., Cassidy K.F., McCuaig T.C., and Kirkland C.L., 2014. Archean komatiite volcanism controlled by the evolution of early continents; Proceedings of the National Academy of Sciences of the United States of America, v. 111(28), p. 10083–10088.

Mukherjee, R., Mondal, S.K., González-Jiménez, J.M., Griffin, W.L., Pearson, N.J., and O'Reilly, S.Y., 2015. Trace-element fingerprints of chromite, magnetite and sulfides from the 3.1 Ga ultramafic–mafic rocks of the Nuggihalli greenstone belt, Western Dharwar craton (India); Contributions to Mineralogy and Petrology, v. 169(6), p. 1–23.

Mungall, J.E., 2014. 13.8 - Geochemistry of Magmatic Ore Deposits; *in* Treatise on Geochemistry (Second Edition), (ed.) H.D. Holland and K.K. Turekian; Elsevier, Oxford, p. 195–218.

Naldrett, A.J., 1999. World-class Ni-Cu-PGE deposits: key factors in their genesis; Mineralium Deposita, v. 34, p. 227–240.

Naldrett, A.J., 2004. Platinum group element (PGE) deposits; *in* Magmatic Sulfide Deposits: Geology, Geochemistry and Exploration, (ed.) A.J. Naldrett; Springer, Berlin Heidelberg, p. 481–612.

Naldrett, A.J., 2005. A history of our understanding of magmatic Ni–Cu sulfide deposits; The Canadian Mineralogist, v. 43(6), p. 2069–2098.

Naldrett, A.J. and Duke, J.M., 1980. Platinum metals magmatic sulfide ores; Science, v. 208(4451), p. 1417–1424.

Natural Resources Canada, 2021. Nickel facts. https://natural-resources.canada.ca/our-natural-resources/minerals-mining/mining-data-statistics-and-analysis/minerals-metals-facts/nickel-facts/20519

Nevalainen, R. 1989. Lithology of fine till fractions in the Kuhmo greenstone belt area, eastern Finland; Geological Survey of Finland, Special Paper 7, p. 59–65.

Nikkarinen, M., Kallio, E., Lestinen, P., and Äyräs, M., 1984. Mode of occurrence of copper and zinc in till over three mineralized areas in Finland; Journal of Geochemical Exploration, v. 21, p. 239–247.

Nilsson, G., 1973. Nickel prospecting and the discovery of the Mjövattnet mineralization, northern Sweden: a case history of the use of combined techniques in drift-covered terrain; *in* Prospecting in Areas of Glaciated Terrain, (ed.) M.J. Jones; Institution of Mining and Metallurgy, London, p. 97–109.

Nurmi, A., 1976. Geochemistry of the till blanket at the Talluskanava Ni-Cu ore deposit, Tervo, central Finland; Geological Survey of Finland, Report of Investigation No. 15.

Paktunc, A.D., 1984. Petrogenesis of ultramafic and mafic rocks of the Thompson Nickel Belt, Manitoba; Contributions to Mineralogy and Petrology, v. 88(4), p. 348–353.

Pagé, P. and Barnes, S-J., 2009. Using trace elements in chromites to constrain the origin of podiform chromitites in the Thetford Mines Ophiolite, Québec, Canada; Economic Geology, v. 104(7), p. 997–1018.

Parsa, M. and McClenaghan, M.B., 2024. Application of machine learning to till geochemical data; *in* Till Geochemistry and Indicator Mineral Methods for Exploration in Glaciated Terrains, (ed.) R.C. Paulen and M.B. McClenaghan; Geological Survey of Canada, Open File 9210, p. 110–114. https://doi.org/10.4095/pbmy2d03m0

Peltonen, P., Huhta, P., and Korsman, K., 1992. Occurrence and mineral chemistry of chrome spinel in till- implications for prospecting for magmatic Ni-Cu sulfide ores in Svecofennian terrain; Geological Survey of Finland, Report of Investigation 111.

Péntek, A., Molnár, F., Watkinson, D.H., and Jones, P.C., 2008. Footwall-type Cu-Ni-PGE mineralization in the Broken Hammer area, Wisner Township, North Range, Sudbury Structure; Economic Geology, v. 103, p. 1005–1028.

Peredery, W.V., 1979. Relationship of ultramafic amphibolites to metavolcanic rocks and serpentinites in the Thompson Belt, Manitoba; The Canadian Mineralogist; v. 17, p. 187–200.

Piña, R., Gervilla, F., Barnes, S-J., Ortega, L., and Lunar, R., 2013. Platinum-group elements-bearing pyrite from the Aguablanca Ni-Cu sulphide deposit (SW Spain): a LA-ICP-MS study; European Journal of Mineralogy, v. 25(2), p. 241–252.

Piña, R., Gervilla, F., Barnes, S.J., Ortega, L., and Lunar, R., 2015. Liquid immiscibility between arsenide and sulfide melts: evidence from a LA-ICP-MS study in magmatic deposits at Serranía de Ronda (Spain); Mineralium Deposita; v. 50(3), p. 265–279.

Piña, R., Gervilla, F., Barnes, S.J., Oberthür, T., and Lunar, R., 2016. Platinum-group element concentrations in pyrite from the Main Sulfide Zone of the Great Dyke of Zimbabwe; Mineralium Deposita, v. 51(7), p. 853–872.

Pronk, A.G., 1987. Pleistocene glacial dispersal and history in Buttle Valley, Vancouver Island, British Columbia: a feasibility study for alpine drift prospecting: Discussion; Canadian Journal of Earth Sciences, v. 24, p. 1504–1505.

Rencz, A.N. and Shilts, W.W., 1980. Nickel in soil and vegetation of glaciated terrains; *in* Nickel in the Environment, (ed.) J.O. Nriagu; Wiley and Sons Inc., New York, 833 p.

Ripley, E.M., 2012. Ni-Cu-PGE mineralization in the Partridge River, South Kawishiwi, and Eagle Intrusions: A review of contrasting styles of sulfide-rich occurrences in the Midcontinent Rift system; Economic Geology, v. 109(2), p. 309–324.

Salminen, R. 1980. On the geochemistry of copper in the Quaternary deposits in the Kiihtelysvaara area, north Karelia, Finland; Geological Survey of Finland, Bulletin 309.

Santaguida, F., Luolavirta, K., Lappalainen, M., Ylinen, J., Voipio, T., and Jones, S., 2015. The Kevitsa Ni-Cu-PGE deposit in the central Lapland greenstone belt in Finland; *in* Mineral Deposits of Finland, (ed.) W.D. Maier, R. Lahtinen, and H. O'Brien; Elsevier, Amsterdam, p. 195–210.

Sappin, A.-A., Dupuis, C., Beaudoin, G., McMartin, I., and McClenaghan, M.B., 2014. Optimal ferromagnetic fraction in till samples along ice-flow paths: case studies from the Sue-Dianne and Thompson deposits, Canada; Geochemistry: Exploration, Environment, Analysis, v. 14, p. 315–329.

Schoneveld, L., Barnes, S.J., Makkonen, H.V., Le Vaillant, M., Paterson, D.J., and Taranovic, V., 2020. Zoned pyroxenes as prospectivity indicators for magmatic Ni-Cu sulfide mineralization; Frontiers in Earth Science; v. 8, 256.

Searcy, C.A., 2001. Preliminary data results for drift exploration for platinum Group Elements, northwestern Ontario; Ontario Geological Survey, Open File Report 6054.

Su, B., Qin, K., Sun, H., Tang, D., Xiao, Q., Liu, P., and Sakyi, P.A., 2012. Olivine compositional mapping of mafic-ultramafic complexes in eastern Xinjiang (NW China); implications for Cu-Ni mineralization and tectonic dynamics; Journal of Earth Science, v. 23(1), p. 41–53.

Shilts, W.W., 1973. Drift prospecting: Geochemistry of eskers and till in permanently frozen terrain, District of Keewatin, Northwest Territories; Geological Survey of Canada, Paper 72–45.

Tardif, N.P., 2000. Regional distribution of platinum, palladium, gold, kimberlite indicators minerals and base metals in surficial sediments, River Valley area, northeastern Ontario; Ontario Geological Survey, Open File Report 6010.

Tuba, G., Molnár, F., Ames, D.E., Péntek, A., Watkinson, D.H., and Jones, P.C., 2014. Multi-stage hydrothermal processes involved in "low-sulfide" Cu (–Ni)–PGE mineralization in the footwall of the Sudbury Igneous Complex (Canada): Amy Lake PGE zone, East Range; Mineralium Deposita, v. 49, p. 7–47.

Ward, L.A., Holwell, D.A., Barry, T.L., Blanks, D.E., and Graham, S.D., 2018. The use of magnetite as a geochemical indicator in the exploration for magmatic Ni-Cu-PGE sulfide deposits: a case study from Munali, Zambia; Journal of Geochemical Exploration, v. 188, p. 172–184.

Yudovskaya, M.A. and Kinnaird, J.A., 2010. Chromite in the Platreef (Bushveld Complex, South Africa): occurrence and evolution of its chemical composition, Mineralium Deposita, v. 45(4), p. 369–91.

Zwanzig, H.V., Macek, J.J., and Mcgregor, C.R., 2007. Lithostratigraphy and geochemistry of the high-grade metasedimentary rocks in the Thompson Nickel Belt and adjacent Kisseynew Domain, Manitoba: implications for nickel exploration; Economic Geology, v. 102, p. 1197–1216.

Lithium signatures in till at the Brazil Lake lithium-cesium-tantalum pegmatites, Nova Scotia

D.M. Brushett[1], C.E. Beckett-Brown[2], M.B. McClenaghan[3], R.C. Paulen[3], and J.M. Rice[3]

[1]Nova Scotia Department of Natural Resources and Renewables, 1701 Hollis St, Halifax, Nova Scotia B3J 2T9
[2]Ontario Geological Survey, Ministry of Mines, 933 Ramsey Lake Road, Sudbury, Ontario P3E 6B5
[3]Geological Survey of Canada, 601 Booth Street, Ottawa, Ontario K1A 0E8

INTRODUCTION

A detailed glacial sediment and bedrock study was carried out around the Brazil Lake lithium-cesium-tantalum (LCT-type) pegmatites in southwestern Nova Scotia, Canada, to develop drift prospecting strategies for Li and related critical mineral resources in glaciated terrain. Lithium resources are key to low CO_2 technologies and the global transition to clean energy as Li is needed to produce Li-ion batteries that are used for transportation and energy storage. This research aims to (1) investigate how spodumene (the key Li ore mineral in the Brazil Lake pegmatites) and associated minerals are glacially dispersed in a region that is extensively covered by unconsolidated glacial sediments; (2) determine the till matrix geochemical signature from this style of mineralization; (3) define net glacial dispersal patterns of the Brazil Lake pegmatites in an area affected by three phases of ice flow; and (4) test analytical methods for Li in till that can be used for the exploration of Li and associated critical minerals in southwest Nova Scotia, and glaciated terrain in general.

This research is being undertaken as part of the Geological Survey of Canada's (GSC) Targeted Geoscience Initiative Program and has been carried out in partnership with the Nova Scotia Department of Natural Resources and Renewables (NSDNRR) and the Ontario Geological Survey. Till geochemistry results are reported in Brushett et al. (2024a) and the indicator mineralogy results will be released in a future GSC report.

GEOLOGY

Geological Setting

The Brazil Lake area is underlain by rocks of the Meguma terrane and is characterized by a thick sequence of Early Cambrian to Early Ordovician metasedimentary rocks, comprising the metasandstone-dominated Goldenville Group and the overlying siltstone- and slate-dominated Halifax Group (White, 2010). Locally, the Meguma Group is unconformably overlain by a thin sequence of Silurian to Early Devonian slate, quartzite, and volcanic rocks of the Rockville Notch Group (White and Barr, 2017; White et al., 2018). The earliest deformation occurred during the Middle Devonian Neoacadian orogeny (ca. 405–365 Ma) resulting in NE- to NNE-trending, upright regional-scale folds. The majority of these rocks were intruded by the ca. 373 Ma peraluminous South Mountain Batholith (SMB) and related granitoid rocks (Fig. 1; White and Barr, 2017). The western edge of the SMB is ~20 km east of the Brazil Lake area and the SMB is host to the East Kemptville Sn deposit and numerous critical mineral occurrences that form the Nova Scotia Tin Domain (Chatterjee, 1983).

Three northeast-trending, steeply dipping pegmatite dykes (referred to as Brazil Lake South, Brazil Lake North, and Army Road pegmatites; Fig. 2) are hosted by the Silurian White Rock Formation (Rockville Notch Group), comprising shallow marine metasedimentary rocks (quartzite, amphibolite, and pelitic schist) interbedded with minor mafic metavolcanic units (Fig. 1, 2; White, 2010; White and Barr, 2017). The Breton Pluton (439 Ma; Keppie and Krough, 2000), located 4.5 km southwest of the Brazil Lake Pegmatites, is a syenogranite to monzogranite intrusion related to the White Rock Formation. It is in fault contact with both the White Rock Formation and Halifax Group (Kontak, 2006). Northeast-southwest-trending shear zones crosscut the area and the metamorphic grade of the White Rock Formation and Halifax Group increases from greenschist to amphibolite facies localized to the contact between the White Rock Formation and Goldenville Group on the south side of the Yarmouth Syncline, which coincides with the Chebogue Shear zone (MacDonald et al., 2003). Field observations by Kontak (2006) suggest that the two Brazil Lake pegmatites were emplaced in an active shear zone where high-temperature ductile deformation occurred during consolidation of the pegmatite. Tantalite U-Pb geochronology from the South pegmatite indicates that pegmatite crystallization occurred at ca. 395 Ma (Kontak et al., 2005; Kontak and Keyser, 2009).

Recommended citation:

Brushett, D.M., Beckett-Brown, C.E., McClenaghan, M.B., Paulen, R.C., and Rice, J.M., 2024. Lithium signatures in till at the Brazil Lake lithium-cesium-tantalum pegmatites, Nova Scotia; *in* Till Geochemistry and Indicator Mineral Methods for Exploration in Glaciated Terrains, (ed.) R.C. Paulen and M.B. McClenaghan; Geological Survey of Canada, Open File 9210, p. 99–109. https://doi.org/10.4095/pbmy2d03m0

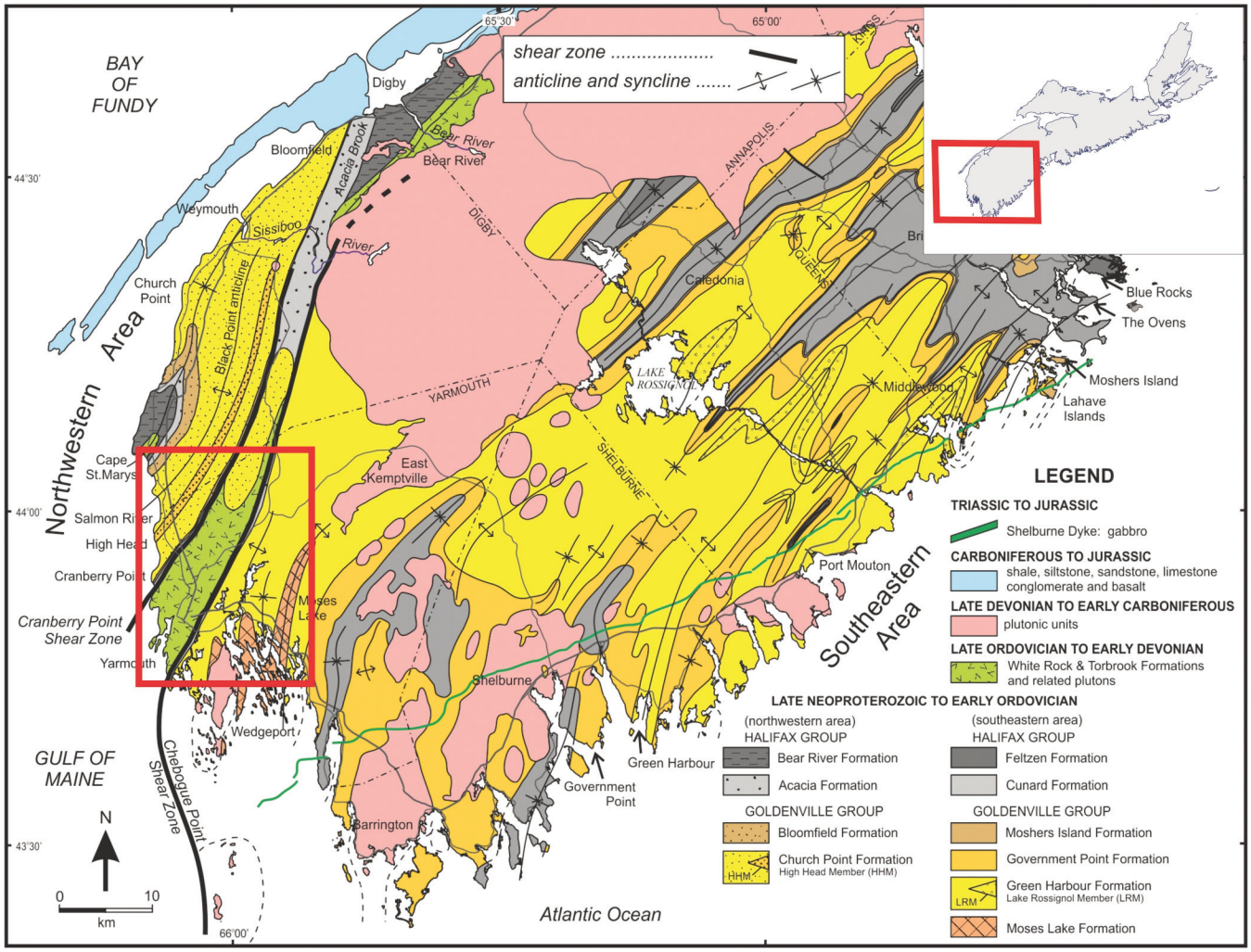


Figure 1. Bedrock geology of southwestern Nova Scotia (modified from White 2010; White et al. 2018). The location of the study area is indicated by the red box; Figure 1 *from* Brushett et al., 2024).

Geology of the Brazil Lake Pegmatites

The North and South Brazil Lake pegmatites are of albite-spodumene type and are characterized by coarse crystals of spodumene and K-feldspar, with intergranular spodumene, muscovite, albite, and quartz. Accessory phases include columbite-tantalite, tourmaline, apatite, beryl, sphalerite, and cassiterite. For a detailed description of the geology of the South Pegmatite, see Kontak (2004). For general descriptions of both pegmatites, refer to Kontak et al. (2005), Kontak (2006), and Kontak and Keyser (2009). Drilling and surface trenching indicate that the North and South pegmatites, which are separated by about 300 m, occur as lenticular forms with wider cores transitioning to thinly tapered ends. The North Pegmatite is at least 700 m in length and reaches a maximum thickness of 21 m at its centre. The South Pegmatite has a defined strike length of ~300 m and a thickness of ~ 8–12 m. Both dykes have southwest-plunging trends of ~ 30–40° (Cullen et al., 2022).

The ore and accessory mineralogy of the Brazil Lake pegmatites are characterized in Table 1. Spodumene ($LiAlSi_2O_6$), the most abundant lithium-bearing mineral in the pegmatites, is a light-coloured, relatively robust silicate mineral (H = 6.5–7) with two perfect cleavages, a vitreous luster that is pearly on its cleavage surface, and a moderate density (3.18 g/cm^3). Of the minerals present in the pegmatites, those that could be useful indicator minerals for drift prospecting include black tourmaline, black tantalite, red garnet, blue apatite, green beryl, cassiterite, wolframite, sphalerite, zircon, epidote, topaz, titanite, and phosphate minerals. Trace elements that are typically enriched in LCT-type pegmatites and may be useful indicator elements for till geochemistry include Li, Be, B, Mn, Rb, Y, Zr, Nb, Sn, Cs, La, Ce, Ta, Th, and U (Černý and Ercit, 2005).

Surficial geology

Much of southwestern Nova Scotia underwent extensive glacial modifications through the late Wisconsin

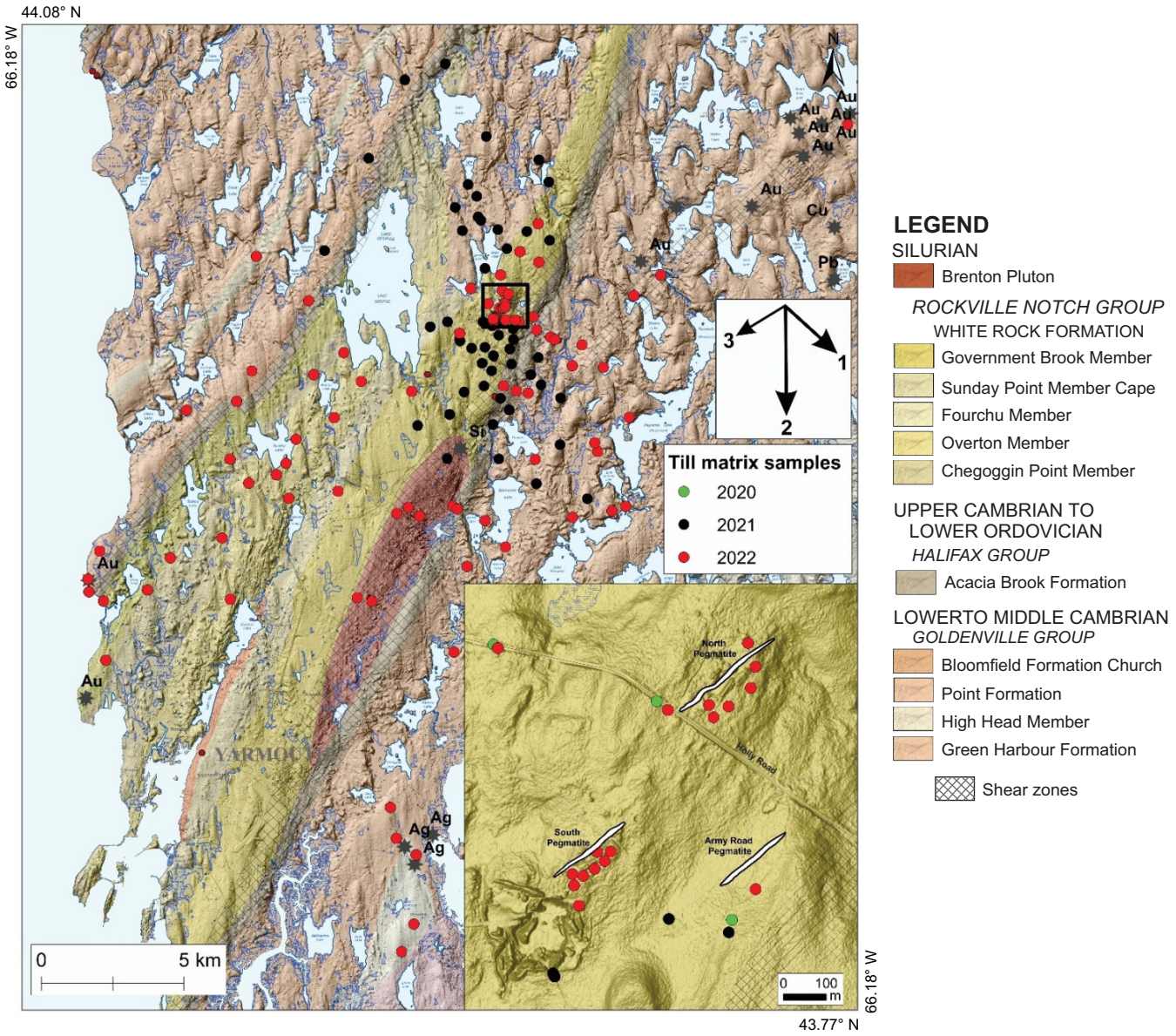


Figure 2. Bedrock geology of the Brazil Lake study area (White et al., 2012) superimposed on a LiDAR hillshade image (azimuth of 315°) showing the location of till samples collected in 2020 (green dots), 2021 (black dots), and 2022 (red dots) and mineral occurrences (grey stars). Generalized ice-flow phases are shown by arrows and their relative age is indicated by numbers, with one being the oldest, based on the regional ice-flow history by Stea and Grant (1982) and Finck and Stea (1995). The inset map shows the location of the Brazil Lake North and South pegmatites and the Army Road pegmatite outlined by white polygons based on their known extents (Critical Raw Materials, 2023). Modified *from* Brushett et al. (2024).

glaciation leaving thick glacial sediments and complex landforms (e.g. Shaw et al., 2006; Stea et al., 2011) that have hindered bedrock mapping and exploration for buried mineralization. The areal extent of the pegmatites at Brazil Lake is not well known due to till cover limiting outcrop exposure. Southeast- to south-trending drumlins are the predominant glacial landform over much of the region. Till thickness in the region ranges from veneers (~2–5 m) over the pegmatites to drumlin ridges > 40 m (Brushett et al., 2024b). In the Brazil Lake area, subtle mega-scale glacial lineations were also identified in LiDAR imagery of this drumlinized terrain; these lineations are indicative of fast-flowing ice during the latter phases of glaciation (i.e. ice streaming: Stokes and Clark, 2002). The area between these till ridges is characterized by thin till (<5 m) overlying bedrock. Glaciofluvial deposits commonly occur in topographic lows, which are now occupied by modern rivers and wetlands.

METHODS

A total of 184 till samples of ~3 to 6 kg were collected for geochemical analysis in 2020, 2021, and 2022. The sites include proximal samples collected up- and down-ice of the Brazil Lake pegmatites and regional samples collected across southwest Nova Scotia to provide

Table 1. Mineralogy of, and potential indicator minerals present in, the Brazil Lake pegmatites summarized from descriptions by Taylor (1967), Corey (1995), and Kontak (2006), as well as indicator minerals recovered from bedrock and till samples in this study.

Mineral	Formula	Specific gravity	Hardness	In bedrock in this study	In till HMC in this study	First reported presence in deposit
spodumene	$LiAlSi_2O_6$	3.1–3.2	6.5–7	yes	yes	Taylor (1967); Kontak (2004)
tourmaline–schorl/dravite	$Na(Fe,Mg)_3Al_6Si_6O_{18}(BO_3)_3(OH)_2$	3.03–3.22	7	yes	yes	Taylor (1967); Kontak (2004)
green beryl	$Be_3Al_2Si_6O_{18}$	2.63–2.9	7.5–8	no	no	Taylor (1967); Kontak (2004)
tantalite	$(Fe,Mn)Ta_2O_6$	6.65–7.95	6–6½	yes	no	Corey (1995); Kontak (2004)
blue apatite	$Ca_5(PO_4)_3(OH,F,Cl)$	3.16–3.22	5	yes	yes	Corey (1995); Kontak (2004)
triplite	$(Mn,Fe)_2(PO_4)(F,OH)$	3.5–3.9	5–5.5	no	no	Kontak (2004)
montebrasite	$LiAlPO_4(OH)$	5.5–6	2.98–3.04	no	no	Kontak (2006)
crandallite	$CaAl_3(PO_4)_2(OH)_5•(H_2O)$	2.78–2.92	4	no	no	Kontak (2006)
goyazite	$SrAl_3(PO_4)_2(OH)_5•(H_2O)$	3.16–3.28	4–5	no	no	Kontak (2006)
lithiophilite	$LiMnPO_4$	3.29–3.50	4	no	no	Corey (1995); Kontak (2004)
fillowite	$Na_3CaMn_{11}(PO_4)_9$	3.43	4.5	no	no	Kontak (2006)
variscite	$Al(PO_4)•2(H_2O)$	2.5–2.52	4–5	no	no	Corey (1995)
florencite	$(La,Ce)Al_3(PO_4)_2(OH)_6$	3.46–3.71	5–6	no	yes	this study (in till only)
heterosite	$(Fe,Mn)PO_4$	4–4.5	3.4	yes	no	this study
uraninite	UO_2	6.5–10.95	5–6	yes	no	this study
zircon	$Zr(SiO_4)$	4.6–4.7	7.5	yes	yes	Corey (1995); Kontak (2004)
cassiterite	SnO_2	6.8–7	6–7	yes	yes	Corey (1995); Kontak (2004)
wolframite	$(Fe, Mn)WO_4$	7–7.5	4–4.5	no	no	Kontak (2004)
scheelite	$CaWO_4$	5.9–6.1	4.5–5	no	yes	this study (in till only)
sphalerite	(Zn,Fe)S	3.9–4.2	3.5–4	yes	yes	Kontak (2004)
pyrite	FeS_2	4.8–5	6–6.5	yes	yes	this study
arsenopyrite	FeAsS	6	5.5–6	yes	no	this study
loellingite	$FeAs_2$	7.43	5–5.5	yes	no	this study
pyrolusite	MnO_2	5	2–6.5	yes	no	this study

Note: HMC = heavy mineral concentrate.

regional context and aid in assessing the potential for additional buried pegmatites. Samples were collected from hand-dug pits and till exposures in borrow pits or along local roads. Samples were also collected from backhoe trenches dug on the down-ice (SSE) side of both the North and South pegmatites where C-horizon (unoxidized to moderately oxidized) till was targeted.

The coarse sand (1.0–2.0 mm) and silt + clay (<0.063 mm) fractions of the till samples were analyzed. For the 2020 samples only, the <0.002 mm (clay) fraction was analyzed. Analyses completed over the 3 years (2020, 2021, 2022) used varying combinations of digestion and fusion methods to test and compare their efficacy for the various pathfinder elements for LCT pegmatites: 1) aqua regia (partial) digestion, 2) Na-peroxide fusion (total), 3) 4-acid (near total) digestion.

A total of 84 large (~10 kg) till samples were collected for indicator mineral analysis in 2020, 2021, and 2022. Fifteen bedrock samples were collected from the North and South pegmatites to document their mineralogy and mineral chemistry, four of these were submitted to Overburden Drilling Management Limited (ODM), Ottawa for heavy mineral processing to identify the suite of indicator minerals that best characterize the pegmatites' indicator mineral signature for comparison with concentrates from the till. Till and bedrock samples were processed to produce 2.8–3.2 specific gravity (SG) and >3.2 SG non-ferromagnetic mid-density and heavy mineral fractions for visual identification and counting of indicator minerals. The 0.25–0.5, 0.5–1.0, and 1.0–2.0 mm non-ferromagnetic >3.2 SG fraction and the 0.25–0.5 mm non-ferromagnetic 2.8–3.2 SG fraction of the bedrock and till samples were examined by ODM and indicator minerals were identified and counted.

RESULTS AND IMPLICATIONS FOR EXPLORATION

Till Characteristics

Two till facies were observed in the study area and both were suitable for till sampling. The first is subglacial traction till (also referred to as subglacial lodgement till) with a silty sand matrix, moderate to high compaction, subhorizontal fissility with visible jointing, angular to subrounded local bedrock clasts, and numer-



Figure 3. Examples of subglacial traction till sampled at various sites in the Brazil Lake study area. Note the compaction of the till as demonstrated by fissility and overconsolidation. **a)** Site 22MPB026 after sampling (photograph by M.B. McClenaghan, NRCan photo 2023-061); **b)** site 22MPB036, overconsolidated chunks of till on the shovel. Note the white spodumene clast indicated by the yellow arrow (photograph by M.B. McClenaghan, NRCan photo 2023-062); **c)** site 22MPB027 after sampling showing well developed A, B, and C soil horizons (photograph by M.B. McClenaghan, NRCan photo 2023-063); **d)** site 22MPB027 overconsolidated chunk of till on shovel (photograph by M.B. McClenaghan, NRCan photo 2023-064); **e)** site 22MPB-038 after sampling showing subhorizontal fissility behind the shovel (photograph by M.B. McClenaghan, NRCan photo 2023-065). Note: width of shovel head is 21 cm; Fig. 6 *from* Brushett et al., 2024).

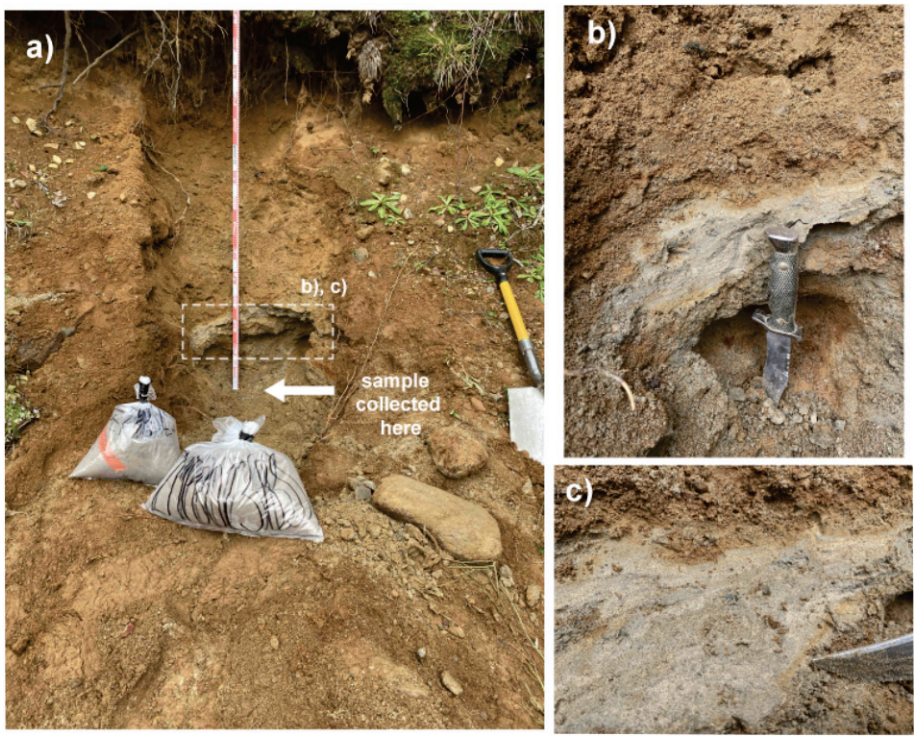


Figure 4. a) Photograph of subglacial melt-out till sampled at site 22MPB023. Subglacial melt-out till is typically looser than subglacial traction till and also contains lenses of sorted sand (**b** and **c**) within the till. The red and white sections on the measuring tape are 10 cm long. Photographs by Jessey Rice: a) NRCan photo 2022-066, b) NRCan photo 2022-67, and c) NRCan photo 2022-068). Figure 10 *from* Brushett et al. (2024).

ous striated and faceted clasts (Fig. 3). Pebbles and cobbles of spodumene were observed in this till facies in trenches just down-ice of the North and South pegmatites. A bedrock subcrop surface, which was revealed by previous stripping of the South pegmatite, is glacially polished and striated (179°) and demonstrates that the bedrock here was in direct contact with southward-flowing ice. This facies is the primary target sample medium.

A second till facies is interpreted as a subglacial meltout till that is sandier, stonier with mostly locally derived clast lithologies, less indurated, has lower compaction, may contain well sorted lenses and layers of sand, and often occurs as a thin (< 2 m) horizon on the drumlin flanks (Fig. 4).

Till Matrix Geochemistry

The 2020 4-acid digestion and aqua regia digestion results were compared for three size fractions, 1.0–2.0 mm, <0.063 mm, and <0.002 mm (Brushett et al., 2022). Although the range of Li, Nb, Cs, and Ta concentrations was greater for the <0.002 mm fraction, the spatial distribution concentration patterns for these elements were similar among all three size fractions.

In 2021 and 2022, only the 1.0–2.0 mm and <0.063 mm till fractions were analyzed using three different analytical methods: Na-peroxide fusion, 4-acid digestion, and aqua regia digestion. Both size fractions were investigated to understand how spodumene breaks down in till and if it occurs in greater abundance in the coarse fraction of the till given its relative robustness and high hardness (6.5–7, Mohs scale).

All three methods identified a Li geochemical signature in till down-ice of the Brazil Lake pegmatite district and some generalizations can be made:

1) Li concentrations are consistently higher in the 1.0–2.0 mm fraction compared to the <0.063 mm fraction of the till; however, the <0.063 mm fraction exhibits a lower standard deviation and variance than its 1.0–2.0 mm counterpart (Fig. 5; Table 2). Note the <0.063 mm fraction is commonly used for mineral exploration for a broad suite of commodities, not solely Li;
2) Na-peroxide fusion results for Li concentrations are generally higher than the concentrations determined by aqua regia for the same till samples (Fig. 6);
3) The most effective method for identifying Li glacial dispersal in till at Brazil Lake is Na-peroxide fusion on the 1.0–2.0 mm fraction. The method shows a net pattern of glacial dispersal from both the North and South pegmatites that is detectable up to 4 km to the south (Fig. 7); and
4) Pathfinder element signatures immediately down-ice (50–200 m) of the three pegmatites are variable. Till just down-ice of the North and South pegmatites is enriched in Li, Be, Cs, Nb, Rb, Ta, and W. Till south of the Army Road pegmatite is characterized by elevated concentrations of Li, Cs, Rb, Sn, and Ta.

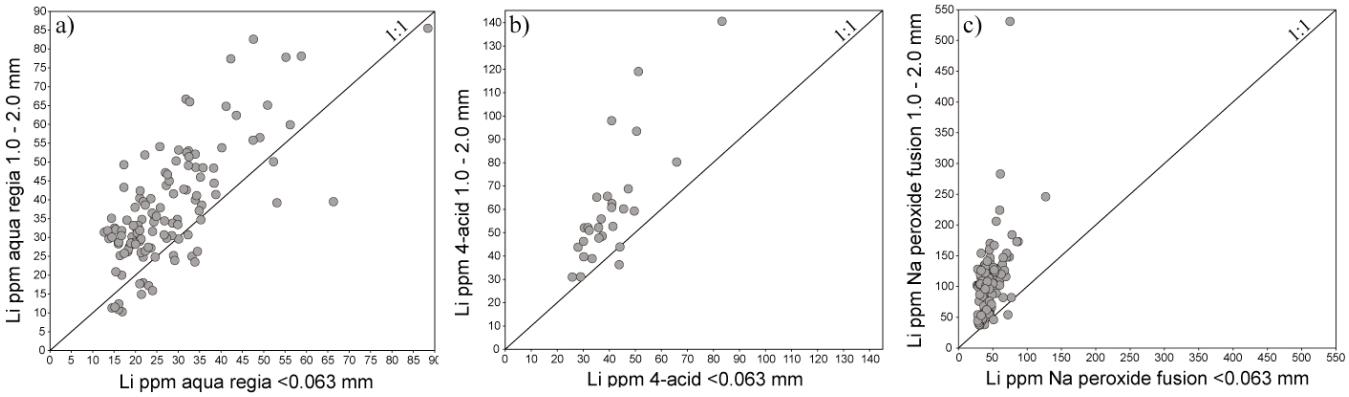


Figure 5. Scatterplots comparing the concentrations of Li (ppm) in the 1–2 mm fraction and the <0.063 mm fraction determined by **(a)** aqua regia (n=104), **(b)** 4-acid (n=28), and **(c)** Na-peroxide fusion (n=121) for till samples collected in 2020 through 2022. Figure 16 *from* Brushett et al. (2024).

Table 2. Comparison of Li concentrations (ppm) for the three digestion methods and two size fractions used to analyze till samples in this study (*from* Brushett et al., 2024).

Digestion method	Size fraction (mm)	Number of analyses	Minimum (ppm)	Maximum (ppm)	Mean (ppm)	Median (ppm)	Standard deviation
Na-peroxide fusion	<0.063 mm	152	17.0	127.0	45.4	42.0	15.3
Na-peroxide fusion	1.0–2.0 mm	104	37.0	531.0	109.1	102.0	61.1
4-Acid	<0.063 mm	91	16.5	97.7	39.3	36.0	13.9
4-Acid	1.0–2.0 mm	29	31.0	140.6	61.2	52.7	25.2
Aqua regia	<0.063 mm	177	9.9	88.4	27.8	24.4	11.4
Aqua regia	1.0–2.0 mm	121	10.3	85.5	37.7	34.4	15.2

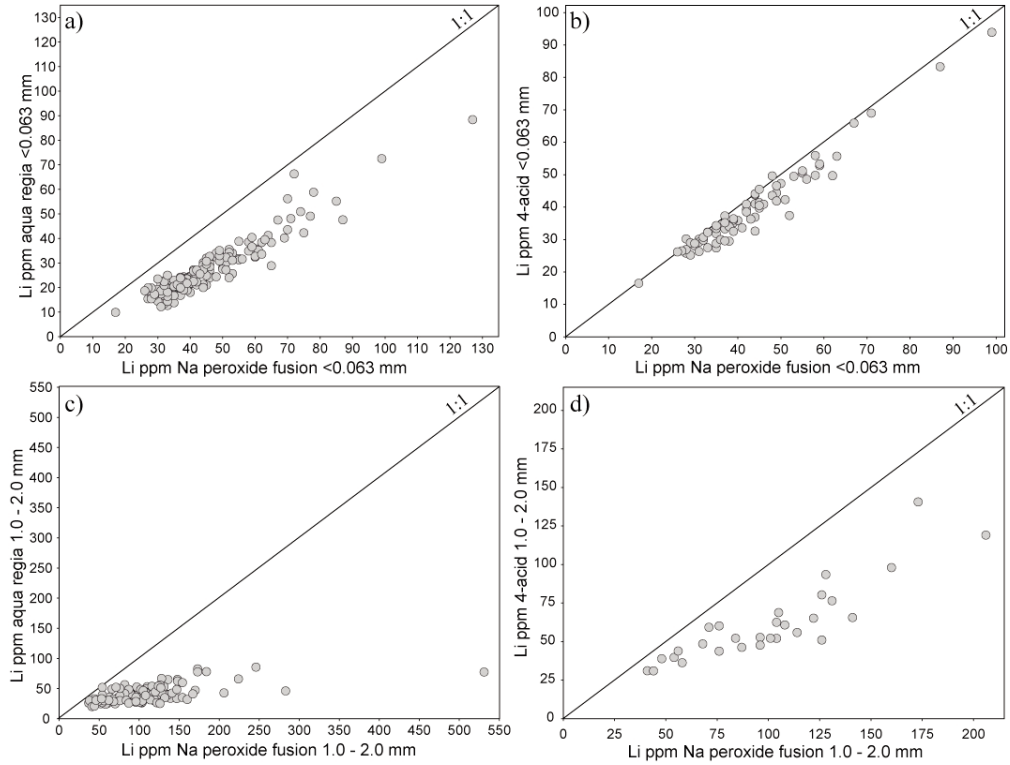


Figure 6. Scatter plots comparing the three digestion methods to their size fraction counterparts (samples from 2020–2022). Concentrations of Li (ppm) in <0.063 mm fraction of till determined by Na-peroxide fusion versus Li concentrations determined by **(a)** aqua regia (n=152) and by **(b)** 4-acid (n=74). Concentrations of Li (ppm) in the 1.0–2.0 mm fraction determined by Na-peroxide fusion versus Li concentrations determined by **(c)** aqua regia (n=104) and by **(d)** 4-acid (n=29). Figure 15 *from* Brushett et al. (2024).

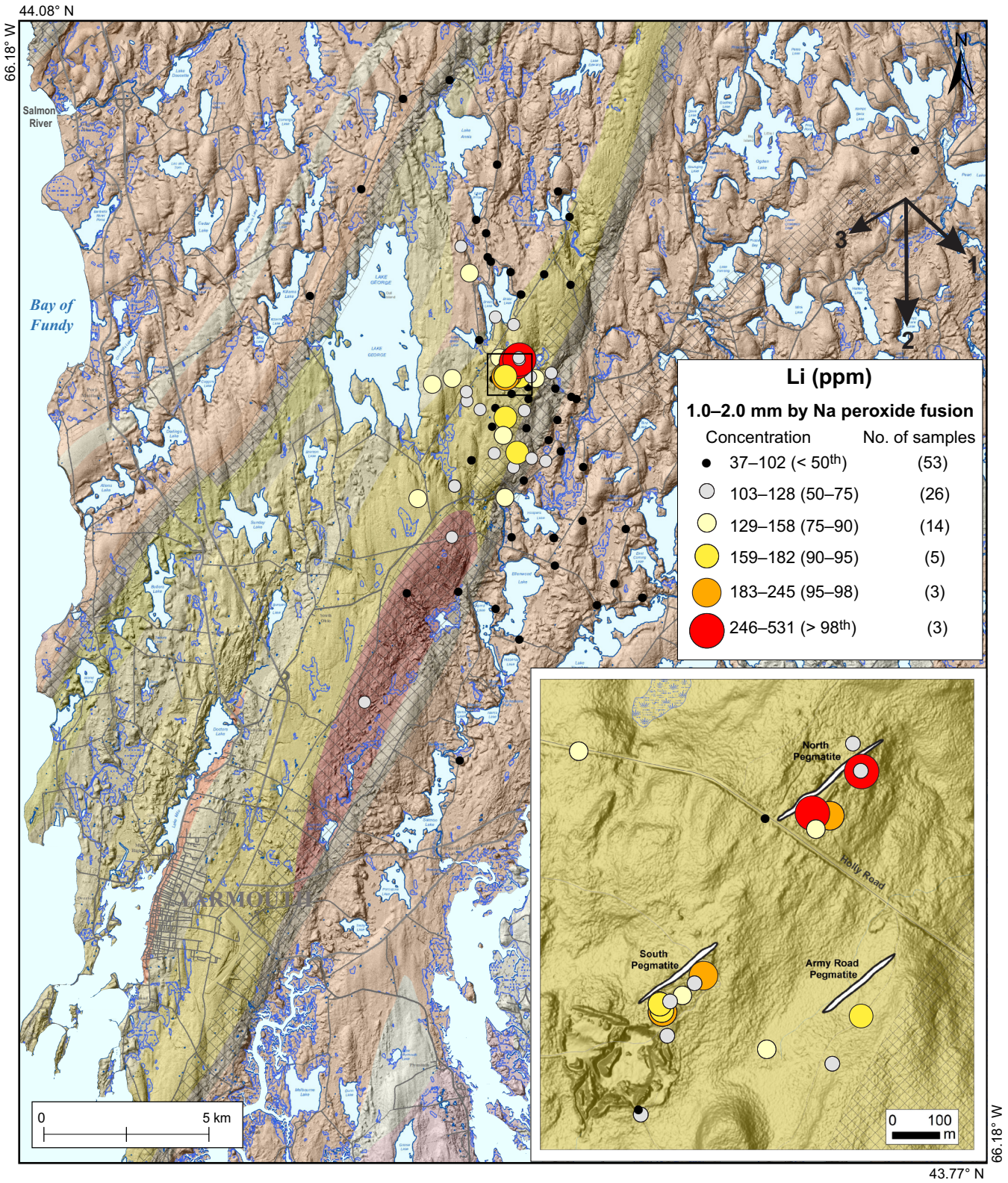


Figure 7. Proportional dot map of Li concentrations from the 1.0–2.0 mm till fraction determined by Na-peroxide fusion/ICP-MS (n = 104). Bedrock geology legend is shown in Figure 2. Data classes for each dot size were determined using percentiles calculated in ArcMap (v. 10.8.1). Figure 14a *from* Brushett et al. (2024).

Table 3. Comparison of Li concentrations (ppm) in till samples collected up-ice and down-ice of the North and South pegmatites. Data for till samples from the East Kemptville area (18CS sample series) are included for comparison and are the average for Li determined by aqua regia/ICP-MS (Smith, 2019). Grey-shaded cells denote values >90th percentile. From Brushett et al. (2024).

Sample	Interpretation	Distance down-ice from the deposit (m)	<0.063 mm			1.0–2.0 mm		
			aqua regia	4-acid	Na-peroxide	aqua regia	4-acid	Na-peroxide
East Kemptville Till (average of 18CS002, 007, 010, 011)	Regional up-ice	-25000	22.5					
22MPB023	background up-ice	-1000	22.3	40.9	42.0	38.6	60.8	108.0
22MPB010	background up-ice	-100	18.6	30.4	32.0	27.6	52.1	104.0
22MPB035	Overlying S-pegmatite	35	31.3	51.2	55.0	42.8	119.1	206.0
22MPB036	Overlying S-pegmatite	50	47.5	65.9	67.0	55.8	80.3	126.0
22MPB009	Down-ice N-pegmatite	500	47.6	83.3	87.0	82.6	140.6	173.0
22MPB015	Down-ice N&S-pegmatite	2500	21.0	40.9	45.0	31.9	98.0	160.0
22MPB030	Down-ice N&S-pegmatite	5400	34.0	49.6	48.0	52.1	59.3	71.0
22MPB029	Down-ice N&S-pegmatite	8400	29.5	45.5	45.0	50.3	60.2	76.0
22MPB027	Down-ice N&S-pegmatite	13000	27.3	44.1	44.0	29.8	43.9	56.0

Note: N = North Pegmatite, S = South Pegmatite, >90th percentile, Upper Crust = 24 ppm.

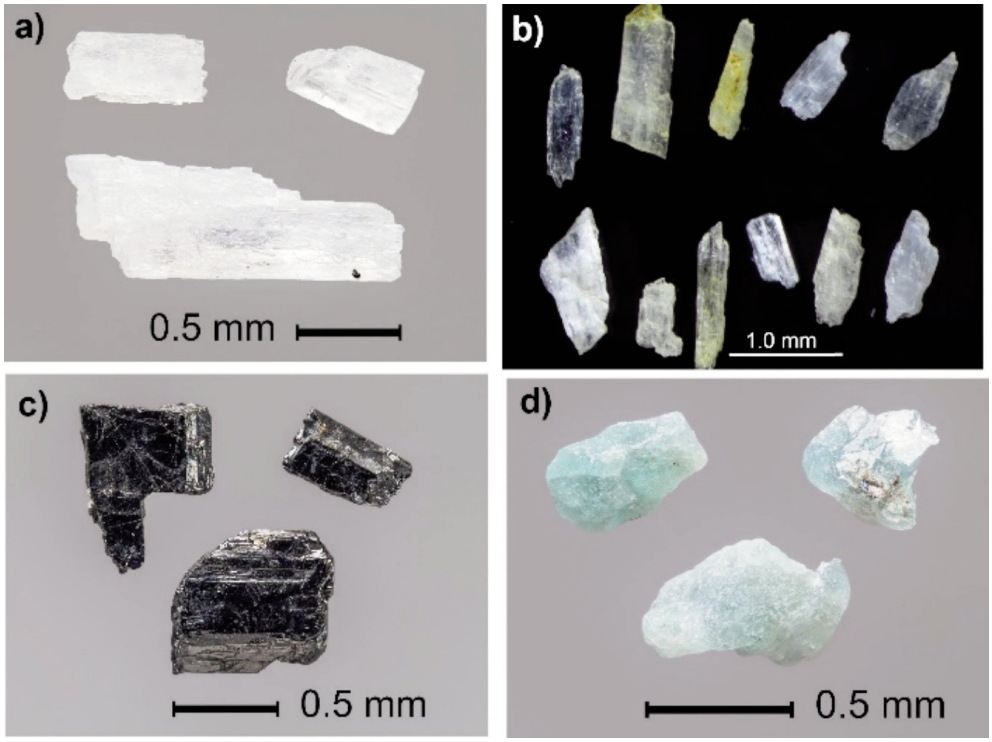


Figure 8. Colour photographs of some of the indicator minerals identified in till samples collected around the Brazil Lake pegmatites. **a)** spodumene (Michael Bainbridge Photography); **b)** spodumene (backlit; Overburden Drilling Management Ltd.); **c)** columbite-tantalite (Michael Bainbridge Photography); and **d)** blue apatite (Michael Bainbridge Photography). Modified *from* McClenaghan et al. (2023).

A summary of the range of concentrations determined for Li in till samples is reported in Table 3.

Indicator Mineral Distribution

Spodumene was identified in mid- and heavy-density mineral fractions of bedrock and till samples by its white colour, prismatic appearance with a generally flattened and elongated shape, striated parallel to commonly massive crystal habit, and brittle fracture (Fig. 8a, b). Other Li pegmatite indicator minerals recovered include black columbite-tantalite (Fig. 8c), blue apatite (Fig. 8d), and black-brown tourmaline. Spodumene

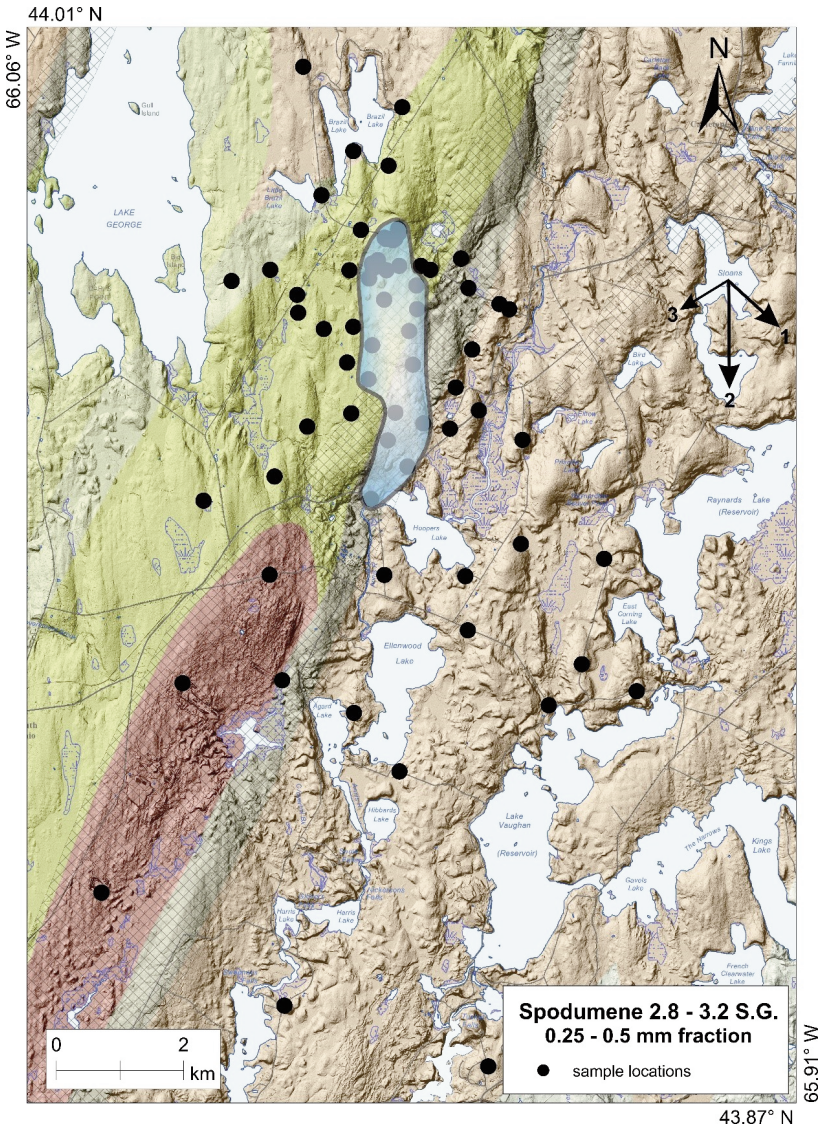


Figure 9. Map showing the of spodumene distribution (>75th percentile values) in the 0.25–0.5 mm 2.8–3.2 SG fraction of till samples normalized to a 10 kg weight of the <2 mm table feed. Spodumene abundances decrease southward but are still detectable in till up to 12 km south of the Brazil Lake pegmatites. The bedrock geology legend is shown in Figure 2. The percentiles used to draw the polygon were calculated using ArcMap (v. 10.8.1). Unpublished Geological Survey of Canada data.

(SG = 3.18) is most abundant in the 0.25–0.5 mm middensity (2.8–3.2 SG) fraction (100s to 1000s of grains per sample) and present, but far less abundant, in the 0.25–0.5 mm heavy mineral (>3.2 SG) fraction (100s of grains). It was also recovered from the 0.5–1.0 mm and the 1–2 mm >3.2 SG fractions (<10 grains). Spodumene is most abundant in till immediately south of the North and South pegmatites (Fig. 9). Abundances decrease southward but are still detectable in till up to 12 km south, which may reflect glacial dispersal from the known pegmatites or another pegmatite source. The background abundance of spodumene in till is zero grains and the presence of any grains in a sample is significant. The spodumene dispersal train is longer and more obvious than the Li (geochemical) dispersal train.

FUTURE WORK

Interpretations of the indicator mineral data for bedrock and till samples are in progress and will be released in a separate report. Examination of the pebble fraction, ad specifically the abundance of spodumene clasts in the till samples, is also underway and will also be reported at a later date. Regional-scale and detailed surficial geological mapping and stratigraphic studies are in progress to further our understanding of the glacial history and stratigraphic context of the depositional record of southwestern Nova Scotia. All geochemical results in this study were from BC- and C-horizon till samples; further work will include a comparison of B- and C-horizon samples to improve the understanding of how spodumene breaks down during glacial transport and how the geochemical response varies between them. Lithium isotope signatures will be determined for selected bedrock and indicator minerals from the North and South pegmatites.

ACKNOWLEDGEMENTS

The authors thank John Wightman, Greg Morris, Cliff Stanley, and Lithium Springs Limited for access to the

Brazil Lake property, field visits, and advice that guided fieldwork. Aber Haji Egeh and Pierre Pelchat are thanked for their important field and lab contributions. Adam Nissen, a Saint Mary's University graduate student, is thanked for field assistance in 2022. Mitch Maracle (NSDNRR summer student) is thanked for field assistance from 2020 to 2022. First Nation representatives Jeff Purdy (Councillor, Acadia First Nation), Greg Hart (NSPI Early Engagement Coordinator, Kwilmu'kw Mawklusuaqn Negotiation Office), and Patrick Butler (Mi'kmaq Energy & Mines Advisor, Kwilmu'kw Mawklusuaqn Negotiation Office) are thanked for their interest and support in the ongoing research.

REFERENCES

Brushett, D.M., McClenaghan, M.B., and Paulen, R.C., 2022. Till geochemical data for the Brazil Lake pegmatite area, southwest Nova Scotia, Canada (NTS 21A/04, 20O/16 and 20P/13): till samples collected in 2020; Nova Scotia Department of Natural Resources and Renewables, Open File Report ME 2022-2.

Brushett, D.M., Beckett-Brown, C.E., McClenaghan, M.B., Paulen, R.C., Rice, J.M., Haji Egeh, A., and Pelchat, P., 2024a. Till geochemical data for the Brazil Lake pegmatite area, southwest Nova Scotia (NTS 21-A/04, 20-O/16 and 20-P/13): samples collected in 2020, 2021, and 2022; Geological Survey of Canada, Open File 9148. https://doi.org/10.4095/332384

Brushett, D.M., Kennedy, G.W., and MacMullen, C.C., 2024b. Sediment thickness and bedrock topography maps of southwest Nova Scotia; Nova Scotia Department of Natural Resources and Renewables, Geoscience and Mines Branch, Open File Map ME 2023-2, scale 1:215 000.

Černý, P. and Ercit, T.S., 2005. The classification of granitic pegmatites revisited; The Canadian Mineralogist, v. 43(6), p. 2005–2026. https://doi.org/10.2113/gscanmin.43.6.2005

Chatterjee, A.K., 1983. Metallogenic map of Nova Scotia; Nova Scotia Department of Mines and Energy, scale 1:500 000.

Corey, M. 1995. Diamond drilling of rare element pegmatites in southwestern Nova Scotia; Nova Scotia Mines and Energy Branches, Open File Report 95-001. https://novascotia.ca/natr/meb/data/pubs/ofr_me_1995-001.pdf

Cullen, M., Harrington, M., and Elgert, L., 2022. NI 43-101 Technical report on the mineral resources estimate for the Brazil Lake project (lithium-bearing pegmatite deposit), Nova Scotia, Canada.

Critical Raw Materials, 2023. Facilitating the energy transition through lithium and rare earth exploration; Retrieved from https://www.innovationnewsnetwork.com/how-will-brazil-lake-lithium-project-power-energy-transition/33307/ <Accessed 2023/08/08>

Finck, P.W. and Stea, R.R., 1995. The compositional development of tills overlying the South Mountain Batholith; Nova Scotia Department of Natural Resources, Mines and Minerals Branch, Paper 95-1, 52 p.

Keppie, J.D. and Krogh, T.E., 2000. 440 Ma igneous activity in the Meguma Terrane, Nova Scotia, Canada; part of the Appalachian overstep sequence?; American Journal of Science, v. 300(6), p. 528–538.

Kontak, D.J., 2004. Geology of the southern lobe of the Brazil Lake LCT-type pegmatite (NTS 21A/04), Yarmouth County, Nova Scotia; Nova Scotia Department of Natural Resources, Mineral Resources Branch, Report of Activities 2003, Report 2004-1, p. 41–68.

Kontak, D.J., 2006. Nature and origin of an LCT-suite pegmatite with late-stage sodium enrichment, Brazil Lake, Yarmouth County, Nova Scotia. I. Geological setting and petrology; The Canadian Mineralogist, v. 44(3), p. 563–598. https://doi.org/10.2113/gscanmin.44.3.563

Kontak, D.J. and Kyser, T.K., 2009. Nature and origin of an LCT-suite pegmatite with late-stage sodium enrichment, Brazil Lake, Yarmouth County, Nova Scotia. II. Implications of stable isotopes ($\delta^{18}O$, δD) for magma source, internal crystallization and nature of sodium metasomatism; The Canadian Mineralogist, v. 47(4), p. 745–764. https://doi.org/10.3749/canmin.47.4.745

Kontak, D.J., Creaser, R.A., Heaman, L.M., and Archibald, D.A., 2005. U-Pb tantalite, Re-Os molybdenite, and $^{40}Ar/^{39}Ar$ muscovite dating of the Brazil Lake pegmatite, Nova Scotia: a possible shear-zone related origin for an LCT-type pegmatite; Atlantic Geology, v. 41(1), p. 17–29.

MacDonald, L.A., Barr, S.M., White, C.E. and Ketchum, J.W.F. 2003. Petrology, age, and tectonic setting of the White Rock Formation, Meguma Terrane, Nova Scotia: evidence for Silurian continental rifting; Canadian Journal of Earth Sciences, v. 39, p. 259–277.

McClenaghan, M.B., Brushett, D.M., Beckett-Brown, C.E., Paulen, R.C., Rice, J.M., Haji Egeh, A., and Nissen, A., 2023. Indicator mineral studies at the Brazil Lake LCT pegmatites, southwest Nova Scotia; Geological Survey of Canada, Scientific Presentation 157. https://doi.org/10.4095/331686

Shaw, J., Piper, D.J.W., Fader, G.B.J., King, E.L., Todd, B., Bell, T., Batterson, M.J., and Liverman, D.G.E., 2006. A conceptual model of the deglaciation of Atlantic Canada; Quaternary Science Reviews, v. 25(17-18), p. 2059–2081. https://doi.org/10.1016/j.quascirev.2006.03.002

Smith, C.G., 2019. Geochemical and mineralogical dispersal in till from the East Kemptville Sn-An-Cu-Ag deposit, southwest Nova Scotia; B.Sc. thesis, Acadia University, Wolfville, Nova Scotia, 128 p.

Stea, R.R. and Grant, D.R., 1982. Pleistocene geology and till geochemistry of southwestern Nova Scotia (sheets 7 and 8); Nova Scotia Department of Mines and Energy, Map 82-10, scale 1:100 000.

Stea, R.R., Seaman, A.A., Pronk, T., Parkhill, M.A., Allard, S., and Utting, D., 2011. The Appalachian Glacier Complex in Maritime Canada; *in* Developments in Quaternary Sciences, v. 15, p. 631–659. https://doi.org/10.1016/S1571-0866(04)80199-4

Stokes, C.R. and Clark, C.D., 2002. Are long subglacial bedforms indicative of fast ice flow?; Boreas, v. 31, p. 239–249. https://doi.org/10.1111/j.1502-3885.2002.tb01070.x

Taylor, F.C., 1967. Reconnaissance geology of the Shelburne map-area, Queen's, Shelburne, and Yarmouth counties, Nova Scotia; Geological Survey of Canada, Memoir 349, p. 73–75.

White, C.E., 2010. Stratigraphy of the lower Paleozoic Goldenville and Halifax groups in southwestern Nova Scotia; Atlantic Geology, v. 46, p. 136–154. https://doi:10.4138/atlgeol.2010.008

White, C.E. and Barr, S.M., 2017. Stratigraphy and depositional setting of the Silurian–Devonian Rockville Notch Group, Meguma terrane, Nova Scotia, Canada; Atlantic Geology, v. 53, p. 337–365. https://doi:10.4138/atlgeol.2017.015

White, C.E., Barr, S.M., and Linnemann, U., 2018. U–Pb (zircon) ages and provenance of the White Rock Formation of the Rockville Notch Group, Meguma terrane, Nova Scotia, Canada: evidence for the "Sardian gap" and West African origin; Canadian Journal of Earth Sciences, v. 55(6), p. 589–603. https://doi.org/10.1139/cjes-2017-0196

Application of machine learning to till geochemical data

Mohammad Parsa and M. Beth McClenaghan

Geological Survey of Canada, 601 Booth Street, Ottawa, Ontario K1A 0E8

ABSTRACT

This paper provides a summary of the application of machine learning tools in the processing and interpretation of till geochemical data. The study utilizes examples drawn from a collection of till geochemical data gathered in the Bathurst Mining Camp, located in northern New Brunswick. This region hosts several Volcanogenic Massive Sulphide (VMS) deposits, including the prominent Brunswick No. 12 Zn-Pb-Cu deposit. The research employs a diverse range of tools, encompassing both unsupervised and supervised techniques. These tools are compared to establish a multi-element geochemical signature that can serve as a vector for delineating exploration targets related to VMS deposits within the study area.

INTRODUCTION

Diminishing rates of deposit discovery, the continuous depletion of existing mineral resources, and the growing demand for various metals collectively contribute to disruptions in the supply chain for many mineral commodities. This is particularly relevant for critical commodities—metals, elements, or minerals that play a pivotal role in modern technologies and may be susceptible to potential supply chain disruptions (Jowitt et al., 2017). It is, therefore, imperative to fully utilize all available exploration tools to favour discovery of new resources of critical commodities. Till geochemistry is a common exploration tool in the glaciated terrains of the Northern Hemisphere (McClenaghan et al., 2000, 2023 and references therein). To harness the full potential of till geochemical data for mineral exploration, several factors affecting this type of data must be considered.

One common challenge in interpreting till geochemical data from a mineral exploration perspective is the process of glacial dispersal on the formation of geochemical anomalies (McClenaghan et al., 2023) and the intricate nature of geochemical data. This paper presents recent advances in methodologies that try to address this latter aspect from a data science standpoint. Firstly, it is essential to recognize that till geochemical data represent closed compositional data, meaning that they consist of strictly positive vectors that sum up to a constant value (Aitchison, 1982). As a result, the enrichment or depletion patterns of different elements are interrelated within a sample, leading to spurious correlations between elements. Compositional data analysis is a field that addresses this aspect of geochemical data. Another issue arises from the complexity of geochemical processes and the interrelationships among different elements. Dealing with this complexity necessitates the use of sophisticated tools and methodologies. This paper showcases the potential of machine learning tools to interpret till geochemical data for mineral exploration. An example of till geochemical data for Bathurst Mining Camp, New Brunswick, which is host to the world-class Brunswick No. 12 Zn-Pb-Cu Volcanogenic Massive Sulphide (VMS) deposit and many others, is illustrated herein to demonstrate the application of machine learning techniques for interpreting till geochemical data. A variety of methods ranging from unsupervised to supervised techniques coupled with their applications are employed and explained herein.

A BRIEF SUMMARY OF MACHINE LEARNING TOOLS

Machine learning tools, a set of frameworks designed to enable computers to learn from data and make predictions, make decisions, or generate insights without being explicitly programmed for each task, have been frequently applied to interpreting geochemical data (Parsa et al., 2022 and references therein). There are two categories of machine learning techniques used in exploration geochemistry, namely supervised and unsupervised tools. The latter does not require much from the user and includes clustering and dimensional reduction techniques.

Clustering is frequently applied to geochemical data for the classification of samples or elements based on their interrelationships. Commonly used dimensional reduction methods, including Principal Component Analysis (PCA) and Factor Analysis (FA), are used to simplify the relationship among elements and facilitate the interpretation of geochemical data. In addition, a

Recommended citation:

Parsa, M. and McClenaghan, M.B., 2024. Application of machine learning to till geochemical data; *in* Till Geochemistry and Indicator Mineral Methods for Exploration in Glaciated Terrains, (ed.) R.C. Paulen and M.B. McClenaghan; Geological Survey of Canada, Open File 9210, p. 110–114. https://doi.org/10.4095/pbmy2d03m0

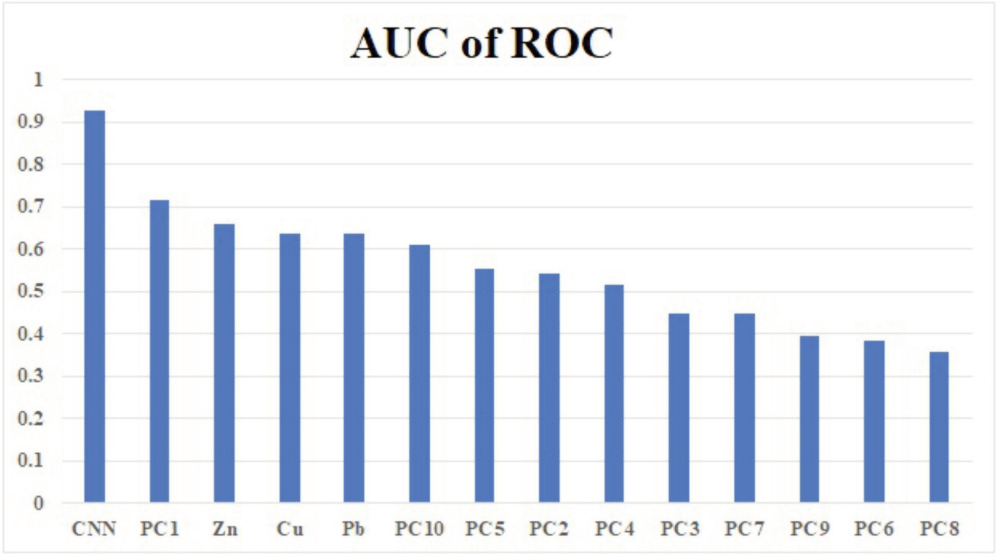


Figure 1. The Area Under the Curve (AUC) of Receiver Operating Characteristics (ROC) plots for convolutional neural networks (CNNs), the first principal component (PC1), and uni-elements maps of Cu, Pb, and Zn derived from till geochemical data of the Bathurst Mining camp. Data are from Parkhill and Dorion (2003).

wide variety of machine learning techniques, ranging from simple regression trees to multi-layer deep neural networks, have been used on geochemical data (*see* Parsa et al., 2022 and references therein). These methods commonly use known mineralized zones as labelled samples and combine univariate geochemical signatures to a predictive multi-element signature. Examples of the use of these methodologies are explained in the case study section.

CASE STUDY

The till data presented herein were collected during the Exploration Science and Technology Program II (EXTECH II) project (Goodfellow et al., 2003) and are sourced from Parkhill and Doiron (2003). Readers are referred to Parkhill and Doiron (2003) and Parsa et al. (2023) for details on the geology, mineral deposits hosted within this area, and sampling and chemical analyses of till samples. Briefly, the till geochemical data used in this study were for the <0.063 mm size fraction, and element concentrations were determined using four-acid digestion followed by inductively coupled plasma-emission spectrometry and inductively coupled plasma-mass spectrometry.

The Area Under the Curve (AUC) within Receiver Operating Characteristic (ROC) plots functions as a metric for assessing the degree of spatial correlation between geochemical signatures and mineral deposits. Typically, higher AUC values indicate stronger correlations between geochemical signatures and mineral deposits. AUC values, as illustrated in Figure 1, indicate that the uni-element geochemical signatures of Cu, Pb, and Zn do not exhibit a complete correlation with the geographical locations of known mineral deposits in the area, although these three elements are the main commodities hosted by these mineral deposits. Compositional PCA was employed in this study to reduce the dimensionality of the geochemical data. Log-ratio transformed values of the analyzed elements, namely Ba, Ce, Co, Cr, Cs, Cu, Dy, Er, Eu, Ga, Gd, Hf, Ho, In, La, Lu, Nb, Nd, Ni, Pb, Pr, Rb, Sc, Sm, Sn, Sr, Ta, Tb, Th, Tl, Tm, U, V, Y, Yb, Zn, and Zr, were used as inputs for PCA. This process yielded a set of uncorrelated Principal Components (PCs). Notably, the first ten PCs account for approximately 90% of the variability within the dataset.

According to the compositional biplot in Figure 2, geochemical anomalies linked to mineralization-related elements, namely Pb, Zn, and Cu, are highlighted in PC1. PC1 also exhibits higher AUC values in comparison to the geochemical signatures of Pb, Zn, and Cu (Fig. 1), signifying that the utilization of PCA has enhanced the identification of geochemical anomalies in this study. Log-ratio transformation, PCA, and biplots were implemented using CODA (http://compositionaldata.com/ codapack.php), an open-source package that can be used for the interpretation of geochemical data.

The initial ten PCs were used as inputs for Convolutional Neural Networks (CNN), a state-of-the-art deep learning tool (O'Shea and Nash, 2015), to generate a geochemical signature that characterizes VMS deposits within the study area. During this process, VMS deposits were utilized as labelled samples to train the neural networks. A fully connected neural network with a convolutional layer and four dense layers was used to generate a regression model. The performance of this model was evaluated by the AUC of ROC plots,

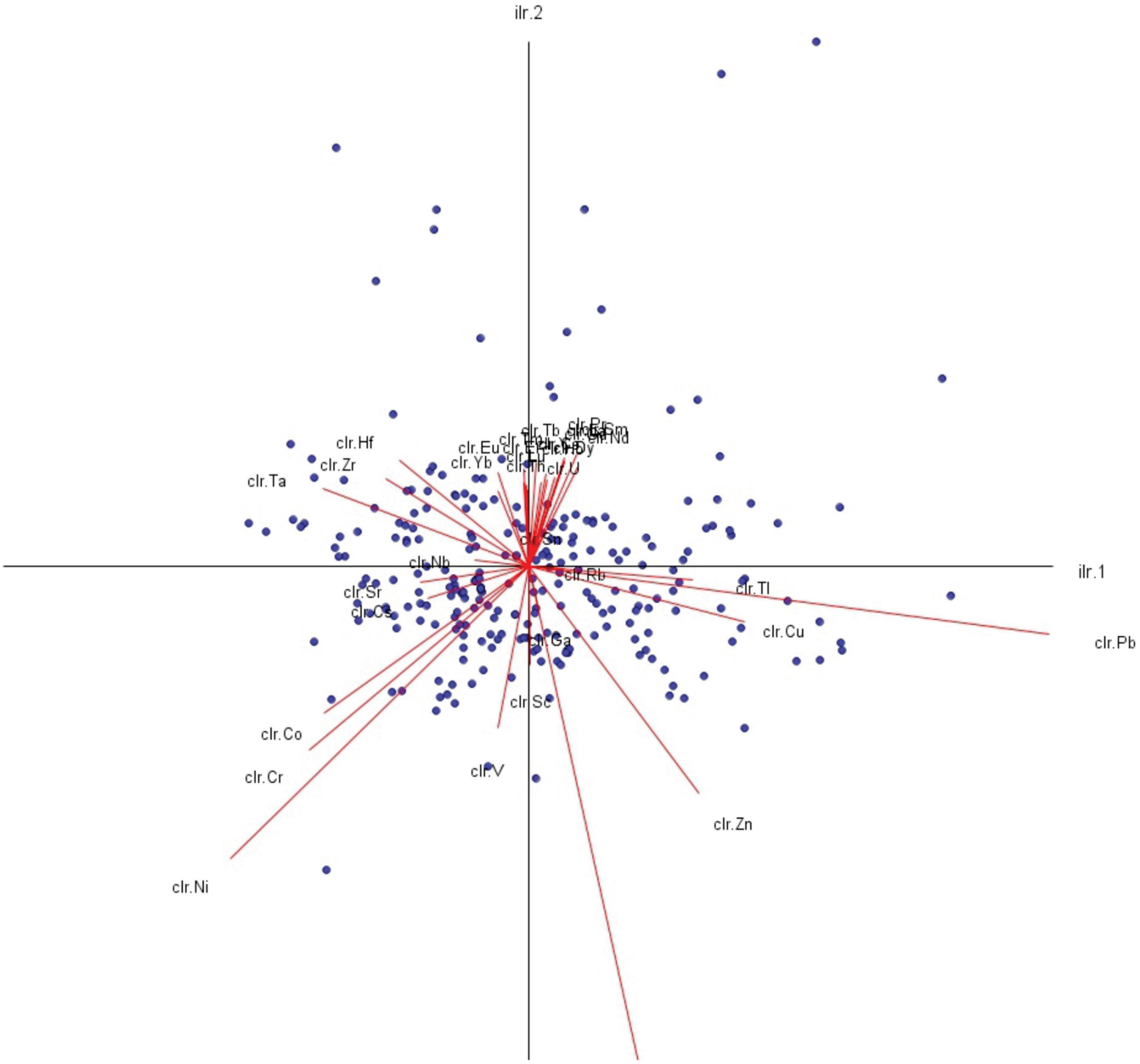


Figure 2. Compositional biplots of till geochemical data for the northern Bathurst Mining Camp. Note the strong association of Cu, Pb, and Zn, elements known to be pathfinder elements for VMS mineralization. Data are from Parkhill and Dorion (2003).

outperforming the AUC of all PCs and geochemical signatures of Cu, Pb, and Zn (Fig. 2).

Figure 3 compares the regression model derived from the application of CNN with the maps of PC1, Cu, Pb, and Zn. According to this figure, the CNN model can serve as a guide for delineating the exploration targets associated with VMS deposits in the study area. The Python script that was used for the integration of geochemical anomalies is publicly available (https://drive.google.com/file/d/1LB5NDmWyJxxeghcZKEFsxmjzIxvpKn92/view?usp=sharing). The dataset used for this regression analysis is also publicly available (https://drive.google.com/file/d/1LB5NDmWyJxxeghcZKEFsxmjzIxvpKn92/view?usp=sharing).

DISCUSSION AND CONCLUSIONS

Interpreting till geochemical data is not without challenges. Knowing the conditions under which samples have been collected can assist in the interpretation. Metadata provides essential context for the geochemical data, helping researchers and geologists understand the conditions under which the samples and subsequent data were collected. It can include information about the location, date, time, and sampling and analytical methodologies. Metadata also allows for an evaluation of quality control data and validation of geochemical data. It also helps identify potential errors or inconsistencies in the geochemical data collection process. By cross-referencing metadata with the actual data,

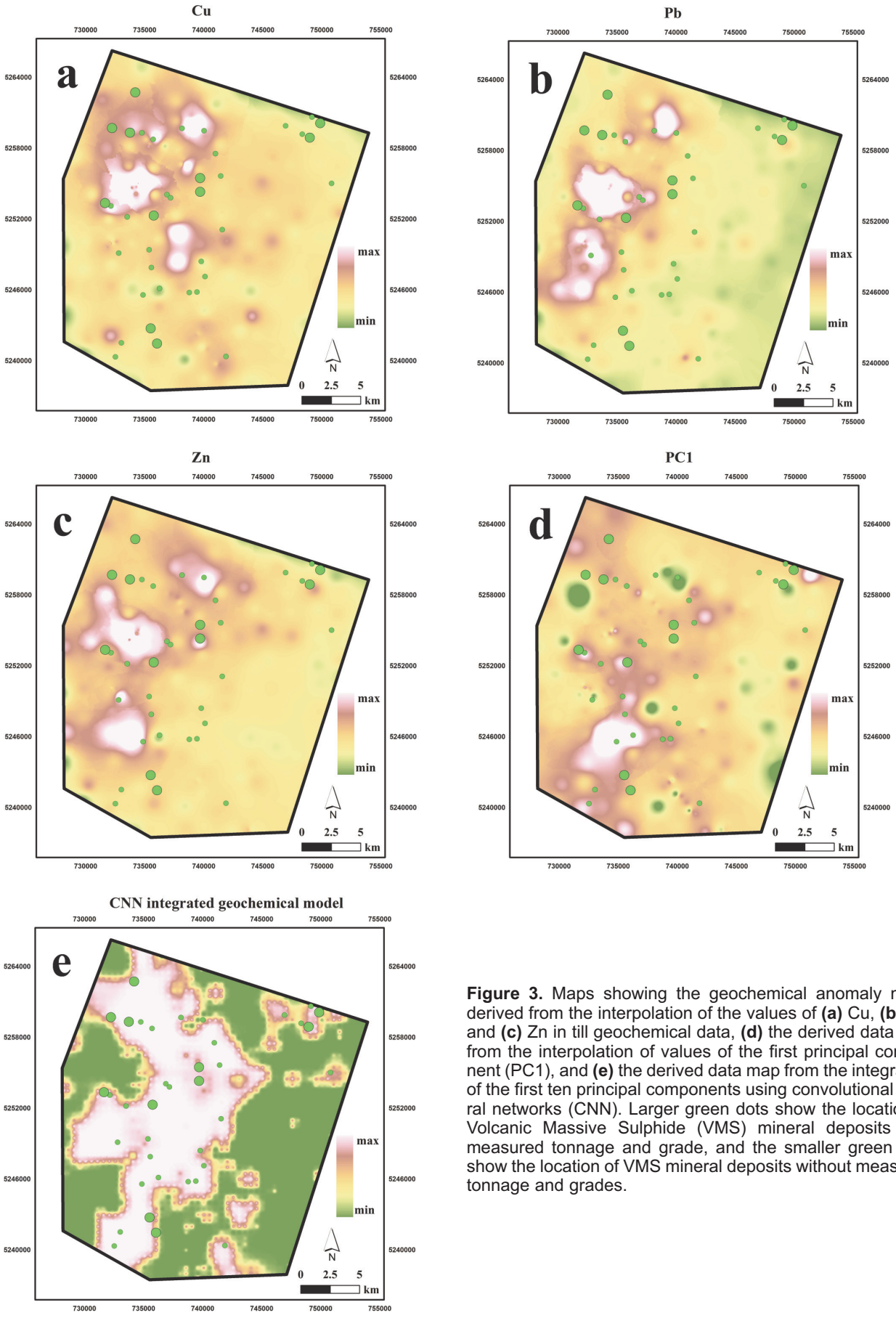


Figure 3. Maps showing the geochemical anomaly maps derived from the interpolation of the values of **(a)** Cu, **(b)** Pb, and **(c)** Zn in till geochemical data, **(d)** the derived data map from the interpolation of values of the first principal component (PC1), and **(e)** the derived data map from the integration of the first ten principal components using convolutional neural networks (CNN). Larger green dots show the location of Volcanic Massive Sulphide (VMS) mineral deposits with measured tonnage and grade, and the smaller green dots show the location of VMS mineral deposits without measured tonnage and grades.

researchers can spot discrepancies and take corrective actions.

The results presented in this study demonstrate that machine learning tools can effectively integrate uni-element geochemical signatures from till data into more robust, multi-element associations that can be utilized to identify exploration targets. However, there are certain challenges associated with using supervised machine-learning tools for geochemical anomaly detection. These challenges primarily stem from the requirement of labelled samples to train supervised algorithms. Labelled samples consist of true positive and true negative samples. The former represents the locations of known mineral deposits, the scarcity of which limits the generalizability of supervised algorithms. The latter indicates non-mineralized zones, which are also challenging to identify. Therefore, future research should prioritize addressing these challenges in the context of geochemical anomaly detection.

ACKNOWLEDGEMENTS

The case study presented in this paper was conducted as part of the first author's post-doctoral research at the University of New Brunswick. The first author would like to express gratitude to David Lentz, James Walker, the Government of New Brunswick, and Brunswick Exploration Co. for their assistance in facilitating the research.

REFERENCES

Aitchison, J., 1982. The statistical analysis of compositional data; Journal of the Royal Statistical Society: Series B (Methodological), v. 44(2), p. 139–160.

Goodfellow, W.D., McCutcheon, S.R., and Peter, J.M., 2003. Massive sulfide deposits of the Bathurst Mining Camp, New Brunswick, and Northern Maine: introduction and summary of findings; *in* Massive Sulfide Deposits of the Bathurst Mining Camp, New Brunswick, and Northern Maine, (ed.) W.D. Goodfellow, S.R. McCutcheon, and J.M. Peter; Society of Economic Geologists, Monograph 11, p. 1–16.

Jowitt, S.M., Wong, V.N.L., Wilson, S.A., and Gore, O., 2017. Critical metals in the critical zone: controls, resources and future prospectivity of regolith-hosted rare earth elements; Australian Journal of Earth Sciences, v. 64, p. 1045–1054.

McClenaghan, M.B., Thorleifson, L.H., and DiLabio, R.N.W., 2000. Till geochemical and indicator mineral methods in mineral exploration; Ore Geology Reviews, v. 16(3-4), p. 145–166.

McClenaghan, M.B., Paulen, R.C., Smith, I.R., Rice, J.M., Plouffe, A., McMartin, I., Campbell, J.E., Lehtonen, M., Parsasadr, M., and Beckett-Brown, C.E., 2023. Review of till geochemistry and indicator mineral methods for mineral exploration in glaciated terrain; Geochemistry: Exploration, Environment, Analysis, v. 23, geochem2023-013.

O'Shea, K. and Nash, R., 2015. An introduction to convolutional neural networks; arXiv preprint arXiv:1511.08458. https://doi.org/10.48550/arXiv.1511.08458

Parkhill, M.A. and Doiron, A., 2003. Quaternary geology of the Bathurst Mining Camp and implications for base metal exploration using drift prospecting; *in* Massive Sulfide Deposits of the Bathurst Mining Camp, New Brunswick, and Northern Maine, (ed.) W.D. Goodfellow, S.R. McCutcheon, and J.M. Peter; Society of Economic Geologists, Monograph 11, p. 631–660.

Parsa, M., Sadeghi, M., and Grunsky, E., 2022. Innovative methods applied to processing and interpreting geochemical data; Journal of Geochemical Exploration, v. 237, 106983. http://dx.doi.org/10.1016/j.gexplo.2022.106983

Parsa, M., Lentz, D.R., and Walker, J.A., 2023. Predictive modeling of prospectivity for VHMS mineral deposits, northeastern Bathurst Mining Camp, NB, Canada, using an ensemble regularization technique; Natural Resources Research, v. 32, p. 19–36.

Abitibi Greenstone Belt: Exploration strategies in thick drift terrain

M.B. McClenaghan[1], R.C. Paulen[1], J.J. Veillette[2], and P.-M. Godbout[1]

[1]Geological Survey of Canada, 601 Booth Street, Ottawa, Ontario K1A 0E8
[2]Emeritus, Geological Survey of Canada, 601 Booth Street, Ottawa, Ontario K1A 0E8

INTRODUCTION

The Abitibi Greenstone Belt (AGB) in northeastern Ontario and northwestern Quebec is one of the largest Neoarchean granite-greenstone terranes in the world, extending 800 km east to west and 300 km north to south (Fig. 1). Mineral deposits within the belt consist of world-class orogenic gold deposits including about 70 gold mines (Veillette et al., 2005), volcanogenic massive sulphide (VMS) deposits including the giant Kidd Creek deposit, komatiite-associated Ni-Cu deposits, molybdenum deposits, Cu-Au vein systems, V-Cr deposits, pegmatite-hosted Li deposits (Mercier-Langevin et al., 2017), and kimberlites (McClenaghan et al., 1996). Many of the orogenic gold deposits are spatially associated with two major fault zones, the Porcupine-Destor Fault Zone and the Cadillac-Larder Lake Fault Zone (Monecke et al., 2017).

Mineral exploration in the belt is challenging because of the thick cover of glacial sediments, much of which is highly conductive glaciolacustrine clay deposits, which have led to the region's informal name, the "Abitibi Clay Belt". The presence of thick clay deposits can impede the use of geophysical methods, such as electrical resistivity, ground penetrating radar, and electromagnetics.

As a result of the extensive thick sediment cover, the lack of bedrock outcrop across the belt has also complicated the search for buried mineral deposits. This chapter reviews the surficial geology and glacial history of this highly prospective region and explains how till geochemistry and indicator mineral methods can be used to "see through" the thick sediment cover to find mineralization.

Since the 1970s, there have been numerous published reports and scientific papers describing till geochemical and indicator mineral methods that have successfully been used in exploration programs and case studies, a selection of which is listed in Table 1. Some of these examples are explained in more detail in this chapter.

QUATERNARY GEOLOGY OF THE ABITIBI GREENSTONE BELT

Much of the bedrock surface across the Abitibi Greenstone Belt (AGB) is covered by 1 to 40 m of unconsolidated sediments that were deposited during or just after multiple cycles of glaciation during the Quaternary (last 2.6 million years) (Veillette et al., 2005). The surface sediments are the products of the retreat of the last ice sheet and the subsequent submergence of the landscape in glacial Lake Barlow-Ojibway. The composition of the surface till and its glacial transport direction(s) are well understood due to the extensive provincial and federal government surficial mapping surveys that have occurred across the AGB.

However, our knowledge of the sediment stratigraphy at depth, where older till units are overlain by other glacial sediments (Fig. 2), is hampered by the lack of exposure. Till sections exposed in the walls of open pits (e.g. Owl Creek, Maude Lake, Selbaie; Fig. 3) have exposed the tills units and older striated bedrock surfaces. These 'windows' into the till stratigraphy have allowed for the documentation of till composition and glacial transport directions (till fabrics, striations) (Averill, 1978; Veillette, 1989; Paulen, 2001; Veillette et al., 2005, 2017) and provided the context in which exploration overburden drillhole stratigraphy can be interpreted (e.g. Bird and Coker, 1987; McClenaghan, 1991, 1994). A generalized till stratigraphic model for the AGB is shown in Figure 2 and is based on the open pit exposures combined with data from drillholes reported in exploration assessment files and government studies (e.g. Skinner, 1972; DiLabio et al., 1988; Smith, 1990, 1992; McClenaghan, 1992a, 1994; Paulen et al., 2006).

Surficial sediments

The surficial geology of the AGB has been mapped in Ontario at a 1:50,000 scale by the Ontario Geological Survey and the Geological Survey of Canada (Fig. 1, Table 2). The portion of the belt within the Quebec borders has been mapped at 1:100,000 to 1:250,000 scale

Recommended citation:
McClenaghan, M.B., Paulen, R.C., Veillette, J.J., and Godbout, P.-M., 2024. Abitibi Greenstone Belt: Exploration strategies in thick drift terrain; *in* Till Geochemistry and Indicator Mineral Methods for Exploration in Glaciated Terrains, (ed.) R.C. Paulen and M.B. McClenaghan; Geological Survey of Canada, Open File 9210, p. 115–132. https://doi.org/10.4095/pbmy2d03m0

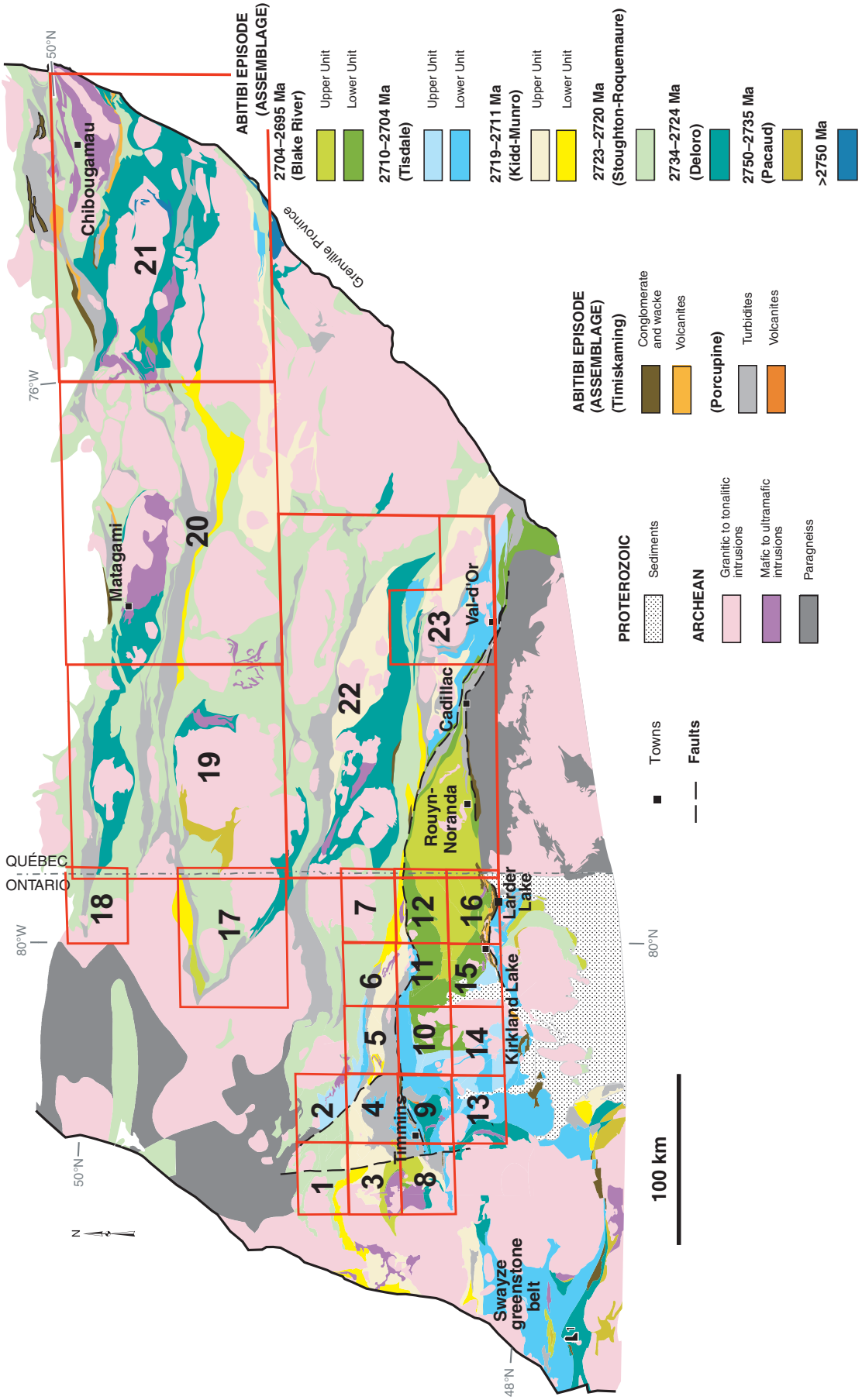


Figure 1. Bedrock geology map of the Abitibi Greenstone Belt (modified *from* Thurston et al., 2008) and the outline of the surficial geology maps that have been published for the belt by the Ontario Geological Survey, the Ministère des Ressources naturelles et des Forêts du Québec, and the Geological Survey of Canada. See Table 2 for a listing of the numbered maps (numbers 1 to 23).

Table 1. Selected listing of till sampling case studies and exploration programs reporting till geochemistry and indicator mineral signatures of gold and VMS deposits and kimberlites that have been reported in the literature.

Deposit/Occurrence	Location	Ore elements	Till geochemistry pathfinder elements	Type of study	Till geochemistry fraction analyzed	Indicator mineral methods used?	Source of information
Kidd Creek	Timmins Mining Camp	Zn-Cu-Pb-Ag	Zn, Cu	government case study	<0.0177 mm		Fortescue and Hughes (1965)
Kidd Creek	Timmins Mining Camp	Zn-Cu-Pb-Ag	Zn, Cu, Ag, Hg	government case study	<0.0177 mm; HMC (>2.96 SG)		Fortescue and Hornbrook (1969); Hornbrook (1975)
Kam Kotia	Timmins Mining Camp	Cu-Zn	Cu, Zn, Ag, Cd, Sb, Se, Ga, Tl, V	government case study	<0.002 mm; <0.063 mm HMC (SG> 3.3)		Smith (1990; 1992)
Kam Kotia	Timmins Mining Camp	Cu-Zn	Cu-Zn	government case study	<0.063 mm; <0.25–0.063 mm HMC (SG >3.3)		Skinner (1972); Shilts (1976)
Jameland	Timmins Mining Camp	Cu-Zn-Au-Ag	Cu-Zn	government case study	<0.063 mm; <0.25–0.063 mm HMC (SG >3.3)		Skinner (1972); Shilts (1976)
Currie (Tillex)	Timmins Mining Camp	Cu	Cu	exploration program	<0.177 mm; <2.0 mm HMC (SG >3.3)		Thompson (1979)
Pamour, Davidson-Tisdale, Bell Creek, Nighthawk, Hislop	Timmins Mining Camp	Au	Au, As, Ag, Cd	government case study	<2.0 mm HMC; <0.063 mm	gold grains	McClenaghan (1999, 2001)
Bell Creek	Timmins Mining Camp	Au	Au	exploration program	<2.0 mm HMC	gold grains	Harron et al. (1987)
Owl Creek	Timmins Mining Camp	Au	Au	exploration case study	<2.0 mm HMC; <0.063 mm	gold grains	Bird and Coker (1987); Shelp and Nichol (1987)
Iso	Noranda Mining Camp	Cu-Zn	Ag, Cu, Zn	university study	matrix and HMC fractions		Telford and Becker (1979)
Horne	Noranda Mining Camp	Cu-Au-Ag	Cu, Zn, Pb	university study	<0.0177 mm		Dreimanis (1958, 1960)
MacDonald (Gallen)	Noranda Mining Camp	Zn-Cu-Au-Ag	Cu, Zn, Pb	university study	<0.177 mm		Dreimanis (1958, 1960)
Magusi River	Noranda Mining Camp	Zn-Cu	Cu, Zn, Ag, Hg	exploration program	whole till; >0.177 mm HMC (SG >2.96); <0.177 mm		Gleeson (1975a)
Bousquet	Noranda Mining Camp	Au	Au	exploration program	<2.0 mm HMC		Gleeson and Sheehan (1987)
Mogador (Vendome)	Val d'Or Mining Camp	Zn-Cu-Pb-Ag-Au	Cu, Zn, Ag	university study	<0.177 mm; >0.177 mm HMC		Dreimanis (1958); Gleeson (1975b)
Louvem	Val d'Or Mining Camp	Zn-Cu-Ag-Au	Cu, Zn	exploration program	<0.177 mm; >0.177 mm HMC (SG >2.96)		Gleeson and Cormier (1971)
Louvem deposit	Val d'Or Mining Camp	Zn-Cu-Ag-Au	Cu, Zn	government case study	<0.177 mm; 0.064–0.177 mm HMC (SG >3.3)		Garrett (1971)
Casa Berardi (Golden Pond)	Casa Berardi	Au	Au, As	exploration program	<2.0 mm HMC	gold grains	Sauerbrei et al. (1987)
Malarctic (Doyon Mine)	Malarctic	Au	Au	exploration program	<2.0 mm HMC		Gleeson and Sheehan (1987)

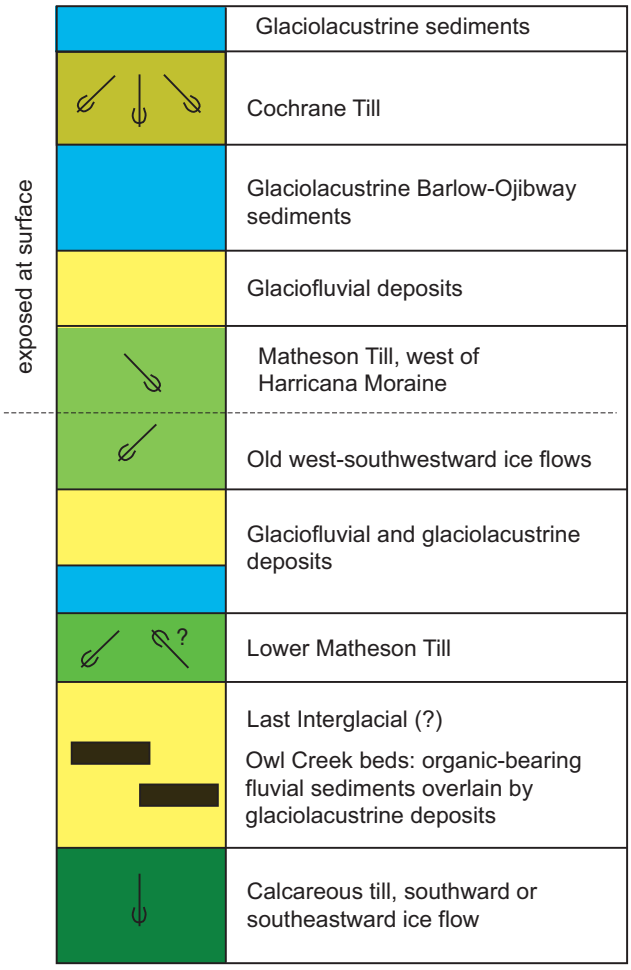


Figure 2. Generalized stratigraphy for the Abitibi Greenstone Belt (modified *from* Veillette et al., 2005) indicating the possibility of intersecting multiple till units in deep overburden drillholes or open pit sections, and their associated ice-flow directions.

Table 2. Listing of the surficial geology maps (numbers 1 to 23) for the Abitibi Greenstone Belt that have been published by the Ontario Geological Survey (OGS), the Ministére des Ressources naturelles et des Forêts du Québec, and the Geological Survey of Canada (GSC). Map locations are shown in Figure 1.

Map number on Figure 1	NTS map sheet	Map/publication	Agency	Author
1	42A/13	Open File 3618	GSC	Paulen and McClenaghan (1998b)
2	42A/14	Open File 3619	GSC	Paulen and McClenaghan (1998a)
3	42A/12	Map 2656	OGS	Richard (2000)
4	42A/11	Map 2655	OGS	Richard (2001)
5	42A/10	Map 2659	OGS	Richard and McClenaghan (2000a)
6	42A/9	Map 2652	OGS	Vagners (2000)
7	32D/12	Map 2651	OGS	Vagners and Courtney (2000)
8	42A/5	Map 2660	OGS	Tucker and Richard (2001)
9	42A/6	Map 2662	OGS	Tucker and Sharpe (2001)
10	42A/7	Map 2658	OGS	Richard and McClenaghan (2000b)
11	42A/8	Map 2650	OGS	Baker (2000b)
12	32D/5	Map 2648	OGS	Baker (2000d)
13	42A/3	Map 2611	OGS	Bajc (2000a)
14	42A/2	Map 2610	OGS	Bajc (2000b)
15	42A/1	Map 2649	OGS	Baker (2000c)
16	32D/4	Map 2647	OGS	Baker (2000a)
17	42H/8, 42H/1, 32E/5, 32E/4	P3770	OGS	Gao (2013a)
18	32E/13, 32E/14	P3769	OGS	Gao (2013b)
19	32E	Open File 6063	GSC	Veillette and Thibadeau (2010)
20	32F	Open File 6062	GSC	Paradis et al. (2010)
21	32G	Open File 6064	GSC	Paradis (2010)
22	32D	Open File 6061	GSC	Veillette et al. (2010)
23	32C/3, 32C/4, 32C/5	BQ 2022-02	MRNF	Dubé-Loubert (2023)

by the Geological Survey of Canada and the Ministère des Ressources naturelles et des Forêts du Québec (Fig. 1, Table 2). These maps are invaluable because they indicate where bedrock is at surface, the trend of glacial striations and landforms, and where till is exposed at surface for sampling. Areas of sand and gravel deposits are also identified, which can be useful for building access roads. Thick clay deposits are mapped out, identifying areas that will require subsurface till sampling techniques.

The main map units that have been identified on surficial geology maps are summarized below.

i) Areas of bedrock outcrop and bedrock with thin till cover are most abundant along an east-west bedrock highland (Abitibi Highland) that forms the drainage divide between James Bay and the St. Lawrence drainage basins (Fig. 3).

ii) Matheson Till, named for thick sequences of sandy silt till (Fig. 4) exposed on the Black River near Matheson, 60 km east of Timmins (Hughes, 1965; McClenaghan, 1992a), occurs at surface as thick (up to 5 m) deposits in isolated patches, thin pockets around the edges of bedrock outcrops, and thin patches (<2 m) overlying bedrock in upland areas. It is olive-grey and contains 5 to 20% carbonate clasts by volume west of the Harricana Moraine (see below), most of which are rock fragments from the Paleozoic Hudson Bay Lowlands (Fig. 5). In places, it is overlain by thick deposits of glaciolacustrine clay and silt. Due to its high sand content, this till is ideal for mineral exploration till geochemical and heavy mineral surveys.

iii) Interlobate moraines and eskers consist of sorted sand and gravel. The largest of these in the AGB is the Harricana Moraine, a major interlobate deglaciation landform (Fig. 3, 5). This feature was deposited between two ice lobes that were retreating towards the northwest and northeast on either side of the moraine during the end of glaciation.

iv) Glaciolacustrine deposits consist of i) shallow-water fine-sand deposits associated with eskers entering the lakes and ii) deep-water deposits of clay and silt varves (Fig. 6). The light coloured silt part of each varve couplet was deposited in the summer during active melting and the dark coloured clay was deposited in calm waters during the winter. These deposits are the main surficial sediment across the AGB (Vincent and Hardy, 1979; Paulen, 2001; Godbout et al., 2019). Areas covered by thick glaciolacustrine clay deposits typically form low-relief plains that have poor drainage and large swampy areas below an elevation of ~300 m. These areas are mostly in the northern half of the AGB and around Frederick Lake and Lake Abitibi (Fig. 3).

v) Clay-rich Cochrane Till (Fig. 4e), which was named for its occurrence near the town of Cochrane (Hughes, 1956, 1965), dominates the surficial landscape north of Timmins and Lake Abitibi. It formed from the erosion and incorporation of underlying glaciolacustrine sediments during a late readvance of the ice and forms a thick (2–8 m) continuous blanket over the northern half of the western AGB. It is a grey-brown to brown, carbonate-rich clayey silt till with 1 to 5% clasts by volume and 25 to 35% carbonate in the matrix. Paleozoic carbonate rocks comprise more than 70% of all clasts in this till. The southern limit of this till sheet, informally referred to as the "Cochrane limit", is shown in Figures 3 and 7. The clast- and sand-poor nature of this till, which indicates very little input from the underlying local bedrock of the AGB, is not suitable for drift prospecting.

Ice-flow patterns

The general ice-flow history of the AGB was reconstructed from the mapping of more than 3000 striated surfaces during more than 20 years of fieldwork overseen by J.J. Veillette and B. McClenaghan (Veillette, 1986, 1989; Veillette and McClenaghan,1996; McClenaghan et al., 1995; Veillette et al., 1999, 2005). Ice-flow indicators, including striations, grooves, crag-and-tail features, and flutings (refer to Paulen et al., 2024), indicate that a complex sequence of ice-flow phases affected the Abitibi region (Fig. 7). Initially, ice flowed to the northwest (290–315°) across the belt from the Quebec Highlands during the growth of the Laurentide Ice Sheet. Striation evidence of this ice-flow phase is scarce, although northwest-oriented striations were found at the Lower Sturgeon hydroelectric dam on the Mattagami River, 30 km north of Timmins (Fig. 3; Paulen and McClenaghan, 1997). Ice flow subsequently shifted counterclockwise, to the west (260–270°) and southwest (230–250°). Striation evidence of these flows is mostly preserved on bedrock surfaces west of the Harricana Moraine. Ice flow then shifted to south and southwest (190–220°) during early deglaciation, as the ice sheet started opening up in the southern Temiskaming area and converging on the Harricana Moraine (Fig. 7). West of the town of Cochrane, a late glacial ice stream (Winisk Ice Stream) surged southeastward from the western margin of Hudson Bay, terminating just northwest of Timmins (Veillette et al., 2017). The last ice-flow phase in the region was from the Cochrane lobes as the deglacial ice margin moved back into glacial Lake Ojibway. Surface till (Matheson Till), sampled in support of mineral exploration and surficial mapping within the AGB, was deposited by the later stages of ice flow to the southwest, south, and

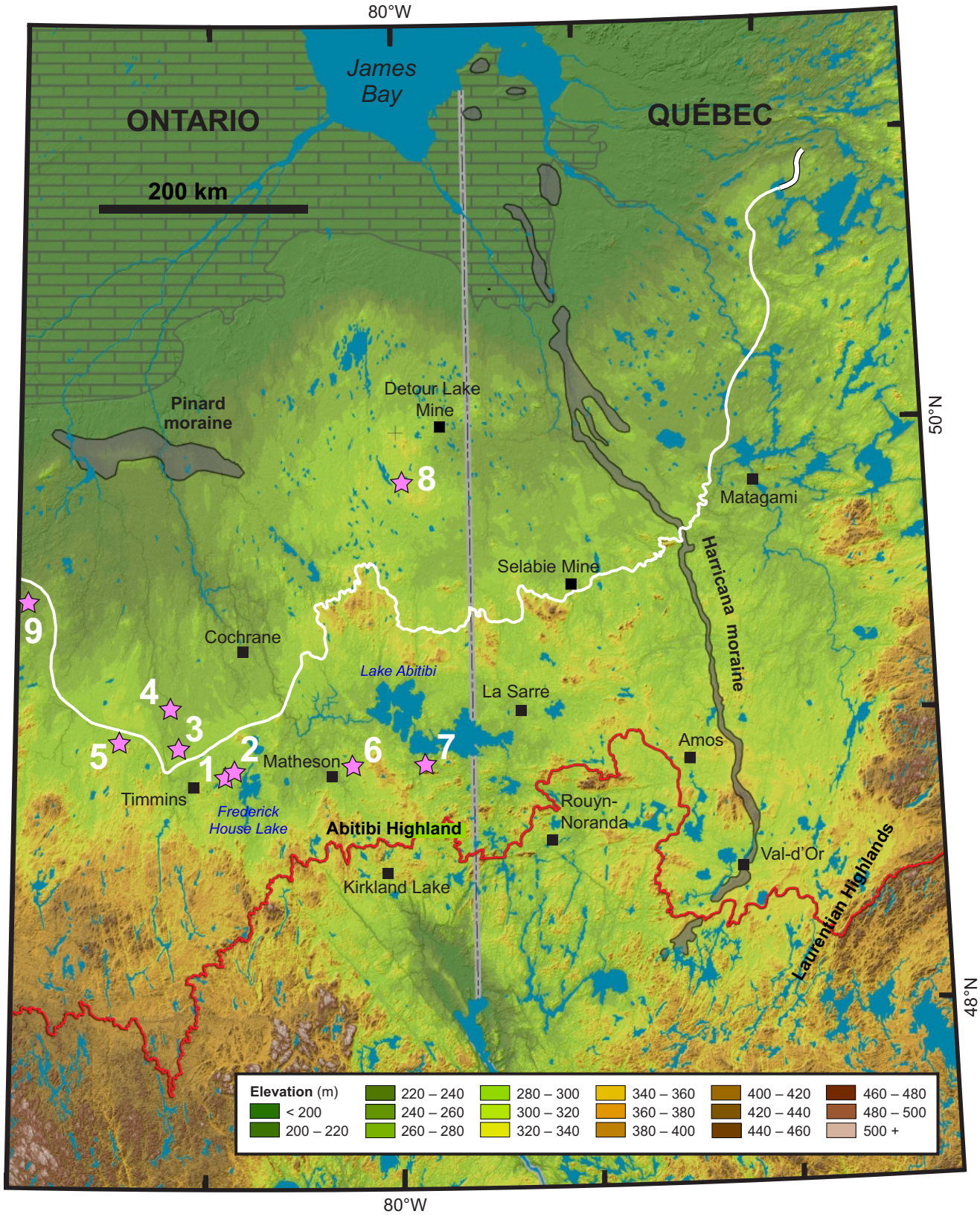


Figure 3. Map showing the topography of the Abitibi Greenstone Belt and the locations of the places mentioned in the text. The long thick white line shows the southern limit of the Cochrane Till. The continuous red line defines the height of land that forms the drainage divide between the Hudson Bay (north) and St. Lawrence River (south) watersheds. Modified from Godbout et al. (2019). Locations: 1 = Pamour Mine, 2 = Owl Creek Mine and Kidd smelter, 3 = Kidd Creek Mine, 4 = Lower Sturgeon generating station, 5 = Loveland Ni-Cu float boulders, 6 = Maude Lake pit, 7 = saprolite in drillhole, 8 = Lawagamau Lake section, 9 = Cargill carbonatite.



Figure 4. Photographs of Matheson and Cochrane tills. **a)** Unoxidized grey silty sand Matheson Till exposed in the walls of the Pamour Au Mine No. 3 open pit in 1995. **b)** Matheson Till exposed in a borrow pit near Timmins. The till sample was collected at a 2 m depth to obtain unoxidized grey till. **c)** Grey unoxidized Matheson Till exposed at the Maude Lake pit. **d)** Matheson Till intersected in a rotasonic drillhole (9 cm diameter core). **e)** Light brown clay-rich Cochrane Till overlying grey silty sand Matheson Till in a borrow pit section near Lawagamau Lake, 25 km southwest of the Detour Lake mine. The site locations are shown in Figure 3.

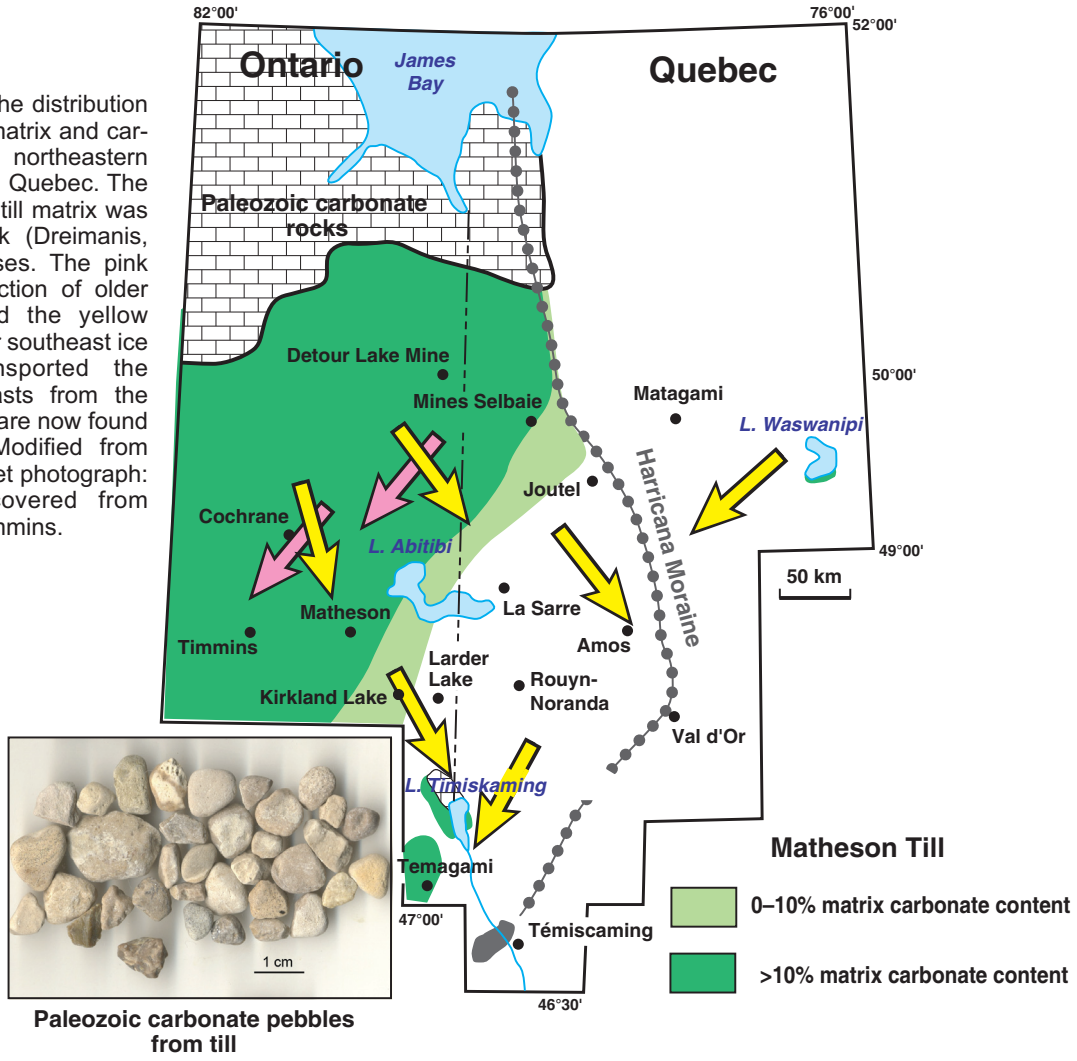


Figure 5. Map showing the distribution of carbonate-rich till (till matrix and carbonate pebbles) across northeastern Ontario and northwestern Quebec. The carbonate content of the till matrix was determined using chittick (Dreimanis, 1962) and LECO analyses. The pink arrows indicate the direction of older southwest ice flow and the yellow arrows represent younger southeast ice that eroded and transported the Paleozoic carbonate clasts from the James Bay Lowland and are now found in the Matheson Till. Modified from Veillette et al. (2005). Inset photograph: Paleozoic pebbles recovered from Matheson Till north of Timmins.

southeast, (depending on the location in the AGB) and is exposed at surface south of the Cochrane Limit.

Matching the erosional ice-flow record with till units is challenging. At a regional scale, it is possible to map the glacial transport of distinct boulder-, cobble- and pebble-sized erratics from remote bedrock sources, such as the Paleozoic carbonate in James Bay (Fig. 5). Most Matheson Till samples collected west of the Harricana Moraine contain a few percent Paleozoic carbonate clasts (Fig. 5 inset photo) and 1–10% matrix carbonate, both of which reflect erosion and southward transport of carbonate debris from the James Bay Lowlands. The highest carbonate clast/matrix concentrations occur in the western and northern parts of the AGB. Note that carbonate clasts are present in till near Kirkland Lake but absent in till further east near Larder Lake (Fig. 5).

An example of how carbonate pebble content in till samples collected from overburden drillholes can be used to identify glacial transport directions is shown in Figure 8. The carbonate content in Matheson Till samples (green in Fig. 8) decreases from west to east in the Matheson-Lake Abitibi area indicating ice flowed due south from the carbonate platform. The carbonate content of till units that are older than the Matheson Till (blue polygons) is consistently high, regardless of location, indicating a sustained south-southeast flow direction that predates the ice-flow patterns shown in Figure 7. This south-southeast ice-flow event (Veillette and McClenaghan, 1996) is likely the source of the older carbonate-rich till intersected in an overburden drillhole 20 km northeast of Kirkland Lake (Fig. 3) and encountered in a depression on the open pit floor of the Selbaie Au mine (Fig. 3; Veillette et al., 2005). Elsewhere in the Selbaie open pit, till samples and till fabrics were collected from a 17 m section of what appeared to be a thick Matheson Till unit. The till stratigraphy records a shift in ice flow from older, southwestward at the bottom to younger southeastward at the top where the till becomes carbonate-rich (Veillette et al., 2005). These ice flows are the same as those shown in Figure 7.

At a local scale, glacial transport directions can be discerned by mapping the distribution of indicator min-

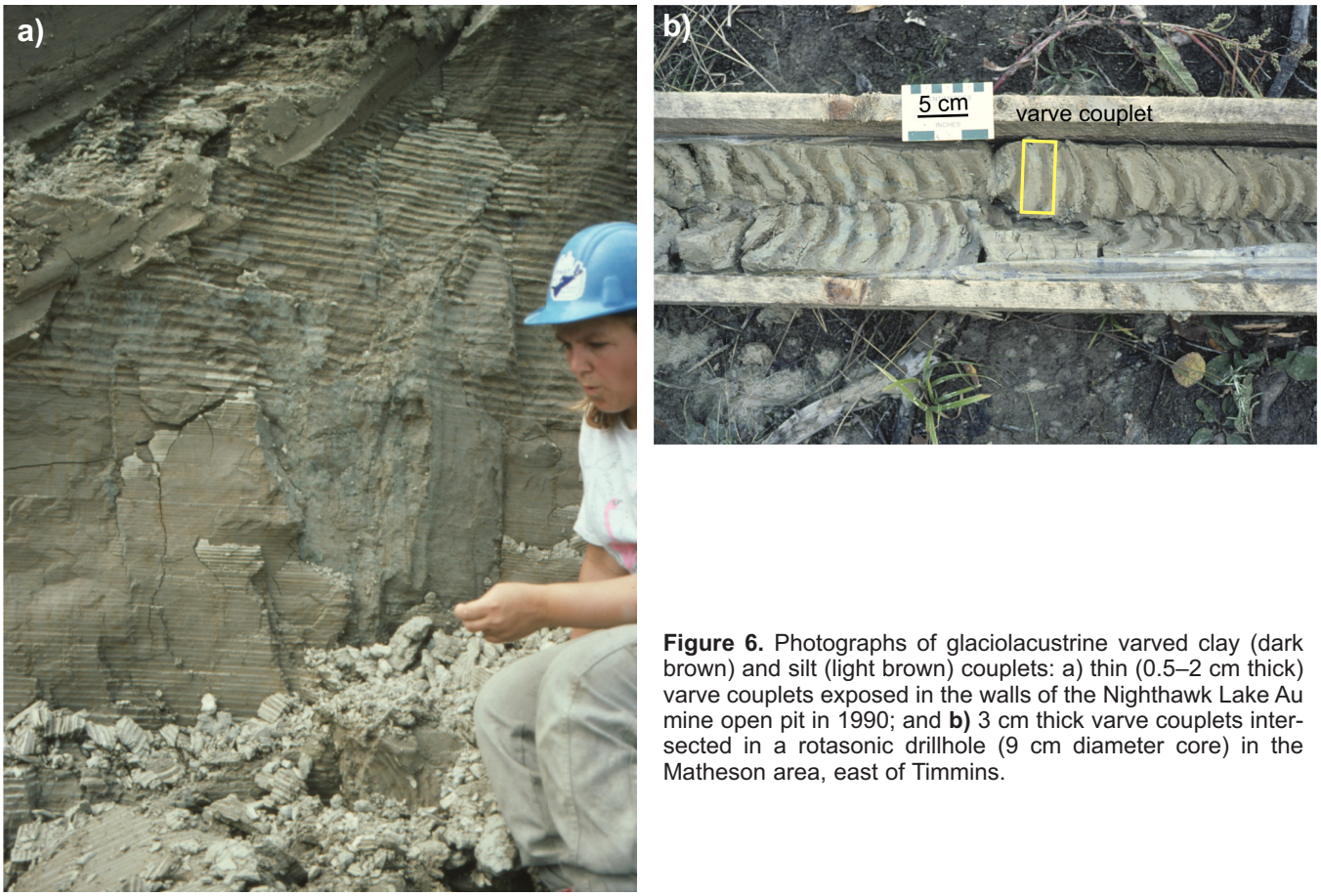


Figure 6. Photographs of glaciolacustrine varved clay (dark brown) and silt (light brown) couplets: a) thin (0.5–2 cm thick) varve couplets exposed in the walls of the Nighthawk Lake Au mine open pit in 1990; and **b)** 3 cm thick varve couplets intersected in a rotasonic drillhole (9 cm diameter core) in the Matheson area, east of Timmins.

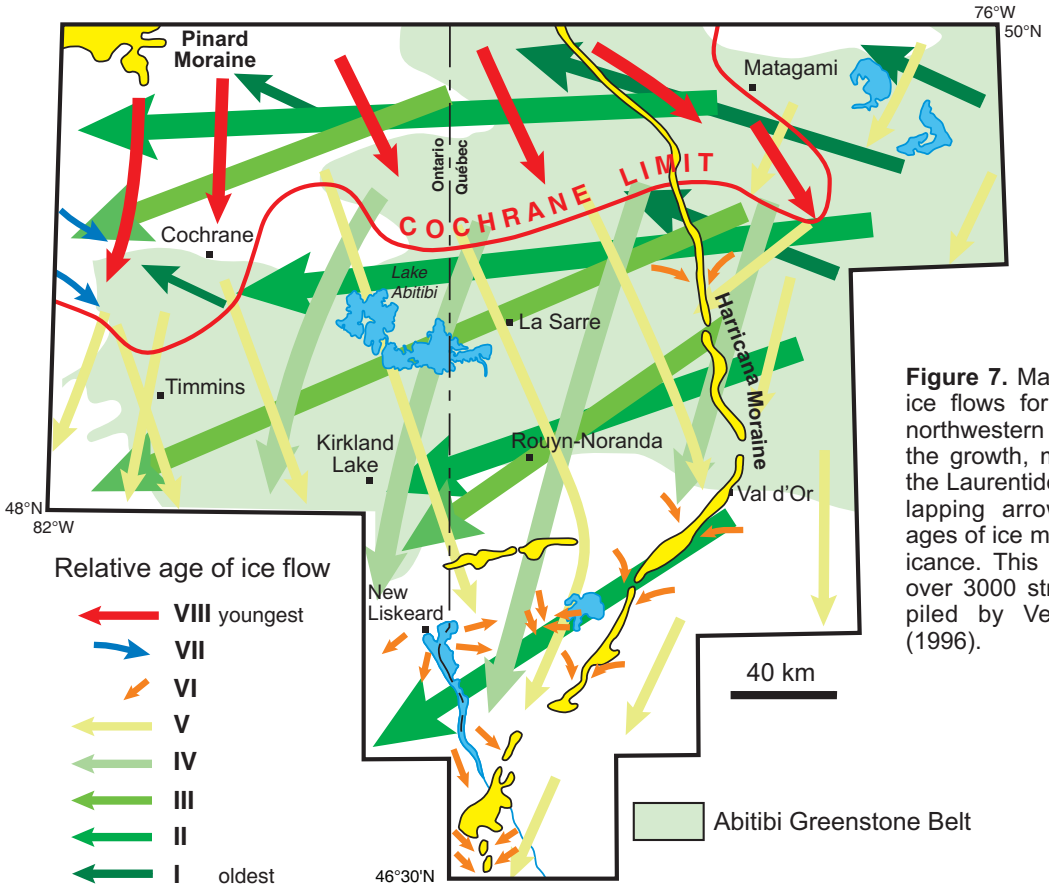


Figure 7. Map showing the sequence of ice flows for northeastern Ontario and northwestern Quebec, which represent the growth, main phases, and decay of the Laurentide Ice Sheet (LIS). The overlapping arrows represent the relative ages of ice movements of regional significance. This reconstruction is based on over 3000 striation measurements compiled by Veillette and McClenaghan (1996).

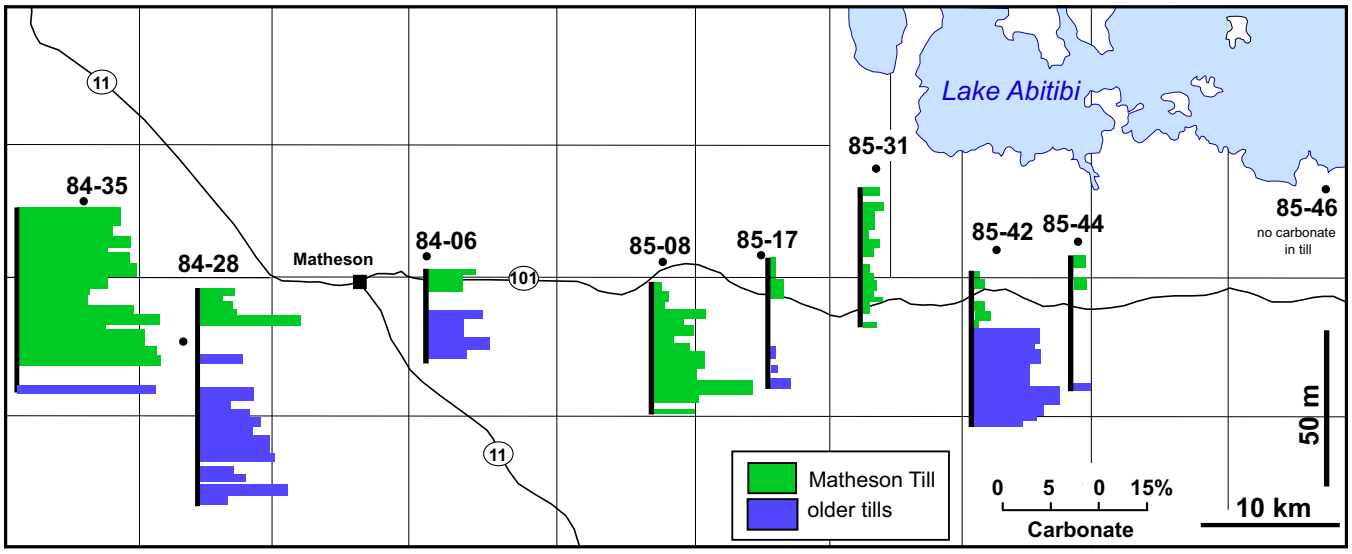


Figure 8. Paleozoic carbonate pebble abundance in till units from selected Ontario Geological Survey sonic overburden drillholes across the Matheson-Lake Abitibi area, showing a decrease in carbonate content in Matheson Till (green polygons) towards the east. Horizontal bar heights correspond to the vertical sample interval in the drillhole. Modified from McClenaghan (1992a).

erals (e.g. gold grains, kimberlite indicator minerals) and/or metal-rich till (geochemistry) from mineralized bedrock. Bird and Coker (1987) demonstrated this using the gold content in Matheson and older till downice from the Owl Creek Au deposit 18 km east of Timmins (labeled 2 in Fig. 3). Another example is the use of As content in till, the distribution pattern for which maps out the location of Cadillac-Larder Lake fault zone in the Rouyn-Noranda area and glacial dispersal from the fault zone to the southwest (*see* Fig. 10 *in* Veillette et al., 2005).

A useful marker horizon that helps distinguish between tills deposited by different glaciations and conduct stratigraphic correlations between drill holes in the western part of the AGB is the stratified Owl Creek beds (Fig. 9), named for its exposure in the walls of the Owl Creek open pit Au mine, 18 km east of Timmins. Its presence has been reported in numerous overburden drill holes in the western Abitibi region (Fig. 9) including those reported by Brereton and Elson (1979), Skinner (1972), McClenaghan (1992a), and Smith (1990, 1992). The beds mark the division between overlying till deposited by the Laurentide Ice Sheet during the Wisconsin stage (ice flows shown in Figure 7) and older tills that underlie the marker horizon. The beds consist of overconsolidated organic-rich silt, clay, and sorted sand. Radiocarbon dates for organic material from the unit are all considered to be infinite (>37,000 BP to >51,000 BP) because they are beyond the limit of the dating methods, thus the beds are thought to have been deposited during the last interglacial between 75,000 and 125,000 years BP, before the last major cycle of glaciation (DiLabio et al., 1988; Mott and DiLabio, 1990).

TILL SAMPLING METHODS

At surface (<2 m depth), till samples can be collected in hand-dug or augered holes, and from natural river or lake shore exposures (Fig. 10). Refer to Rice and McClenaghan (2024) for a description of till sampling methods. Additionally, samples may be collected from excavator trenches, open pits, borrow pits, or road cuts. Government surficial geology maps and LiDAR imagery are useful for identifying areas where till is accessible at or near surface. See the chapter by Bukhari et al. (2024) for an explanation of how LiDAR can be used to preselect surface till sample sites.

Where sediments are thick (>2 m depth) and till is not exposed at surface, till samples are collected using excavators (up to 5 m depth), portable drills, or drilling rigs (Fig. 10). In the AGB, till units can be thick and several tills can be encountered, thus overburden drilling allows multiple till samples to be collected at depth. The most common subsurface till sampling method used across the AGB is reverse circulation (RC) drilling, which recovers a mud and chip slurry while continuously drilling (e.g. Bird and Coker, 1987; Harron et al., 1987). Thousands of RC holes have been drilled into bedrock to sample till across the AGB by exploration companies since the method was first developed in the 1970s (Skinner, 1972). Rotasonic drilling has also been used to collect till samples from continuous core sequences that have been recovered from surface into bedrock (e.g. Smith, 1992; McClenaghan, 1994; McClenaghan et al., 1996; Paulen, 2001; Fig. 4d). Both drilling methods are described in detail in McMartin and McClenaghan (2001). Many of the exploration RC and sonic drillhole

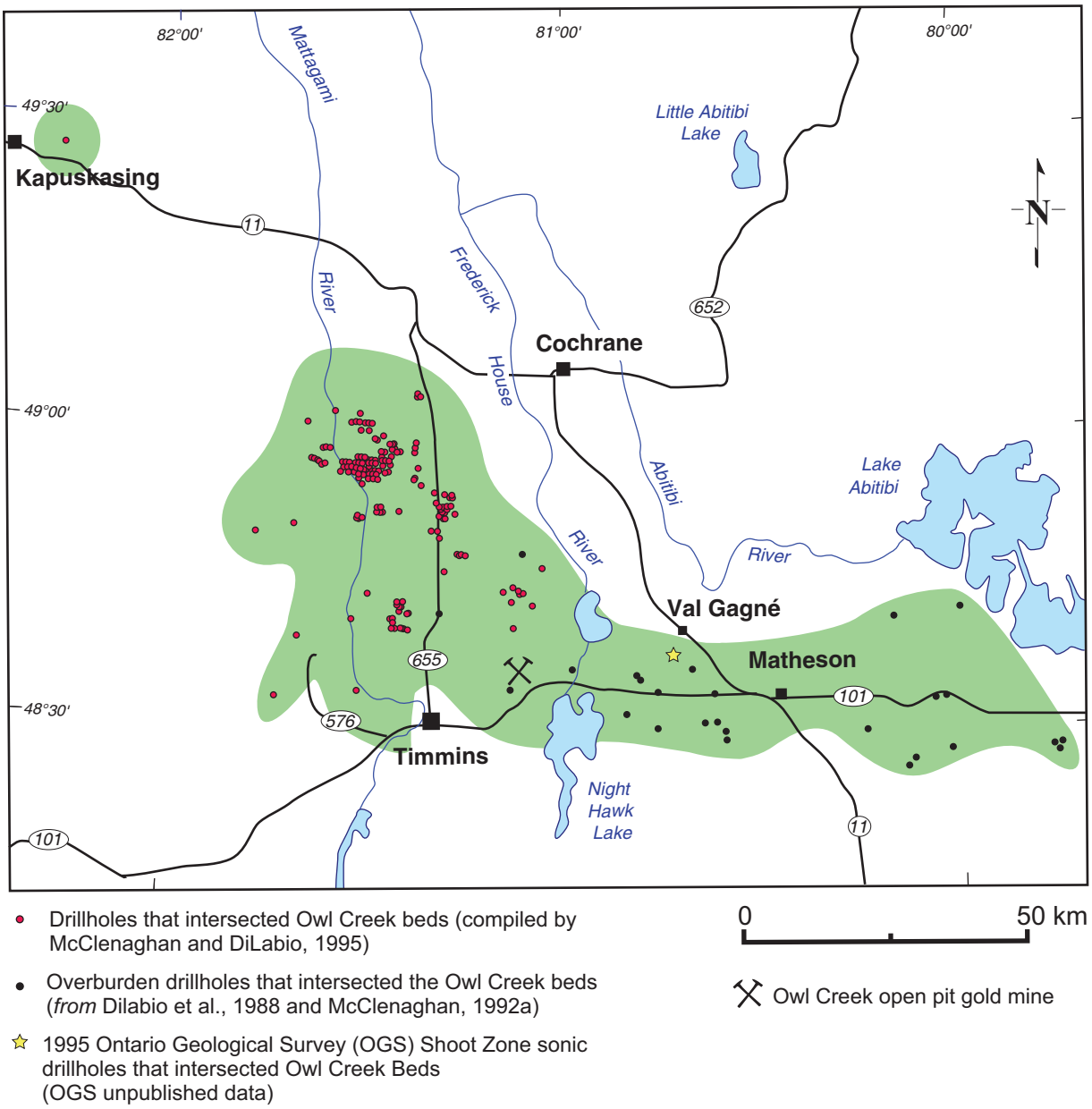


Figure 9. Map showing the area (green polygon) where exploration and government overburden drillholes have intersected Owl Creek beds in the western Abitibi region. Modified from Paulen (2001).

logs are available in provincial government assessment files and provide insights into the depth to bedrock, as well as the thicknesses of clay and till units. A digital compilation of overburden drillhole stratigraphy and depth to bedrock in diamond drillholes is available for part of the western AGB (McClenaghan and DiLabio, 1995).

In overburden drillholes, multiple till samples should be collected from vertical till sequences and not just from the till/bedrock interface because geochemical and/or indicator mineral dispersal trains do not only occur at the till/bedrock interface but may also occur higher up in a till unit, as shown in Figure 11. Sampling an entire till sequence increases the chances of inter-

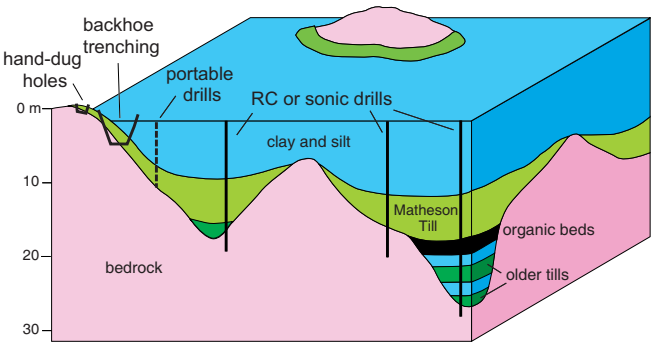


Figure 10. Schematic block diagram of the Abitibi region showing till distribution and thickness and the optimal till sampling strategies for various overburden thicknesses. Modified from McClenaghan (2001).

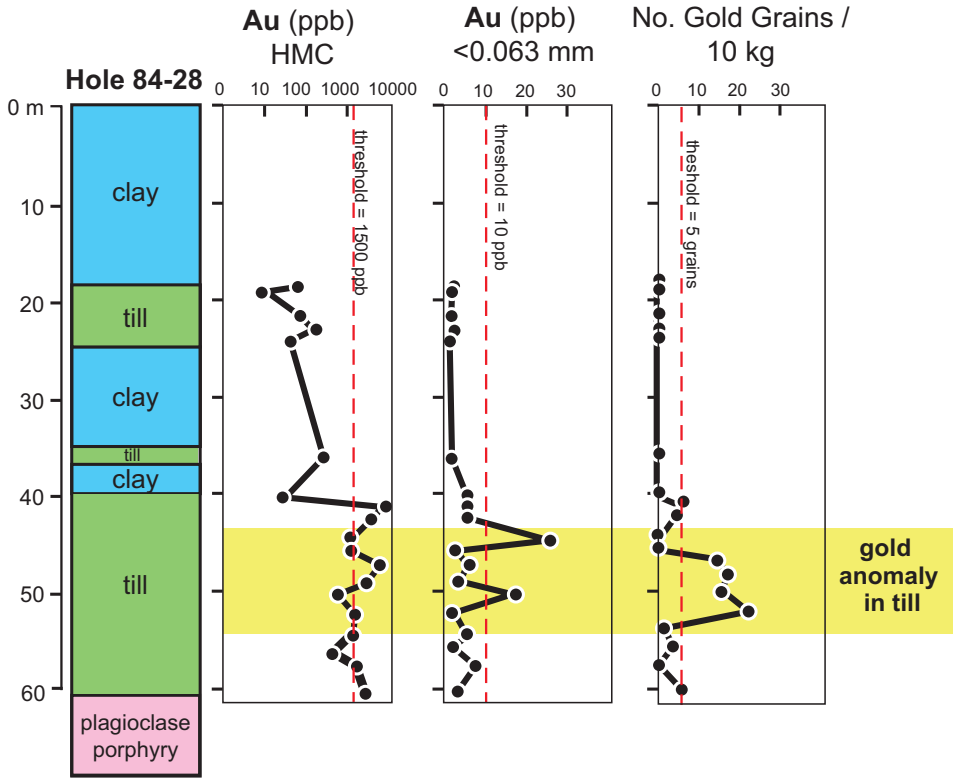


Figure 11. Gold concentrations in the till matrix and heavy mineral fractions (HMC) and gold grain abundance in till intersected in Ontario Geological Survey sonic overburden drillhole 84-28 in Currie Township, east of Timmins. The gold anomaly is at least 5 m above the till/bedrock interface, indicating the importance of collecting multiple samples through an entire till sequence and not just the lowermost metre of till on bedrock. Modified from McClenaghan (1994).

secting a dispersal train from more distal sources.

TILL GEOCHEMISTRY

A 2–3 kg sample is commonly collected for till matrix geochemical analysis of the <0.063 mm fraction. Using aqua regia/inductively coupled plasma-mass spectrometry (ICP-MS) on a 30 g aliquot allows for the determination of 65 elements in the till samples, including reproducible values for Au. It is a strong partial digestion for most elements and is optimal for determining the common ore elements Au, Ag, Cu, Pb, Zn, and Ni, as well as the pathfinder elements As, Bi, Cd, Co, Ga, Ge, Hg, In, Sb, Se, Te, and Tl. A total digestion method, such as lithium meta/tetra borate fusion, is recommended for determining the total concentration of the more difficult-to-digest minerals that host Cr, Sn, REE, and W. For lithium exploration, 4-acid digestion or Na-peroxide fusion can be used to determine near total (90%) or total Li concentrations, respectively, in till (Li-FT Power, 2022; Brushett et al., 2024). Several regional-scale till geochemical surveys have been conducted over parts of the AGB (listed in Table 3) and these have identified anomalous areas that warrant further investigation and provide the regional context in which to interpret results from exploration programs. For a more detailed review of till geochemical methods, see McClenaghan et al. (2023) and Beckett-Brown and McClenaghan (2024).

INDICATOR MINERAL METHODS

Government regional-scale surveys (Table 3) and exploration programs conducted in the AGB have been systematically reporting gold-grain abundance and shape data from till sampling programs since the 1980s (e.g. DiLabio, 1990; Alcock, 1991; McClenaghan, 1992a,b; Bajc, 1996, 1997; Bajc et al., 1996; McClenaghan et al., 1998a; Bajc and Crabtree, 2001). This 40+ year time span has allowed thresholds to be established between background and anomalous gold-grain abundances in till from the AGB. In general, background gold-grain abundance increases southward (Fig. 12) and is related to the amount of mineralized metavolcanic bedrock that is present up-ice (Averill and Huneault, 1991). For specific areas in the AGB, government regional-scale till surveys have defined more precise thresholds between background and anomalous concentrations. For example, the threshold between anomalous concentrations of gold grains in the Timmins area is five grains/10 kg (McClenaghan et al., 1998a), whereas, in the Peterlong-Radisson lakes area, 25 km south of Timmins, the threshold is ten grains/10 kg (Bajc, 1996).

Kimberlite indicator mineral methods have been used in diamond exploration in the Kirkland Lake area since the 1980s (e.g. Fortescue et al., 1984; Brummer et al., 1992a,b; McClenaghan et al., 1996, 1998b, 1999a,b) and have led to the discovery of the Kirkland Lake kimberlite field. Modern heavy mineral methods now allow for the recovery of indicator minerals from

Table 3. Listing of government studies for which stratigraphic information and till geochemistry and/or indicator mineral data have been published.

Area	Drilling method	Regional till survey?	Publications
Timmins to Smoky Falls	rotasonic drilling	no	DiLabio et al. (1988); Smith (1990, 1992)
Timmins to Val d'Or transect	reverse circulation drilling	no	Skinner (1972); DiLabio (1983)
Kirkland Lake	reverse circulation drilling	yes	Fortescue et al. (1984); McClenaghan and Wyatt (1990)
Black-River Matheson (Lake Abitibi)	rotasonic drilling	yes	McClenaghan (1991, 1992a, 1994)
Kirkland Lake kimberlite field	rotasonic drilling	no	McClenaghan et al. (1996, 1998b, 1999a,b)
Rouyn-Val d'Or	cobra drilling	yes	Gilbert et al. (1972); LaSalle et al. (1975a,b, 1976, 2005); Kish et al. (1979); Lalonde and LaSalle (1982); Beaumier (1983); Beaumier and Henry (1987); LaSalle and Henry (1987); Beaumier et al. (1994); LaSalle et al. (2005)
Peterlong-Raddison Lake	No drilling	yes	Bajc (1996); Bajc and Crabtree (2001)
Matchewan	No drilling	yes	Bajc (1997)
Timmins	No drilling	yes	McClenaghan et al. (1998a)
Shining Tree	No drilling	yes	Alcock (1991)

till for a broad suite of deposit types (e.g. McClenaghan and Paulen, 2018, and references therein).

MINERALIZED BOULDERS

In addition to till geochemistry and indicator mineral methods, mineralized boulders on surface can be used to explore the Abitibi region. Ferguson and Freeman (1978) and McClenaghan et al. (1998a) have documented some of the reports of mineralized boulders (float) found on surface in the Timmins region that were glacially transported down ice of mineralized bedrock. Most notable is the Loveland Township Ni-Cu mineralized boulder occurrence northwest of Timmins (Fig. 3), known informally as the Loveland nickel property, which is likely sourced from mineralized ultramafic rocks 1 km to the northwest (Ferguson and Freeman, 1978; Katchen, 2020).

PREGLACIAL SAPROLITE

The formation of preglacial saprolite (in situ weathered bedrock) may, in places, concentrate certain elements that are economically of interest. The presence of saprolite has been reported in drillholes in several locations across the AGB. The weathering that formed the

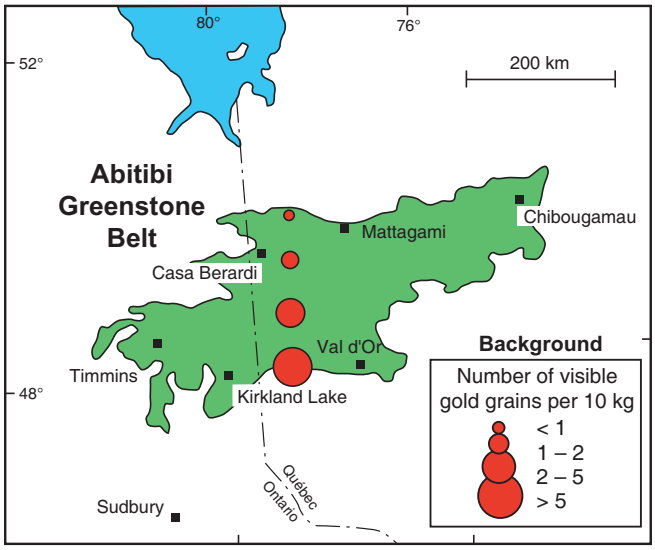


Figure 12. Southward increasing threshold between background and anomalous abundances of gold grains in the heavy mineral fraction of till across the Abitibi Greenstone Belt. Modified from Averill and Huneault (1991)..

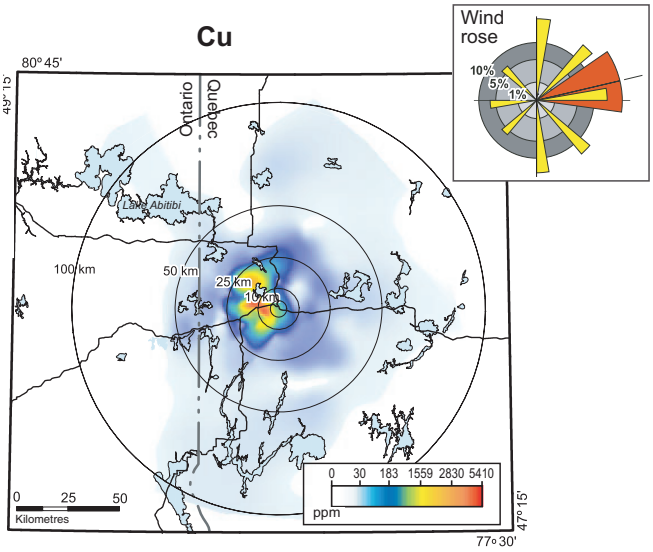


Figure 13. Interpolated surface showing the regional distribution of Cu (ppm, aqua regia ICP-AES) in the <2.0 mm fraction of humus samples collected within 100 m of the Noranda Smelter. Inset is a wind rose diagram showing the percentage of the time (1%, 5%, 10%) that the wind blows along 8 principal wind directions (yellow vectors) and the average wind direction in orange (*from* Henderson and Knight, 2005).

saprolite is thought to be preglacial due to the depth and extent that the bedrock has been severely altered. Rongier et al. (2014) published a depth-to-bedrock map for the western Quebec part of the AGB, with one of its stated purposes being to identify areas where saprolite may be preserved in depressions in the bedrock surface that escaped glacial erosion.

The Cargill carbonatite, 100 km northwest of Timmins, is one of the best examples of preserved preglacial weathering of bedrock in northeastern Ontario. The following description is summarized from Sage (1988) and Sandvik and Erdosh (1977). Beneath ~2 m of glaciolacustrine clay and, on average, 15 m of grey-green till, is deeply weathered bedrock that consists of organic-rich quartz sand with numerous 1 to 4 m thick layers of peat, kaolinite, and clean, white, well sorted sand. These sediments are underlain by deeply weathered carbonatite consisting of apatite-bearing residuum, a few meters to 170 m in thickness, which developed during Cretaceous weathering. Other examples of preserved saprolite were intersected in sonic overburden drillholes south of Lake Abitibi (Fig. 3), including a 14 m section of bedrock that consisted of "orange clay" with black pyrolusite stringers (Steele et al., 1986a) and a second nearby drillhole had highly kaolinized bedrock (Steele et al., 1986b). Smith (1992) reported the intersection of 1.5 to 13 m of strongly weathered bedrock in four sonic overburden drillholes 80 km northwest of Timmins and 40 km south of Kapuskasing.

SMELTER EFFECTS

The AGB hosts two smelters, which are known to be sources of airborne particles that settle onto the local landscape. GSC studies showed that concentrations of Ag, As, Bi, Cd, Cu, Mo, Pb, and Zn are enriched in humus and B-horizon soils within a 50 km radius of the Noranda smelter (Fig. 13; Henderson et al., 2002). McClenaghan et al. (1998a) showed that concentrations of Cu, Zn, Pb, Cd, Ag, Bi, Mo, and Se in humus are enriched within a 10 km radius of the Kidd smelter (Fig. 3) just east of Timmins. The presence of fallout from the smelters should be considered when interpreting any geochemical data of humus and B-horizon soil from within 100 km of these sites in the AGB, especially when using soil selective leach analysis.

CONCLUSIONS

- There is great potential within the world-class AGB for the discovery of additional orogenic gold, VMS, komatiite-associated Ni-Cu, Mo, Cu-Au veins, V-Cr, and pegmatite-hosted Li deposits, and kimberlites.
- The thick cover of glacial sediments overlying bedrock in most parts of the belt is challenging for exploration.
- The mineral-deposit types listed above have distinct geochemical and mineralogical signatures that can be readily detected by analyzing the till units within the thick cover of glacial sediments using primarily till geochemistry and indicator mineral methods
- The application of till sampling as an exploration tool is well established in the AGB, with a more than 40 year history.
- Our understanding of the ice-flow history and glacial stratigraphy of the AGB has benefitted from access to exploration properties and mine sites as well as exploration drillhole logs in assessment files and confidential company files.

ACKNOWLEDGEMENTS

Our knowledge of the glacial geology of the Abitibi Greenstone Belt and drift exploration methods is the result of the GSC's long-term research in the 1970s through to the 2000s. This summary is an output of the GSC's Targeted Geoscience Initiative (TGI-6) indicator minerals methods activity. Richard Fortin (GSC) is thanked for his advice on geophysical methods. Janet Campbell (GSC) is thanked for her review of this chapter

REFERENCES

Alcock, P.W., 1991. Quaternary geology of the Shining Tree area; Ontario Geological Survey, Open File Report 5810.

Averill, S.A., 1978. Overburden exploration and the new glacial history of Northern Canada; Canadian Mining Journal, v. 99, p. 58–64.

Averill, S.A. and Huneault, R.,1991. Using silt-sized visible gold grains to explore for gold deposits concealed by Quaternary overburden: Nevada vs. Canada; EXPLORE, v. 72, p. 10–12.

Baker, C.L., 2000a. Quaternary Geology, Larder Lake Area; Ontario Geological Survey Map M2647.

Baker, C.L., 2000b. Quaternary Geology, Ramore Area; Ontario Geological Survey Map M2650.

Baker, C.L., 2000c. Quaternary Geology, Kirkland Lake Area; Ontario Geological Survey Map M2649.

Baker, C.L., 2000d. Quaternary Geology, Magusi River area; Ontario Geological Survey Map M2648.

Bajc, A.F., 1996. Regional distribution of gold in till in the Peterlong Lake-Radisson Lake area, Southern Abitibi subprovince; potential exploration targets; Ontario Geological Survey, Open File Report 5941.

Bajc, A.F., 1997. A regional evaluation of gold potential along the western extension of the Larder-Lake Cadillac break, Matachewan area; results of regional till sampling; Ontario Geological Survey, Open File Report 5957.

Bajc, A.F., 2000a. Quaternary Geology, Peterlong Lake area; Ontario Geological Survey, Map 2611.

Bajc, A.F., 2000b. Quaternary Geology, Radisson Lake area; Ontario Geological Survey, Map 2610.

Bajc, A.F. and Crabtree, D.C., 2001. Results of regional till sampling for kimberlite and base metal indicator minerals, Peterlong Lake–Radisson Lake area, northeastern Ontario; Ontario Geological Survey, Open File Report 6060.

Bajc, A.F., Hamilton, S.M., Ayer, J., and Jensen, L.S., 1996. New exploration targets in the Peterlong Lake-Radisson Lake area, southern Abitibi subprovince; till, lake sediment and lake water sampling programs; Ontario Geological Survey, Open File Report 5942.

Beaumier, M. and Henry, J., 1987. Compilation des aires d'intérêt géochimique (Abitibi-Témiscamingue), Québec. Ministère de l'Énergie et des Ressources, Document divers DV 87–22.

Beckett-Brown, C.E. and McClenaghan, M.B., 2024. Using indicator minerals to explore for porphyry Cu deposits and their related critical minerals; *in* Till Geochemistry and Indicator Mineral Methods for Exploration in Glaciated Terrains, (ed.) R.C. Paulen and M.B. McClenaghan; Geological Survey of Canada, Open File 9210, p. 147–156. https://doi.org/10.4095/pbmy2d03m0

Bird, D.J. and Coker, W.B., 1987. Quaternary stratigraphy and geochemistry at the Owl Creek Gold Mine, Timmins, Ontario, Canada; Journal of Geochemical Exploration, v. 28, p. 267–284.

Brummer, J.J., MacFadyen, and Pegg, C.C., 1992a. Discovery of kimberlites in the Kirkland Lake area northern Ontario, Canada PART I: early surveys and the surficial geology; Exploration and Mining Geology, v. 1, p. 339–350.

Brummer, J.J., MacFadyen, D.A., and Pegg, C.C., 1992b. Discovery of kimberlites in the Kirkland Lake area, northern Ontario, Canada. Part II: kimberlite discoveries, sampling, diamond content, ages and emplacement; Exploration and Mining Geology, v. 1, p. 351–370.

Brushett, D.M., Beckett-Brown, C.E., McClenaghan, M.B., Paulen, R.C., Rice, J.M., Haji Egeh, A., and Pelchat, P., 2024. Till geochemical data for the Brazil Lake pegmatite area, southwest Nova Scotia (NTS 21A/04, 20-O/16 and 20P/13): samples collected in 2020, 2021, and 2022; Geological Survey of Canada, Open File 9148.

Bukhari, S., Eyles, N., and Paulen, R.C., 2024. LiDAR in glacial geology and drift exploration: The prospectors' ice-stream landsystem; *in* Till Geochemistry and Indicator Mineral Methods for Exploration in Glaciated Terrains (ed.) R.C. Paulen and M.B. McClenaghan; Geological Survey of Canada, Open File 9210, p. 132–138. https://doi.org/10.4095/pbmy2d03m0

DiLabio, R.N.W., 1983. Gold content of overburden samples in the Abitibi Clay Belt; Geological Survey of Canada, Open File 945.

DiLabio, R.N.W., 1990. Classification and interpretation of the shapes and surface textures of gold grains from till on the Canadian Shield; *in* Current Research, Part C; Geological Survey of Canada, Paper 90-1C, p. 323–329.

DiLabio, R.N.W., Miller, R.F., Mott, R.J., and Coker, W.B., 1988. The Quaternary stratigraphy of the Timmins area, Ontario, as an aid to mineral exploration by drift prospecting; *in* Current Research, Part C; Geological Survey of Canada, Paper 88-1C, p. 61–65.

Dreimanis, A., 1958. Tracing ore boulders as a prospecting method in Canada; The Canadian Mining and Metallurgical Bulletin, v. 51, p. 73–79.

Dreimanis, A., 1960. Geochemical prospecting for Cu, Pb, and Zn in glaciated areas, eastern Canada; *in* 21st International Geological Congress, Norden, Part II Results of Applied Geochemistry and Geophysics, p. 7–19.

Dreimanis, A., 1962. Quantitative gasometric determination of calcite and dolomite by using chittick apparatus; Journal of Sedimentary Petrology, v. 32, p. 520–539.

Ferguson, S.A. and Freeman, E.B., 1978. Ontario occurrences of float, placer gold and other heavy minerals; Ontario Geological Survey, Mineral Deposits Circular 17.

Fortescue, J.A.C. and Hornbrook, E.H.W., 1969. Copper, zinc, nickel, and lead in lower till material collected near a massive sulphide ore body in the clay belt of northern Ontario; Geological Survey of Canada, Paper 65-2, p. 23–27.

Fortescue, J.A.C. and Hughes, O.L., 1965. Section F Two quick projects, one at a massive sulphide orebody near Timmins, Ontario and the other at a copper deposit in Gaspé Park, Quebec; *in* Progress Report on Biogeochemical Research at the Geological Survey of Canada 1963–1966 (Part 2); Geological Survey of Canada, Paper 67-23, p. 39–63.

Fortescue, J.A.C., Lourim, J., Gleeson, C.F., Jensen, L., and Baker, C., 1984. A synthesis and interpretation of basal till geochemical and mineralogical data obtained from the Kirkland Lake (KLIP) area (1979-1982) Part I and Part II; Ontario Geological Survey, Open File Report 5506.

Garrett, R.G., 1971. The dispersion of copper and zinc in glacial overburden at the Louvem deposit, Val d'Or, Quebec; *in* Proceedings, 3rd International Geochemical Exploration Symposium, Toronto, April 16–18, 1970, (ed.) R.W. Boyle; Canadian Institute of Mining and Metallurgy, Special Volume 11, p.157–158.

Gao, C., 2013a. Quaternary Geology, Burntbush Area, northeastern Ontario; Ontario Geological Survey, Map 3770.

Gao, C., 2013b. Quaternary Geology, Detour Lake area, northeastern Ontario; Ontario Geological Survey, Map 3769.

Gleeson, C.F., 1975a. Magusi River Zn-Cu deposit, Quebec; Journal of Geochemical Exploration, v. 4, p. 172–173.

Gleeson, C.F., 1975b. Consolidated Mogador Cu-Pb-Zn-Ag-Au deposit, Quebec; Journal of Geochemical Exploration, v. 4, p. 172–173.

Gleeson, C.F. and Cormier, R., 1971. Evaluation by geochemistry of geophysical anomalies and geological targets using overburden sampling at depth; Proceedings, 3rd International Geochemical Exploration Symposium, Toronto, April 16–18, 1970, (ed.) R.W. Boyle; Canadian Institute of Mining and Metallurgy, Special Volume 11, p. 159–165.

Gleeson, C.F. and Hornbrook, E.H.W., 1975. Semi-regional geochemical studies demonstrating the effectiveness of till sampling at depth; *in* Geochemical Exploration 1974, (ed.) I.L. Elliott and W.K. Fletcher; Association of Applied Geochemists, Special Publication No. 2, Elsevier, p. 611-630.

Gleeson, C.F. and Sheehan, D., 1987. Humus and till geochemistry over the Doyon, Bosquet and Williams Au deposits; Canadian Institute of Mining and Metallurgy Bulletin, v. 80, p. 58–66.

Godbout, P.-M., Roy, M., and Veillette, J.J., 2019. High-resolution varve sequences record one major late-glacial ice re-advance and two drainage events in the eastern Lake Agassiz-Ojibway basin; Quaternary Science Reviews, v. 223, 105942.

Harron, G.A., Middleton, R.S., Durham, R.B., and Philipp, A., 1987. Geochemical and geophysical gold exploration in the Timmins area, Ontario; a case history; Canadian Institute of Mining and Metallurgy Bulletin, v. 80, p. 52–57.

Henderson, P.J. and Knight, R.D., 2005. The regional distribution and mobility of copper and lead in soils near the Horne copper smelter at Rouyn-Noranda, Quebec; Chapter 3 *in* Metals in the Environment around Smelters at Rouyn-Noranda, Quebec, and Belledune, New Brunswick: Results and conclusions of the GSC MITE Point Sources Project, (ed.) G. Bonham-Carter; Geological Survey of Canada, Bulletin 584.

Henderson, P.J., Knight, R.D., and I. McMartin, I., 2002. Geochemistry of soils within a 100 km radius of the Horne Cu smelter, Rouyn-Noranda, Quebec; Geological Survey of Canada, Open File 4169.

Hornbrook, E.H.W., 1975. Kidd Creek Cu-Zn-Ag deposit, Ontario; Journal of Geochemical Exploration, v. 4, p. 165–168.

Hughes, O.L., 1956. Surficial geology of Smooth Rock, Cochrane District, Ontario; Geological Survey of Canada, Paper 55-41.

Hughes, O.L., 1965. Surficial geology of part of the Cochrane District, Ontario, Canada; *in* International Studies on the Quaternary, (ed.) H.E. Wright Jr. and D.G. Frey; Geological Society of America, Special Paper 84, p. 535–565.

Lalonde, J-P. and LaSalle, P., 1982. Atlas géochimique de l'argile et du till de base de l'Abitibi, Québec; Ministère des richesses naturelles du Québec, DPY-830.

LaSalle, P. and Henry, J., 1987. Géochimie du till de la région de l'Abitibi (projet Cadillac, or, arsenic, antimoine, tungstène); Ministère de l'Énergie et des Ressources, Dossier public DP 87-22.

LaSalle, P., Warren, B., Gilbert, P., Jacob, H.L., and La Salle, Y.R., 1975a. Moraine sampling under varved clays in the Rouyn-Val d'Or area: general results; *in* Geochemical Exploration 1974, (ed.) I.L. Elliot and W.K. Fletcher; Association of Exploration Geochemists, Special Publication No., 2, Elsevier Science, New York, p. 595–610.

LaSalle, P., Warren, B., and Gilbert, P. ,1975b. Till sampling at depth in the Rouyn-Val d'Or area; *in* Glacial Till, (ed.) R.F. Legget; Royal Society of Canada, Special Publications, No. 12, p. 24–248.

LaSalle, P., Warren, B., and LaSalle, Y.R., 1976. Minéraux métalliques dans des échantillons de till d'Abitibi, Québec. Ministère des Richesses naturelles, Dossier public DP-348.

LaSalle, Y., LaSalle, P., and Beaumier, M., 2005. Fractions lithiques et minéralogiques du till de base de la partie sud de l'Abitibi (données numériques du MB 85-29). Ministère des Ressources naturelles et de la Faune, DP 2005-01.

Li-FT Power, 2022. Li-FT Power provides exploration results for 2022 Rupert project exploration program; Junior Mining Network, Accessed Oct. 23, 2023. https://www.juniorminingnetwork.com/junior-miner-news/press-releases/3217-cse/lift/130848-li-ft-provides-exploration-results-from-2022-rupert-project-exploration-program.html

McClenaghan, M.B., 1991. Geochemistry of tills from the Black River-Matheson (BRiM) sonic overburden drilling program and implications for exploration; Ontario Geological Survey, Open File Report 5800.

McClenaghan, M.B., 1992a. Quaternary geology of the Matheson-Lake Abitibi area, Ontario Geological Survey, Open File Report 5836.

McClenaghan, M.B., 1992b. Surface till geochemistry and implications for exploration, Black River- Matheson area, northeastern Ontario; Exploration and Mining Geology, v. 1, p. 327–337.

McClenaghan, M.B., 1994. Till geochemistry in areas of thick drift and its application to gold exploration, Matheson area, northeastern Ontario; Exploration and Mining Geology, v. 3, p. 17–30.

McClenaghan, M.B., 1999. Till geochemical signatures associated with gold deposits in the Timmins-Matheson areas, Western Abitibi greenstone Belt, northeastern Ontario; Geological Survey of Canada, Open File 3707.

McClenaghan, M.B., 2001. Regional and local-scale gold grain till geochemical signatures of lode Au deposits in the western Abitibi Greenstone Belt, central Canada; *in* Drift Exploration in Glaciated Terrain, (ed.) M.B. McClenaghan, P.T. Bobrowsky, G.E.M. Hall, and S. Cook; Geological Society of London, Special Publication 185, p. 201–223.

McClenaghan, M.B. and DiLabio, R.N.W., 1995. Overburden database compilation, Timmins, Ontario (NTS 42A/11, 12, 13, 14): Geological Survey of Canada, Open File Report 3086.

McClenaghan, M.B. and Wyatt, P.H., 1990. Summary of overburden and bedrock trace element data from the Kirkland Lake Initiatives Program (KLIP) reconnaissance till sampling program; Ontario Geological Survey, Open File Report 5737.

McClenaghan, M.B. and Paulen, R.C., 2018. Chapter 20 *in* Mineral Exploration in Glaciated Terrain; *in* Past Glacial Environments (Sediments, Forms and Techniques) A new & revised edition, (ed.) J. Menzies, J. and J.J-M. van der Meer; Elsevier, p. 689–751.

McClenaghan, M.B., Veillette, J.J., and DiLabio, R.N.W., 1995. Ice flow patterns in the Timmins and Kirkland Lake areas, northeastern Ontario; Geological Survey of Canada, Open File 3014, scale 1:100 000.

McClenaghan, B.M., Kjarsgaard, I.M., Schulze, D.J., Stirling, J.A.R., Pringle, G., and Berger, B.R., 1996. Mineralogy and geochemistry of the B30 kimberlite and overlying glacial sediments, Kirkland Lake, Ontario; Geological Survey of Canada, Open File 3295.

McClenaghan, M.B., Paulen R.C., Ayer, J.A., Trowell, N.F., and Bauke, S., 1998a. Regional till and humus geochemistry of the Timmins-Kamiskotia (NTS 42A/11, 12, 13, 140 area, northeastern Ontario; Geological Survey of Canada, Open File 3675.

McClenaghan, M.B. Kjarsgaard, I.M., Schulze, D.J., Berger, B., Stirling, J.A.R., and Pringle, G., 1998b. Mineralogy and geochemistry of the Diamond Lake kimberlite and associated esker sediments, Kirkland Lake, Ontario; Geological Survey of Canada, Open File 3576.

McClenaghan, M.B., Kjarsgaard, I.M., Stirling, J.A.R., Pringle, G., Kjarsgaard, B.A., and Berger, B.R., 1999a. Mineralogy and geochemistry of the C14 kimberlite and associated glacial sediments, Kirkland Lake, Ontario; Geological Survey of Canada, Open File 3719.

McClenaghan, M.B., Kjarsgaard, I.M., Kjarsgaard, B.A., Stirling, J.A.R., Pringle, G., and Berger, B.R., 1999b. Mineralogy and geochemistry of the A4 kimberlite and associated glacial sediments, Kirkland Lake, Ontario; Geological Survey of Canada, Open File 3769.

McClenaghan, M.B., Paulen, R.C., Smith, I.R., Rice, J.M., Plouffe, A., McMartin, I., Campbell, J.E., Lehtonen, M., Parsasadr, M., and Beckett-Brown, C.E., 2023. Review of till geochemistry and indicator mineral methods for mineral exploration in glaciated terrain; Geochemistry: Exploration, Environment, Analysis, v. 23, p. 1–43

McMartin, I,, McClenaghan, M.B., 2001. Till geochemistry and sampling techniques in glaciated shield terrain: a review; *in* Drift Exploration in Glaciated Terrain, (ed.) M.B. McClenaghan, P.T. Bobrowsky, G.E.M. Hall, and S.J. Cook; Geological Society of London, Special Publication 185, p. 19–43.

Monecke, T., Mercier-Langevin, P., Dubé, B., and Frieman, B.M., 2017. Geology of the Abitibi Greenstone Belt; Chapter 1 *in* Archean Base and Precious Metal Deposits, southern Abitibi Greenstone Belt, Canada, (ed.) T. Monecke, P. Mercier-Langevin, and B. Dubé; Society of Economic Geology, Reviews in Economic Geology, v. 19, p. 7–49.

Mercier-Langevin, P., Goutier, J., and Dubé, B., 2017. Introduction; Chapter 1 *in* Precious- and base-metal deposits of the southern Abitibi greenstone belt, Superior Province, Ontario and Quebec: 14th Biennial Society for Geology Applied to Mineral Deposits meeting field trip guidebook; Geological Survey of Canada, Open File 8317.

Paradis, S.J., 2010. Surficial geology, Chibougamau, Quebec; Geological Survey of Canada, Open File 6064.

Paradis, S.J., Veillette, J.J., and Pomares, J.-S., 2010. Surficial geology, Rivière Bell, Quebec; Geological Survey of Canada, Open File 6062.

Paulen, R.C., 2001. Quaternary geology of the Timmins Area, northeastern Ontario; M.Sc. thesis, University of Waterloo, Waterloo, Ontario Canada.

Paulen, R.C. and McClenaghan, M.B., 1997. Surficial mapping and Quaternary stratigraphic studies in the western Abitibi greenstone belt, Timmins, Ontario; *in* Current Research 1997-C; Geological Survey of Canada, p. 191–200.

Paulen, R.C. and McClenaghan, M.B., 1998a. Surficial geology of the Buskegau River (NTS 42A/14) area, northeastern Ontario; Geological Survey of Canada, Open File Map 3619, scale 1:50 000.

Paulen, R.C. and McClenaghan, M.B., 1998b. Surficial geology of the Manning Lake (NTS 42A/13) area, northeastern Ontario; Geological Survey of Canada, Open File Map 3618, scale 1:50 000.

Paulen, R.C., McClenaghan, M.B., and Harris, J.R., 2006. Bedrock topography and drift thickness models from the Timmins Area, northeastern Ontario: An application of GIS to the Timmins overburden drillhole database; *in* GIS for the Earth Sciences, (ed.) H.R. Harris; Geological Association of Canada, Special Publication 44, p. 414–434.

Paulen, R.C., Eyles, N., and Ross, M., 2024. Glacial dispersal trains and ice streams on the Canadian Shield; *in* Till Geochemistry and Indicator Mineral Methods for Exploration in Glaciated Terrains, (ed.) R.C. Paulen and M.B. McClenaghan; Geological Survey of Canada, Open File 9210, p. 139–146. https://doi.org/10.4095/pbmy2d03m0

Rice, J. and McClenaghan, M.B., 2024. Dirt detectives: Unravelling buried mineral potential with advanced till sampling techniques; *in* Till Geochemistry and Indicator Mineral Methods for Exploration in Glaciated Terrains, (ed.) R.C. Paulen and M.B. McClenaghan; Geological Survey of Canada, Open File 9210, p. 24–34. https://doi.org/10.4095/pbmy2d03m0

Richard, J.A., 2000. Quaternary geology of the Kamiskotia Lake area; Ontario Geological Survey, Map M2556.

Richard, J.A., 2001. Quaternary geology of the Pamour area; Ontario Geological Survey, Map M2655.

Richard, J.A. and McClenaghan, M.B., 2000a. Quaternary Geology, Porquis Junction area; Ontario Geological Survey, Map M2659.

Richard, J.A. and McClenaghan, M.B., 2000b. Quaternary Geology, Watabeag River area; Ontario Geological Survey, Map M2658.

Rongier, G., Allard, G., and Rabeau, R., 2014. Évaluation du recouvrement quaternaire et topographie du roc de la Ceinture de roches vertes de l'Abitibi : implications pour l'exploration minérale; Énergie et Ressources naturelles du Québec, MB 2014-35.

Sauerbrei, J.A., Pattison, E.F., and Averill, S.A., 1987. Till sampling in the Casa-Berardi gold area, Quebec: a case history in orientation and discovery (Canada); Journal of Geochemical Exploration, v. 28, p. 297–314.

Shelp, G.S. and Nichol, I., 1987: Distribution and dispersal of gold in glacial till associated with gold mineralization in the Canadian Shield; *in* Geochemical Exploration 1985, Part 1, (ed.) R.G. Garrett; Journal of Geochemical Exploration, v. 28, p. 315–336.

Shilts, W.W., 1976. Glacial till and mineral exploration; *in* Glacial Till, (ed.) R.F. Legget; Royal Society of Canada, Special Publication N. 12, p. 205–224.

Skinner, R.G., 1972. Drift prospecting in the Abitibi Clay Belt; Geological Survey of Canada, Open File 116.

Smith, S.L., 1990. Geochemical and lithological data from overburden drill cores, and descriptive core logs, Timmins to Smoky Falls, Ontario; Geological Survey of Canada, Open File 2278, 214 p.

Smith, S.L.,1992. Quaternary stratigraphic drilling transect, Timmins to the Moose River Basin, Ontario; Geological Survey of Canada, Bulletin 415, 94 p.

Steele, K.G., McClenaghan, M.B., Baker, C.L., and Jensen, L.S., 1986a. Geophysical/geochemical series, sonic drillholes 85-43 and 85-44, Lamplugh Township, Cochrane District; Ontario Geological Survey, Map M80881.

Steele, K.G., McClenaghan, M.B., Baker, C.L., and Jensen, L.S., 1986b. Geophysical/geochemical series, sonic drillhole 85-42, Lamplugh Township, Cochrane District; Ontario Geological Survey, Map M80880.

Telford, W. M. and Becker, A., 1979. Exploration case histories of the Iso and New Insco orebodies; *in* Geophysics and geochemistry in the search for metallic ores, (ed.) P.J. Hood; Geological Survey of Canada, Economic Geology Report 31, p. 605–629.

Thompson, I.S., 1979. Till prospecting for sulphide ores in the Abitibi Clay Belt of Ontario; Canadian Institute of Mining and Metallurgy, v. 72, p. 65–72.

Thomson, I., Burns, J.G., and Faulkner, F.H., 1987. Gold exploration in deep glaciated overburden: experiences from the Belore case history; Journal of Geochemical Exploration, v. 29, p. 435–436.

Thurston, P.C., Ayer, J.A., Gouthier, J., and Hamilton, M.A., 2008. Depositional gaps in Abitibi Greenstone Belt stratigraphy: A key to exploration for syngenetic mineralization; Economic Geology, v. 103, p. 1097–1134.

Tucker, C.M. and Richard, J.A., 2001. Quaternary geology of the Dan Lake area; Ontario Geological Survey, Map M2660.

Tucker, C.M. and Sharpe, D., 2001. Quaternary geology of the Timmins area; Ontario Geological Survey, Map M2662.

Vagners, U.J., 2000. Quaternary Geology, Matheson area; Ontario Geological Survey, Map M2652.

Vagners, U.J. and Courtney, S.J., 2000. Quaternary geology, Lightning River area; Ontario Geological Survey, Map M2651.

Veillette, J.J., 1986. Former southwesterly ice flows in the Abitibi-Témiscamingue; implications for the configuration of the Late Wisconsinan Ice Sheet; Canadian Journal of Earth Science, v. 23, p. 1724–1741.

Veillette, J.J., 1989. Ice movements, till sheets and glacial transport in the Abitibi-Timiskaming, Québec and Ontario; *in* Drift Prospecting (ed.) R.N.W. DiLabio and W. Coker; Geological Survey of Canada, Paper 89-20, p. 139–154.

Veillette, J.J. and McClenaghan, M.B., 1996. Sequence of ice flow in the Abitibi-Timiskaming region: implications for mineral exploration and dispersal of carbonate rocks from the Hudson Bay Basin, Quebec and Ontario; Geological Survey of Canada, Open File 3033.

Veillette, J.J. and Thibadeau, P., 2010. Surficial geology, Villebois, Quebec; Geological Survey of Canada, Open File 6063.

Veillette, J.J., Dyke, A.S., and Roy, M., 1999. Ice-flow evolution of the Labrador Sector of the Laurentide Ice Sheet: a review, with new evidence from northern Quebec; Quaternary Science Reviews, v. 18, p. 993–1019.

Veillette, J.J., Paradis, S., and Buckle, J., 2005. Bedrock and surficial geology of the general area around Rouyn-Noranda, Quebec and Ontario; *in* Metals in the Environment around Smelters at Noranda, Quebec and Belledune, New Brunswick: Results and Conclusions of the GSC MITE Point Sources Project, (ed.) G.F. Bonham-Carter; Geological Survey of Canada, Bulletin 584, 16 p.

Veillette, J.J., Paradis, S. J., and Thibaudeau, P., 2010. Surficial geology, Rouyn-Noranda-Senneterre, Quebec; Geological Survey of Canada, Open File 6061.

Veillette, J.J., Roy, M., Paulen, R.C., Mènard, M., and St-Jacques, G., 2017. Uncovering the hidden part of a large ice stream of

the Laurentide Ice Sheet, northern Ontario, Canada; Quaternary Science Reviews, v. 155, p. 136–158.

Vincent, J.-S. and Hardy, L., 1979. The evolution of glacial lakes Barlow and Ojibway, Quebec and Ontario; Geological Survey of Canada, Bulletin 316.

Wolfe, W.J., 1975. CANAGAU Zn-Pb-Cu-Ag deposit (Ben Nevis area) Ontario; Journal of Geochemical Exploration, v. 4, p. 151–155.

LiDAR in glacial geology and drift exploration: The prospectors' ice-stream landsystem

Syed Bukhari[1], Nick Eyles[1], and Roger C. Paulen[2]

[1]University of Toronto at Scarborough, 1265 Military Trail, Scarborough ON M1C 1A4
[2]Geological Survey of Canada, 601 Booth Street, Ottawa, Ontario K1A 0E8

INTRODUCTION

Rapidly evolving digital mapping technologies have resulted in a renewed understanding of ancient and modern ice-sheet beds and their glaciological structure, in particular the presence of fast-flowing ice streams where ice-flow velocities may have been as high as 10 km/yr within the Laurentide and Cordilleran ice sheets (Margold et al., 2015; Eyles et al., 2018). High-resolution-LiDAR (Light Detection and Ranging) data-derived digital terrain models (DTMs), with resolutions of ≤0.5 metres, now allow for rapid semi-automated assessment of terrain types and landforms (e.g. Sookhan et al., 2021, 2022; Eyles et al., 2023; Fig. 1).

Mapping of fast-flowing low-profile 'ice streams' is based on the distinct geomorphology of their beds characterized by highly elongated closely-spaced ridges and grooves called megascale glacial lineations (MSGLs; Stokes, 2011; Evans et al., 2014; Spagnolo et al., 2014; Otteson et al., 2016; Stokes et al., 2016) that are cut into pre-existing glacial landsystems from earlier streaming and non-streaming phases of ice flow (Eyles et al., 2016, 2018, 2023). The presence of ice streams and the need to establish a map of their full extent and number within paleo-ice sheets has far-reaching applications for mineral exploration programs because of the contrasting nature of debris transport

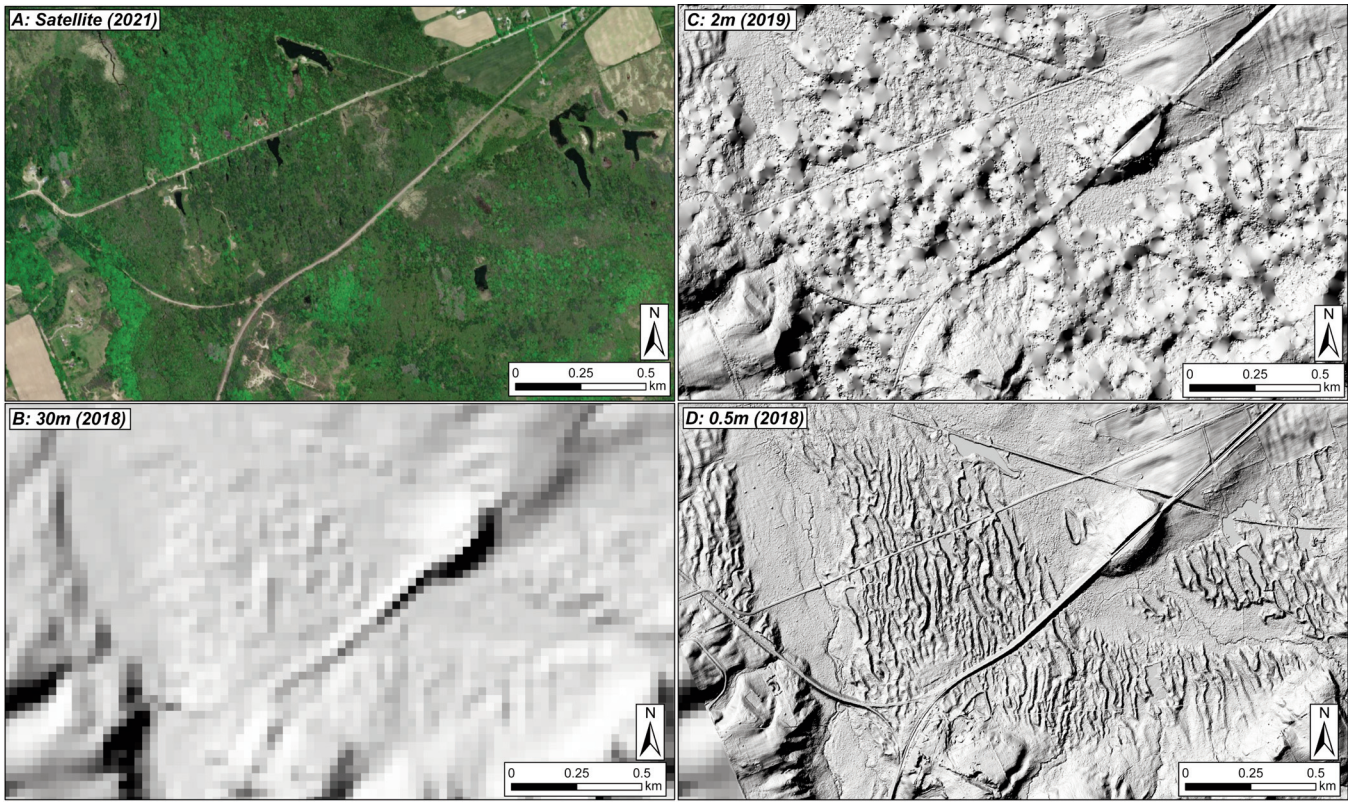


Figure 1. The resolving power of LiDAR compared with other topographic data sets, using the same study area in all cases. **A)** A Maxar high-resolution satellite imagery (released 2021). **B)** An Ontario Provincial 30 m resolution digital elevation model (DEM; released 2018). **C)** A 2 m resolution imagery derived DEM (released 2019), **D)** A high-resolution (0.5 metre) LiDAR-derived image revealing De Geer moraine ridges that mark the annual stillstands of the retreating Laurentide Ice Sheet margin in shallow water (*from* Bukhari et al., 2024).

Recommended citation:

Bukhari, S., Eyles, N., and Paulen, R.C., 2024. LiDAR in glacial geology and drift exploration: The prospectors' ice-stream landsystem; *in* Till Geochemistry and Indicator Mineral Methods for Exploration in Glaciated Terrains (ed.) R.C. Paulen and M.B. McClenaghan; Geological Survey of Canada, Open File 9210, p. 133–139. https://doi.org/10.4095/pbmy2d03m0

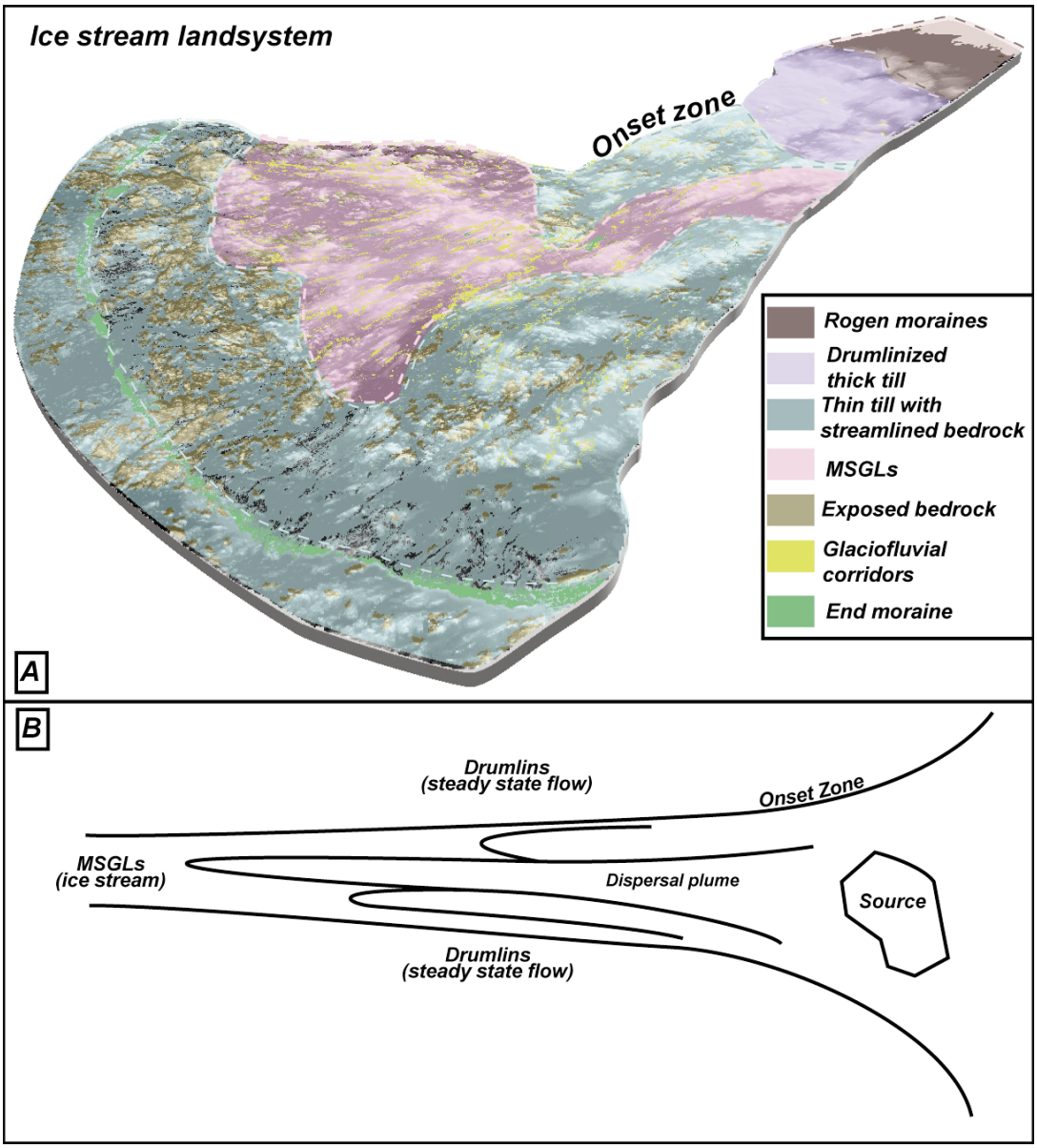


Figure 2. A) Prospectors' ice-stream landsystem. Up-ice transverse moraines such as Rogen moraines, in areas of slow ice flow, transition down-glacier into drumlinized thick till and large areas of thin till with streamlined bedrock. The main trunk of the ice stream consists of individual sub-ice flow units identified by flow sets of MSGLs interspersed with narrow corridors of ice-contact glaciofluvial sediment containing eskers along the margins of flow units. See subsequent figures 3 to 7 for examples of each landsystem element. **B)** A generalized dispersal train, with multiple fingers, reflects the composite structure of ice streams.

and mineral dispersion under fast-flowing ice compared to non-streaming flow (Dredge, 2000; Primmer et al., 2015; McClenaghan et al., 2015; Paulen et al., 2017, 2024). Previous inventories of ice streams have identified more than 100 ice streams within the Laurentide Ice Sheet (Margold et al., 2015) but recent work shows this is a considerable underestimate (Bukhari et al., 2024). Currently, this represents a major uncertainty in mineral exploration across the Canadian Shield. How many ice streams were there at different phases during the lifetime of the ice sheet, what was their duration, and what was their extent?

LIDAR: A PARADIGM SHIFT

New work using LiDAR to map the beds of former ice streams reveals a distinct internal structure consisting of multiple sub-ice flow units based on the identification of multiple en echelon flow sets of MSGLs (Sookhan et al., 2021, 2022; Bukhari et al., 2024; Fig. 2). LiDAR data also provides crucial information regarding the presence and origins of hybrid palimpsest beds resulting from phases of fast flow that were superimposed on the Last Glacial Maximum or older surfaces that hitherto have been poorly documented. Till

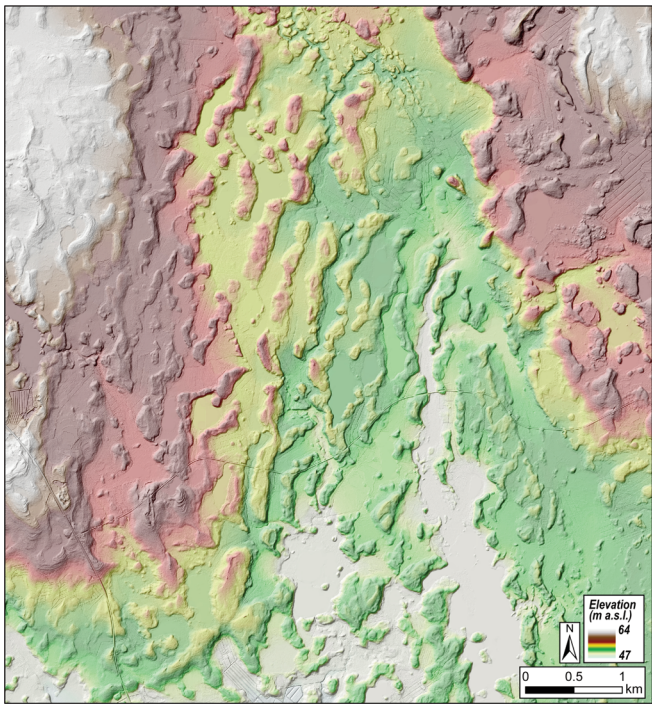


Figure 3. Rogen moraines transverse to ice flow in an area of cold-based slowly flowing ice. The ice-flow direction is west to east. Data are sourced *from* Putkinen et al.(2017).

sampling surveys conducted without this contextual information about the nature of former ice-flow dynamics and, in particular, the presence or absence of fast-flowing ice are of limited value.

This paper integrates previous high-resolution (≤0.5m) LiDAR digital topographic data from various parts of Canada to develop a composite 'Prospectors ice stream' landsystem model (Fig. 2) to contextualize and guide mineral exploration programs. This process is akin to facies modelling that relates surface forms to underlying genetically related sediment types, which has been particularly useful in understanding complex depositional systems left behind by former ice sheets in a range of settings (e.g. Eyles and Eyles, 2010).

A number of distinct landform elements can be identified within the ice stream landsystem model. Moraine ridges oriented transverse to ice flow (e.g. ribbed and Rogen moraines) demarcate areas of slow-flowing cold-based or polythermal ice upstream of the zone of ice streaming (Fig. 3). Down-glacier, drumlinized surfaces typically flank the main ice-stream bed, which in turn is characterized by highly elongated low-relief MSGLs (Eyles et al., 2023; Fig. 4) that are underlain by tills and older pre-existing sediments drumlinized earlier under moderate ice-flow velocities (< ca. 150 m/yr.). There may be large areas of associated streamlined bedrock or crag-and-tail features in areas of thin or discontinuous till cover (Fig. 5). The boundaries of sub-ice flow units within the trunk of the ice stream are marked by narrow (< 1 km) irregular corridors of ice-

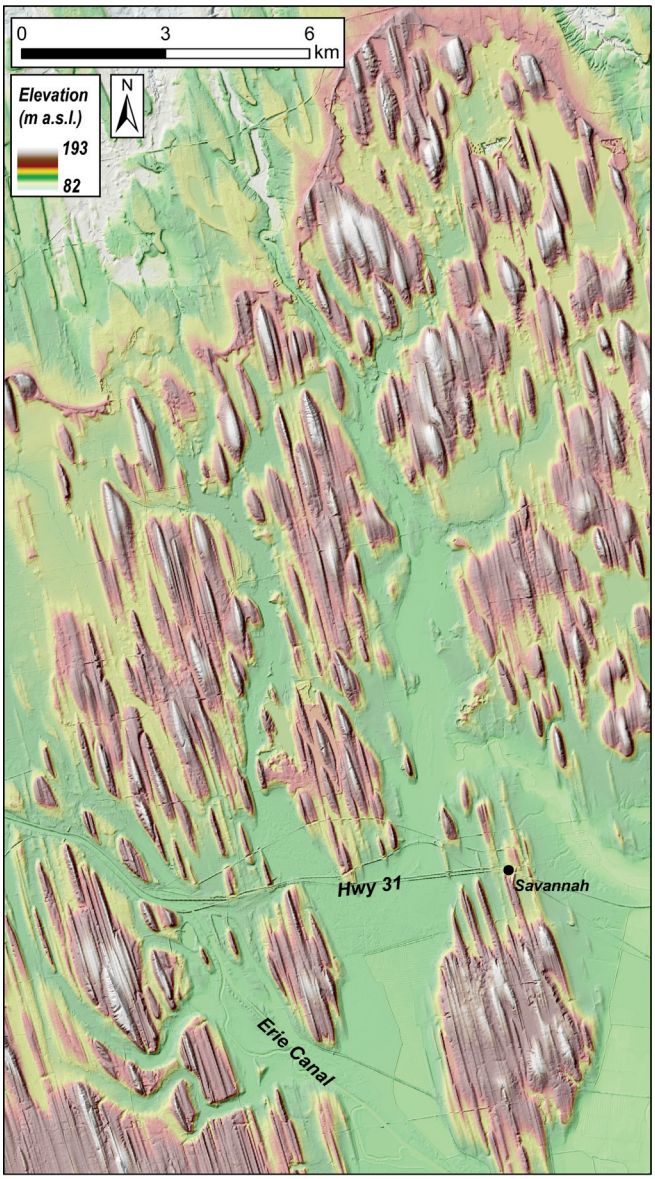


Figure 4. Mega-scale glacial lineations are cut under ice streams. The ice-flow direction is north to south. Data sourced *from* the United States Geological Survey 3DEP LiDAR library.

contact glaciofluvial sediments with hummocky uncontrolled surfaces characteristic of complex sub-ice marginal processes, and associated eskers and fan deltas (Fig. 6). The location of these fluvially dominated corridors is commonly structurally controlled and follows the boundaries or sutures of ice-flow subunits and, as such, are quasi-regularly spaced. This is thought to arise because subglacial tunnels carrying meltwater and sediment occur preferentially along the slower moving boundaries of ice-flow units as such tunnels cannot be kept open under fast-flowing ice under the trunk of streaming glaciers (e.g. Dowdeswell et al., 2015). In some cases, these corridors show elevated concentrations of indicator minerals relative to adjacent belts of MSGLs whereby indicator minerals

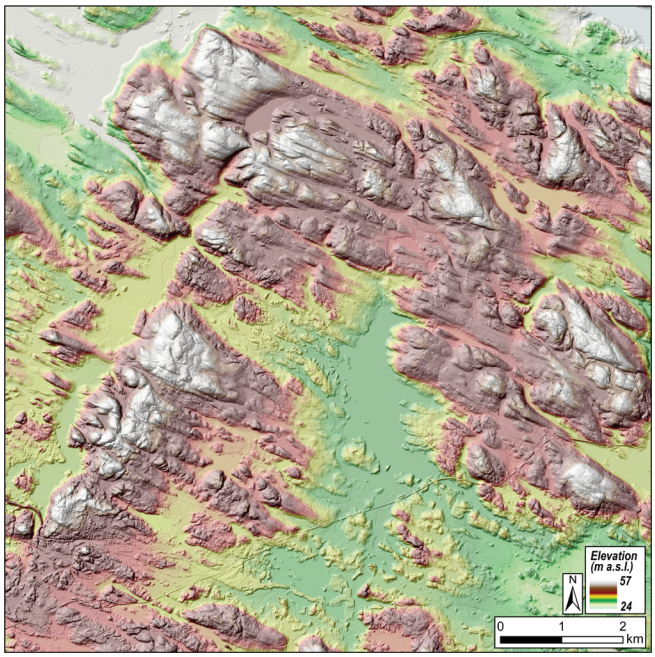


Figure 5. Glacially scoured and partly streamlined bedrock with a thin discontinuous till veneer; ice-flow direction is from west to east. Data are sourced *from* Putkinen et al. (2017).

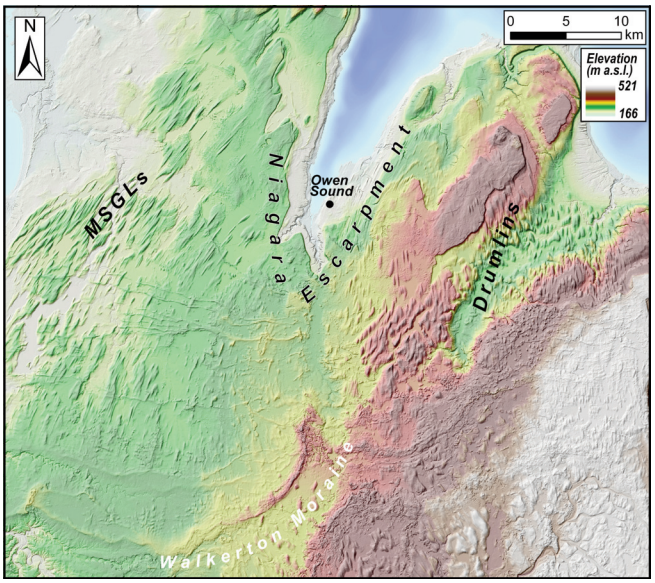


Figure 7. An ice-stream bed on thick sediment shows the distribution of mega-scale glacial lineations (MSGLs) in the central axis of the ice stream with drumlins to the east along its slower flowing margins. Note the large, looped end moraine and the smaller recessional moraines. Data are sourced *from* the Ontario GeoHub digital library (DEDSFM Huron-Georgian Bay).

extend much further down ice because of more rapid and extended debris transport (DesRosiers, P., 2021; Sookhan et al., 2021). MSGLs characterize the bed along the central trunk of the ice stream and become less elongated and transitional to drumlins near the slower flowing margins (Fig. 7).

The various elements of the ice-stream landsystem model are illustrated in this presentation using the newly available 2 m resolution ArcticDEM data set (Fig. 6). An informative example of extended down-glacier indicator clast dispersal by fast-flowing ice is shown in Figure 8, which depicts the extent and structure of a complexly structured ice stream that was mapped using high-resolution LiDAR. In this case, conspicuous red and green quartzite clasts (6.3–12.6 mm in diameter), sourced from a 60 kilometre-long lin-

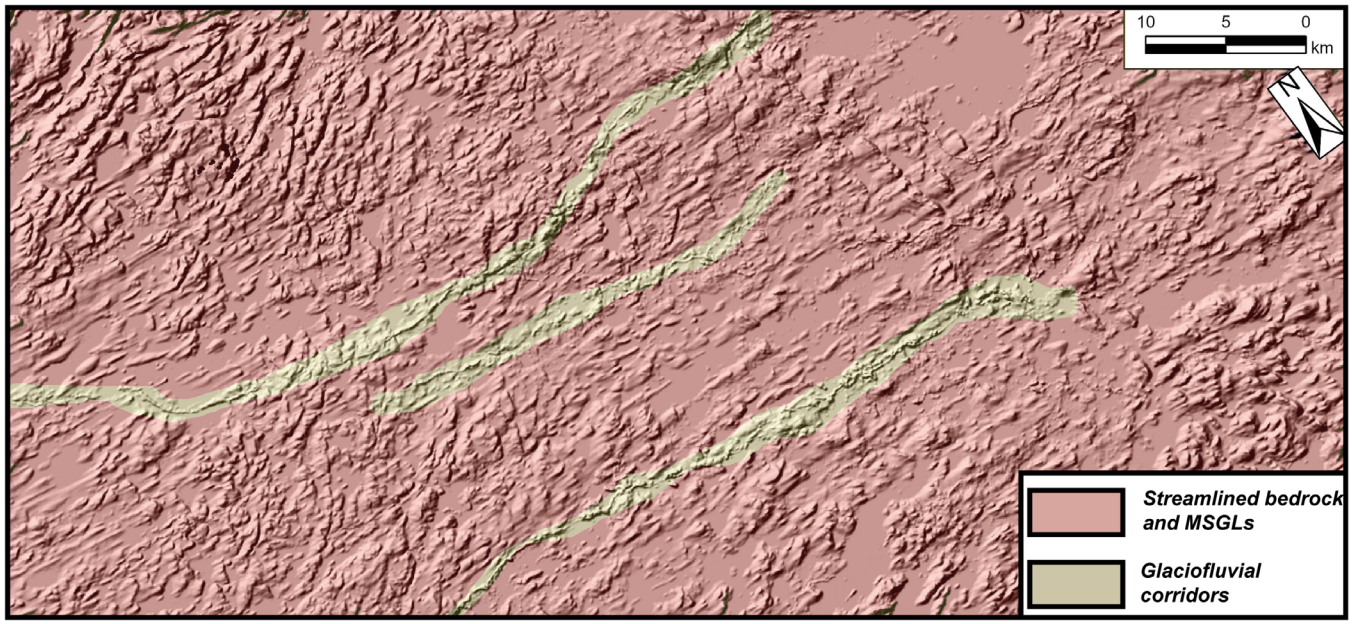


Figure 6. Ice-contact glaciofluvial corridors define the margins of former sub-ice flow units of mega-scale glacial lineations (MSGLs) and streamlined bedrock; the ice-flow direction is from east to west. Data are sourced *from* ArcticDEM (Porter et al., 2018).

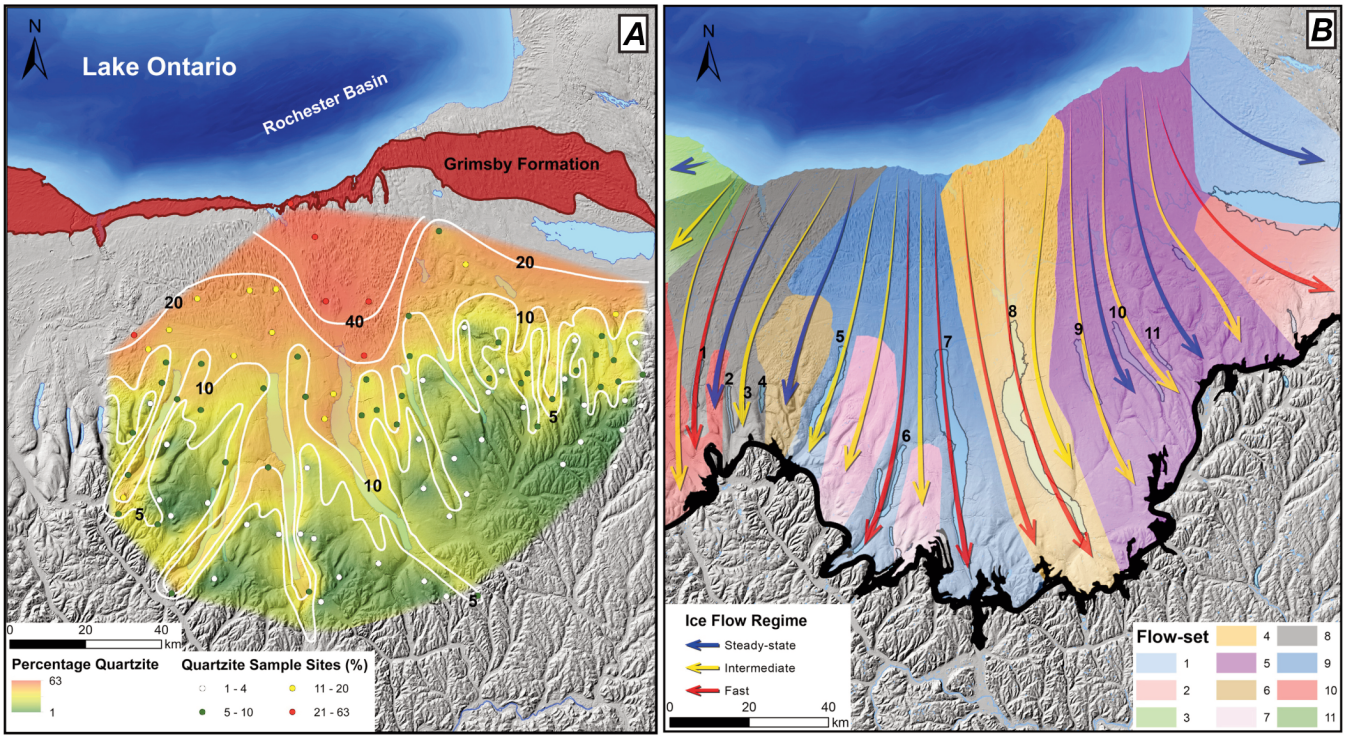


Figure 8. A, B) Maps showing the distribution and percentage of red and green Paleozoic quartzite clasts (6.3–12.6 mm in diameter) in ice-stream tills derived from a west-east oriented outcrop area immediately south of Lake Ontario. Note the enhanced subglacial transport of quartzite by ice-stream flow units (modified *from* Sookhan et al., 2021).

ear outcrop oriented transverse to the ice flow can be traced in near-surface tills down ice. LiDAR mapping and statistically validated quantitative analysis of bedform elongation across its bed (e.g. Sookhan et al., 2021) confirms the presence of discrete flow sets of MSGLs (sub-ice flow units) as depicted in the ice-stream model (Fig. 2B). Enhanced subglacial transport of debris at the base of each component unit is expressed as narrow radiating, finger-like plumes of till containing red-green quartzite (Sookhan et al., 2021; Fig. 8).

Glacial geological mapping using LiDAR backscatter and reflectivity parameters has been used successfully for mapping boulder trains and identifying ice-flow directions as well as subglacial erosional and depositional processes from subtle streamlined landforms on modern and ancient glacier beds. It is now clear that access to LiDAR-derived topographic data (or other high-resolution elevation datasets) and a detailed glacial geological analysis is a fundamental requirement of mineral exploration programs. A key step in such an analysis is to identify areas of non-streaming ice flow in inter ice-stream areas, which is necessary for contextualizing regional broad-scale geochemical data and sampling programs with the associated variation in the spatial geometry of dispersal trains. An additional consideration is to identify areas of palimpsest beds of cross-cutting lineations (Fig. 9), where the direction of ice streaming was counter to former ice-flow directions, resulting in a superposition of dispersal trains. 'Flow switching' was a common process during deglaciation and thinning of the Laurentide Ice Sheet as it became increasingly susceptible to underlying topography and the influence of large ice-frontal waterbodies, and has major implications for stratigraphic work and subsurface till sampling programs. Rapid semi-automated digital mapping of regional LiDAR data sets to identify glacial landsystem types on contrasting beds (rock, sediment) and under contrasting thermal regimes (cold-based, wet-based, polythermal) is in progress.

IMPLICATIONS FOR MINERAL EXPLORATION

LiDAR technology can contribute critical contextual information regarding the geological evolution of areas targeted for mineral exploration studies. It provides geologists with the ability to penetrate vegetation and visualize bare earth topography using a non-invasive and cost-effective method. A key component in mineral exploration, as highlighted previously, is the identification of the number and extent of ice streams within a glaciated terrain. Ice streams play the most significant role in erosion and transport of glacial sediments and the modern landscape in Canada is a product of hundreds of, as yet unmapped, ice streams. Furthermore, the prospectors' ice-stream model presented herein, requires that extra attention be given to developing till

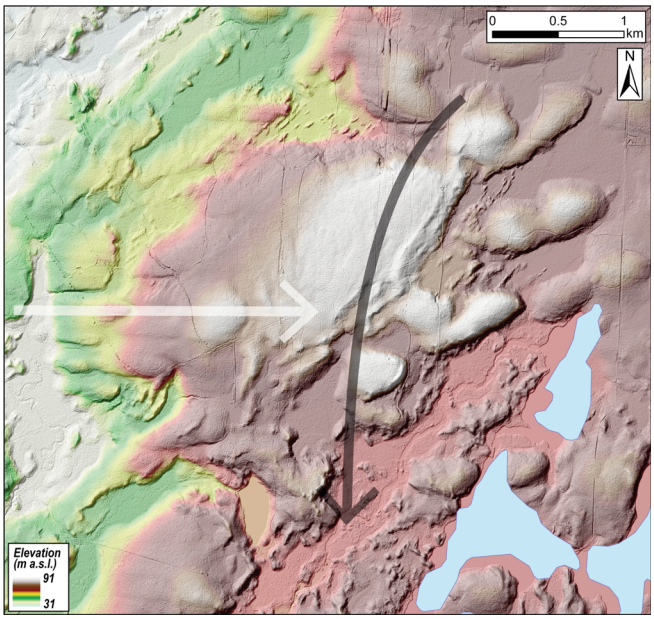


Figure 9. Palimpsest terrain illustrating cross-cutting relationships between an older drumlinized surface overprinted by a younger streamlined surface (older ice-flow phase is shown by a grey arrow, younger ice-flow phase is in white). Data sourced *from* the Nova Scotia GeoNova LiDAR database.

sampling programs as the glacial processes within individual ice-stream beds are temporally and spatially variable, and as such, are reflected in heterogenous types of sediments and landforms. This approach is already being applied to determine the mineral potential of lithium-bearing pegmatites in Finland (Chudasama and Sarala, 2022), a glaciated bed very similar to that of the Canadian Shield. Mineral exploration in Canada must advance with modern technology and exploit the benefits of LiDAR.

REFERENCES

Bukhari, S., Eyles, N., Mulligan, R., Burt, A., Eyles, C., Paulen, R., Ross, M., and Putkinen, N., 2024. Laurentide Ice Sheet configuration in southern Ontario, Canada during the last glaciation (MIS 4 to 2) from stratigraphic drilling and LiDAR-based surficial mapping; Canadian Journal of Earth Science, 2023-0091. https://doi.org/10.1139/cjes-2023-0091

Chudasama, B. and Sarala, P., 2022. Mineral prospectivity mapping of lithium-spodumene pegmatites in the Kaustinen region of Finland: Implications for lithium exploration in Finland; Geological Survey of Finland, Open File Work Report 28/2022. 21 p. https://tupa.gtk.fi/raportti/arkisto/28_2022.pdf

DesRosiers, P., 2021. The effect of deglacial meltwater processes on kimberlite indicator mineral concentrations in glacial sediments. M.Sc. thesis, Simon Fraser University, 132 p.

Dowdeswell, J.A., Hogan, K.A., Arnold, N.S., Mugford, R.I., Wells, M., Hirst, J.P.P., and Decalf, C., 2015. Sediment-rich meltwater plumes and ice-proximal fans at the margins of modern and ancient tidewater glaciers: Observations and modelling; Sedimentology, v. 62, p. 1665–1692. https://doi.org/10.1111/sed.12198

Dredge, L.A., 2000. Carbonate dispersal trains, secondary till plumes, and ice streams in the west Foxe Sector, Laurentide Ice Sheet; Boreas, v. 29, p. 144–156. https://doi.org/10.1111/j.1502-3885.2000.tb01207.x

Evans, D.J.A., Young, N.J.P., and Ó Cofaigh, C., 2014. Glacial geomorphology of terrestrial-terminating fast flow lobes/ice stream margins in the southwest Laurentide Ice Sheet; Geomorphology, v. 204, p. 86–113. https://doi.org/10.1016/j.geomorph.2013.07.031

Eyles, C.H. and Eyles, N., 2010. Glacial Facies 4; *in* Facies Models 4, (ed.) N.P. James and G. Dalrymple; Geological Association of Canada, GEOtext 6, p. 73–104.

Eyles, N., Putkinen, N., Sookhan, S., and Arbelaez-Moreno, L., 2016. Erosional origin of drumlins and megaridges; Sedimentary Geology, v. 338, p. 2–23. https://doi.org/10.1016/j.sedgeo.2016.01.006

Eyles, N., Arbelaez Moreno, L., and Sookhan, S., 2018. Ice streams of the Late Wisconsin Cordilleran Ice Sheet in western North America; Quaternary Science Reviews, v. 179, p. 87–122. https://doi.org/10.1016/j.quascirev.2017.10.027

Eyles, N., Bukhari, S., Sookhan, S., Ruscica, P., and Paulen, R., 2023. LiDAR-based semi-automated mapping of drumlins and mega-scale glacial lineations of the Green Bay Lobe, Wisconsin, USA: Ice sheet beds as glaciotribological systems; Earth Surface Processes and Landforms, v. 48, p. 295–321. https://doi.org/10.1002/esp.5486

Margold, M., Stokes, C.R., and Clark, C.D., 2015. Ice streams in the Laurentide Ice Sheet: Identification, characteristics and comparison to modern ice sheets; Earth-Science Reviews, v. 143, p. 117–146. https://doi.org/10.1016/j.earscirev.2015.01.011

McClenaghan, M.B., Paulen, R.C., Layton-Matthews, D., Hicken, A.K., and Averill, S.A., 2015. Glacial dispersal of gahnite from the Izok Lake Zn-Cu-Pb-Ag VMS deposit, northern Canada; Geochemistry: Exploration, Environment, Analysis, v. 15, p. 333–349. https://doi.org/10.1144/geochem2014-317

Ottesen, D., Stokes, C.R., Bøe, R., Rise, L., Longva, O., Thorsnes, T., Olesen, O., Bugge, T., Lepland, A., and Hestvik, O.B., 2016. Landform assemblages and sedimentary processes along the Norwegian Channel Ice Stream; Sedimentary Geology, v. 338, p. 115–137. https://doi.org/10.1016/j.sedgeo.2016.01.024

Paulen, R.C., Stokes, C.R., Fortin, R., Rice, J.M., Dubé-Loubert, H., and McClenaghan, M.B., 2017. Dispersal trains produced by ice streams: an example from Strange Lake, Labrador, Canada; *in* Proceedings of Exploration 17, (ed.) V. Tschirhart and M.D. Thomas; Sixth Decennial International Conference on Mineral Exploration, p. 871–875. https://geochem.nrcan.gc.ca/cdogs/content/pub/pub03698_e.htm

Porter, C., Morin, P., Howat, I., Noh, M. J., Bates, B., Peterman, K., Keesey, S., Schlenk, M., Gardiner, J., Tomko, K., Willis, M., Kelleher, C., Cloutier, M., Husby, E., Foga, S., Nakamura, H., Platson, M., Wethington, M., Williamson, C., and Bojesen, M., 2018. ArcticDEM, Harvard Dataverse, V1. https://doi.org/10.7910/DVN/OHHUKH

Paulen, R.C., Eyles, N., and Ross, M., 2024. Glacial dispersal trains and ice streams on the Canadian Shield; *in* Till Geochemistry and Indicator Mineral Methods for Exploration in Glaciated Terrains, (ed.) R.C. Paulen and M.B. McClenaghan; Geological Survey of Canada, Open File 9210, p. 139–146. https://doi.org/10.4095/pbmy2d03m0

Primmer, S., Bell, T., and Batterson, M., 2015. The role of ice dynamics on drift dispersal in the Newfoundland Ice Cap: Preliminary investigations; *in* Current Research (2015); Newfoundland and Labrador Department of Natural Resources, Geological Survey Report 15–1, p. 277–285.

Putkinen, N., Eyles, N., Putkinen, S., Ojala, A.E.K., Palmu, J.-P., Sarala, P., Väänänen, T., Räisänen, J., Saarelainen, J., Ahtonen, N., Rönty, H., Kiiskinen, A., Rauhaniemi, T., and Tervo, T., 2017. High-resolution LiDAR mapping of glacial landforms

and ice stream lobes in Finland; Bulletin of the Geological Society of Finland, v. 89, p. 64–81. https://doi.org/10.17741/bgsf/89.2.001

Sookhan, S., Eyles, N., Bukhari, S., and Paulen, R.C., 2021. LiDAR-based quantitative assessment of drumlin to mega-scale glacial lineation continuums and flow of the paleo Seneca-Cayuga paleo-ice stream; Quaternary Science Reviews, v. 263, 107003. https://doi.org/10.1016/j.quascirev.2021.107003

Sookhan, S., Eyles, N., and Bukhari, S., 2022. Drumlins and mega-scale glacial lineations as a continuum of subglacial shear marks: A LiDAR based morphometric study of streamlined surfaces on the bed of a Canadian paleo-ice stream; Quaternary Science Reviews, v. 292, 107679. https://doi.org/10.1016/j.quascirev.2022.107679

Spagnolo, M., Clark, C.D., Ely, J.C., Stokes, C.R., Anderson, J.B., Andreassen, K., Graham, A.G.C., and King, E.C., 2014. Size, shape and spatial arrangement of mega-scale glacial lineations from a large and diverse dataset; Earth Surface Processes and Landforms, v. 39, p. 1432–1448. https://doi.org/10.1002/esp.3532

Stokes, C.R., 2011. Palaeo-ice stream; in Encyclopedia of Snow, Ice and Glaciers, (ed.) V.P. Singh, P. Singh, and U.K. Haritashya; Springer Netherlands, Dordrecht, p. 803–808. https://doi.org/10.1007/978-90-481-2642-2_630

Stokes, C.R., Margold, M., Clark, C.D., and Tarasov, L., 2016. Ice stream activity scaled to ice sheet volume during Laurentide Ice Sheet deglaciation; Nature, v. 530, p. 322–326. https://doi.org/10.1038/nature16947

Glacial dispersal trains and ice streams on the Canadian Shield

Roger C. Paulen[1], Nick Eyles[2], and Martin Ross[3]

[1]Geological Survey of Canada, 601 Booth Street, Ottawa, Ontario K1A 0E8
[2]University of Toronto at Scarborough, 1265 Military Trail, Scarborough ON M1C 1A4
[3]University of Waterloo, 200 University Avenue West, Waterloo, Ontario, N2L 3G1

ABSTRACT

The identification of glacial dispersal landforms and sedimentary deposits formed by fast-flowing glaciers was important to the earliest recognition of paleo-ice streams of the Laurentide Ice Sheet in the 1970s and 1980s. The spectacular continental-scale Dubawnt dispersal train in northern Canada was one of the first to be identified as the product of a high glacial flow rate. Subsequently, dispersal plumes of Paleozoic carbonate rocks imprinted on Precambrian Canadian Shield terrain in northern Canada were interpreted to be products of ice streams.

The geomorphic imprint of ice streams over hard-bed, higher relief areas tends to be less obvious because of thinner till cover and an absence of diagnostic geomorphic features such as shear margin moraines. Despite the relatively thin till cover in some regions of the Canadian Shield, the extremely high concentrations of mineralized (exotic) debris within the till 10s of kilometres down-ice from their sources is quite remarkable. Typically, under normal ice-flow conditions in areas of hard-beds on the Canadian Shield, dispersal trains formed by erosive ice are diluted over relatively short distances (<5 km) down-ice. The long (10s of km) dispersal trains of till with distinct chemical and/or mineralogical compositions, coupled with obvious erosive/depositional corridors of streamlined landforms, provide a means of identifying hard-bedded ice streams elsewhere in northern Canada.

INTRODUCTION

Ice streams are corridors that occur within an ice sheet that flow more rapidly than the surrounding ice; ice streams erode and disperse large amounts of glacial debris, and produce well defined tracts of far-travelled and exotic glacial debris (e.g. Bennett, 2003; Dyke, 2008; Ross et al., 2009; Spagnolo et al., 2016; Sookhan et al., 2021). These fast-flowing corridors can be tens of metres to tens of kilometres wide and are identified by streamlined glacial morphology with highly attenuated landforms, or mega-scale glacial lineations (MSGLs) having length:width ratios exceeding 10:1 (Hart, 1999; Spagnolo et al., 2014) and sharply delineated margins (Stokes and Clark, 1999). In hard-bedded terrains, such as the Canadian Shield, thinner till deposits may mean that glacial geomorphic features may not be present and ice-stream identification criteria include strongly eroded and sculpted bedrock forms (Krabbendam et al., 2016) and the long-distance dispersal of exotic clasts and till (e.g. Paulen et al., 2017; Sookhan et al., 2021).

Numerous paleo-ice stream footprints have been identified in areas that were covered in Canada by the Laurentide, Cordilleran, and Innuitian ice sheets (e.g. Dyke and Morris, 1988; Dredge, 2000; Winsborrow et al., 2004; De Angelis and Kleman, 2007; Margold et al., 2015; Veillette et al., 2017; Eyles et al., 2018; McMartin et al., 2021). Glacial dispersal trains emanating from mineralized point sources within trunks of larger paleo-ice streams have been identified in northern Canada (Fig. 1). This paper highlights the differences between documented dispersal trains created by 'normal' (steady state) glacial flow and those created by faster flowing ice.

The Strange Lake glacial dispersal train in northern Quebec and Labrador is a remarkably linear ribbon defined by till geochemistry and airborne gamma-ray data that extends >60 km down-ice (northeast) from a mineralized rare earth element-rich peralkaline intrusion (Paulen et al., 2017; McClenaghan et al., 2019). This dispersal train formed within one of several ice streams that operated over a hard bed near the centre of the Labrador Dome of the Laurentide Ice Sheet (Margold et al., 2015). Further north, a kimberlite indicator mineral-rich dispersal train (referred to as the Tremblay Corridor) extends 65 km down-ice (northwest) from a cluster of kimberlite intrusions on northern Melville Peninsula, Nunavut (Armstrong, 2009; Paulen et al., 2019). This glacial dispersal train was also formed over a hard bed by an ice-stream flow within the Gulf of Boothia Ice Stream, which originated from the Foxe Dome of the Laurentide Ice Sheet (Tremblay and Paulen, 2012).

Recommended citation:

Paulen, R.C., Eyles, N., and Ross, M., 2024. Glacial dispersal trains and ice streams on the Canadian Shield; *in* Till Geochemistry and Indicator Mineral Methods for Exploration in Glaciated Terrains, (ed.) R.C. Paulen and M.B. McClenaghan; Geological Survey of Canada, Open File 9210, p. 140–147. https://doi.org/10.4095/pbmy2d03m0

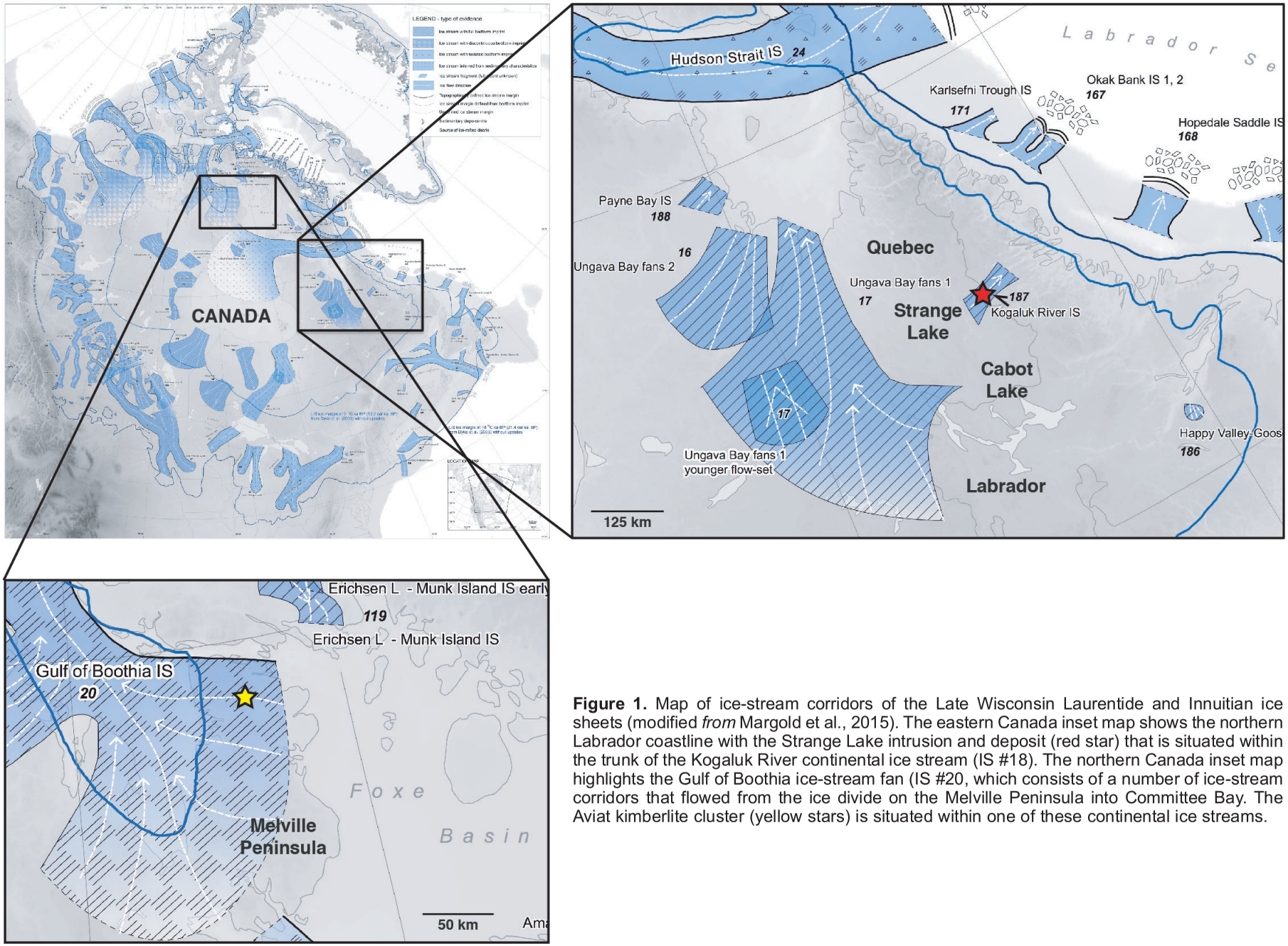


Figure 1. Map of ice-stream corridors of the Late Wisconsin Laurentide and Innuitian ice sheets (modified *from* Margold et al., 2015). The eastern Canada inset map shows the northern Labrador coastline with the Strange Lake intrusion and deposit (red star) that is situated within the trunk of the Kogaluk River continental ice stream (IS #18). The northern Canada inset map highlights the Gulf of Boothia ice-stream fan (IS #20, which consists of a number of ice-stream corridors that flowed from the ice divide on the Melville Peninsula into Committee Bay. The Aviat kimberlite cluster (yellow stars) is situated within one of these continental ice streams.

STRANGE LAKE DISPERSAL TRAIN

In the mid-1980s, the Geological Survey of Canada and the Geological Survey of Newfoundland and Labrador carried out high-density surficial geochemical studies (1 sample site per 1.97 km^2) around the Strange Lake intrusion and associated Strange Lake Zr-Y heavy rare earth element (REE) deposit in eastern Canada. The purpose of the surveys was to determine the ice-flow history and patterns of glacial dispersal, and to determine the surficial geochemical signatures of the rare earth element-rich intrusion (Batterson, 1989). A glacial dispersal train trending northeast from the Strange Lake intrusion and its mineralized zones for a minimum of 50 km was defined using airborne gamma-ray spectrometry, radioactive boulders, lake sediment geochemistry, and till geochemistry (Geological Survey of Canada, 1980; McConnell and Batterson, 1987; Batterson and Taylor, 2009).

The till survey outlined an exceptional linear dispersal train, with a width comparable to the bedrock source along its entire length (Fig. 2). Single-element geochemical patterns for ore-related elements (Y, Zr, Nb, Be, La) define a ribbon-shaped dispersal train for at least 40 km down-ice from the peralkaline complex. The formation of this train was originally attributed to sustained, unidirectional steady-state glacial flow (Batterson, 1989). Geochemical reanalysis of regional lake sediment showed that this dispersal train likely extended right out to the Labrador coast (Amor et al., 2018).

Surficial mapping conducted along the Ancestral Labrador Ice Divide (*see* Rice et al., 2023, and references therein for an overview) and heavy mineral glacial dispersal studies at Strange Lake (McClenaghan et al., 2019), which included examination of the Shuttle Radar Topographic Mission (SRTM) Digital Elevation Model (DEM) imagery of the Strange Lake deposit, highlighted that the surficial geomorphology was dominated by MSGLs formed from fast-flowing ice. The Strange Lake intrusion and deposit, and resultant dispersal train, were situated within the trunk of the Kogaluk River ice stream (Margold et al., 2015) that strongly eroded the deposit and carried out mineral-rich debris to the Labrador coast.

AVIAT DISPERSAL TRAIN

The Aviat kimberlite cluster is located in the northern part of the Melville Peninsula in northern Canada. Reconnaissance heavy mineral sampling surveys of till, eskers, and beaches over the northern portion of the Melville Peninsula commenced in 2001 by an exploration company as part of their diamond exploration program. Recovery of diamond indicator minerals was reported in these early samples (Armstrong, 2009). Follow-up sampling resulted in the recovery of diamond indicators with adhering kimberlite. Since the initial discovery, more than 80 000 line kilometres of airborne geophysics have been flown and approximately 11 000 surficial samples have been collected across the property (Armstrong et al., 2008).

The combined sampling surveys revealed a kimberlite indicator mineral-rich zone in till approximately 65 km long and 10 km wide, trending 286°, which is parallel to the observed dominant glacial-flow direction (Fig. 3). This regional-scale indicator mineral train is referred to as the Tremblay Corridor and all presently known kimberlites occur within a 10 km long by 3 km portion at the eastern terminus of the Tremblay corridor (Armstrong, 2009).

The linear nature of the dispersal train and overall indicator mineral abundances aided diamond exploration. Armstrong (2009) originally reported that the linear dispersal trains were attributed to sustained, unidirectional steady-state glacial flow, similar to the initial interpretation of the Strange Lake dispersal train. However, mapping of glacial landforms in the northern Melville Peninsula (De Angelis and Kleeman, 2005; Tremblay and Paulen, 2012) shows that the kimberlite dispersal train occurs within a region of several ice-stream flow units. These ice streams were driven by westward flow from the former spreading ice centre (the Foxe sector of the Laurentide Ice Sheet) over the Foxe basin, which overrode the northern Melville Peninsula and streamed ice into the Gulf of Boothia-Lancaster Sound trough (Fig. 4).

IMPLICATIONS FOR MINERAL EXPLORATION

Dispersal trains from point sources in non-ice-stream areas of northern Canada tend to be much shorter (<10 km; cf. McClenaghan and Paulen, 2018). Dispersal trains created by ice streams, however, are tens of kilometres long, and their geometry, due to higher subglacial erosion and formation by faster flowing ice, tend to be linear, narrow ribbons (Paulen et al., 2017; McClenaghan and Paulen, 2018; Sookhan et al., 2021).

The geometry of dispersal trains and the nature of till deposited by paleo-ice streams can have significant impacts on the application of till geochemistry and indicator mineral methods to mineral exploration because their glacial transport distances can be significant (>50 km). The distally derived till within a paleo-ice-stream footprint will reflect bedrock source(s) much farther up ice than till adjacent to ice streams, creating a mosaic of tills of different provenances at surface (e.g. Ross et al., 2009). When ice streams erode a point source, such as a mineral deposit, it forms a large linear exploration target. When ice streams erode

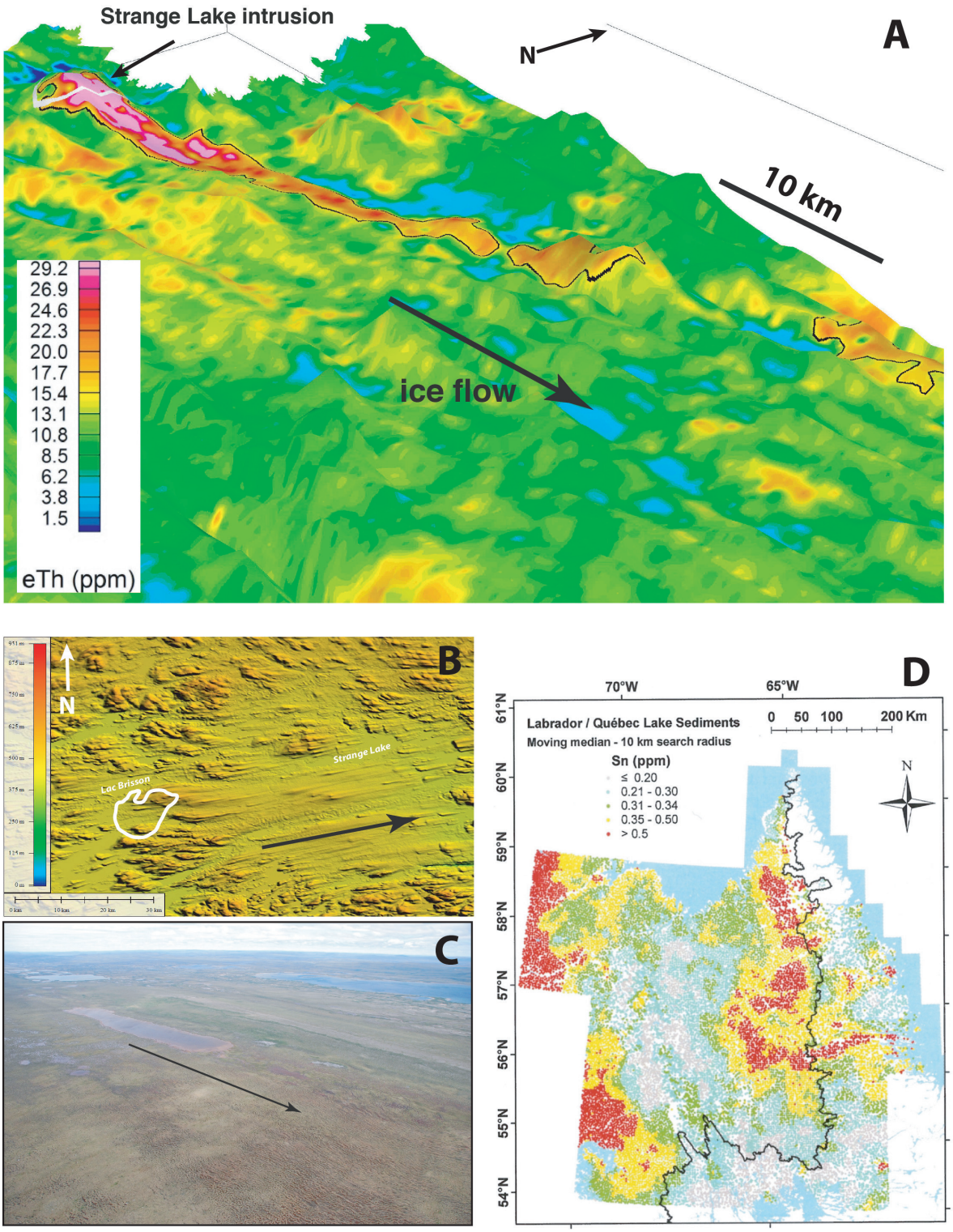


Figure 2. A) The Strange Lake till dispersal train from airborne gamma-ray spectrometry survey data (Geological Survey of Canada, 1980), overlain on a Digital Elevation Model (DEM; applied with 10x vertical exaggeration) of the Strange Lake region and viewed obliquely from the southeast. The linear mega-scale glacial lineations (MSGLs) dominate the landscape and mirror the ribbon-shaped dispersal train. **B)** Shuttle Radar Topographic Mission (SRTM) DEM image of the Strange Lake deposit (outlined in white) highlighting the mega-scale glacial lineations from the Kogaluk River ice stream that eroded the deposit from left to right (black arrow) and created the elongated ribbon dispersal train. **C)** Oblique aerial photo of the MSGLs that occur in the Strange Lake area, with landforms showing large length-to-width ratios, indicative of fast-flowing ice. **D)** Plot of lake sediment geochemistry for tin (Sn; *from* Amor et al., 2018), an element affiliated with peralkaline granitic intrusions. A long linear Sn anomaly extends from the host granite of the Strange Lake deposit and continues for more than 100 km out to the Labrador coast.

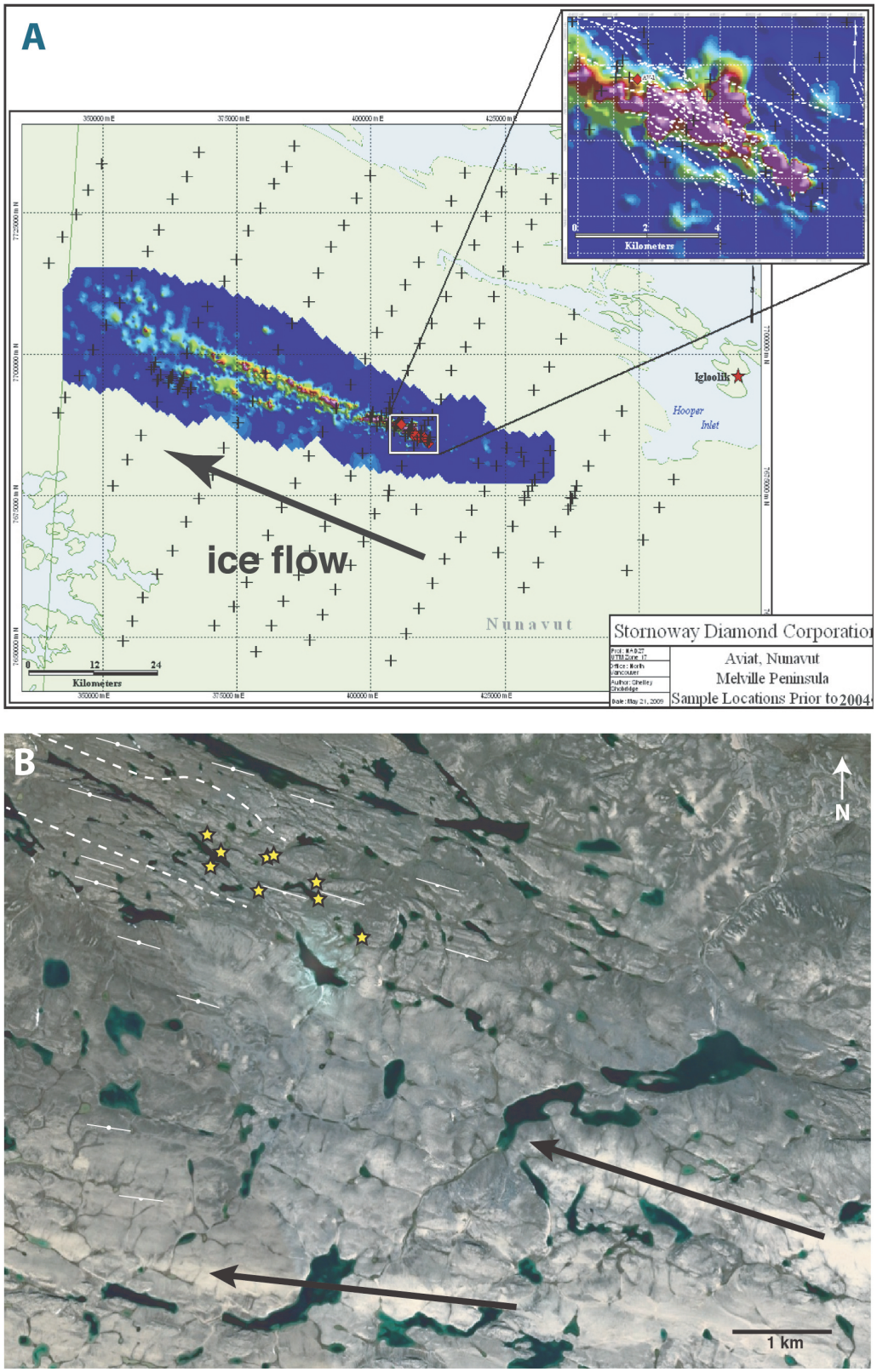


Figure 3. A) Colour-shaded map of total kimberlite indicator mineral abundance in all surficial samples (2004–2008) over the entire Tremblay corridor, with an inset of the eastern terminus of the dispersal train. The original 2004 surficial samples that were used to discover the dispersal train are shown as crosses (modified *from* Armstrong, 2009). **B)** Satellite image of the Aviat cluster of kimberlites. The small yellow stars indicate outcropping kimberlites. The white dashed line is the linear dispersal train proximal to the kimberlite field. This region is the onset zone for the northern tracts of the Gulf of Boothia ice streams (*see* Fig. 1). Mega-scale glacial lineations can be seen on the landscape (shown as white fluting symbols), as well as large carbonate dispersal trains (black arrows) formed by streaming ice (image source: Landsat 7 with 15 m resolution panchromatic band).

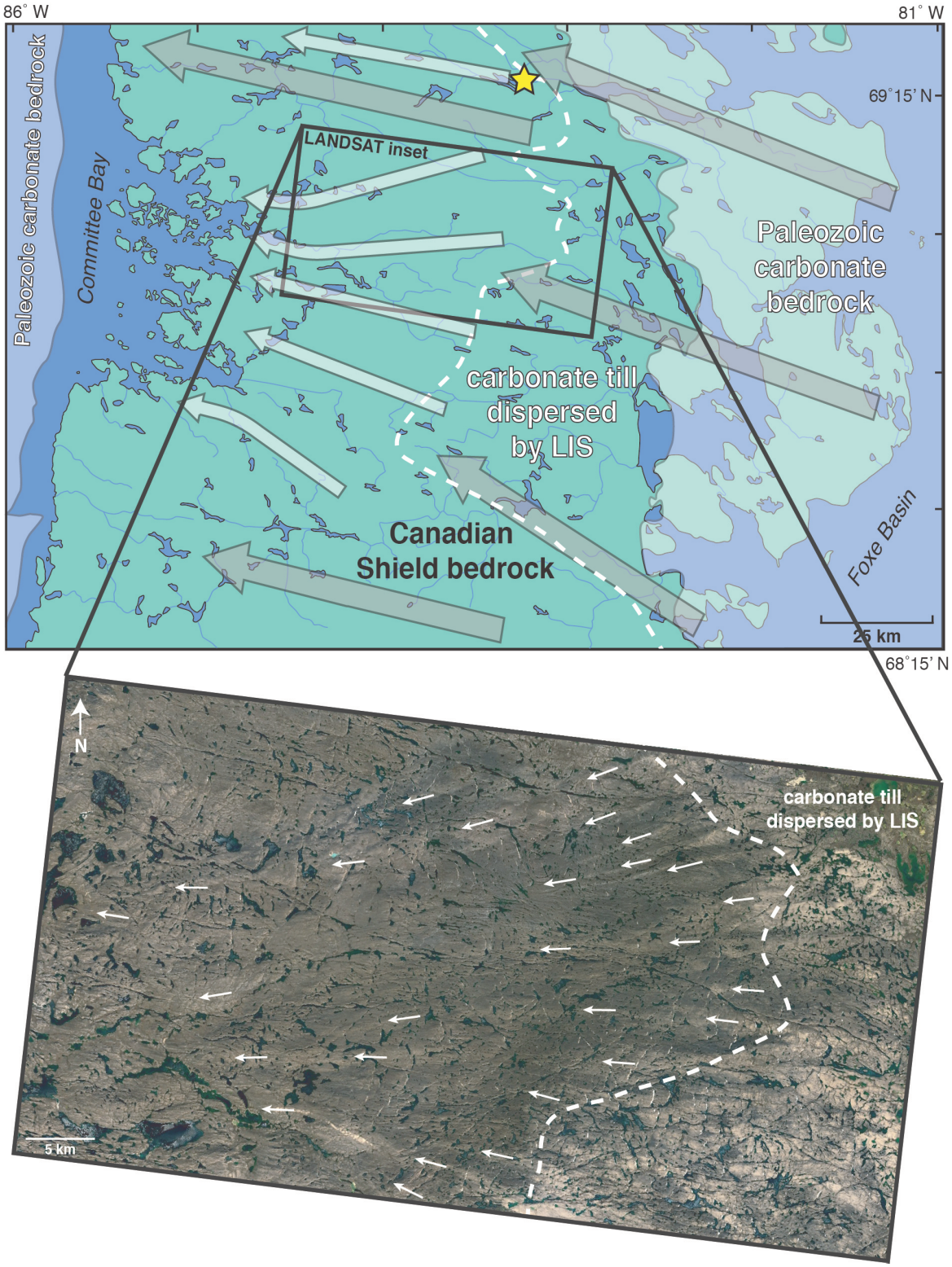


Figure 4. The carbonate dispersal trains of central Melville Peninsula, Nunavut (*see* Dredge, 2000). During the last glacial event, the Laurentide Ice Sheet eroded Paleozoic carbonate bedrock from the Foxe Basin and eastern Melville Peninsula and deposited a light coloured carbonate till inland over Canadian Shield bedrock (dark arrows and white dashed line; Tremblay and Paulen, 2012). During deglaciation, several ice streams formed as part of a large fan in Committee Bay (white arrows), with their onset zones at the western edge of the carbonate till zone, producing elongate ribbons, or fingers, of carbonate-rich till that extend almost 50 km to Committee Bay (yellow star is the Aviat kimberlite field). Lower inset is a satellite image of the central Melville Peninsula, showing the elongate tracts of carbonate till ribbons (lighter tones, demarked by small arrows) created by ice streams that flowed westward to Committee Bay. The onset zones for these ice streams is in the region with carbonate till previously deposited by the Laurentide Ice Sheet (image source: Landsat 7 with 15 m resolution panchromatic band).

non-mineralized bedrock, the resultant exotic till that is deposited masks the geochemical and mineralogical signature of the underlying bedrock. The long glacial transport distances observed in glacial sediments deposited by ice streams should be taken into consideration when collecting till samples and interpreting till geochemistry and heavy mineral patterns in these regions of Shield terrain in the northern hemisphere.

ACKNOWLEDGMENTS

This summary of ice stream dispersal trains is an output of the GSC's Critical Minerals Geoscience and Data Program (CMGD) under the "Ice stream paradigm and search for critical minerals in Canada: exploiting the power of automated geospatial mapping techniques' sub-activity (2023–2027)". Fruitful discussions and contributions to some of the ideas this paper draws upon are also acknowledged from Niko Putkinen (Geological Survey of Finland) and Syed Bukhari (University of Toronto, Scarborough Campus).

REFERENCES

Amor, S., McCurdy, M., and Garrett, R., 2018. Creation of an atlas of lake-sediment geochemistry of Western Labrador and Northeastern Quebec; Geochemistry: Exploration, Environment, Analysis, v. 19, p. 369–393. https://doi.org/10.1144/geochem2018-061

Armstrong, J.P., 2009. Kimberlite indicator mineral anomalies in a regional, local, and bedrock context: Examples from Canada; *in* Workshop B: Indicator Mineral Methods in Mineral Exploration, (ed.) M.B. McClenaghan and L.H. Thorleifson; 24th International Applied Geochemistry Symposium, 31 May 2009, Fredericton, Canada, p. 47–53.

Armstrong, J.P., Stubley, M.P., and Chang, F.Y., 2008. Geology and exploration history of the Aviat kimberlite cluster, northern Rae Craton, Melville Peninsula, Nunavut, Canada; *in* Extended Abstracts; 9th International Kimberlite Conference, Frankfurt, Extended Abstract No. 9IKC-A-00266. https://doi.org/10.29173/ikc3498

Batterson, M.J., 1989. Glacial dispersal from the Strange Lake alkalic complex, northern Labrador; *in* Drift Prospecting, (ed.) R.N.W. DiLabio and W.B. Coker; Geological Survey of Canada, Paper 89-20, p. 31–40. https://doi.org/10.4095/127362

Batterson, M.J. and Taylor, D.M., 2009. Geochemical re-analysis of till samples from the Strange Lake area, Labrador (NTS Map Sheets 14D/5 and 24A/8); Government of Newfoundland and Labrador, Department of Natural Resources, Geological Survey, Open File LAB/1479. https://www.gov.nl.ca/iet/files/mines-geoscience-publications-openfiles-oflab1479.pdf

Bennett, M.R., 2003. Ice streams as the arteries of an ice sheet: their mechanics, stability and significance; Earth-Science Reviews, v. 61, p. 309–339. https://doi.org/10.1016/S0012-8252(02)00130-7

De Angelis, H. and Kleman, J., 2005. Palaeo-ice streams in the northern Keewatin sector of the Laurentide Ice Sheet; Annals of Glaciology, v. 42, p. 135–144. https://doi.org/10.3189/172756405781812925

De Angelis, H. and Kleman, J., 2007. Palaeo-ice streams in the Foxe/Baffin sector of the Laurentide Ice Sheet; Quaternary Science Reviews, v. 26, p. 1313–1331. https://doi.org/10.1016/j.quascirev.2007.02.010

Dredge, L.A., 2000. Carbonate dispersal trains, secondary till plumes, and ice streams in the west Foxe Sector, Laurentide Ice Sheet; Boreas, v. 29, p. 144–156. https://doi.org/10.1111/j.1502-3885.2000.tb01207.x

Dyke, A.S., 2008. The Steensby Inlet ice stream in the context of the deglaciation of northern Baffin Island, eastern Arctic Canada; Earth Surface Processes and Landforms, v. 33, p. 573–592. https://doi.org/10.1002/esp.1664

Dyke, A.S. and Morris, T.F., 1988, Drumlin fields, dispersal trains, and ice streams in Arctic Canada; Canadian Geographer / Le Géographe canadien, v. 32, p. 86–90. https://doi.org/10.1111/j.1541-0064.1988.tb00860.x

Eyles, N., Arbelaez-Moreno, L., and Sookhan, S., 2018. Ice streams within the last Cordilleran Ice Sheet of western North America; Quaternary Science Reviews, v. 179, p. 87–122. https://doi.org/10.1016/j.quascirev.2017.10.027

Geological Survey of Canada, 1980. Airborne gamma ray spectrometric map, Dihourse Lake; Quebec–Newfoundland Geophysical Series, Map 35124(08)G. https://doi.org/10.4095/124881

Hart, J.K., 1999. Identifying fast ice flow from landform assemblages in the geological record: a discussion; Annals of Glaciology, v. 28, p. 59–66. https://doi.org/10.1016/0037-0738(94)90133-3

Krabbendam, M., Eyles, N., Putkinen, N., Bradwell, T., and Arbelaez-Moreno, L., 2016. Streamlined hard beds formed by palaeo-ice streams: A review; Sedimentary Geology, v. 338, p. 24–50. https://doi.org/10.1016/j.sedgeo.2015.12.007

Margold M., Stokes C.R., and Clark C.D., 2015. Ice streams in the Laurentide Ice Sheet: a new mapping inventory; Journal of Maps, v. 11. p. 380–395. https://doi.org/10.1080/17445647.2014.912036

McClenaghan, M.B. and Paulen, R.C., 2018. Mineral Exploration in Glaciated Terrain, Chapter 20; *in* Past Glacial Environments (Sediments, Forms and Techniques) A new & revised edition, (ed.) J. Menzies and J.J-M. van der Meer; Elsevier, p. 689–751. https://doi.org/10.1016/B978-0-08-100524-8.00022-1

McClenaghan, M.B., Paulen, R.C., and Kjarsgaard, I.M., 2019. Rare metal indicator minerals in bedrock and till at the Strange Lake peralkaline complex, Quebec and Labrador, Canada; Canadian Journal of Earth Sciences, v. 56, p. 857–869. https://doi.org/10.1139/cjes-2018-0299

McConnell, J.W. and Batterson, M.J., 1987. The Strange Lake Zr-Y-Nb-Be-REE deposit, Labrador: A geochemical profile in till, lake and stream sediment, and water; Journal of Geochemical Exploration, v. 29, p. 105–127. https://doi.org/10.1016/0375-6742(87)90073-2

McMartin, I., Godbout, P.-M., Campbell, J.E., Tremblay, T., and Behnia, P., 2021. A new map of glacigenic features and glacial land systems in central mainland Nunavut, Canada; Boreas, v. 50, p. 51–75. https://doi.org/10.1111/bor.12479

Paulen, R.C., Stokes, C.R., Fortin, R., Rice, J.M., Dubé-Loubert, H., and McClenaghan, M.B., 2017. Dispersal trains produced by ice streams: an example from Strange Lake, Labrador, Canada; *in* Proceedings of Exploration 17, (ed.) V. Tschirhart and M.D. Thomas; Sixth Decennial International Conference on Mineral Exploration, p. 871–875. https://geochem.nrcan.gc.ca/cdogs/content/pub/pub03698_e.htm

Paulen, R.C., Stokes, C., and McClenaghan, M.B., 2019. Mineral dispersal trains as products of hard-bedded ice streams in northern Canada; 20th Congress of the International Union for Quaternary Research (INQUA), Abstract P-4840. https://virtual.oxfordabstracts.com/#/event/public/574/submission/2181

Rice, J.M., Paulen, R.C., Ross, M., McClenaghan, M.B., and Campbell, H.E., 2023. Quaternary geology of the southern Core Zone area, Quebec and Newfoundland and Labrador; *in* Surficial Geology of Northern Canada: a Summary of Geomapping for Energy and Minerals Program Contributions, (ed.)

I. McMartin; Geological Survey of Canada, Bulletin 611, p. 221–265. https://doi.org/10.4095/331426

Ross, M., Campbell, J.E., Parent, M., and Adams, R.S., 2009. Palaeo-ice streams and the subglacial landscape mosaic of the North American mid-continent prairies; Boreas, v. 38, p. 421–439. https://doi.org/10.1111/j.1502-3885.2009.00082.x

Sookhan, S., Eyles, N., Bukhari, S., and Paulen, R.C., 2021. LiDAR-based quantitative assessment of drumlin to mega-scale glacial lineation continuums and flow of the paleo Seneca-Cayuga paleo-ice stream; Quaternary Science Reviews, v. 263. https://doi.org/10.1016/j.quascirev.2021.107003

Spagnolo, M., Clark, C.D., Ely, J.C., Stokes, C.R., Anderson, J.B., Andreassen, K., Graham, A.G.C., and King, E.C., 2014. Size, shape and spatial arrangement of mega-scale glacial lineations from a large and diverse dataset; Earth Surface Processes and Landforms, v. 39, p. 1432–1448. https://doi.org/10.1002/esp.3532

Spagnolo, M., Phillips, E., Piotrowski, J.A., Rea, B.R., Clark, C.D., Stokes, C.R., Carr, S.J., Ely, J.C., Ribolini, A., Wysota, W., and Szuman, I., 2016. Ice stream motion facilitated by a shallow-deforming and accreting bed. Nature Communications, v. 7, 10723. https://doi.org/10.1038/ncomms10723

Stokes, C.R. and Clark, C.D., 1999. Geomorphological criteria for identifying Pleistocene ice streams; Annals of Glaciology, v. 28, p. 67–74. https://doi.org/10.3189/172756499781821625

Tremblay, T. and Paulen, R.C., 2012. Glacial geomorphology and till geochemistry of Central Melville Peninsula, Nunavut; Geological Survey of Canada, Open File 7115. https://doi.org/10.4095/290993

Veillette, J.J., Roy, M., Paulen, R.C., Ménard, M., and St-Jacques, G., 2017. Uncovering the hidden part of a large ice stream of the Laurentide Ice Sheet, northern Ontario, Canada; Quaternary Science Reviews, v. 155, p. 136–158. https://doi.org/10.1016/j.quascirev.2016.11.008

Winsborrow, M.C.M., Clark, C.D., and Stokes, C.R., 2004. Ice streams of the Laurentide Ice Sheet; Géographie physique et Quaternaire, v. 58, p. 269–280. https://doi.org/10.7202/013142ar

Using indicator minerals to explore for porphyry Cu deposits and their related critical minerals

Christopher E. Beckett-Brown[1,2] and M. Beth McClenaghan[3]

[1]Ontario Geological Survey, Ministry of Mines, 933 Ramsey Lake Road, Sudbury, Ontario P3E 6B5
[2]Harquail School of Earth Sciences, Laurentian University, Sudbury, Ontario P3E 2C6
[3]Geological Survey of Canada, 601 Booth Street, Ottawa, Ontario K1A 0E8

ABSTRACT

The porphyry indicator mineral (PIMs) suite was developed in the 2000s for exploration in arid unglaciated regions but subsequently, this method has been applied to exploration in the glaciated terrains of Canada and Alaska. Although the use of PIM techniques in glaciated terrain has not yet contributed to a mineral discovery, it is actively being applied in exploration. Porphyry copper exploration using indicator minerals is somewhat challenged by the disseminated nature of ore minerals, the small grain size (in the case of gold grains), and the inability to survive glacial transport, thus significant work has been undertaken to examine alternative indicators (i.e. accessory minerals) that form in reasonable abundances in these systems and also have characteristics (e.g. mineral chemistry, luminescence, isotopic signatures) that identify them as being sourced from a porphyry system.

INTRODUCTION

Porphyry Cu-Mo-Au deposits are large (hundreds of millions of tonnes of ore) and generally low-grade systems genetically related to porphyritic intrusions (Sinclair, 2007). The distribution of hypogene ore minerals is generally structurally controlled in stockworks, breccias, and veins, which are primary sources for Cu, Mo, and Au mineralization. These systems also contain significant critical mineral byproduct metals, including Re, W, In, Pt, Pd, and Se. The alteration zonation of porphyry systems has been well documented (Sinclair, 2007; Sillitoe, 2010; Cooke et al., 2014a, and references therein), with many exhibiting predictable zonation patterns that reflect a temperature gradient from the base of the systems upward and outward from sodic-calcic, potassic, propylitic, chlorite-sericite, sericitic (phyllic), and advanced argillic (Fig. 1).

There are limited case studies documenting the spatial patterns of indicator mineral signatures for porphyry Cu deposits in till samples collected in glaciated terrain (Kelley et al., 2011, 2013; Plouffe et al., 2013, 2022; Hashmi et al., 2015). Of these, only one example of the application of indicator mineral methods to porphyry Cu exploration has been reported for unglaciated terrains (Averill, 2011). Several other studies have documented the indicator minerals in the deposits themselves and their distinctive mineral chemistry (Plouffe and Ferbey, 2017, and references therein). This chapter provides an overview of best practices for applying indicator mineral methods for porphyry Cu exploration to till sampling in Canada.

INDICATOR MINERALS

Porphyry indicator minerals (PIMs) are minerals that indicate the presence of ore minerals or hydrothermal alteration. Indicator mineral (IM) abundance is widely dependent on content in the source rocks, the degree of alteration, and the ore assemblages that are present. The large footprint of porphyry systems can also be of benefit in generating subsequently large IM dispersal trains (Plouffe and Ferbey, 2017); conversely, the large and disseminated nature of ore minerals in porphyry systems can hinder their potential for forming distinct IM anomalies.

There are two groups of PIMs (Table 1): 1) “type 1”, which includes ore minerals and their alteration minerals, and 2) “type 2”, which are minerals that are readily found in porphyry copper deposits, such as magmatic/hydrothermal or alteration minerals that require additional information (e.g. chemical, isotopic, age constraints) that link them to porphyry mineralization. Type 1 minerals include gold, chalcopyrite, molybdenite, pyrite, jarosite, and secondary Cu minerals (Cu-oxides and -sulphates can also be present, although it is very rare to find them preserved in till). Type 2 minerals include apatite, epidote, garnet (andradite), magnetite, rutile, titanite, tourmaline, and zircon.

PIMs assist in determining the bedrock sources, the nature of the mineralization, the element source, the mineralogy (Type 1), and mineral fertility (Type 2). Porphyry Cu indicator mineral dispersal patterns/fans/trains are generally larger than geochemical anomalies (e.g. Anderson et al., 2011; Kelley et al., 2011;

Recommended citation:

Beckett-Brown, C.E. and McClenaghan, M.B., 2024. Using indicator minerals to explore for porphyry Cu deposits and their related critical minerals; *in* Till Geochemistry and Indicator Mineral Methods for Exploration in Glaciated Terrains, (ed.) R.C. Paulen and M.B. McClenaghan; Geological Survey of Canada, Open File 9210, p. 148–157. https://doi.org/10.4095/pbmy2d03m0

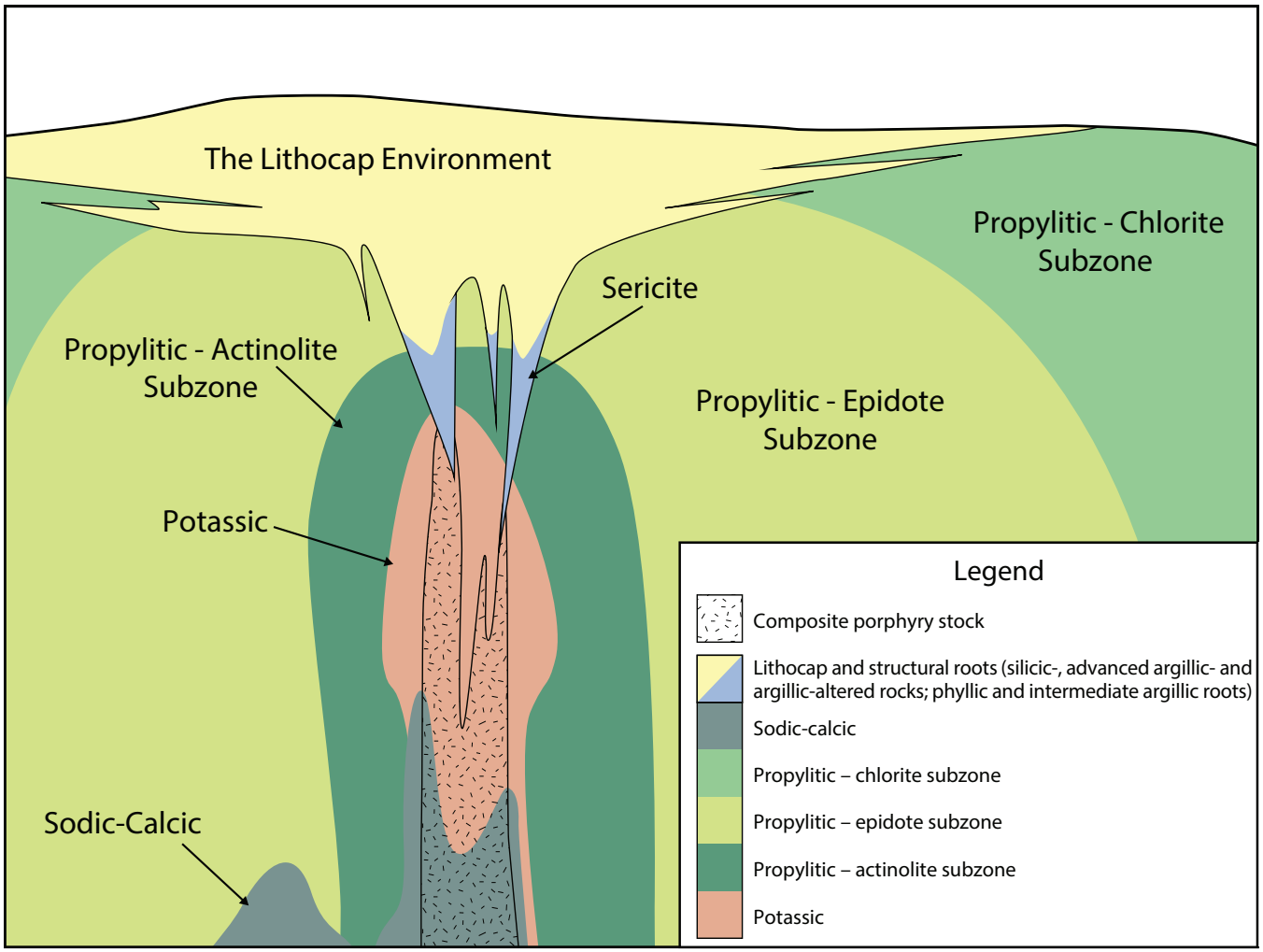


Figure 1. Generalized porphyry alteration zonation (modified *after* Cooke et al., 2020). The type 1 and type 2 porphyry indicator minerals that occur in each alteration zone are listed in Table 1.

Table 1. Table of porphyry Cu indicator minerals (Kelley et al., 2011; Plouffe and Ferbey, 2017) grouped according to typical alteration assemblages and subdivided into two subtypes, type 1 and type 2.

Alteration type	Defining mineralogy	Type 1 indicators	Type 2 indicators
Sodic-Calcic	albite, actinolite, magnetite		magnetite, diopside, epidote, garnet (andradite), tourmaline, titanite
Potassic	biotite, K-feldspar	pyrite, chalcopyrite, gold, bornite, molybdenite	epidote, tourmaline, magnetite, andalusite, apatite
Propylitic	chlorite, epidote, albite, carbonate	pyrite, gold, sphalerite, galena	epidote, magnetite, tourmaline, apatite
Chlorite-Sericite	chlorite, sericite, illite, hematite	pyrite, gold, chalcopyrite	epidote, tourmaline
Sericite (Phyllic)	quartz, sericite	pyrite, chalcopyrite, gold, bornite, enargite, tennantite	tourmaline, apatite
Argillic	vuggy quartz, alunite, pyrophyllite, dickite, kaolinite	pyrite, gold, enargite	andalusite, corundum, dumortierite, topaz
Supergene	quartz, hematite, goethite, jarosite	chalcocite, covellite, digenite, jarosite	goethite

Eppinger et al., 2013). PIMs may be of use in determining the potential for porphyry Cu mineralization in large, glaciated regions, notably western Canada, which has been relatively underexplored due to little bedrock exposure. However, another reason that PIM methods have been under-utilized in western Canada is because of the low abundance of type 1 PIMs in mineralized rocks, the small grain size (typically <0.25 mm) of these minerals, their susceptibility for oxidation and breaking down in till and stream sediments, and the lack of case studies documenting this method.

SAMPLE PROCESSING/PREPARATION FOR PORPHYRY INDICATOR MINERALS

Indicator mineral separation, which is routinely conducted at commercial laboratories, generally follows a similar pattern (Fig. 3 *in* Beckett-Brown and McClenaghan, 2024), a description of which is described in detail in McClenaghan et al. (2020, 2023). Due to the lack of physically robust type 1 IMs, type 2 IMs are much more useful for porphyry Cu exploration. Many of the type 2 IMs have a specific gravity (SG) at or close to 3.2, which is the common threshold between heavy (>3.2 SG) and mid-density (2.8–3.2 SG) mineral fractions produced during sample processing. Thus, when processing till samples, both the mid-density and heavy mineral fractions should be recovered and examined for PIMs. The densities of key PIMs are listed below along with the mineral descriptions.

PORPHYRY CU INDICATOR MINERALS AND METHODS

Porphyry Cu Indicator minerals are briefly described below, along with colour photographs, and are organized based on their type (1 or 2) and alphabetical order. More detailed descriptions of some of the minerals and their characteristic chemistries are reported in Bouzari et al. (2011) and Plouffe and Ferby (2017).

Type 1

Chalcopyrite (Fig. 2a, $CuFeS_2$, SG=4.1–4.3, H=3.5–4] is the primary hypogene Cu ore mineral in porphyry systems (e.g. Kelley et al., 2011). It has been recovered in till down-ice of known porphyry systems in British Columbia, Canada (e.g. Mount Polly, Gibraltar, Woodjam, Highland Valley Copper), with counts ranging from 0 to 4630 grains/10 kg till sample (Hashmi et al., 2015; Plouffe et al., 2016). Glacial dispersal of chalcopyrite in till extends more than 10 km from the main mineralized zones at the Mount Polly and Highland Valley copper deposits (Plouffe and Ferbey, 2017). Although chalcopyrite can be susceptible to oxidation and physical degradation (i.e. preglacial and/or postglacial weathering), it can be an important type 1 indicator for porphyry deposits.

Gold [Fig. 2b, Au, SG=15.5–19.3, H=2.5–3] is an excellent type 1 indicator of porphyry Cu-Mo-Au mineralization but is not always present in porphyry systems. Its presence alone, i.e., without other PIMs present, could be diagnostic of other ore systems, not only porphyry Cu systems. Gold grains in porphyry systems are generally small, ranging from 5 to 100 µm in diameter, and occur as inclusions in, or overgrowths of, other minerals (Kesler et al., 2002). These physical features pose challenges for gold liberation from its bedrock host phase, its ability to be visually identified during mineral picking, and reduces its potential to survive glacial transport. Gold grains have been reported to agglomerate during surficial transport but this seems to be restricted to fluvial systems (Osovetsky, 2016). Additionally, the gold concentrations in porphyry systems are low (0.004–0.35 g/t, for porphyry Cu-Au systems: Sinclair, 2007). At the Pebble porphyry Cu-Au deposit, Alaska, an investigation of 138 polished thin sections of ore samples identified 89 sections that contained gold, totaling 323 grains. These gold grains varied in size from 0.6 to 74.5 µm (average diameter) with 96% of those being <15 µm in size (Gregory et al., 2013), which poses a challenge as gold grains are only readily recovered from till samples for diameters of more than ~10 µm using the sample processing methods discussed above (McClenaghan and Cabri, 2011).

Chapman et al. (2022) have used inclusion assemblages and the population of gold particles in placers to identify their bedrock source. Porphyry gold grains from calc-alkaline systems can be identified by their Bi-Pb-Te-S inclusion signature (Chapman et al., 2018) and from alkalic porphyry systems by their Ag-Pb inclusion signature (Chapman et al., 2017). Gold grains were recovered in till surrounding the Mount Polly deposit (0–105 grains/10 kg) with anomalous gold counts being observed up to 5 km down-ice of the deposit (Hashmi et al., 2015; Plouffe et al., 2016).

Molybdenite [Fig. 2c, MoS_2, SG=4.62–4.73, H=1–1.5] is potentially a useful type 1 indicator of porphyry Cu-Mo-Au mineralization but lacks the physical and chemical robustness to survive glacial erosion and transport and is generally fine-grained (<0.25 mm in diameter) in the bedrock source. Molybdenite grains have not yet been recovered from till down ice of a known porphyry system (Plouffe and Ferbey, 2017), however, it has been recovered in till down ice of the intrusion-hosted Sisson W-Mo deposit in New Brunswick and in stream sediments downstream of the Casino porphyry Cu deposit in Yukon (McClenaghan et al., 2023), indicating that it can survive erosion and transport. Numbers of grains are expected to be low (<10 grains per sample) if detected.

Pyrite [Fig. 2d, FeS_2, SG=4.8–5.01, H=6–6.5], is a pseudo type 1 indicator of porphyry Cu-Mo-Au miner-



Figure 2. Photographs of porphyry indicator minerals: **a)** chalcopyrite, **b)** gold, **c)** molybdenite, **d)** pyrite, **e)** jarosite, **f)** epidote (from till surrounding the Woodjam prospect, British Columbia), **g)** andradite, **h)** magnetite, **i)** red rutile (from till in the Thompson Ni-belt area), **j)** titanite, **k)** prismatic tourmaline, and **l)** clustered tourmaline. Plates a, b, c, d, e, g, h, j, k, and l from stream sediments around the Casino porphyry Cu deposit, Yukon. Photographs taken by Michael Bainbridge Photography.

alization as it is associated with sulphide mineralization but is not an ore mineral. Pyrite is the most common accessory sulphide mineral in porphyry systems and is moderately stable in till due to its hardness. It can be easily recovered in heavy mineral concentrates (Averill, 2011). Pyrite grains have been recovered in till surrounding the Gibraltar deposit in British Columbia (0–27397 grains/10 kg) with anomalous pyrite counts observed up to 5 km down-ice of some deposits (Plouffe and Ferbey, 2019). However, pyrite can be susceptible to oxidation, and occurrences of geothite-altered pyrite grains have been recovered (Plouffe and Ferbey, 2016), which may limit its utility as a type 1 indicator for porphyry deposits.

Jarosite [Fig. 2e, $KFe_3(SO_4)_2(OH)_6$, SG=3.25, H=2.5–3.5] is a pseudo type 1 indicator of porphyry Cu-Mo-Au mineralization as it reflects the dissolution and reprecipitation of primary sulphides in supergene zones

(Anderson, 1982; Desborough et al., 2010). Despite its low hardness (2.5–3.5), jarosite has been recovered in abundance as rounded amorphous grains from till samples down-ice of porphyry deposits (1000s of grains/10 kg sample, Kelley et al., 2011). Recent work on jarosite from stream sediments surrounding a known porphyry deposit shows promise for its use as an effective indicator (Walli, 2022). Jarosite grains were recovered in till surrounding the Woodjam prospect (0–5455 grains/10 kg) with anomalous jarosite counts being observed directly overlying the deposit and up to 1 km down-ice (Plouffe and Ferbey, 2019).

Type 2

Apatite [$Ca_5(PO_4)_3(OH,F,Cl)$, SG=3.17–3.23, H=5] is a type 2 indicator of porphyry Cu-Mo-Au mineralization. It is a common magmatic/hydrothermal accessory phase that is found throughout a porphyry system and has received significant scientific interest (e.g. Roegge et al., 1974; Streck and Dilles, 1998; Bouzari et al., 2016; Mao et al., 2016). Apatite forming in porphyry copper systems is known to be Cl-rich (Roegge et al., 1974). Apatite cathodoluminescence (CL) was studied at four porphyry systems in British Columbia and used to identify hydrothermal alteration intensity. Apatite found in unaltered rocks exhibits a yellow CL response, apatite forming in K-silicate-altered rocks exhibits a green CL response, and apatite found in sericite-altered rocks exhibits grey CL (Bouzari et al., 2016). Rukhlov et al. (2016) showed that apatite trace-element chemistry in till up to 15 km down-ice could be correlated with apatite from nearby porphyry deposits, demonstrating that it can be a useful exploration tool. Apatite grains were recovered in till surrounding the Mount Polly deposit (0–3 modal % of the >3.2 heavy mineral concentrate) with anomalous apatite counts being observed directly overlying the deposit and up to 1 km down-ice (Hashmi et al., 2015).

Epidote [Fig. 2f, $Ca_2(Fe,Al)_3(SiO_4)_3(OH)$, SG=3.2–3.6, H=6–7] is another type 2 indicator of porphyry Cu-Mo-Au mineralization that has been investigated by various authors (Hashmi et al., 2015; Plouffe et al., 2016; Cooke et al., 2020; Plouffe et al., 2022). It is a common hydrothermal alteration mineral, mostly concentrated in the propylitic halo of porphyry systems (Cooke et al., 2020). The Fe^{3+} member (epidote) of the epidote supergroup is most common due to the relatively oxidizing conditions that are typical of a porphyry copper system (Cooke et al., 2020). Epidote abundance in till samples collected around porphyry systems has also been investigated (Kelley et al., 2011, Hashmi et al., 2015; Plouffe et al., 2016) with anomalous samples consisting of up to 95 modal % epidote in the heavy mineral concentrates (>3.2 SG) (Plouffe et al., 2016). In addition to abundance, mineral chemistry is an important aspect of this type 2 mineral. Epidote supergroup minerals are known to permit the substitution of porphyry Cu pathfinder elements such as As, Sb, Pb, and V, thus epidote trace element chemistry is of particular interest when attempting to detect a porphyry Cu system footprint (Cooke et al., 2014b; Baker et al., 2020; Plouffe et al., 2022).

Andradite garnet [Fig. 2g, $Ca_3Fe_2Si_3O_{12}$, SG=3.9, H=6.5–7.5] has also been identified as a type 2 indicator for porphyry Cu-Mo-Au systems but specifically related to skarns associated with these deposits (Sillitoe, 2010; Kelley et al., 2011). Yellow andradite grains were recovered from till surrounding the Pebble deposit (0–1866 grains/10kg sample) with andradite counts anomalous down-ice of the deposit (Kelley et al., 2011). It was recovered in till surrounding the Mount Polly deposit (0–78125 grains/10kg) with anomalous counts reported directly overlying the deposit and up to 1 km down-ice (Hashmi et al., 2015). The major-, minor-, and trace-element chemistry of andradite garnets have been investigated (Meinert et al., 2005; Li et al., 2021) but clear distinctions between prospective and non-prospective grains have not been identified yet.

Magnetite [Fig. 2h, $Fe^{2+}Fe^{3+}{}_2O_4$, SG=5.17, H=5.5–6] another type 2 indicator of porphyry Cu-Mo-Au mineralization (Canil et al., 2016; Pisiak et al., 2017), forms as a hydrothermal alteration mineral in porphyry systems. Pisiak et al. (2017) provide the first test of magnetite in till as a potential PIM and McCurdy et al. (2022) further tested its use in stream sediments using mineral chemistry criteria that could be applied to glaciated terrain. Linear discriminant analysis (LDA) was used to differentiate barren igneous, hydrothermal porphyry, and ore-related igneous magnetite, but the models are primarily affected by concentrations of Mn, Ni, and V.

Rutile [Fig. 2i, TiO_2, SG=4.2, H=6–6.5] is a type 2 indicator of porphyry Cu-Mo-Au mineralization that forms in the potassic and phyllic zones of porphyry systems. It is commonly a hydrothermal alteration product of biotite, ilmenite, titanomagnetite, and titanite. Bouzari et al. (2011) noted that red rutile is prospective due to its high Cu content, in addition to other elements (V, Ta, and Sc). In porphyries that contain Mo, concentrations of Mo in rutile can be high. Rabbia et al. (2009) reported rutile from El Teniente, Chile, contained 186 ± 20 ppm Mo and Kelley et al. (2011) reported black rutile in several altered and mineralized bedrock samples from the Pebble deposit, Alaska, although it was not directly observed in till samples. Based on chemical analyses, rutile associated with Cu porphyry mineralization has a distinct signature (Kelley et al., 2010).

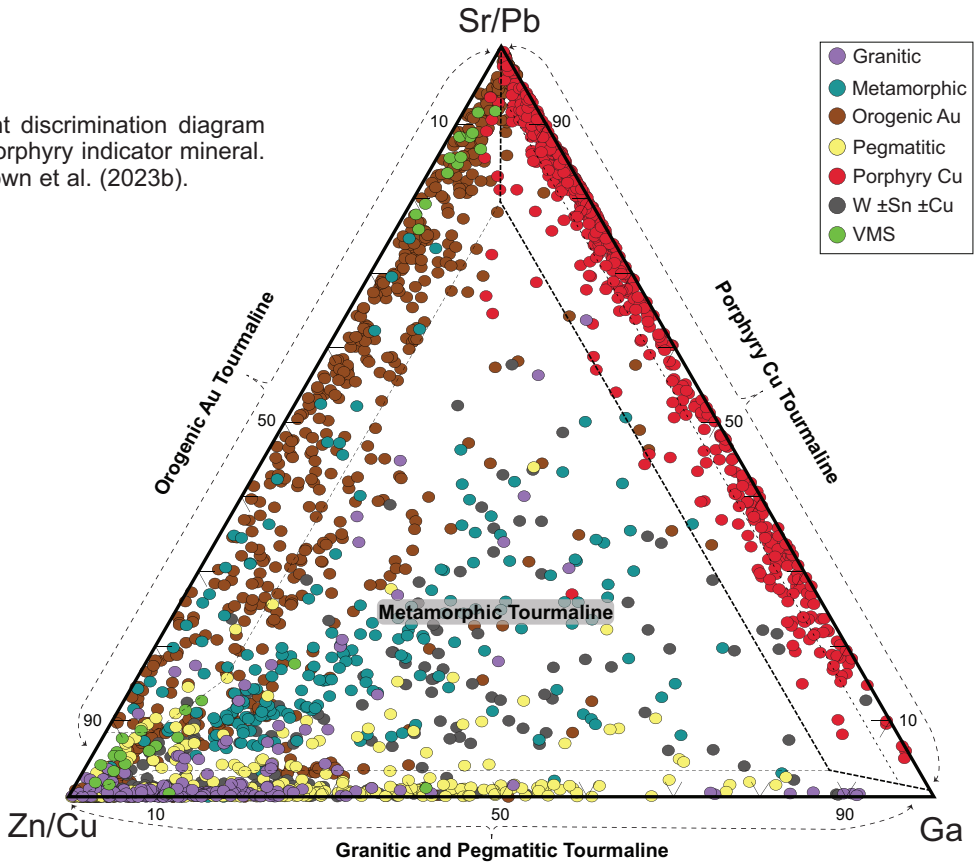


Figure 3. A trace-element discrimination diagram for tourmaline, a type 2 porphyry indicator mineral. Diagram *from* Beckett-Brown et al. (2023b).

Titanite [Fig. 2j, $CaTiSiO_5$, SG=3.5, H=5–5.5] has also been investigated as a type 2 indicator for porphyry Cu-Mo-Au systems (Celis et al. 2013; Celis 2015), forming as a magmatic/hydrothermal accessory mineral (Bouzari et al., 2011). Xu et al. (2015) measured titanite grains from mineralized intrusions and postulated that grains with high REE+Y contents (>15,000 ppm) are prospective. Titanite can reach 10 modal % in till samples near the Highland Valley Copper deposit (Plouffe and Ferbey, 2017). Prospective magmatic titanite from porphyry W and Mo deposits in western Canada are enriched in W (up to 103 ppm), and Mo (up to 174 ppm), which are interpreted to reflect a high concentration in the melt (Che et al., 2013). Titanite chemistry was investigated in porphyry Cu deposits from the Junshajian – Red River belt, China (Xu et al., 2015). These authors reported that titanite in mineralized intrusions is chemically distinct from that forming in barren intrusions with higher values of Fe_2O_3/Al_2O_3, ΣREE+Y, LREE/HREE, Ce/Ce*, (Ce/Ce*)/(Eu/Eu*), U, Th, Ta, Nb and Ga, and lower values for Al_2O_3, CaO, Eu/Eu*, Zr/Hf, Nb/Ta, and Sr (Xu et al., 2015).

Tourmaline [Fig. 2k, $XY_3Z_6T_6O_{18}(BO_3)_3V_3W$, SG=2.8–3.2, H=7–7.5] is another type 2 indicator of porphyry Cu-Mo-Au mineralization. It is commonly found in zones of phyllic alteration (Sillitoe, 2010) but can be found throughout the various zones of hydrothermal alteration in a porphyry system (Beckett-Brown et al., 2023a). The major and minor element composition of tourmaline has been investigated by a number of authors (Baksheev et al., 2012; Chapman et al., 2015) who concluded that grains from mineralized porphyry systems contain a constant 2 *apfu* Mg, and follow the oxydravite-povondraite trend (*see* Fig. 3: Baksheev et al., 2012). The use of tourmaline as an indicator mineral for porphyry systems had not been investigated in detail until recently (Chapman et al., 2015; Beckett-Brown et al., 2023a,b). Tourmaline texture (radiating clusters of prismatic grains; Fig. 2l) and chemistry (high Sr/Pb with low Zn/Cu and intermediate Ga; Fig. 3) can be used to distinguish prospective porphyry grains from background non-prospective ones following a step-wise decision tree (Fig. 4). Tourmaline can be recovered in both the heavy and mid-density fractions of till samples but is most abundant in the latter. Tourmaline abundance in till surrounding the Woodjam porphyry Cu-Au porphyry system, British Columbia, can range from 0–545 grains/10 kg (Fig. 5). A subset of tourmaline from till samples surrounding the Woodjam prospect were classified based on the tourmaline porphyry Cu decision tree (Fig. 4) and show that prospective tourmaline grains can be detected at least 13 km down-ice of the deposit (Fig. 6).

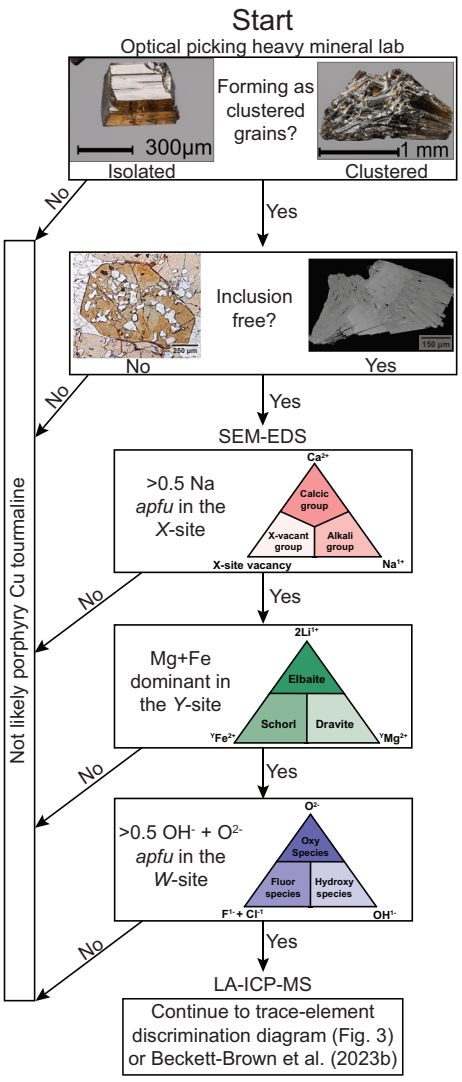


Figure 4. A stepwise decision tree to identify detrital tourmaline [$XY_3Z_6T_6O_{18}(BO_3)_3V_3W$] derived from porphyry Cu systems, based on physical and chemical data (from Beckett-Brown et al., *in press*). **Step 1)** Tourmaline morphology: grains forming in clusters are significantly more prospective than individual isolated grains. **Step 2)** Inclusion populations: porphyry-related tourmaline grains rarely contain mineral inclusions (zircon and rutile are the most common). To simplify classification, if inclusions are observed in the tourmaline grains, the grains are not considered to be derived from a porphyry Cu system. **Step 3)** X-site: Only porphyry Cu tourmaline is dominated by Na in the X-site. **Step 4)** Y-site constituents: porphyry Cu tourmaline is almost exclusively dominated by Mg and only rarely by Fe or Al. The Y-site of porphyry Cu tourmaline is never Li-dominant. **Step 5)** W-site: Porphyry Cu tourmaline is oxy- or hydroxyl- dominant (i.e. OH^- or O^{2-}); **Step 6)** Trace-element discrimination: plot the results using the Sr/Pb–Zn/Cu–Ga ternary diagram (Fig. 3, Beckett-Brown et al., 2023b). Tourmaline that plots outside the porphyry field is less likely to have been derived from a porphyry Cu system.

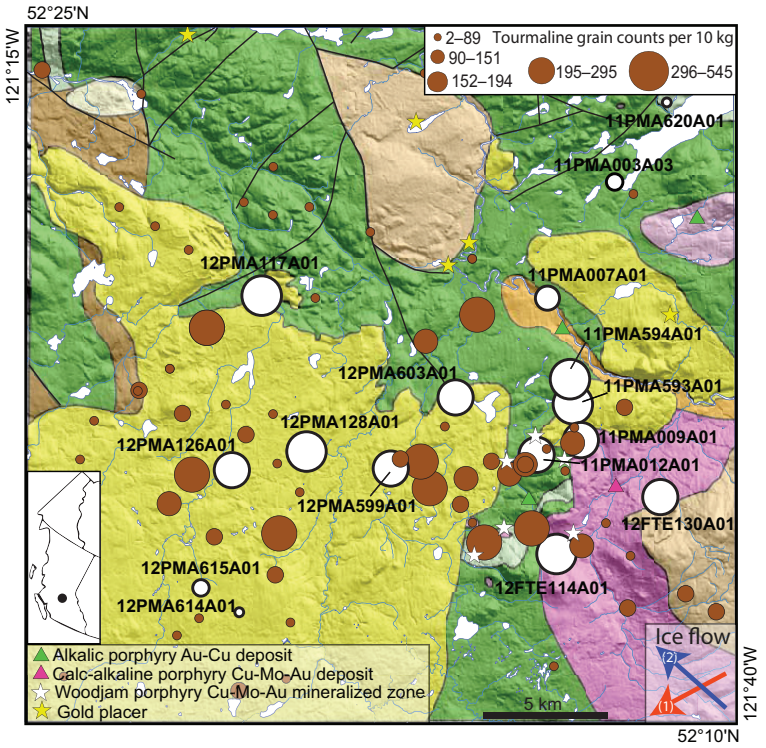


Figure 5. Map showing the location of surficial sediment samples from which tourmaline grains were recovered and examined; inset map shows the location of the Woodjam deposit in British Columbia. Proportional dot map of tourmaline abundance (grain counts, normalized to 10 kg) in the mid-density (2.8–3.2 SG) 0.25 to 0.5 mm fraction of till samples collected around the Woodjam deposit cluster, British Columbia. *See* Plouffe and Ferbey (2017) for bedrock geology. White dots with the thick black outline indicate till samples from which tourmaline grains were investigated.

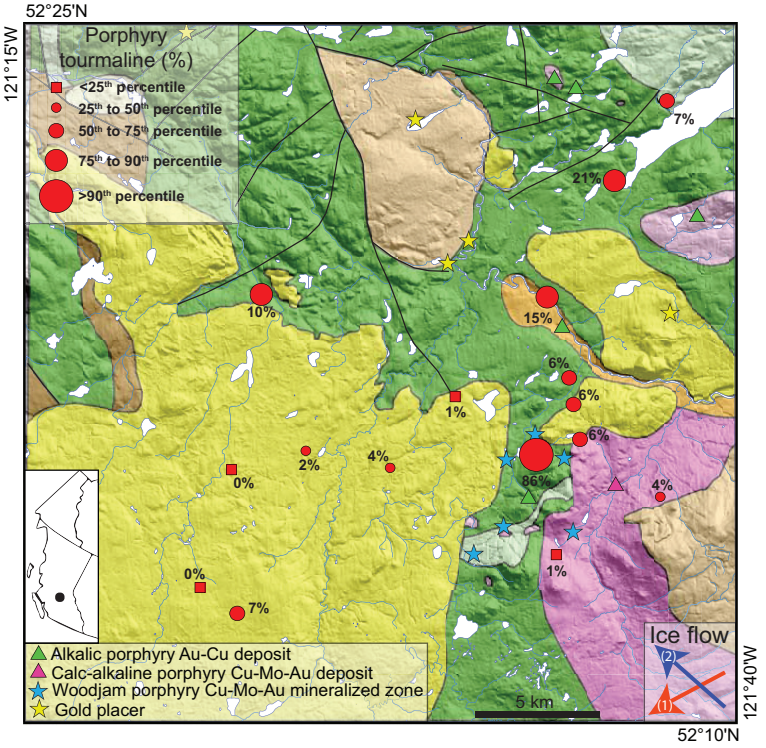


Figure 6. Map showing the same location as Figure 5 showing the percentage of tourmaline grains found in till samples that were classified as porphyry Cu-related based on the decision tree presented in Figure 4.

Zircon [$ZrSiO_4$, SG=4.6–4.7, H=7.5] is a type 2 indicator of porphyry Cu-Mo-Au mineralization whose mineral chemistry has been investigated by various authors (Lu et al., 2016; Pizzaro et al., 2020, 2024; Lee et al., 2021a,b). Zircon is a common magmatic accessory mineral in porphyritic intrusions. Lee et al. (2021b) investigated detrital zircons in till around the Highland Valley copper deposit, British Columbia, using LA-ICP-MS U-Pb and trace-element chemistry. Eu/Eu*N values >0.4 were used to define fertile versus barren zircons. A unimodal age population of zircon grains was observed but was not a key discriminator for this study, likely due to the proximal till sampling of this study. In British Columbia, up to 2000 rose-coloured zircon grains/10 kg were recovered in till samples collected surrounding the Highland Valley Copper deposit, where as other deposits (Mount Polley) yielded a maximum of 11 grains/10 kg (Plouffe and Ferbey, 2017). Pizarro et al. (2024) examined detrital zircons in alluvial sediments in Chile to identify porphyry Cu mineralization using the following geochemical classification: Hf >8750 (ppm), Ce/Nd >1, Eu/Eu* >0.4, 10 000 × (Eu/Eu*)/Y > 1, (Ce/Nd)/Y > 0.01, Dy/Yb <0.3 and 0.1 < Th/U < 1.

THE FUTURE AND CONCLUSIONS

Identifying indicator minerals in till can be an effective tool for detecting the presence of porphyry Cu-Mo-Au deposits in glaciated terrains (Kelley et al., 2011; Plouffe and Ferbey, 2017; Plouffe et al., 2022). Due to the challenges that type 1 PIMs present, additional focus should be put on type 2 PIMs. Subsequently, picking of the mid-density PIMs in addition to the routine high-density PIMs should be a procedure when exploring regions that are prospective for porphyry mineralization. Type 2 PIMs in their definition, require additional information to distinguish their source as being porphyry-related, thus more efficient workflows must be developed to streamline the assessment of these features. For example, the automated mineral counting by µXRF (discussed in Beckett-Brown and McClenaghan, 2024) and a robotic sample loading process could be followed by LA-ICP-MS using the existing stage positions to re-locate mineral grains of interest. Many of the type 2 PIMs listed above have distinct characteristics that distinguish grains forming in background environments from those forming in porphyry Cu-Mo-Au systems, now we need to put these methods to the test.

REFERENCES

Anderson, J.A., 1982. Characteristics of leached capping and techniques of appraisals; *in* Advances in Geology of the Porphyry Copper Deposits, Southwest North America, (ed.) S.R. Titley; The University of Arizona Press, Tucson, p. 275–295.

Anderson, E.D., Smith, S.M., Giles, S.A., Granitto, M., Eppinger, R.G., Bedrosian, P.A., Shah, A.K., Kelley, K.D., Fey, D.L., Minsley, B.J., and Brown, P.J., 2011. Geophysical, geochemical, and mineralogical data from the Pebble Cu-Au-Mo porphyry deposit area, southwest Alaska: Contributions to assessment techniques for concealed mineral resources (No. 608). US Geological Survey, p. 1–46.

Averill, S.A., 2011. Viable indicators in surficial sediments for two major base metal deposit types: Ni-Cu-PGE and porphyry Cu; Geochemistry: Exploration, Environment, Analysis, v. 11, p. 279–291.

Baker, M.J., Wilkinson, J.J., Wilkinson, C.C., Cooke, D.R., and Ireland, T., 2020. Epidote trace element chemistry as an exploration tool in the Collahuasi district, northern Chile; Economic Geology, v. 115, p. 749–770.

Baksheev, I.A., Yu Prokof'ev, V., Zaraisky, G.P., Chitalin, A.F., Yapaskurt, V.O., Nikolaev, Y.N., Tikhomirov, P.L., Nagornaya, E.V., Rogacheva, L.I., Gorelikova, N.V., and Kononov, O.V., 2012. Tourmaline as a prospecting guide for the porphyry-style deposits; European Journal of Mineralogy, v. 24, p. 957–979.

Beckett-Brown, C.E. and McClenaghan, M.B., 2024. Using indicator minerals to explore for porphyry Cu deposits and their related critical minerals; *in* Till Geochemistry and Indicator Mineral Methods for Exploration in Glaciated Terrains, (ed.) R.C. Paulen and M.B. McClenaghan; Geological Survey of Canada, Open File 9210, p. 147–156. https://doi.org/10.4095/pbmy2d03m0

Beckett-Brown, C.E., McDonald, A.M., and McClenaghan, M.B., 2023a. Recognizing tourmaline in mineralized porphyry copper systems: textures and major-element chemistry; The Canadian Journal of Mineralogy and Petrology, v. 61, p. 3–29.

Beckett-Brown, C.E., McDonald, A.M., and McClenaghan, M.B., 2023b. Trace element characteristics of tourmaline in porphyry copper systems: development and application to discrimination; The Canadian Journal of Mineralogy and Petrology, v. 61, p. 31–60.

Beckett-Brown, C.E., McDonald, A.M., and McClenaghan, M.B., 2024. Evaluating the application of texture and chemistry of detrital tourmaline as an indicator of porphyry Cu mineralization: A case study from the Casino porphyry Cu-Au-Mo deposit, Yukon, Canada; Journal of Geochemical Exploration, v. 262, 107469. https://doi.org/10.1016/j.gexplo.2024.107469

Bouzari, F., Hart, C.J.R., Barker, S., and Bissig, T., 2011. Porphyry indicator minerals (PIMS): a new exploration tool for concealed deposits in south-central British Columbia; Geoscience BC, Report 17, p. 31.

Bouzari, F., Hart, C.J., Bissig, T., and Barker, S., 2016. Hydrothermal alteration revealed by apatite luminescence and chemistry: A potential indicator mineral for exploring covered porphyry copper deposits; Economic Geology, v. 111, no. 6, p. 1397–1410.

Canil, D., Grondhal, C., Lacourse, T., and Pisiak, L.K. 2016. Trace elements in magnetite from porphyry Cu-Mo-Au deposits in British Columbia, Canada; Ore Geology Reviews, v. 72, p. 1116–1128.

Celis, A., 2015. Titanite as an indicator mineral for alkalic Cu-Au porphyry deposits in south central British Columbia; M.Sc. thesis, University of British Columbia, Vancouver, British Columbia, 247 p.

Celis, M.A., Bouzari, F., Bissig, T., Hart, C.J.R., and Ferbey, T., 2013. Petrographic characteristics of porphyry indicator minerals from alkalic porphyry copper-gold deposits in south-central British Columbia (NTS 092, 093); Geoscience BC Summary of Activities, p. 2014–1.

Chapman, J.B., Plouffe, A., and Ferbey, T., 2015. Tourmaline: the universal indicator? in Application of Indicator Mineral

Methods to Exploration, Short Course No. 2, (ed.) B. McClenaghan and E. Layton-Matthews; 27th International Applied Geochemistry Symposium, Tucson, Arizona, Association of Applied Geochemists, p. 25–31.

Chapman, R., Mileham, T., Allan, M., and Mortensen, J., 2017. A distinctive Pd-Hg signature in detrital gold derived from alkalic Cu-Au porphyry systems; Ore Geology Reviews, v. 83, p. 84–102.

Chapman, R.J., Allan, M.M., Mortensen, J.K., Wrighton, T.M., and Grimshaw, M.R., 2018. A new indicator mineral methodology based on a generic Bi-Pb-Te-S mineral inclusion signature in detrital gold from porphyry and low/intermediate sulfidation epithermal environments in Yukon Territory, Canada; Mineralium Deposita, v. 53, p. 815–834.

Chapman, R.J., Mortensen, J.K., Allan, M.M., Walshaw, R.D., Bond, J., and MacWilliam, K., 2022. A new approach to characterizing deposit type using mineral inclusion assemblages in gold particles; Economic Geology, v. 117, no. 2, p. 361–381.

Che, X.D., Linnen, R.L., Wang, R.C., Groat, L.A., and Brand, A.A., 2013. Distribution of trace and rare earth elements in titanite from tungsten and molybdenum deposits in Yukon and British Columbia, Canada; The Canadian Mineralogist, v. 51, p. 415–438.

Cooke, D.R., Hollings, P., Wilkinson, J.J. and Tosdal, R.M. 2014a. Geochemistry of porphyry deposits; *in* Treatise on Geochemistry, 2nd Edition, (ed.) K.K. Turekian and H.D. Holland; Elsevier, p. 357–381.

Cooke, D.R., Baker, M., Hollings, P., Sweet, G., Chang, Z., Danyushevsky, L., Gilbert, S., Zhou, T., White, N.C., Gemmell, J.B., and Inglis, S., 2014b. New advances in detecting the distal geochemical footprints of porphyry systems—epidote mineral chemistry as a tool for vectoring and fertility assessments; *in* Building Exploration Capability for the 21st Century (ed.) K.D. Kelley and H.C. Golden; Society of Economic Geology, Special Publication Volume 18, p. 127–152.

Cooke, D.R., Agnew, P., Hollings, P., Baker, M., Chang, Z., Wilkinson, J.J., Ahmed, A., White, N.C., Zhang, L., Thompson, J., and Gemmell, J.B., 2020. Recent advances in the application of mineral chemistry to exploration for porphyry copper–gold–molybdenum deposits: detecting the geochemical fingerprints and footprints of hypogene mineralization and alteration; Geochemistry: Exploration, Environment, Analysis, v. 20, no. 2, p. 176–188.

Desborough, G.A., Smith, K.S., Lowers, H.A., Swayze, G.A., Hammarstrom, J.M., Diehl, S.F., Leinz, R.W., and Driscoll, R.L., 2010. Mineralogical and chemical characteristics of some natural jarosites; Geochimica et Cosmochimica Acta, v. 74, no. 3, p. 1041–1056.

Eppinger, R.G., Fey, D.L., Giles, S.A., Grunsky, E.C., Kelley, K.D., Minsley, B.J., Munk, L., and Smith, S.M., 2013. Summary of exploration geochemical and mineralogical studies at the giant Pebble porphyry Cu-Au-Mo deposit, Alaska: Implications for exploration under cover; Economic Geology, v. 108, no. 3, p. 495–527.

Gregory, M.J., Lang, J.R., Gilbert, S., and Hoal, K.O., 2013. Geometallurgy of the Pebble porphyry copper-gold-molybdenum deposit, Alaska: Implications for gold distribution and paragenesis; Economic Geology, v. 108, no. 3, p. 463–482.

Hashmi, S, Ward, B.C., Plouffe, A., Leybourne, M.I., and Ferbey, T., 2015. Geochemical and mineralogical dispersal in till form the Mount Polley Cu-Au porphyry deposit, central British Columbia; Canada; Geochemistry: Exploration, Environment, Analysis, v. 15, p. 234–249.

Kelley, K.D., Lang, J., and Eppinger, R.G., 2010. Exploration geochemistry at the giant Pebble porphyry Cu-Au-Mo deposit, Alaska; Society of Economic Geologists, Newsletter, v. 80, p. 1–23

Kelley, K.D., Eppinger, R.G., Lang, J., Smith, S.M., and Fey, D.L., 2011. Porphyry Cu indicator minerals in till as an exploration tool: Example from the giant Pebble porphyry Cu-Au-Mo deposit, Alaska, USA; Geochemistry: Exploration, Environment, Analysis, v. 11, no. 4, p. 321–334.

Kelley, K.D., Lang, J.R., and Eppinger, R.G., 2013. The giant pebble Cu-Au-Mo deposit and surrounding region, Southwest Alaska: introduction; Economic Geology, v. 108, p. 397–404.

Kesler, S.E., Chryssoulis, S.L., and Simon, G., 2002. Gold in porphyry copper deposits: its abundance and fate; Ore Geology Reviews, v. 21, no. 1-2, p. 103–124.

Lee, R.G., Byrne, K., D'Angelo, M., Hart, C.J., Hollings, P., Gleeson, S.A., and Alfaro, M., 2021a. Using zircon trace element composition to assess porphyry copper potential of the Guichon Creek batholith and Highland Valley Copper deposit, south-central British Columbia; Mineralium Deposita, v. 56, p. 215–238.

Lee, R.G., Plouffe, A., Ferbey, T., Hart, C.J., Hollings, P., and Gleeson, S.A., 2021b. Recognizing porphyry copper potential from till zircon composition: A case study from the Highland Valley Porphyry district, south-central British Columbia; Economic Geology, v. 116, no. 4, p. 1035–1045.

Li, Y., Yuan, F., Jowitt, S.M., Li, X., Deng, Y., Li, X., and Zhou, T., 2021. Garnet major and trace element evidence of the alteration and mineralizing processes associated with genesis of the Qiaomaishan skarn deposit, Xuancheng ore district, eastern China; Ore Geology Reviews, v. 137, p. 104304.

Lu, Y.-J., Loucks, R.R., Fiorentini, M., McCuaig, T.C., Evans, N.J., Yang, Z.-M., Hou, Z.-Q., Kirkland, C.L., Parra-Avila, L.A., and Kobussen, A., 2016. Zircon composition as a pathfinder for porphyry Cu±Mo±Au deposits; *in* Tectonics and Metallogeny of the Thetyan Orogenic Belt, (ed.) J. Richards; Society of Economic Geologists, Special Publication No. 19, Littleton, Colorado, p. 329–347.

Mao, M., Rukhlov, A.S., Rowins, S.M., Spence, J., and Coogan, L.A., 2016. Apatite trace element compositions: A robust new tool for mineral exploration; Economic Geology, v. 111, no. 5, p. 1187–1222.

McClenaghan, M.B. and Cabri, L.J., 2011. Gold and platinum group element indicator minerals in surficial sediments; Geochemistry: Exploration, Environment, Analysis, v. 11, p. 251–263.

McClenaghan, M.B., Spirito, W.A., Plouffe, A., McMartin, I., Campbell, J.E., Paulen, R.C., Garrett, R.G., Hall, G.E.M., Pelchat, P., and Gauthier, M.S., 2020. Geological Survey of Canada till-sampling and analytical protocols: from field to archive, 2020 update; Geological Survey of Canada, Open File 8591, 1 zip file.

McClenaghan, M.B., Beckett-Brown, C.E., McCurdy, M.W., and Casselman, S.G., 2023. Stream sediment indicator mineral signatures of the Casino porphyry Cu-Au-Mo deposit, Yukon, Canada; Economic Geology, v. 118, p. 411–431.

McCurdy, M., Peter, J.M., McClenaghan, M.B., Gadd, M.G., Layton-Matthews, D., Leybourne, M.I, Garrett, R.G., Petts, D.C., Jackson, S.E., and Casselman, S., 2022, Evaluation of magnetite as an indicator mineral for porphyry Cu exploration: A case study using bedrock and stream sediments at the Casino porphyry Cu-Au-Mo deposit, Yukon, Canada; Geochemistry: Exploration, Environment, Analysis, v. 22, geochem2021-072.

Meinert, L.D., Dipple, G.M., and Nicolescu, S., 2005. World skarn deposits; *in* One Hundredth Anniversary Volume, 1905–2005, (ed.) J.W. Hedenquist, J.F.H. Thompson, R.J. Goldfarb, and J.P. Richards; Society of Economic Geology, p. 299–336.

Osovetsky, B.M., 2016. Aggregation of nanogold particles in the environment; Natural Resources Research, v. 25, p. 241–253.

Pisiak, L.K., Canil, D., Lacourse, T., Plouffe, A., and Ferbey, T., 2017. Magnetite as an indicator mineral in the exploration of porphyry deposits: A case study in till near the Mount Polley Cu-Au deposit, British Columbia, Canada; Economic Geology, v. 112, no. 4, p. 919–940.

Pizarro, H., Campos, E., Bouzari, F., Rousse, S., Bissig, T., Gregoire, M., and Riquelme, R., 2020. Porphyry indicator zircons (PIZs): Application to exploration of porphyry copper deposits; Ore Geology Reviews, v. 126, p. 103771.

Pizarro, H., Rousse, S., Bouzari, F., Bissig, T., Gregoire, M., Riquelme, R., Carretier, S., Townley, B., Hoareau, G., and Mpodozis, C., 2024. Use of porphyry indicator zircons (PIZs) in the sedimentary record as an exploration tool for covered porphyry copper deposits in the Atacama Desert, Chile; Journal of Geochemical Exploration, v. 256, p. 107351.

Plouffe, A. and Ferbey, T., 2016. Till geochemistry, mineralogy and textural data near four porphyry Cu deposits in British Columbia; Geological Survey of Canada, Open File 8038, British Columbia Geological Survey Geofile 2016-10, 1 zip file.

Plouffe, A. and Ferbey, T., 2017. Porphyry Cu indicator minerals in till: A method to discover buried mineralization; *in* Indicator Minerals in Till and Stream Sediments of the Canadian Cordillera, (ed.) T. Ferbey, A. Plouffe, and A. Hickin; Mineral Association of Canada, Topics in Mineral Sciences Volume 47; Geological Association of Canada, Special Paper 50, p. 129–159.

Plouffe, A. and Ferbey, T., 2019. Indicator-mineral content of bedrock and till at the Gibraltar porphyry Cu-Mo deposit and the Woodjam porphyry Cu-Au-Mo prospect, south-central British Columbia; Geological Survey of Canada, Open File 8580; British Columbia Geological Survey, Open File 2019–10, 1 zip file.

Plouffe, A., Ferbey, T., Anderson, R.G., Hashmi, S., and Ward, B.C., 2013. New TGI-4 till geochemistry and mineralogy results near the Highland Valley, Gibraltar, and Mount Polley mines, and Woodjam District: an aid to search for buried porphyry deposits; Geological Survey of Canada, Open File 7473, 58 p.

Plouffe, A., Ferbey, T., Hashmi, S., and Ward, B.C., 2016. Till geochemistry and mineralogy: vectoring towards Cu porphyry deposits in British Columbia, Canada; Geochemistry: Exploration, Environment, Analysis, v. 16, p. 213–232.

Plouffe, A., Kjarsgaard, I.M. Ferbey, T., Wilton, D.H.C., Petts, D.C., Percival, J.B., Kobylinski, C.H., and McNeil, R., 2022. Detecting buried porphyry Cu mineralization in a glaciated landscape: a case study from the Gibraltar Cu-Mo deposit, British Columbia, Canada; Economic Geology, v. 117, p. 777–799.

Rabbia, O.M., Hernández, L.B., French, D.H., King, R.W., and Ayers, J.C., 2009. The El Teniente porphyry Cu-Mo deposit from a hydrothermal rutile perspective; Mineralium Deposita, v. 44, p. 849–866.

Roegge, J.S., Logsdon, M.J., Young, H.S., Barr, H.B., Borcsik, M., and Holland, H.D., 1974. Halogens in apatites from the Providencia area, Mexico; Economic Geology, v. 69, p. 229–240.

Rukhlov, A.S., Plouffe, A., Ferbey, T., Mao, M., and Spence, J., 2016. Application of trace-element compositions of detrital apatite to explore for porphyry deposits in central British Columbia; *in* Geological Fieldwork 2015; British Columbia Ministry of Energy and Mines, British Columbia Geological Survey, Paper 2016-1, p. 145–179.

Sillitoe, R.H., 2010. Porphyry copper systems; Economic Geology, v. 105, no. 1, p. 3–41.

Sinclair, W.D., 2007. Porphyry deposits; *in* Mineral Deposits of Canada: A Synthesis of Major Deposit Types, District Metallogeny, the Evolution of Geological Provinces, and Exploration Methods, (ed.) W.D. Goodfellow; Geological Association of Canada, Mineral Deposits Division, Special Publication No. 5, p. 983–1006.

Streck, M.J. and Dilles, J.H., 1998. Sulfur evolution of oxidized arc magmas as recorded in apatite from a porphyry copper batholith; Geology, v. 26, no. 6, p. 523–526.

Walli, C., 2022. Crystal Chemistry of Jarosite-Group Minerals from the Casino Deposit, Yukon; Unpublished thesis, Chemistry, Laurentian University, 52 p.

Xu, L., Xianwu, B., Ruizhong, H., Yongyong, T., Wang, X., and Xu, Y., 2015. LA-ICP-MS mineral chemistry of titanite and geological implications for exploration of porphyry Cu deposits in the Jinshajiang - Red River alkaline igneous belt, SW China; Mineralogy and Petrology, v. 109, p. 181–200.